Thesis

Asymptotic analysis of optimized waveform relaxation methods for RC circuits and RLCG transmission lines

KUMBHAR, Pratik Mahadeo

Abstract

Waveform Relaxation (WR) methods are iterative methods to solve time-dependent problems and large systems of ordinary differential equations arising from large scale electronic circuits. These methods are based on partitioning large circuits into smaller sub-circuits, which are then solved separately for multiple time steps and the overall solution is obtained by iteration between sub-circuits. The slow convergence of these methods especially for large time windows led to the introduction of Optimized Waveform relaxation (OWR) methods, which are based on optimizing parameters. In this thesis, we study the application of these methods to infinite RC and RLCG type circuits. We consider both the overlapping and nonoverlapping WR methods and find the optimized parameters in the transmission conditions. We then developed a novel algorithm that is based on model order reduction techniques for the simplified analysis of OWR methods when applied to infinitely long electric circuits.

Reference

KUMBHAR, Pratik Mahadeo. *Asymptotic analysis of optimized waveform relaxation methods for RC circuits and RLCG transmission lines*. Thèse de doctorat : Univ. Genève, 2020, no. Sc. 5434

DOI : 10.13097/archive-ouverte/unige:136729
URN : urn:nbn:ch:unige-1367299

UNIVERSITÉ DE GENÈVE
Section de mathématiques

FACULTÉ DES SCIENCES
Professeur Martin J. Gander

Asymptotic Analysis of Optimized Waveform Relaxation Methods for RC Circuits and RLCG Transmission Lines

THÈSE

Présentée á la Faculté des Sciences de l'Université de Genève
pour obtenir le grade de Docteur ès Sciences, mention Mathématiques

par

Pratik Mahadeo KUMBHAR

de

Mumbai (Inde)

Thèse N° 5434

GENÈVE
Atelier d'impression ReproMail
2020

UNIVERSITÉ
DE GENÈVE

FACULTÉ DES SCIENCES

DOCTORAT ÈS SCIENCES, MENTION MATHEMATIQUES

Thèse de Monsieur Pratik Mahadeo KUMBHAR

intitulée :

«Asymptotic Analysis of Optimized Waveform Relaxation Methods for RC Circuits and RLCG Transmission Lines»

La Faculté des sciences, sur le préavis de Monsieur M. GANDER, professeur ordinaire et directeur de thèse (Section de mathématiques), Monsieur G. VILMART, docteur (Section de mathématiques), Madame L. HALPERN, professeure (Laboratoire Analyse, Géométrie et Applications, Université Paris 13, Villetaneuse, France), autorise l'impression de la présente thèse, sans exprimer d'opinion sur les propositions qui y sont énoncées.

Genève, le 29 janvier 2020

Thèse - 5434 -

Le Décanat

N.B. - La thèse doit porter la déclaration précédente et remplir les conditions énumérées dans les "Informations relatives aux thèses de doctorat à l'Université de Genève".

To my Aai, Baba, family and friends,

Abstract

The ultimate aim of this thesis is to study the application of the nonoverlapping and overlapping Waveform Relaxation (WR) and Optimized Waveform Relaxation (OWR) methods to electric circuits, to be precise, RC circuits and RLCG transmission lines. We analyze for the first time the influence of overlap on the convergence of both WR and OWR methods. The thesis is divided into four chapters.

Chapter 1 is devoted to the introduction of basic concepts. We start by giving a background about various Domain Decomposition (DD) methods. We mention and discuss the most popular DD methods and their applications. We also explain WR methods in detail and give some convergence estimates. We then move toward electric circuits and recall Kirchoff's voltage law, Kirchoff's current law and the Modified Nodal Analysis (MNA) formulation.

In Chapter 2, we build a mathematical model of circuit equations for an infinitely long RC circuit. This process is carried out using the well known MNA formulation. We apply the classical WR method to this circuit and study its convergence in the Laplace space. We further introduce OWR methods to overcome the problem of slow convergence of the WR methods when large time windows are used. OWR methods require us to solve a min-max problem to find the optimizing parameters involved in the transmission conditions of the OWR methods. This min-max problem cannot be solved using the available complex analysis tools and hence we use asymptotic analysis with respect to two different parameters: one with respect to final time going to infinity and the other with respect to the reaction terms going to zero. We considered both nonoverlapping and overlapping WR and OWR methods, and found the optimizing parameters for both of these cases. We proved that overlap increases the convergence rate for both WR and OWR methods. We also proved that OWR methods produce far more rapid convergence than the WR methods. Finally, we performed numerical tests to support our theoretical results.

In Chapter 3, we considered a complicated electric circuit, the infinitely long RLCG transmission line. We analyzed both nonoverlapping and overlapping decompositions for WR and OWR methods. For this circuit, the unknowns are voltages at the nodes and currents in the circuit branches, and thus for overlapping methods, the type of partitioning of the circuit is interesting. We considered two types of partitioning for the circuit: one at a voltage node and the other at a current node, and showed that the convergence rate of the overlapping WR method is the same irrespective of the type of partitioning, while for the overlapping OWR method, the one with partitioning at a voltage node converges faster than that of a partitioning at a current node. We further solved min-max problems to find optimized parameters for three cases: the nonoverlapping OWR method, the overlapping OWR with splitting at a voltage node and overlapping OWR with splitting at a current node.

In Chapter 4, we developed a novel algorithm for the analysis of OWR methods when applied to infinitely long electric circuits. We proposed first to reduce the infinitely long circuit into a smaller equivalent circuit, and then to apply the WR and OWR methods. The expression of the convergence factor for the OWR method is thus simpler and hence the optimization problem to find optimized parameters can be easily solved without using asymptotic analysis. Though we carried out this algorithm only for the nonoverlapping OWR method applied to an infinitely long RC circuit, this algorithm can be extended to other circuits and time dependent PDEs.

Résumé

Le but ultime de cette thèse est d'étudier l'application des méthodes de relaxation de forme d'onde (WR) et de relaxation de forme d'onde optimisée (OWR) à des circuits électriques, pour être précis, un circuit RC infiniment long et une ligne électrique RLCG infiniment longue. Nous analysons pour la première fois l'influence des chevauchements sur la convergence des méthodes WR et OWR. La thèse est divisée en quatre chapitres.

Le chapitre 1 est consacré à l'introduction des concepts de base. Nous commençons par donner un aperçu des différentes méthodes de décomposition de domaine (DD). Nous mentionnons et discutons des méthodes populaires de DD et de leurs applications. Nous expliquons ensuite en détail les méthodes WR et donnons quelques estimations de convergence. Nous passons ensuite aux circuits électriques et rappelons la loi de tension de Kirchoff, la loi de courant de Kirchoff et la formulation de l'analyse nodale modifiée (MNA).

Dans le chapitre 2, nous construisons un modèle mathématique des équations d'un circuit RC infiniment long. Ce processus est réalisé à l'aide de la formulation MNA bien connue. Nous appliquons la méthode WR classique à ce circuit et étudions sa convergence dans l'espace de Laplace. Nous introduisons en outre des méthodes OWR pour résoudre le problème de la lente convergence des méthodes WR lorsque de grandes fenêtres temporelles sont utilisées. Cependant, les méthodes OWR nous obligent à résoudre un problème min-max pour trouver les paramètres d'optimisation impliqués dans les conditions de transmission des méthodes OWR. Ce problème min-max ne peut pas être résolu en utilisant l'analyse complexe disponible et par conséquent, nous utilisons l'analyse asymptotique en fonction de deux paramètres diffrents : l'un avec par rapport au temps final allant à l'infini et l'autre par rapport aux termes de réaction allant jusqu'à zéro. Nous avons examiné les méthodes WR et OWR qui se chevauchent et qui ne se chevauchent pas, et nous avons constaté que l'optimisation pour ces deux cas. Nous avons prouvé que le chevauchement augmente le taux de convergence pour les méthodes WR et OWR. Nous avons également prouvé que les méthodes OWR produisent une convergence beaucoup plus rapide que les méthodes WR. Nous avons ensuite effectué des tests numériques pour étayer nos résultats théoriques.

Dans le chapitre 3, nous avons considéré un circuit électrique compliqué, les lignes de transmission RLCG infiniment longues. Nous avons analysé les deux cas : décomposition sans chevauchement et décomposition avec chevauchement pour les méthodes WR et OWR. Pour ce circuit, les inconnues étaient les tensions aux nœuds et les courants dans les branches du circuit, et donc pour les méthodes de chevauchement, le type de partitionnement du circuit est intéressant. Nous avons considéré deux types de partitionnement du circuit : l'un à un nœud de tension et l'autre un nœud de courant. Nous avons observé que le taux de convergence de la méthode WR à chevauchement

est le même quel que soit le type de partitionnement, alors que pour la méthode OWR à chevauchement, celle avec à un nœud de tension converge plus rapidement que celui d'un nœud de courant. Nous avons en outre résolué problèmes min-max pour trouver des paramètres d'optimisation dans trois cas : méthode OWR sans chevauchement, OWR chevauchant avec division au niveau d'un nœud de tension et OWR chevauchant avec division au niveau d'un courant nœud.

Dans le chapitre 4, nous avons développé un nouvel algorithme pour l'analyse des méthodes OWR appliquées aux circuits électriques infiniment longs. Nous proposons d'abord de réduire le circuit infiniment long en un circuit équivalent plus petit, puis d'appliquer les méthodes WR et OWR. L'expression du facteur de convergence pour la méthode OWR est donc plus simple et donc le problème d'optimisation pour trouver les paramètres d'optimisation peut être facilement résolué sans utiliser l'analyse asymptotique. Bien que nous n'ayons effectué cet algorithme que pour la méthode OWR non chevauchante appliquée à un circuit RC infiniment long, cet algorithme peut être étendu à d'autres circuits et aux EDP dépendants du temps.

Acknowledgement

First of all, I would like to express my sincere gratitude to my Ph.D. supervisor Prof. Martin J. Gander for all his guidance, support, motivation and immense knowledge. He always trusted my work, and without his active guidance, it would not have been possible for me to complete this work. I also wish to express my gratitude to Dr. Albert Ruehli, Missouri University of Science and Technology, for explaining us how to build a mathematical model of electric circuits and providing me with important inputs related to circuits.

My sincere thanks to Prof. Laurence Halpern and Dr. Gilles Vilmart for being the jury for my Ph.D. defense.

I would like to express my thankfulness to all the faculty members and my fellow colleagues of the department for their valuable suggestions and encouragement. Special thanks to my collaborators Tommaso Vanzan and Dr. Faysal Chaouqui for numerous discussions on DD methods and related topics. I thank my officemates Eiichi and Ibrahim for creating motivating atmosphere in the office. I thank the members of numerical analysis group: Bart, Marco, Ding, Gabriele, Parisa, Adrien, Guillaume, Giancarlo, Thibaut, Julian, Conor, Pablo, Michal, Yongxiang, Sandie and Bo. I also thank my friends from other groups of the department: Aitor, Yaroslav, Renaud, Pascaline, Louis-Hadrien and Fathi. Special thanks to Jhih-Huang and Aurelie for helping me to learn French. Not to forget the contribution of the Mrs. Joselle Besson who helped in with the administrative work in Geneva. I am happy to acknowledge my friend Monika, who is ever encouraging and supporting in all aspects of my life. I thank my Indian friends in Geneva namely Bharat, Sneh, Pramod, Somnath, Sujata, Manish and Jimit for making me feel like home.

My eternal gratitude goes to my parents, Mrs. Sangeeta Kumbhar and Mr. Mahadeo Kumbhar, and other family members including my sister Mrs. Priyanka Raje, brother in law Mr. Nishikant Raje for their support and continuous motivation. I am also very grateful to my M.Sc. thesis supervisors Prof. Amiya Pani from IIT-Bombay, Prof. Thierry Goudon and Prof. Boniface Nkonga from University of Nice for their support. There are many others who played an important role in my life and would like to thank them also.

Finally, I would like to thank God Almighty for giving me the strength, knowledge, ability and opportunity to undertake this research study and to persevere and complete it satisfactorily.

Contents

Chapter 1

Introduction

Scientific computing deals with modeling a physical phenomena, and then solving it using available numerical tools. These models are systems of Partial Differential Equations (PDEs) such as the heat equation, the Laplace equation and so on. Over the last century, numerous numerical methods have been developed to solve these models. Most of these methods are sequential in nature and developed to be implemented on a single processor. However the size of these systems can be of millions of order and take a large amount of time due to their large computational cost. Since 2004, the CPU frequency is stagnating around 3 GHz and there is hardly any hope that it will improve in the near future [18]. But one can make use of the availability of a large number of processors.

Instead of solving a large system on a single processor, we can divide it into multiple subsystems which then can be solved on multiple processors and an algorithm can be developed to merge these solutions from different processors. Domain Decomposition (DD) methods are one such classical method which is based on a divide and conquer rule. Numerous DD methods have been introduced and well studied in the last few decades. The main two types of DD methods are the nonoverlapping and the overlapping DD methods. The classical overlapping DD methods like the alternating Schwarz and parallel Schwarz methods converge, while the nonoverlapping versions of these methods do not converge [18, 22]. Nonoverlapping DD methods like Dirichlet-Neumann (DN), Neumann-Neumann (NN) methods and Finite Element Tearing and Interconnecting (FETI) methods are also widely used. For a two subdomain case, DN methods are based on solving a Dirichlet and a Neumann problem iteratively [69]. NN methods were first introduced in 1988 [6] and their various versions were analyzed for two and multiple subdomain cases by many researchers all over the world [8, 10–12, 66]. FETI and Balancing DD method are similar to NN method and have also been well studied [13, 19, 20, 50, 58, 59]. Nonoverlapping DD methods are widely applied to heterogeneous problems, where the domain is divided into nonoverlapping subdomains such that each subdomain solves one particular type

of PDE [40, 41, 47]. Further, for the class of overlapping methods, both classical Schwarz and optimized Schwarz methods were analyzed for numerous types of PDEs like Laplace, Helmholtz, advection-diffusion and so on by Gander et al [22, 42–44, 56]. The classical methods are not scalable and hence one needs to use two level or multilevel methods to make them scalable. A recent paper deals with scalability of these methods in one dimension [9, 14].

For time dependent PDEs, similar methods have also been introduced. One of the well known and widely used parallel computing tool for time dependent PDEs or time dependent systems of Ordinary Differential Equations (ODEs) is Waveform Relaxation (WR). The history of WR methods goes back to 1982, where they were proposed to solve very large systems of ODEs arising from electric circuits by Lelarasmee, Ruehli and Sangiovanni-Vincentelly in [53]. The rapidly increasing size of the integrated circuits made them difficult to simulate. The availability of multiple processors allows us to divide the huge circuits into smaller sub-circuits which are solved on different processors and information is exchanged between them at the end of each iteration. In [53], Ruehli and his team considered a MOS ring oscillator to explain how this method works. Nonoverlapping WR methods have been studied for small RC circuits in [2, 37], and for infinitely long RC circuits in [3, 70], while for their overlapping version we refer to [32, 34]. These methods were also analyzed for RLCG transmission lines by Gander et al [1, 25, 26, 33, 36].

Further, a similar algorithm was developed for solving time dependent PDEs. This algorithm is called Schwarz Waveform Relaxation (SWR) [21]. Similar to WR methods, the space is divided into multiple subdomains and solved over the entire time interval. SWR and OSWR methods are studied for the heat equation in [27, 38, 45], for the wave equation in [30, 48], for advection diffusion equations in [28, 60], and for Maxwell's equations in [5, 16, 17]. Moreover for the nonoverlapping case, Neumann Neumann Waveform Relaxation (NNWR) and Dirichlet Neumann Waveform Relaxation (DNWR) were recently analyzed in [35, 51, 62, 65].

Recently, WR methods were also applied to the field circuit coupled problems, where the computational domain is divided into two subdomains, and a time dependent PDE is solved on one subdomain and the circuit equations on the other [4, 15, 46]. Note that in WR or SWR methods, the space domain is divided into multiple subdomains, and not the time domain. Hence, once the space parallelism stagnates, these methods can be combined with other time parallel methods like Parareal [31, 39, 54, 55, 67], Pipelining methods [52, 64] and others to achieve an extra speedup.

In this thesis, we will study the application of nonoverlapping and overlapping WR methods to electric circuits, to be specific infinitely long RC circuits and infinitely long RLCG transmission lines. But before moving towards it, we will give an overview of WR methods and explain some basic concepts of electric circuits and their modeling.

1.1 Time Parallel Methods

Time parallel integration methods are gaining a lot of importance and are currently an active field of research for solving systems of time dependent ODEs and time dependent PDEs, for example, the heat equation, wave equations, Maxwell's equations and transport equations. Solving these PDEs using any finite difference scheme or finite element method is computationally costly and one needs to use parallel computing. This will lead to a small computational cost for each processor. However the communication cost between these processors needs to be considered which may be large, and hence using too many processors will make the overall method ineffective. We thus need to use an appropriate number of processors. Further, usually space parallelism is analyzed and implemented, while time direction is not used for parallelism because the time evolution is considered as sequential process, that is, the solution at a particular time depends on the solution at the earlier time. However, when the space parallelization saturates, we are left with the only choice of using parallelization methods for time direction.

Time parallel methods can be divided into four major classes:

- Methods based on multiple shooting,
- Methods based on domain decomposition,
- Methods based on multigrid,
- Direct time parallel methods.

We shall not explain all of these methods and let the reader refer to [23] and its references for more details on these methods. In this section we shall explain WR methods in detail and recall some important convergence theorems and their proofs.

1.1.1 Waveform Relaxation methods

As discussed earlier, WR methods are iterative methods to solve time dependent problems. These methods belong to the group of time parallel methods based on domain decomposition, where the space is divided into multiple subdomains as illustrated in Figure 1.1. The basic idea of WR methods is simple. We first divide the space domain Ω_x into several subdomains, say Ω_i, $i = 1, 2, \ldots, n$. Then, on each subdomain, we solve the given problem on the entire time window $(0, T]$, where T is the final time. At the end of each iteration, we transfer the information between the neighboring subdomains using some transmission conditions, and again solve the problem. This process continues until the solution converges. Note that, this process of finding the solution on each subdomain can be done in parallel, and the communication between the subdomains takes place at the start of each iteration. A notable

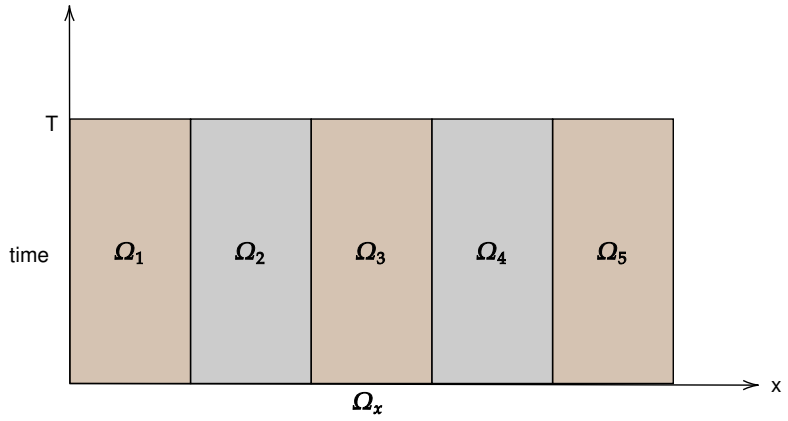

Figure 1.1: Space-time domain decomposition for WR methods.

advantage of WR methods is that different time integration methods with different time stepping can be used in different subdomains.

1.1.1.1 Convergence of WR

For the convergence analysis of WR methods, we refer to Gander's lectures notes on WR methods [24]. Note that the convergence of WR methods and SWR methods depends solely on the types of equations being solved for. In this section, we shall show the general estimate for the WR algorithm for systems of ODEs of the form

$$\begin{aligned} &\tfrac{d}{dt}\mathbf{u}(t) = \mathbf{f}(t,\mathbf{u}(t)), \qquad t \in (0,T], \\ &\mathbf{u}(0) = \mathbf{u}_0. \end{aligned} \tag{1.1}$$

We now use a partition function $\tilde{\mathbf{f}}(t,\mathbf{v},\mathbf{v})$ that satisfies

$$\tilde{\mathbf{f}}(t,\mathbf{v},\mathbf{v}) = \mathbf{f}(t,\mathbf{v}), \quad \forall \mathbf{v} \in \mathbb{R}^d, t \in (0,T].$$

We then define the WR iterations associated with the partition functions. For the iteration index $k = 0, 1, 2, \ldots$, we have

$$\begin{aligned} &\frac{d}{dt}\mathbf{u}^{k+1}(t) = \tilde{\mathbf{f}}(t,\mathbf{u}^{k+1}(t),\mathbf{u}^{k}(t)), \qquad t \in (0,T], \\ &\mathbf{u}^{k+1}(0) = \mathbf{u}_0. \end{aligned} \tag{1.2}$$

To study the convergence of these iterations, we need the following two lemmas.

Lemma 1.1.1. *(Gronwall Lemma) Let $u(t)$, $\alpha(t)$ and $\beta(t)$ be continuous functions on $[0,T]$. If $\beta(t) \geq 0$ and*

$$u(t) \leq \alpha(t) + \int_0^t \beta(s)u(s)ds \qquad \forall t \in [0,T],$$

then

$$u(t) \leq \alpha(t) + \int_0^t \alpha(s)\beta(s)e^{\int_s^t \beta(\tau)d\tau}ds \qquad \forall t \in [0,T].$$

Lemma 1.1.2. *Let* $I_0(t) := \int_0^t e^{L_1 s}ds = \frac{1}{L_1}\left(e^{L_1 t}-1\right)$ *and*

$$I_k(t) = \frac{1}{L_1}e^{L_1 t}\frac{(L_2 t)^k}{k!} - \frac{L_2}{L_1}I_{k-1}(t), \quad k = 1,2,\ldots, \tag{1.3}$$

where L_1 *and* L_2 *are two positive constants. Then*

$$L_2 I_k(t) + L_1 L_2 \int_0^t I_k(s)e^{L_1(t-s)ds} = \frac{(L_2 t)^{k+1}}{(k+1)!}e^{L_1 t}. \tag{1.4}$$

Proof. The proof follows by induction on k and can be found in [24]. □

Using these two lemmas, we prove a convergence estimate for the general WR method.

Theorem 1.1.1. *If the partition function* $\tilde{\mathbf{f}}(t,\mathbf{v},\mathbf{w})$ *is Lipschitz continuous in both arguments uniformly for all* $t \in [0,T]$*, that is,*

$$\begin{aligned} \|\tilde{\mathbf{f}}(t,\mathbf{v}_1,\mathbf{w}) - \tilde{\mathbf{f}}(t,\mathbf{v}_2,\mathbf{w})\| &\leq L_1\|\mathbf{v}_1 - \mathbf{v}_2\|, \\ \|\tilde{\mathbf{f}}(t,\mathbf{v},\mathbf{w}_1) - \tilde{\mathbf{f}}(t,\mathbf{v},\mathbf{w}_2)\| &\leq L_2\|\mathbf{w}_1 - \mathbf{w}_2\|, \end{aligned} \tag{1.5}$$

then the waveform relaxation algorithm (1.2) *satisfies the error estimate*

$$\|\mathbf{u} - \mathbf{u}^k\|_T \leq e^{L_1 T}\frac{(L_2 T)^k}{k!}\|\mathbf{u} - \mathbf{u}^0\|_T, \tag{1.6}$$

where $\|\cdot\|_T$ *denotes the maximum norm in* $[0,T]$*, that is,* $\|\mathbf{u}\|_T := \max_{0\leq t\leq T}\|\mathbf{u}(t)\|$.

Proof. This proof can be found in [24], but since it is an important proof we show important steps. Subtracting the integral form of the WR iterations (1.2) from the integral form of the WR system (1.1) leads to,

$$\mathbf{u}(t) - \mathbf{u}^k(t) = \int_0^t \left[\mathbf{f}(s,\mathbf{u}(s)) - \tilde{\mathbf{f}}(s,\mathbf{u}^k(s),\mathbf{u}^{k-1}(s))\right]ds.$$

The function $\mathbf{f}$ satisfies $\mathbf{f}(s,\mathbf{u}(s)) = \tilde{\mathbf{f}}(s,\mathbf{u}(s),\mathbf{u}(s))$, and hence using the Lipschitz continuity (1.5), we have

$$\begin{aligned} \|\mathbf{u}(t) - \mathbf{u}^k(t)\| &= \left\| \int_0^t \left[\tilde{\mathbf{f}}(s,\mathbf{u}(s),\mathbf{u}(s)) - \tilde{\mathbf{f}}(s,\mathbf{u}^k(s),\mathbf{u}^{k-1}(s))\right]ds \right\| \\ &= \left\| \int_0^t \left[\tilde{\mathbf{f}}(s,\mathbf{u}(s),\mathbf{u}(s)) - \tilde{\mathbf{f}}(s,\mathbf{u}^k(s),\mathbf{u}(s))\right]ds \right. \\ &\quad \left. + \int_0^t \left[\tilde{\mathbf{f}}(s,\mathbf{u}^k(s),\mathbf{u}(s)) - \tilde{\mathbf{f}}(s,\mathbf{u}^k(s),\mathbf{u}^{k-1}(s))\right]ds \right\| \\ &\leq L_1\int_0^t \|\mathbf{u}(s) - \mathbf{u}^k(s)\|ds + L_2\int_0^t \|\mathbf{u}(s) - \mathbf{u}^{k-1}(s)\|ds. \end{aligned}$$

We define $\beta(t) := L_2$ and $\alpha(t) := L_2 \int_0^t \|\mathbf{u}(s) - \mathbf{u}^{k-1}(s)\| ds$. Applying the Gronwall Lemma 1.1.1, the above inequality reduces to

$$\|\mathbf{u}(t)-\mathbf{u}^k(t)\| \leq L_2 \int_0^t \|\mathbf{u}(s)-\mathbf{u}^{k-1}(s)\| ds + L_1 L_2 \int_0^t \int_0^s \|\mathbf{u}(\tau)-\mathbf{u}^{k-1}(\tau)\| d\tau e^{L_1(t-s)} ds. \tag{1.7}$$

For $k = 1$, we obtain

$$\begin{aligned} \|\mathbf{u}(t) - \mathbf{u}^1(t)\| &\leq L_2 \int_0^t \|\mathbf{u}(s) - \mathbf{u}^0(s)\| ds + L_1 L_2 \int_0^t \int_0^s \|\mathbf{u}(\tau) - \mathbf{u}^0(\tau)\| d\tau e^{L_1(t-s)} ds \\ &\leq L_2 t \|\mathbf{u}(t) - \mathbf{u}^0(t)\|_t + L_1 L_2 \int_0^t s \|\mathbf{u}(s) - \mathbf{u}^0(s)\|_s e^{L_1(t-s)} ds \\ &\leq \left(L_2 t + L_1 L_2 e^{L_1 t} \int_0^t s e^{-L_1 s} ds \right) \|\mathbf{u}(t) - \mathbf{u}^0(t)\|_t. \end{aligned} \tag{1.8}$$

Using integration part, the term in the parenthesis can be simplified to

$$\begin{aligned} L_2 t + L_1 L_2 e^{L_1 t} \int_0^t s e^{-L_1 s} ds &= \frac{L_2}{L_1} \left(e^{L_1 t} - 1 \right) \\ &= \frac{L_2}{L_1} \left(1 + L_1 t + \frac{(L_1 t)^2}{2} + \dots \right) \leq L_2 t e^{L_1 t}. \end{aligned}$$

We thus arrive for all $t \in [0, T]$ at

$$\|\mathbf{u}(t) - \mathbf{u}^1(t)\|_T \leq L_2 T e^{L_1 T} \|\mathbf{u}(t) - \mathbf{u}^0(t)\|_T.$$

We proved the required inequality (1.6) for $k = 1$. Assuming that the inequality (1.6) holds for $k - 1$, we prove that it holds for k. From (1.7),

$$\begin{aligned} \|\mathbf{u}(t) - \mathbf{u}^k(t)\| \leq L_2 &\int_0^t e^{L_1 s} \frac{(L_2 s)^{k-1}}{(k-1)!} \|\mathbf{u} - \mathbf{u}^0\|_s ds \\ &+ L_1 L_2 \int_0^t \int_0^s e^{L_1 t} \frac{(L_2 \tau)^{k-1}}{(k-1)!} \|\mathbf{u} - \mathbf{u}^0\|_\tau d\tau e^{L_1(t-s)} ds. \end{aligned} \tag{1.9}$$

Using integration by parts, the first term can be bounded by

$$\begin{aligned} \int_0^t e^{L_1 s} \frac{(L_2 s)^{k-1}}{(k-1)!} \|\mathbf{u} - \mathbf{u}^0\|_s ds &\leq \int_0^t e^{L_1 s} \frac{(L_2 s)^{k-1}}{(k-1)!} ds \|\mathbf{u} - \mathbf{u}^0\|_t \\ &= \left(\frac{1}{L_1} e^{L_1 t} \frac{(L_2 t)^{k-1}}{(k-1)!} - \frac{1}{L_1} \int_0^t e^{L_1 s} \frac{(L_2 s)^{k-2}}{(k-2)!} ds \right) \|\mathbf{u} - \mathbf{u}^0\|_t. \end{aligned}$$

Define $I_{k-1}(t) := \int_0^t e^{L_1 s} \frac{(L_2 s)^{k-1}}{(k-1)!} ds$. Then the above equation can be written as

$$I_{k-1}(t) \|\mathbf{u} - \mathbf{u}^0\|_t \leq \left(\frac{1}{L_1} e^{L_1 t} \frac{(L_2 t)^{k-1}}{(k-1)!} - \frac{L_2}{L_1} I_{k-2}(t) \right) \|\mathbf{u} - \mathbf{u}^0\|_t.$$

Substituting this into (1.9) leads to

$$\|\mathbf{u}(t) - \mathbf{u}^k(t)\| \leq \left(L_2 I_{k-1}(t) + L_1 L_2 \int_0^t I_{k-1}(s) e^{L_1(t-s)} ds \right) \|\mathbf{u}(t) - \mathbf{u}^0(t)\|_t,$$

which can be further bounded using the estimate of Lemma 1.1.2 to yield the required error estimate (1.6). This completes the proof of this theorem. □

Remark 1.1.1. Theorem 1.1.1 states that the WR algorithm converges superlinearly for finite time intervals.

1.2 Electric Circuits

In this section we discuss electric circuits and their simulation. Most of the content of this section has been summarized from the book [63], and one may refer to this book for more details.

Circuit simulation is a process of constructing and checking the design of an electric circuit before its manufacturing. In other words, it is a process of developing a mathematical model to replicate the behavior of the real circuit, and then solve this model numerically. Simulations help the circuit designers to test their ideas, and optimize circuit parameters to achieve the desired output. They thus save a lot of time and cost when designing circuits, and one can minimize the risk of unwanted hazards. Further, the number of electronic devices is continuously increasing which in turn increases the need for new design tools and techniques. Circuit solvers like SPICE is no exception. Not only new approaches are desired but the tools need to have an ever increasing capacity to solve larger problems.

The first step of circuit simulation is building a mathematical model using the well known Kirchoff's Current Law (KCL) and Kirchoff's Voltage Law (KVL). We first recall some basic definitions which will be required to build a model.

Definition 1.2.1. An *element* is a two-terminal electrical device. An *electrical network*, or *circuit* is a system consisting of a set of elements and a set of *nodes*, where every element terminal is identified with a unique node, and every node is identified with at least one element terminal.

Using the above definition, we can represent an electrical network by a graph whose vertices corresponds to circuit nodes and edges corresponds to circuit elements. We now define two of the most fundamental Laws, KCL and KVL.

Definition 1.2.2. (KCL) The *Kirchoff's Current Law* states that in an electric circuit, the total amount of current flowing into any node is equal to the total amount of current flowing out of it. In order words, the algebraic sum of currents in a circuit meeting at a node is zero, that is, $\sum_{k=1}^{n} i_k = 0$, where i_k represents the current in the k^{th} edge.

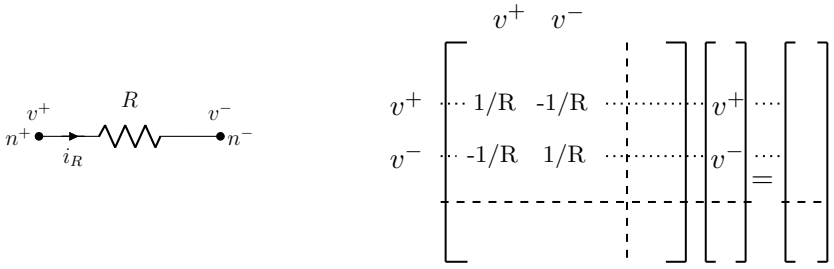

Figure 1.2: Element stamp for a resistor R.

Definition 1.2.3. (KVL) The *Kirchoff's Voltage Law* states that the algebraic sum of all the voltages around any closed loop in a circuit is equal to zero. In other words, the algebraic sum of all the potential differences (voltages) around the loop must be equal to zero, that is, $\sum_{k=1}^{n} V_k = 0$.

The method used to build a mathematical model of any circuit is one of the important factors which determines the circuit simulation time. The amount of time required to build these circuit equations, computational cost, storage requirements and the execution time of the computer programming affects the efficiency of the method used. In most cases, the mathematical model is developed using one of the two popular approaches: the Sparse Tableau Analysis (STA) formulation and the Modified Nodal Analysis (MNA) formulation. In this chapter, we explain the MNA formulation in detail and recommend the reader to refer to the book [63] to understand the STA formulation.

1.2.1 Modified Nodal Analysis

We summarize the MNA formulation based on Section 2.4.4 of [63]. The MNA formulation was originally described by Ho et al [49] in 1975. Depending on the circuit elements, MNA leads to a system of differential equations in time or a system of algebraic equations. To assemble the MNA system, we first define an *element stamp*, and give some examples of stamps.

Definition 1.2.4. The contribution of every element to the matrix equation is described by means of a template, which is called an *element stamp*.

For an example, consider a resistor with resistance R and whose terminals are denoted by n^+ and n^-. Let i_R be the current passing through it which has a standard reference direction from n^+ to n^-. Further, let v^+ and v^- be the voltages at nodes n^+ and n^- respectively. This is shown in Figure 1.2. By Ohm's Law, the current $i_R = \frac{v^+ - v^-}{R} = v^+\left(\frac{1}{R}\right) + v^-\left(\frac{-1}{R}\right)$, and hence the element stamp for this resistor is given on the right of Figure 1.2. For a capacitor, the current i_C through it takes the form $i_C = C\left(\frac{dv^+}{dt} - \frac{dv^-}{dt}\right)$, where C is its capacitance. The element stamp of

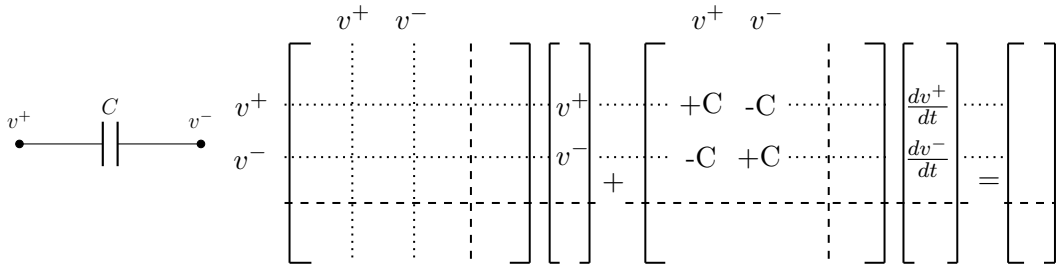

Figure 1.3: Element stamp for a capacitor C.

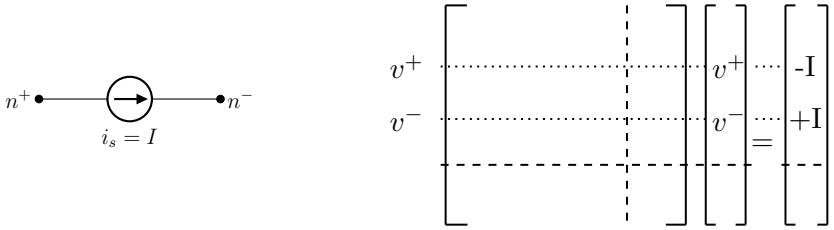

Figure 1.4: Element stamp for an independent current source i_s.

a capacitor thus contains one more matrix which is multiplied with the derivative of voltages in time. This is illustrated in Figure 1.3. Further, the electric circuit is driven by some independent current source which provides an external current i_s. The element stamp for such a current source can be seen in Figure 1.4. For most of the electrical circuits, the MNA formulation builds a system of differential equations in time, and it has the form $M\dot{\mathbf{v}} = K\mathbf{v} + \tilde{\mathbf{f}}$.

We explain now the assembling process of the MNA formulation for an RC circuit. We start with a zero RHS vector $\tilde{\mathbf{f}} \in \mathbb{R}^N$, and zero matrices M, $K \in \mathbb{R}^{N\times N}$, where N is the number of nodes in the circuit. The vector $\mathbf{v}$ contains the unknown voltages at the nodes and remains unchanged throughout this process. We then read every element of the circuit one by one. As an element is read, its element stamp is added to the matrices M and K. Since the element stamp of a capacitor contains derivative terms, its element stamp is added to the matrix M, while the element stamp of a resistor is added to the matrix K. The source terms are stamped into the vector $\tilde{\mathbf{f}}$. This process continues until all elements of the circuit are read and thus we obtain a system of differential equations in time of the form $\dot{\mathbf{v}} = A\mathbf{v} + \mathbf{f}$, where $A := M^{-1}K$ and $\mathbf{f} := M^{-1}\tilde{\mathbf{f}}$.

Remark 1.2.1. This assembling process is similar to that of the well known Finite Element Methods (FEM) described in [7]. In FEM, the domain is divided into smaller triangles, which are popularly called *elements*. These elements can be of the shape of other basic polygons. While assembling the mass and stiffness matrices, the basis functions are evaluated on each individual elements separately, which are then added in these matrices. This process is the same as that are followed by MNA.

Chapter 2

Waveform Relaxation Methods Applied to RC circuits

In this chapter, we will study the application of both Waveform Relaxation (WR) methods and Optimized Waveform Relaxation (OWR) methods to an infinitely long RC circuit.

A Resistor-Capacitor (RC) circuit, which is also called an RC filter, is a simple electric circuit whose components are only resistors and capacitors. Of course, this circuit contains also of a voltage source and a load resistor. The simplest RC circuit is shown in Figure **??**. In this circuit, the energy stored in the capacitor C is discharged through the resistor R.

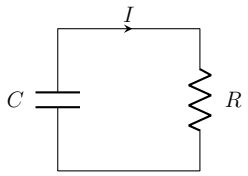

Figure 2.1: A simple RC circuit[1]

Often, RC circuits are used as filters, that is, they block signals of a certain range of frequencies and allow the rest to pass. In this chapter, we will consider infinitely long low pass RC filters (see Figure 2.2). As the name suggests, these circuits allow only low frequency signals ranging from 0 Hz to a fixed cutoff frequency to pass, and thus blocking other signals. Note that in Figure 2.2, an independent current source with current I_s supplies the required current to the circuit. Also the voltage $v_{-\infty}$ just denotes that the RC circuit is infinitely long.

[1] https://en.wikipedia.org/wiki/RC_circuit

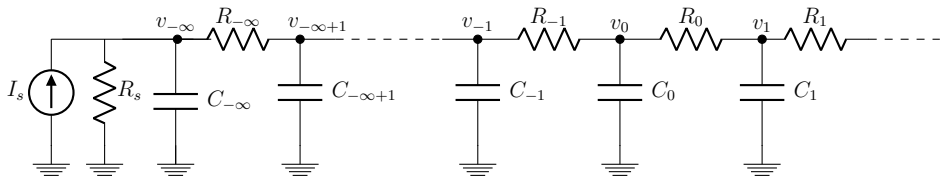

Figure 2.2: RC Circuit of infinite length.

Today, the tremendously increasing size and complexities of an integrated circuit makes their simulation computationally very costly. As discussed in Section 1.1, WR methods provides a quick and computationally cheap way for their simulations. In order to implement WR methods, these integrated circuits need to be divided into smaller circuits. Usually, RC circuits are part of these large integrated circuits, and hence analyzing the application of WR methods to RC circuits will provide us with a better understanding of transmission conditions at the RC circuit interface. One can then opt to divide circuits at an RC circuit interface and then use the transmission conditions developed in this chapter, which will ultimately lead to quick simulation of large integrated circuits. Further, such RC circuit interfaces can also be found in Field-circuit coupled problems as discussed in Chapter 1.

The structure of this chapter is as follows: first we develop the mathematical model of the infinitely long RC circuit as shown in Figure 2.2. Then we will explain the WR algorithm for this circuit and study its convergence. We will then introduce OWR methods and show how these methods are faster than classical WR methods. Next, we will find the optimized parameters involved in the transmission conditions by considering asymptotic analysis with respect to the final time and the reaction term. Finally, we support our theoretical results with numerical experiments.

2.1 Mathematical Model

We are interested in determining the voltages v_i, $i \in \mathbb{Z}$ at the nodes of the circuit shown in Figure 2.2. The Modified Nodal Analysis (MNA), originally described by Ho, Ruehli and Brennan in 1975 [49], is used to build a mathematical model of such electric circuits. MNA has been explained in detail in Section 1.2.1. MNA produces a system of ODEs of the form $\dot{\mathbf{v}} = A\mathbf{v} + \mathbf{f}$, where the entries of the matrix A contain the elements of the circuit, $\mathbf{v}$ is the unknown vector of voltages at the nodes, and $\mathbf{f}$ contains the source terms. For the infinite RC circuit, this system looks like

$$\frac{d\mathbf{v}}{dt} = \begin{bmatrix} \ddots & \ddots & \ddots & & & & \\ & a_{-1} & b_0 & c_0 & & & \\ & & a_0 & b_1 & c_1 & & \\ & & & a_1 & b_2 & c_2 & \\ & & & & \ddots & \ddots & \ddots \end{bmatrix} \mathbf{v} + \mathbf{f}, \tag{2.1}$$

where

$$a_i := \frac{1}{R_i C_{i+1}}, \quad b_i := -\left(\frac{1}{R_{i-1}} + \frac{1}{R_i}\right)\frac{1}{C_i}, \quad c_i := \frac{1}{R_i C_i}, \quad i \in \mathbb{Z},$$

and $\mathbf{f} := (I_s(t)/C_{-\infty}, 0, 0, \ldots, 0)^\top$. Further, initial conditions $\mathbf{v}(0)=\mathbf{v}_0$ need to be supplied to solve the system of equations (2.1).

For a small vector $\mathbf{v}$, one can solve the system of ODEs (2.1) by employing explicit (for example, forward Euler) or implicit (for example, backward Euler) time stepping methods. However if the size of the vector $\mathbf{v}$ is in the millions, implicit methods are computationally costly and requires a lot of time since large matrices need to be inverted at each time step. For an explicit method, small time steps need to be used which adds up the computational cost. One therefore needs to use parallel methods. WR methods are parallel methods used to simulate time dependent and multi-scale problems. These methods are explained in detail in Section 1.1.1.

2.1.1 Relation with the Heat equation

The heat equation is a partial differential equation in space and time that describes the distribution of heat over an object and its evolution as time progresses. To give a glimpse of this equation, we consider an one dimensional infinite bar, which is denoted by $\Omega_x := (-\infty, \infty)$, and a time interval $(0, T]$, where T is the final time. Let $v(x,t)$ denote the temperature on the bar at position $x \in \Omega_x$ at time $t \in (0,T]$. The heat equation is then given by

$$\begin{aligned} \frac{\partial v(x,t)}{\partial t} &= \frac{\partial^2 v(x,t)}{\partial x^2} + f(x,t), \quad x \in \Omega_x, \quad t \in (0,T], \\ v(x,0) &= v_0(x), \quad x \in \Omega_x, \end{aligned} \tag{2.2}$$

where $v_0(x)$ is the given initial temperature and $f(x,t)$ denotes the external heat source. We further include boundary conditions $u(x,t) \to 0$ for all t as $x \to \pm\infty$.

We observe that the system of ODEs (2.1) can also be viewed as a semi-discretization by the method of lines of the heat equation (2.2) in space-time: if we consider small resistors and capacitors, $R_i \approx \Delta x$ and $C_i \approx \Delta x$, then each equation of the system (2.1) takes the form

$$\frac{dv_i}{dt} = \frac{v_{i-1} - 2v_i + v_{i+1}}{\Delta x^2} + f_i, \tag{2.3}$$

and as $\Delta x \to 0$, we arrive at the heat equation (2.2). Hence we can consider the RC circuit of infinite length as an approximation for the one dimensional heat equation on the unbounded domain $\Omega_x = (-\infty, \infty)$.

The application of WR and OWR methods to the heat equation have been studied by Gander et al [27, 38, 45]. Further different types of WR methods namely Dirichlet-Neumann and Neumann-Neumann methods were studied for the heat equation by Mandal et al in [57].

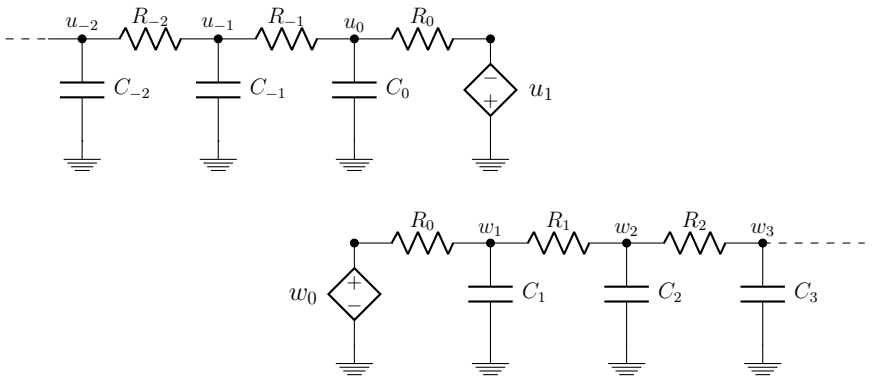

Figure 2.3: Classical nonoverlapping WR algorithm decomposition.

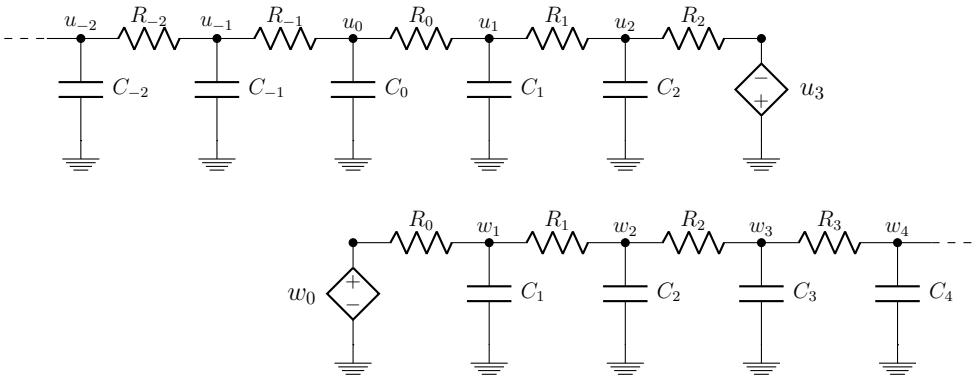

Figure 2.4: Classical WR algorithm with 2 circuit nodes overlap.

2.2 Waveform Relaxation Algorithm

In this section, we will study the application of WR methods to this circuit and analyze its convergence in the Laplace space.

For a general WR algorithm, one decomposes the system (2.1) into many subsystems, but to understand the key features of WR, we consider a decomposition into two subsystems only. We decompose the infinitely long RC circuit from Figure 2.2 at node 0 into two equal sub-circuits. This corresponds to the nonoverlapping WR decomposition. We then consider a overlapping WR decomposition where n nodes of the circuit are overlapped. In this decomposition, we include an overlap of n nodes in the first sub-circuit and keep the other sub-circuit unchanged. Let us denote the first subsystem unknowns by $\mathbf{u}(t)$ and the second subsystem unknowns by $\mathbf{w}(t)$, where $\mathbf{u}(t) := (\dots, u_{-1}, u_0, \dots, u_n)^\top = (\dots, v_{-1}, v_0, \dots, v_n)^\top$ and $\mathbf{w}(t) := (w_1, w_2, \dots)^\top = (v_1, v_2, \dots)^\top$. Figures 2.3 and 2.4 show the decomposition of the infinitely long

RC circuit into nonoverlapping and overlapping circuits. We observe that when we decompose the circuit, we need to add two voltage sources, one for the first sub-circuit $\mathbf{u}$ and the other for the second sub-circuit $\mathbf{w}$. At each iteration k, these voltage sources are given by transmission conditions which transfer information between the sub-circuits. The systems of differential equations for the decomposed overlapping sub-circuits are

$$\begin{aligned}
\tfrac{d}{dt}\mathbf{u}^{k+1}(t) &= \begin{bmatrix} \ddots & \ddots & \ddots & \\ & a_{n-2} & b_{n-1} & c_{n-1} \\ & & a_{n-1} & b_n \end{bmatrix} \begin{bmatrix} \vdots \\ u_{n-1}(t) \\ u_n(t) \end{bmatrix}^{k+1} + \begin{bmatrix} \vdots \\ 0 \\ u_{n+1}(t) \end{bmatrix}^{k+1} + \begin{bmatrix} \vdots \\ f_{n-1}(t) \\ f_n(t) \end{bmatrix}, \\
\tfrac{d}{dt}\mathbf{w}^{k+1}(t) &= \begin{bmatrix} b_1 & c_1 & & \\ a_1 & b_2 & c_2 & \\ & \ddots & \ddots & \ddots \end{bmatrix} \begin{bmatrix} w_1(t) \\ w_2(t) \\ \vdots \end{bmatrix}^{k+1} + \begin{bmatrix} a_0 w_0(t) \\ 0 \\ \vdots \end{bmatrix}^{k+1} + \begin{bmatrix} f_1(t) \\ f_2(t) \\ \vdots \end{bmatrix},
\end{aligned} \tag{2.4}$$

where the unknowns $u_{n+1}^{k+1}(t)$ and $w_0^{k+1}(t)$ are determined by the transmission conditions

$$u_{n+1}^{k+1}(t) = w_{n+1}^{k}(t), \quad \text{and} \quad w_0^{k+1}(t) = u_0^{k}(t). \tag{2.5}$$

Note that at the start of each iteration, these transmission conditions transfer voltages at the interface. Comparing this with Schwarz Waveform Relaxation methods applied to PDEs in [27, 38], these conditions can be interpreted as Dirichlet boundary conditions.

To start the algorithm, we specify an initial guess for the solutions $w_{n+1}^0(t)$ and $u_0^0(t)$, and then solve the subsystems (2.1) for all time $t \in (0, T]$, where T is the final time of simulation. These two subsystems can be solved in parallel, since in the transmission conditions (2.5) both subsystems use data from the previous iteration, like in a block Jacobi method from linear algebra. One could also do the solves sequentially, and use the newest value available in the second transmission condition, $w_0^{k+1}(t) = u_0^{k+1}(t)$, which would be more like a block Gauss Seidel iteration from linear algebra. The convergence analysis for both parallel and sequential methods is similar. Hence we will focus only on the parallel version here and a similar analysis can be done also for the sequential version.

2.2.1 Convergence Analysis of the classical WR Algorithm

The presence of different resistors R_i and capacitors C_i makes the convergence analysis difficult, so to simplify, we assume that all resistors and capacitors have the same value, that is, $R_i := R$ and $C_i := C$ for all $i \in \mathbb{Z}$ which leads to $a_i = a$, $b_i = -2a$ and $c_i = a$ for all $i \in \mathbb{Z}$. We now define the Laplace transformation:

Definition 2.2.1. If $f(t)$ is a real or complex valued function of the non negative

real variable t, then the Laplace transformation is defined by the integral

$$\mathcal{L}(s) = \hat{f}(s) := \int_0^\infty e^{-st} f(t)dt, \qquad s \in \mathbb{C}.$$

The Laplace transformation transforms a system of differential equations into a system of algebraic equations which are relatively easy to analyze. We now study the convergence of the WR algorithm (2.4) in the Laplace space using the transmission conditions (2.5).

Since the systems (2.4) are linear, the error equations correspond to the homogeneous problem, $\mathbf{f} = \mathbf{0}$, with zero initial conditions, $\mathbf{u}^{k+1}(0) = \mathbf{w}^{k+1}(0) = \mathbf{0}$. For $s \in \mathbb{C}$, let $\hat{\mathbf{u}}$ and $\hat{\mathbf{w}}$ denote the Laplace transformation of these two subsystems $\mathbf{u}$ and $\mathbf{w}$ respectively. Note that we do the convergence analysis in the Laplace space. The following lemma will prove that the convergence of WR in the Laplace domain implies convergence in the time domain. For this, we define a weighted L^2 norm: For $\sigma \geq 0$,

$$\|x(t)\|_\sigma := \|e^{-\sigma t} x(t)\|_{L^2}. \tag{2.6}$$

Lemma 2.2.1. *For any $\sigma \geq 0$, where $s = \sigma + i\omega$, with $\sigma, \omega \in \mathbb{R}$, if $\hat{x}(s) = \rho(s)\hat{y}(s)$, then*

$$\|x(t)\|_\sigma \leq \left(\sup_{\omega \in \mathbb{R}} |\rho(s)| \right) \|y(t)\|_\sigma.$$

Proof. Let $v(t) := e^{-\sigma t}x(t)$ and $p(t) := e^{-\sigma t}y(t)$. Then using the definition of the weighted norm defined in (2.6), we have

$$\begin{aligned} \|x(t)\|_\sigma^2 &= \|e^{-\sigma t}x(t)\|_{L^2}^2 = \|v(t)\|_{L^2}^2, \quad \text{and,} \\ \|y(t)\|_\sigma^2 &= \|e^{-\sigma t}y(t)\|_{L^2}^2 = \|p(t)\|_{L^2}^2. \end{aligned} \tag{2.7}$$

To avoid the ambiguity of symbols, we denote the Fourier transformation of the function $x(t)$ by $\hat{\hat{x}}(\omega)$, where the frequency $\omega \in \mathbb{R}$. The Parseval identity states that

$$\int_0^\infty |v(t)|^2 \, dt = \int_{-\infty}^\infty \left| \hat{\hat{v}}(\omega) \right|^2 d\omega,$$

where we have restricted the range of t to $[0, \infty)$. The definition of the Fourier transformation and some basic calculus leads to

$$\begin{aligned} \int_0^\infty |v(t)|^2 \, dt &= \int_{-\infty}^\infty \left| \int_0^\infty e^{-i\omega t} v(t) dt \right|^2 d\omega = \int_{-\infty}^\infty \left| \int_0^\infty e^{-i\omega t} e^{-\sigma t} x(t) dt \right|^2 d\omega \\ &= \int_{-\infty}^\infty \left| \int_0^\infty e^{-st} x(t) dt \right|^2 d\omega, \end{aligned}$$

and thus we arrive at

$$\|v(t)\|_{L^2}^2 = \int_{-\infty}^\infty |\hat{x}(s)|^2 \, d\omega. \tag{2.8}$$

Doing the same calculations one can also arrive at

$$\|p(t)\|_{L^2}^2 = \int_{-\infty}^{\infty} |\hat{y}(s)|^2 \, d\omega.$$

Substituting $\hat{x}(s) = \rho(s)\hat{y}(s)$ into (2.8), and since $\sigma \geq 0$ is fixed,

$$\begin{aligned} \|v(t)\|_{L^2}^2 &= \int_{-\infty}^{\infty} |\rho(s)\hat{y}(s)|^2 \, d\omega \\ &\leq \left(\sup_{\omega\in\mathbb{R}} |\rho(s)|\right)^2 \int_{-\infty}^{\infty} |\hat{y}(s)|^2 \, d\omega \\ &= \left(\sup_{\omega\in\mathbb{R}} |\rho(s)|\right)^2 \|p(t)\|_{L^2}^2. \end{aligned}$$

Finally, using the relation (2.7), the above equation leads to the required relation,

$$\|x(t)\|_\sigma \leq \left(\sup_{\omega\in\mathbb{R}} |\rho(s)|\right) \|y(t)\|_\sigma.$$

□

Remark 2.2.1. We infer from Lemma 2.2.1 that the convergence in the Laplace space with the convergence factor $|\rho(s)| < 1$ implies convergence in the time domain in the weighted norm $\|\cdot\|_\sigma$, and for $\sigma = 0$, we obtain convergence in L^2.

We now find a closed form for the convergence factor, which we denote by $\rho_{n,cla}$. The Laplace transformation for $s \in \mathbb{C}$ of the WR algorithm (2.4) is given by

$$\begin{aligned} s\hat{\mathbf{u}}^{k+1} &= \begin{bmatrix} \ddots & \ddots & \ddots & \\ & a & b & a \\ & & a & b \end{bmatrix} \begin{bmatrix} \vdots \\ \hat{u}_{n-1} \\ \hat{u}_n \end{bmatrix}^{k+1} + \begin{bmatrix} \vdots \\ 0 \\ a\hat{w}_{n+1}^k \end{bmatrix}, \\ s\hat{\mathbf{w}}^{k+1} &= \begin{bmatrix} b & a & & \\ a & b & a & \\ & \ddots & \ddots & \ddots \end{bmatrix} \begin{bmatrix} \hat{w}_1 \\ \hat{w}_2 \\ \vdots \end{bmatrix}^{k+1} + \begin{bmatrix} a\hat{u}_0^k \\ 0 \\ \vdots \end{bmatrix}, \end{aligned} \tag{2.9}$$

where we have already included the transmission conditions (2.5); this shows the dependence of $\hat{\mathbf{u}}$ on $\hat{\mathbf{w}}$ and vice-versa. In order to find the convergence factor of the WR algorithm, we need the following lemma.

Lemma 2.2.2. *Let $a > 0$, $b < 0$, $i := \sqrt{-1}$, and $s := \sigma + i\omega$, with $\sigma \geq 0$. For $-b \geq 2a$, the roots $\lambda_{1,2}(s) := \frac{s-b\pm\sqrt{(b-s)^2-4a^2}}{2a}$ of the characteristic equation $ay_{j-1} + (b-s)y_j + ay_{j+1} = 0$ of the subsystems in (2.9) satisfy $|\lambda_2(s)| \leq 1 \leq |\lambda_1(s)|$.*

Proof. Solving the subsystems (2.9) requires solving a recurrence relation of the form $ay_{j-1} + (b-s)y_j + ay_{j+1} = 0$, where $y_j = \hat{u}_j^{k+1}(s)$, $\hat{w}_j^{k+1}(s)$ for $j \in \mathbb{Z}$. This equation has the characteristics equation $a\lambda^2 + (b-s)\lambda + a = 0$, where λ is a parameter. We denote the roots of this equation by $\lambda_1(s)$ and $\lambda_2(s)$,

$$\lambda_{1,2}(s) := \frac{s - b \pm \sqrt{(b-s)^2 - 4a^2}}{2a}. \tag{2.10}$$

Now, since $a > 0$, $b < 0$ and $-b \geq 2a$, we can write $b = -(2+\epsilon)a$ for some $\epsilon \geq 0$. Let $p + iq := \sqrt{(b-s)^2 - 4a^2}$, where p, $q \in \mathbb{R}$, with $p > 0$. We then obtain with $\sigma \geq 0$

$$\begin{aligned} |\lambda_1(s)| &= \left| \frac{s - b + \sqrt{(b-s)^2 - 4a^2}}{2a} \right| = \left| \frac{\sigma + i\omega + (2+\epsilon)a}{2a} + \frac{p + iq}{2a} \right| \\ &= \left| 1 + \frac{\epsilon a + \sigma + p}{2a} + \frac{i(\omega + q)}{2a} \right| \geq 1. \end{aligned}$$

Now by Vieta's formulas, the product $\lambda_1(s)\lambda_2(s) = 1$, which implies $|\lambda_2(s)| \leq 1$ and this completes the proof. □

From now onward, we shall use simplified notations $\lambda_1 := \lambda_1(s)$, $\lambda_2 := \lambda_2(s)$, $\hat{u}_j^{k+1} := \hat{u}_j^{k+1}(s)$ and $\hat{w}_j^{k+1} := \hat{w}_j^{k+1}(s)$, and show their dependence on s only when necessary.

Remark 2.2.2. Under the conditions $\omega > 0$ or $\epsilon > 0$, where $s = \sigma + i\omega$, $\sigma \geq 0$ and $b = -(2+\epsilon)a$, the roots λ_1 and λ_2 defined in (2.10) satisfy $|\lambda_2| < 1 < |\lambda_1|$.

Theorem 2.2.1. *The convergence factor $\rho_{n,cla}(s)$ of the classical WR algorithm (2.9) with n nodes overlap for an RC circuit of infinite length is given by*

$$\rho_{n,cla}(s) = \left(\frac{1}{\lambda_1^2} \right)^{n+1}. \tag{2.11}$$

Proof. The iterates $\hat{\mathbf{u}}^{k+1}$ and $\hat{\mathbf{w}}^{k+1}$ for the subsystems in (2.9) satisfy the recurrence relation

$$a\hat{u}_{j-1}^{k+1} + (b-s)\hat{u}_j^{k+1} + a\hat{u}_{j+1}^{k+1} = 0 \qquad \text{for} \qquad j = \ldots, n-2, n-1, n, \tag{2.12}$$

$$a\hat{w}_{j-1}^{k+1} + (b-s)\hat{w}_j^{k+1} + a\hat{w}_{j+1}^{k+1} = 0 \qquad \text{for} \qquad j = \mathbb{N}, \tag{2.13}$$

whose solutions are $\hat{u}_j^{k+1} = A^{k+1}\lambda_1^j + B^{k+1}\lambda_2^j$ for $j = \ldots, n-2, n-1, n$ and $\hat{w}_j^{k+1} = C^{k+1}\lambda_1^j + D^{k+1}\lambda_2^j$ for $j \in \mathbb{N}$. Observe that $|\lambda_2| < 1 < |\lambda_1|$ and thus $\lambda_2^j \to \infty$ as $j \to -\infty$ and $\lambda_1^j \to \infty$ as $j \to \infty$. The solutions must remain bounded for all j, which implies $B^{k+1} = 0$ and $C^{k+1} = 0$, and hence we obtain $\hat{u}_j^{k+1} = A^{k+1}\lambda_1^j$ and $\hat{w}_j^{k+1} = D^{k+1}\lambda_2^j$. Substituting $j = n$ into (2.12), we get

$$a\hat{u}_{n-1}^{k+1} + (b-s)\hat{u}_n^{k+1} = -a\hat{w}_{n+1}^k \implies A^{k+1}\lambda_1^{n-1} + \left(\frac{b-s}{a} \right) A^{k+1}\lambda_1^n = -D^k\lambda_2^{n+1}.$$

From the definition of $\lambda_{1,2}$ given in (2.10), we have $\lambda_1 + \lambda_2 = -\left(\frac{b-s}{a}\right)$ and $\lambda_1\lambda_2 = 1$, and these relations reduce the above equation to

$$A^{k+1}\left(\lambda_1^{n-1} - \lambda_1^{n+1} - \lambda_1^{n-1}\right) = -D^k\lambda_2^{n+1},$$

and thus

$$A^{k+1} = D^k\left(\frac{\lambda_2^{n+1}}{\lambda_1^{n+1}}\right) = D^k\left(\frac{1}{\lambda_1^{n+1}}\right)^2. \tag{2.14}$$

Similarly, substituting $j = 1$ in (2.13) leads to

$$\begin{aligned} a\hat{u}_0^k + (b-s)\hat{w}_1^{k+1} + a\hat{w}_2^k = 0 \quad &\Longrightarrow \quad A^k + \left(\frac{b-s}{a}\right)D^{k+1}\lambda_2 + D^{k+1}\lambda_2^2 = 0 \\ &\Longrightarrow \quad A^k + D^{k+1}\lambda_2(-\lambda_1 - \lambda_2 + \lambda_2) = 0 \\ &\Longrightarrow \quad D^{k+1} = A^k. \end{aligned} \tag{2.15}$$

Combining (2.14) and (2.15) gives us $A^{k+1} = \rho_{n,cla}(s)A^{k-1}$ and $D^{k+1} = \rho_{n,cla}(s)D^{k-1}$, where $\rho_{n,cla}(s)$ is given in (2.11). Since the solutions are given by $\hat{u}_j^{k+1} = A^{k+1}\lambda_1^j$ and $\hat{w}_j^{k+1} = D^{k+1}\lambda_2^j$, we conclude $\hat{u}_j^{k+1} = \rho_{n,cla}(s)\hat{u}_j^{k-1}$ and $\hat{w}_j^{k+1} = \rho_{n,cla}(s)\hat{w}_j^{k-1}$. This completes the proof. □

We observe that the convergence factor $\rho_{n,cla}(s)$ is the same for all nodes in both subsystems. Remark 2.2.2 states that $|\lambda_1| > 1$, when the frequency $\omega > 0$ or $\epsilon > 0$, and hence the convergence factor $|\rho_{n,cla}| < 1$ under either of these two conditions. The condition $\omega > 0$ with $\omega \to 0$ corresponds to considering a large time interval $(0, T]$ with $T \to \infty$ and under this condition $|\rho_{n,cla}| \to 1$. The second condition $\epsilon > 0$, where $b = -(2+\epsilon)a$ corresponds to adding reaction term of the type $-\epsilon\hat{\mathbf{u}}$ and $-\epsilon\hat{\mathbf{w}}$ in the first and second subsystems of (2.9). This corresponds to simulating circuit for infinite time and considering the reaction terms $\epsilon\hat{\mathbf{u}}$ and $\epsilon\hat{\mathbf{w}}$ going to zero. In the left plot of Figure 2.5, we observe that $|\rho_{0,cla}| \to 1$ when $\omega = 0$ and $\epsilon \to 0$. For circuits, the introduction of ϵ leads to the addition of a resistor $\tilde{R} = R/\epsilon$ at each node of the circuit (see Figure 2.6). We also add that the limit $\epsilon \to 0$ leads to the limit $\tilde{R} \to \infty$, which means that no current passes through this resistor. Thus considering $b = -(2+\epsilon)a$ and taking the limit $\epsilon \to 0$ states that the circuit in Figure 2.6 is a good approximation to the circuit in Figure 2.4. Note that the addition of large resistors $\tilde{R}$ corresponds to small leakage of current in the dielectric medium. This is typical condition observed in the real world. Theorem 2.2.1 also reveals the effect of overlap on the convergence factor $\rho_{n,cla}$. Increasing the overlap decreases the convergence factor $\rho_{n,cla}$ and hence increases the convergence rate of the WR method. Numerically, we show this effect in the right plot of Figure 2.5, where we also observe that the effect is very small for ω close to zero when $s = i\omega$.

Further, large time corresponds to small frequency ω in $s = \sigma + i\omega$ in the Laplace space. From Theorem 2.2.1, we observe that as $\omega \to 0$, $|\lambda_1| \to 1$, and hence $|\rho_{n,cla}| \to$

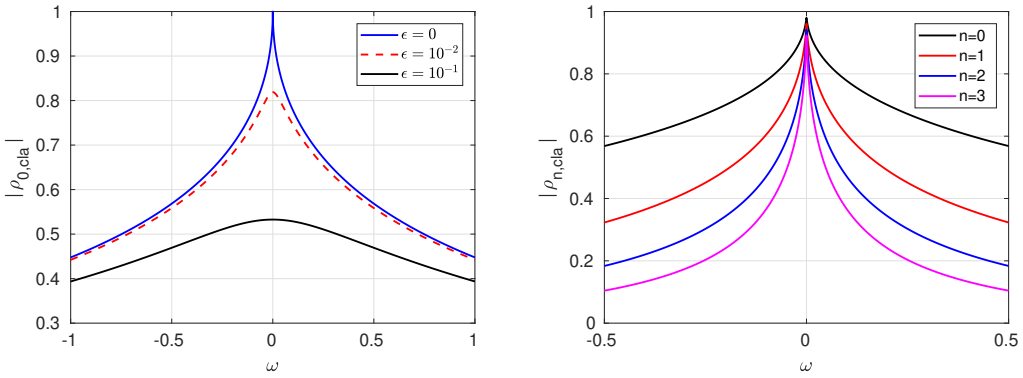

Figure 2.5: Convergence factor for $s = i\omega$ for different values of ϵ (left) and for different overlaps with $\epsilon = 10^{-4}$ (right).

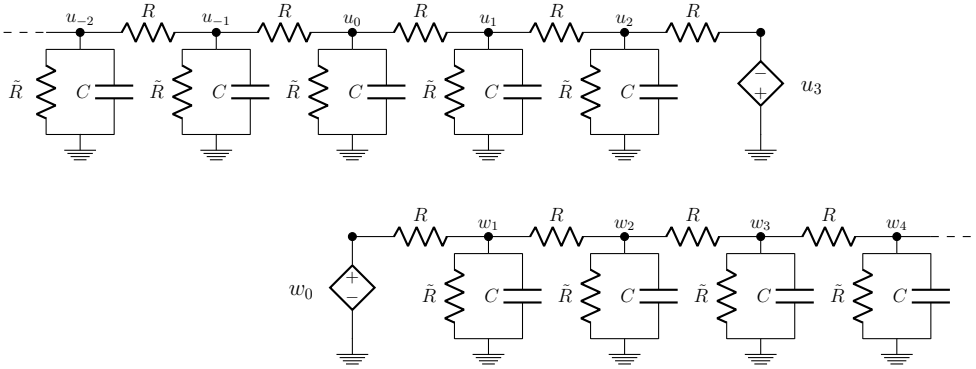

Figure 2.6: WR algorithm with $b = -(2+\epsilon)a$ and $\tilde{R} = R/\epsilon$.

1. This slow convergence especially for large time windows is the main drawback of the classical WR methods. Moreover, when $\epsilon \to 0$ with $b = -(2+\epsilon)a$, we observe that $|\rho_{n,cla}(0)| \to 1$, which means as $\epsilon \to 0$, the convergence rate slows down for small ω, and increasing the overlap does mostly improve the convergence of higher frequencies ω, as one can see in Figure 2.5 on the right. The Dirichlet transmission conditions (2.5) which exchange just voltages at the interfaces are the main reason for this slow convergence. We thus search for better transmission conditions to exchange information between the sub-circuits. This leads to the OWR algorithm, which we shall discuss in the next section.

2.3 Optimized Waveform Relaxation Algorithm

Optimized transmission conditions were first introduced and analyzed in 1999 by Gander et al [29] for Schwarz Waveform Relaxation (SWR) methods. In this paper, optimal transmission conditions were derived, which were approximated by zeroth

and second order approximations. The zeroth order approximations can be viewed as Robin boundary conditions, and these new transmission conditions lead to tremendous increase in the convergence rate. This idea was further applied for the nonoverlapping decomposition of infinitely long RC circuit in [3, 37], and for small RC circuit in [2]. Inspired by these articles, we define similar transmission conditions for the overlapping case with n nodes overlap

$$\begin{aligned}(u_{n+1}^{k+1} - u_n^{k+1}) + \alpha u_{n+1}^{k+1} &= (w_{n+1}^k - w_n^k) + \alpha w_{n+1}^k,\\ (w_1^{k+1} - w_0^{k+1}) + \beta w_0^{k+1} &= (u_1^k - u_0^k) + \beta u_0^k,\end{aligned} \tag{2.16}$$

where $\alpha, \beta \in \mathbb{R}$ and k is the iteration index. Note that the voltages u_i and w_i depend on time t. These transmission conditions exchange both voltages and currents at the interface, which can be seen by dividing the first equation by α and the second by β. Considering α as a resistor, the term $\frac{u_{n+1}^{k+1} - u_n^{k+1}}{\alpha}$ can be viewed as a current and u_{n+1}^{k+1} as a voltage. These transmission conditions are called optimized transmission conditions since we need to find the best (optimized) values for α and β such that the convergence factor is as small as possible. We now rearrange the optimized transmission conditions (2.16) as

$$\begin{aligned}u_{n+1}^{k+1} &= \tfrac{u_n^{k+1}}{1+\alpha} + w_{n+1}^k - \tfrac{w_n^k}{1+\alpha},\\ w_0^{k+1} &= -\tfrac{w_1^{k+1}}{\beta-1} + u_0^k + \tfrac{u_1^k}{\beta-1}.\end{aligned} \tag{2.17}$$

Substituting these rearranged transmission conditions into (2.4) leads to

$$\begin{aligned}\tfrac{d}{dt}\mathbf{u}^{k+1}(t) &= \begin{bmatrix} \ddots & \ddots & \ddots & \\ & a & b & a \\ & & a & b+\frac{a}{\alpha+1} \end{bmatrix} \begin{bmatrix} \vdots \\ u_{n-1}(t) \\ u_n(t) \end{bmatrix}^{k+1} + \begin{bmatrix} \vdots \\ 0 \\ aw_{n+1}^k(t) - \frac{a}{\alpha+1} w_n^k(t) \end{bmatrix} + \begin{bmatrix} \vdots \\ f_{n-1}(t) \\ f_n(t) \end{bmatrix}\\ \tfrac{d}{dt}\mathbf{w}^{k+1}(t) &= \begin{bmatrix} b-\frac{a}{\beta-1} & a & & \\ a & b & a & \\ & \ddots & \ddots & \ddots \end{bmatrix} \begin{bmatrix} w_1(t) \\ w_2(t) \\ \vdots \end{bmatrix}^{k+1} + \begin{bmatrix} au_0^k + \frac{a}{\beta-1} u_1^k \\ 0 \\ \vdots \end{bmatrix} + \begin{bmatrix} f_1(t) \\ 0 \\ \vdots \end{bmatrix}.\end{aligned} \tag{2.18}$$

Initial conditions $\mathbf{u}(0) = \mathbf{u}_0$ and $\mathbf{w}(0) = \mathbf{w}_0$ are again supplied to solve these systems of differential equations.

For circuits, the introduction of the new transmission conditions (2.16) means two voltage sources need to be added at the interface of each sub-circuit. From Figure 2.7, we see that the resistors $R_\alpha := R(1+\alpha)$ and $R_\beta := R(1-\beta)$, which depend on the parameters α and β, are added. Similar to the WR algorithm, at each iteration the voltage sources w_{n+1}, w_n, u_0, u_1 are transferred between the sub-circuits.

We can also interpret these new transmission conditions (2.16) as Robin transmission conditions for the discretized heat equation (2.3) if we divide the first equation of

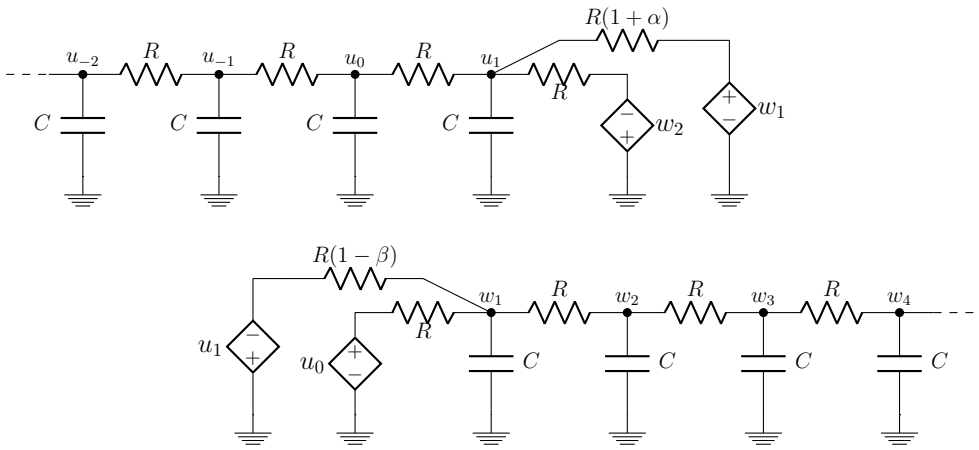

Figure 2.7: OWR algorithm with 1 circuit node overlap.

(2.16) by $\bar{\alpha} := \frac{\alpha}{p}$ for some $p > 0$ and the second equation by $\bar{\beta} := \frac{-\beta}{p}$, to obtain

$$\begin{aligned} \frac{u_{n+1}^{k+1} - u_n^{k+1}}{\bar{\alpha}} + p u_{n+1}^{k+1} &= \frac{w_{n+1}^k - w_n^k}{\bar{\alpha}} + p w_{n+1}^k, \\ \frac{w_1^{k+1} - w_0^{k+1}}{\bar{\beta}} - p w_0^{k+1} &= \frac{u_1^k - u_0^k}{\bar{\beta}} - p u_0^k. \end{aligned}$$

If we now consider $\bar{\alpha} \approx \Delta x$ and $\bar{\beta} \approx \Delta x$, then the fractions inside the above equations represent discretizations for the derivatives $\frac{\partial u}{\partial x}$ and $\frac{\partial w}{\partial x}$, and we thus obtain in the limit Robin transmission conditions,

$$\begin{aligned} \left(\frac{\partial}{\partial x} + p\right) u_{n+1}^{k+1} &= \left(\frac{\partial}{\partial x} + p\right) w_{n+1}^k, \\ \left(\frac{\partial}{\partial x} - p\right) w_0^{k+1} &= \left(\frac{\partial}{\partial x} - p\right) u_0^k. \end{aligned}$$

2.3.1 Convergence Analysis of OWR

In this subsection, we derive an expression for the convergence factor ρ_n of the OWR method defined above. Again, for the derivation and analysis of ρ_n, we consider the error equations, and hence $\mathbf{f} = \mathbf{0}$, $\mathbf{u}_0 = \mathbf{0}$, and $\mathbf{w}_0 = \mathbf{0}$. We transform the systems of equations (2.18) into the Laplace space using the Laplace transformation defined in

2.2.1 to arrive at

$$
\begin{aligned}
s\hat{\mathbf{u}}^{k+1} &= \begin{bmatrix} \ddots & \ddots & \ddots & \\ & a & b & a \\ & & a & b+\frac{a}{\alpha+1} \end{bmatrix} \begin{bmatrix} \vdots \\ \hat{u}_{n-1} \\ \hat{u}_n \end{bmatrix}^{k+1} + \begin{bmatrix} \vdots \\ 0 \\ a\hat{w}_{n+1}^k - \frac{a}{\alpha+1}\hat{w}_n^k \end{bmatrix}, \\
s\hat{\mathbf{w}}^{k+1} &= \begin{bmatrix} b-\frac{a}{\beta-1} & a & & \\ a & b & a & \\ & \ddots & \ddots & \ddots \end{bmatrix} \begin{bmatrix} \hat{w}_1 \\ \hat{w}_2 \\ \vdots \end{bmatrix}^{k+1} + \begin{bmatrix} a\hat{u}_0^k + \frac{a}{\beta-1}\hat{u}_1^k \\ 0 \\ \vdots \end{bmatrix}.
\end{aligned} \tag{2.19}
$$

The above systems of equations clearly show their dependence on each other. Further, we need to give initial guesses $\hat{w}_{n+1}^0$, $\hat{w}_n^0$, $\hat{u}_0^0$ and $\hat{u}_1^0$ to start this algorithm.

Theorem 2.3.1. *The convergence factor $\rho_n(s,\alpha,\beta)$ of the OWR algorithm (2.19) for an RC circuit of infinite length is given by*

$$
\rho_n(s,\alpha,\beta) := \left(\frac{\alpha+1-\lambda_1}{\lambda_1(1+\alpha)-1}\right)\left(\frac{\lambda_1+\beta-1}{1+(\beta-1)\lambda_1}\right)\left(\frac{1}{\lambda_1^2}\right)^n. \tag{2.20}
$$

Proof. To find the convergence factor, we proceed as in the proof of Theorem 2.2.1 to arrive at $\hat{u}_j^{k+1} = A^{k+1}\lambda_1^j$ for $j = \ldots, n-1, n$, and $\hat{w}_j^{k+1} = D^{k+1}\lambda_2^j$ for $j \in \mathbb{N}$. To determine the constants A^{k+1} and D^{k+1}, we use the optimized transmission conditions (2.17) and equations (2.12)-(2.13). Substituting $j = n$ in (2.12) and then using the rearranged transmission conditions (2.17) gives

$$
\begin{aligned}
& a\hat{u}_{n-1}^{k+1} + (b-s)\hat{u}_n^{k+1} = -a\hat{u}_{n+1}^{k+1} = -\frac{a\hat{u}_n^{k+1}}{1+\alpha} - a\hat{w}_{n+1}^k + \frac{a\hat{w}_n^k}{1+\alpha} \\
\implies & \hat{u}_{n-1}^{k+1} + \left(\frac{b-s}{a} + \frac{1}{1+\alpha}\right)\hat{u}_n^{k+1} = -\hat{w}_{n+1}^k + \frac{\hat{w}_n^k}{1+\alpha}.
\end{aligned}
$$

Using the properties of λ_1 and λ_2 defined in (2.10), namely $\lambda_1 + \lambda_2 = -\frac{b-s}{a}$ and $\lambda_1\lambda_2 = 1$, we have

$$
\begin{aligned}
& A^{k+1}\lambda_1^{n-1} + \left(-\lambda_1 - \lambda_2 + \frac{1}{1+\alpha}\right)A^{k+1}\lambda_1^n = -D^k\lambda_2^{n+1} + \frac{D^k\lambda_2^n}{1+\alpha} \\
\implies & A^{k+1}\lambda_1^n\left(\frac{1}{\lambda_1} - \lambda_1 - \lambda_2 + \frac{1}{1+\alpha}\right) = D^k\lambda_2^n\left(\frac{1}{1+\alpha} - \lambda_2\right) \\
\implies & A^{k+1}\lambda_1^n\left(\frac{1-\lambda_1(1+\alpha)}{1+\alpha}\right) = D^k\lambda_2^n\left(\frac{1-\lambda_2(1+\alpha)}{1+\alpha}\right) \\
\implies & A^{k+1} = D^k\left(\frac{\lambda_2(1+\alpha)-1}{\lambda_1(1+\alpha)-1}\right)\left(\frac{\lambda_2}{\lambda_1}\right)^n.
\end{aligned} \tag{2.21}
$$

Similarly substituting $j = 1$ in (2.13) results in

$$
\begin{aligned}
& (b-s)\hat{w}_1^{k+1} + a\hat{w}_2^{k+1} = -a\hat{w}_0^{k+1} = \frac{a\hat{w}_1^{k+1}}{\beta-1} - a\hat{u}_0^k - \frac{a\hat{u}_1^k}{\beta-1} \\
\Longrightarrow \quad & \left(\frac{b-s}{a} - \frac{1}{\beta-1}\right)\hat{w}_1^{k+1} + \hat{w}_2^{k+1} = -\hat{u}_0^k - \frac{\hat{u}_1^k}{\beta-1} \\
\Longrightarrow \quad & \left(-\lambda_1 - \lambda_2 - \frac{1}{\beta-1}\right) D^{k+1}\lambda_2 + D^{k+1}\lambda_2^2 = -A^k - \frac{A^k\lambda_1}{\beta-1} \\
\Longrightarrow \quad & D^{k+1}\lambda_2\left(-\lambda_1 - \lambda_2 - \frac{1}{\beta-1} + \lambda_2\right) = -A^k\left(1 + \frac{\lambda_1}{\beta-1}\right) \\
\Longrightarrow \quad & -D^{k+1}\left(\frac{\beta-1+\lambda_2}{\beta-1}\right) = -A^k\left(\frac{\beta-1+\lambda_1}{\beta-1}\right) \\
\Longrightarrow \quad & D^{k+1} = A^k\left(\frac{\beta-1+\lambda_1}{\beta-1+\lambda_2}\right). \qquad (2.22)
\end{aligned}
$$

Using $\lambda_1\lambda_2 = 1$ and equations (2.21)-(2.22), we arrive for $j = \ldots, -2, -1, 0, \ldots, n$ at

$$
\begin{aligned}
\hat{u}_j^{k+1} &= A^{k+1}\lambda_1^j \\
&= \left(\frac{\lambda_2(1+\alpha)-1}{\lambda_1(1+\alpha)-1}\right)\left(\frac{\lambda_1+\beta-1}{\lambda_2+\beta-1}\right)\left(\frac{\lambda_2}{\lambda_1}\right)^n A^{k-1}\lambda_1^j \\
&= \left(\frac{\alpha+1-\lambda_1}{\lambda_1(1+\alpha)-1}\right)\left(\frac{\lambda_1+\beta-1}{1+(\beta-1)\lambda_1}\right)\left(\frac{1}{\lambda_1^2}\right)^n \hat{u}_j^{k-1} \\
&=: \rho_n(s,\alpha,\beta)\hat{u}_j^{k-1},
\end{aligned}
$$

where the convergence factor $\rho_n(s,\alpha,\beta)$ is given by (2.20). Similarly, we can also show that $\hat{w}_j^{k+1} = \rho_n(s,\alpha,\beta)\hat{w}_j^{k-1}$, for $j \in \mathbb{N}$, and this completes the proof. □

In Section 2.2, we proved that the convergence factor of the classical WR method is less than 1, that is, $|\rho_{n,cla}| < 1$ under two conditions: first, when the frequency $\omega > 0$ and second, when $\epsilon > 0$, where $b = -(2+\epsilon)a$. We shall find similar conditions for the convergence factor $\rho_n(s,\alpha,\beta)$.

Lemma 2.3.1. *For $\alpha > 0$, $\beta < 0$, and either $\omega > 0$ or $\epsilon > 0$, where $b = -(2+\epsilon)a$, the modulus of the convergence factor $\rho_n(s,\alpha,\beta)$ of the OWR algorithm is less than 1, that is, $|\rho_n(s,\alpha,\beta)| < 1$ for all $n \geq 0$.*

Proof. Since $\lambda_1 \in \mathbb{C}$, we assume $\lambda_1 = x + iy$, where x,$y \in \mathbb{R}$. Remark 2.2.2 states that under the condition, either $\omega > 0$ or $\epsilon > 0$, where $b = -(2+\epsilon)a$, we have $|\lambda_1| > 1$

and hence $x^2+y^2>1$. Further for $\alpha>0$, $(\alpha+1)^2-1>0$ and hence,

$$\begin{aligned}
&(\alpha+1)^2-1<[(\alpha+1)^2-1](x^2+y^2)\\
\iff\quad &(\alpha+1)^2+x^2+y^2<(\alpha+1)^2x^2+(\alpha+1)^2y^2+1\\
\iff\quad &(\alpha+1)^2+x^2+y^2-2x(\alpha+1)<(\alpha+1)^2x^2+(\alpha+1)^2y^2+1-2x(\alpha+1)\\
\iff\quad &(\alpha+1-x)^2+y^2<((\alpha+1)x-1)^2+(\alpha+1)^2y^2\\
\iff\quad &|\alpha+1-x-iy|^2<|(\alpha+1)(x+iy)-1|^2.
\end{aligned}$$

Taking the square root on both sides leads to $|\alpha+1-\lambda_1|<|(\alpha+1)\lambda_1-1|$. Similarly, for $\beta<0$, we can show $|\lambda_1+\beta-1|<|1+(\beta-1)\lambda_1|$ and this completes the proof. □

We observe from (2.11) and (2.20) that the effect of overlap on the convergence factor which is given by $\left(\frac{1}{\lambda_1^2}\right)^n$ is the same for both the WR and the OWR algorithm. This means increasing the overlap increases the rate of convergence also for OWR. Further, the convergence factor is the same for all the circuit nodes irrespective of which sub-circuit they belong to. Finally, for fast convergence, we would like to have the convergence factor $|\rho_n(s,\alpha,\beta)|$ as small as possible.

Lemma 2.3.2. *If $\alpha\to\infty$ and $\beta\to-\infty$, then the convergence factor (2.20) of the OWR method is equal to the convergence factor (2.11) of the classical WR method, that is, $\rho_n(s,\infty,-\infty)=\rho_{n,cla}(s)$.*

Proof. This is a straightforward result and can be proved by taking the limits $\alpha\to\infty$ and $\beta\to-\infty$ of the expression (2.20):

$$\begin{aligned}
\rho_n(s,\infty,-\infty) &= \lim_{\alpha\to\infty}\lim_{\beta\to-\infty}\rho_n(s,\alpha,\beta)\\
&= \lim_{\alpha\to\infty}\lim_{\beta\to-\infty}\left(\frac{\alpha+1-\lambda_1}{\lambda_1(1+\alpha)-1}\right)\left(\frac{\lambda_1+\beta-1}{1+(\beta-1)\lambda_1}\right)\left(\frac{1}{\lambda_1^2}\right)^n\\
&= \lim_{\alpha\to\infty}\lim_{\beta\to-\infty}\left(\frac{1+\frac{1-\lambda_1}{\alpha}}{\lambda_1+\frac{\lambda_1-1}{\alpha}}\right)\left(\frac{\frac{\lambda_1-1}{\beta}+1}{\lambda_1+\frac{1-\lambda_1}{\beta}}\right)\left(\frac{1}{\lambda_1^2}\right)^n\\
&= \left(\frac{1}{\lambda_1^2}\right)\left(\frac{1}{\lambda_1^2}\right)^n=\left(\frac{1}{\lambda_1^2}\right)^{n+1}\\
&= \rho_{n,cla}(s).
\end{aligned}$$

□

Remark 2.3.1. For the circuit interpretation of Lemma 2.3.2, we refer to the circuit shown in Figure 2.7. For $\alpha\to\infty$ and $\beta\to-\infty$, the resistances $R(1+\alpha)\to\infty$ and $R(1-\beta)\to\infty$, which means that no current flows through these resistors. We can remove these resistors and attached voltage sources w_1 and u_1. These sub-circuits then reduce to the WR sub-circuits with one node overlap similar to the one shown in Figure 2.4.

The parameters a, b represent circuit elements and cannot be changed, but we can choose α and β such that $|\rho_n(s,\alpha,\beta)|$ becomes as small as possible. So what is the best possible choice for the parameters α and β?

Theorem 2.3.2. *The OWR method for the two subdomain case converges in two iterations, independently of the initial guess and the overlap, if*

$$\alpha_{opt} := \lambda_1 - 1, \qquad \textit{and} \qquad \beta_{opt} := 1 - \lambda_1. \tag{2.23}$$

Proof. Setting the convergence factor $\rho_n(s,\alpha,\beta) = 0$, we find $\alpha = \lambda_1 - 1$ and $\beta = 1 - \lambda_1$. Since, $\hat{u}_j^{k+1} = \rho_n(s,\alpha,\beta)\hat{u}_j^{k-1}$ and $\hat{w}_j^{k+1} = \rho_n(s,\alpha,\beta)\hat{w}_j^{k-1}$, we have $\hat{u}_j^2$ and $\hat{w}_j^2$ identically zero and hence the OWR has converged in two iterations. □

One can see that this is the best choice, since the solution in each subsystem depends on all the source terms f_j and during the first iteration, each subsystem uses only the local f_j to compute the approximation. It is only for the second iteration that information is transferred. Therefore, convergence cannot be achieved in less than 2 iterations.

Since λ_1 is a complicated function of $s \in \mathbb{C}$, its inverse Laplace transformation leads to non-local operators in time for α_{opt} and β_{opt}. These non-local operators are expensive to use since they require convolution operations. It is therefore of interest to approximate α_{opt} and β_{opt} by a polynomial in s. In this thesis, we will focus on approximation of α_{opt} and β_{opt} by a constant.

2.4 Optimization

In this section, we shall find asymptotic expressions for the optimized α and β. We shall consider asymptotic analysis in two different cases: first, when $\omega \to 0$ with $\epsilon = 0$, and second, when $\epsilon \to 0$ with fixed minimum frequency $\omega = 0$. Recall that the first case corresponds to simulation on large time intervals $(0, T]$ with final time $T \to \infty$, while the second case corresponds to the simulation on infinitely large time intervals and letting the reaction terms $\epsilon a\hat{\mathbf{u}}$, $\epsilon a\hat{\mathbf{w}} \to 0$. Before considering these two cases, we first build and simplify the optimization problem.

In order to have rapid convergence of the OWR method discussed in Section 2.3, we want $|\rho_n(s,\alpha,\beta)| \ll 1$, which leads to solving the min-max problem

$$\min_{\alpha,\beta} \left(\max_{\Re(s)\geq 0} |\rho_n(s,\alpha,\beta)| \right), \tag{2.24}$$

where $\Re(s)$ denotes the real part of s. Since $s \in \mathbb{C}$ with $s = \sigma + i\omega$ and $\sigma \geq 0$, the above optimization problem is in four variables and hence already very difficult to solve. We simplify the problem using some assumptions and the following lemmas.

Lemma 2.4.1. *For $\alpha > 0$, $\beta < 0$, the maximum of $|\rho_n(s, \alpha, \beta)|$ lies on the imaginary axis of the complex plane.*

Proof. The idea is to show that the convergence factor $\rho_n(s, \alpha, \beta)$ is analytic in the right half of the complex plane and then use the maximum modulus principle for analytic functions [68].

We first show by contradiction that the denominator of $\rho_n(s, \alpha, \beta)$ does not have any zeros in the right half of the complex plane. Assume there is a zero. Then $\lambda_1 = 0$, or $(1 + \alpha)\lambda_1 - 1 = 0$, or $1 + (\beta - 1)\lambda_1 = 0$. The first case is not possible since from Lemma 2.2.2, we have $|\lambda_1| \geq 1$. Considering the second case we have $\lambda_1 = \frac{1}{1+\alpha}$. Since $\alpha > 0$, $|\lambda_1| = \left|\frac{1}{1+\alpha}\right| < 1$ which is again a contradiction. Similarly, the third case can not hold since $\beta < 0$. Thus $\rho_n(s, \alpha, \beta)$ is analytic in the right half of the complex plane, that is, for $s = \sigma + i\omega$, with $\sigma \geq 0$, and hence by the maximum modulus principle for analytic functions, its maximum in modulus is attained on the boundary.

Further, any complex number in the right half of the complex plane can be expressed in polar coordinates as $s = re^{i\theta}$, where $r \in [0, \infty)$ and $\theta \in [-\pi/2, \pi/2]$. From the definition of λ_1 given in Lemma 2.2.2, we observe that $\lim_{r\to\infty} |\lambda_1| = \infty$ and hence

$$\begin{aligned}
\lim_{r\to\infty} |\rho_n(s, \alpha, \beta)| &= \lim_{|\lambda_1|\to\infty} \left| \left(\frac{\alpha + 1 - \lambda_1}{\lambda_1(1 + \alpha) - 1} \right) \left(\frac{\lambda_1 + \beta - 1}{1 + (\beta - 1)\lambda_1} \right) \left(\frac{1}{\lambda_1^2} \right)^n \right| \\
&= \lim_{|\lambda_1|\to\infty} \left| \left(\frac{\alpha + 1 - \lambda_1}{\lambda_1(1 + \alpha) - 1} \right) \left(\frac{\lambda_1 + \beta - 1}{1 + (\beta - 1)\lambda_1} \right) \right| \lim_{|\lambda_1|\to\infty} \left| \left(\frac{1}{\lambda_1^2} \right)^n \right| \\
&= \lim_{|\lambda_1|\to\infty} \left| \left(\frac{\frac{\alpha+1}{\lambda_1} - 1}{1 + \alpha - \frac{1}{\lambda_1}} \right) \left(\frac{1 + \frac{\beta-1}{\lambda_1}}{\frac{1}{\lambda_1} + \beta - 1} \right) \right| \lim_{|\lambda_1|\to\infty} \left| \left(\frac{1}{\lambda_1^2} \right)^n \right| \\
&= \left| \left(\frac{-1}{1 + \alpha} \right) \left(\frac{1}{\beta - 1} \right) \right| \lim_{|\lambda_1|\to\infty} \left| \left(\frac{1}{\lambda_1^2} \right)^n \right| \\
&= 0.
\end{aligned}$$

Thus the maximum lies on the boundary when $\theta = \pm\pi/2$ and $r < \infty$, that is, when $\sigma = 0$. This boundary corresponds to the imaginary axis of the complex plane. □

Lemma 2.4.2. *For $\sigma = 0$, $|\rho_n(\omega, \alpha, \beta)|$ is an even function of ω.*

Proof. At the boundary, $\sigma = 0$, from the definition of λ_1 and the assumption $b =$

$-(2+\epsilon)a$, with $\epsilon \geq 0$, we obtain

$$\begin{aligned}\lambda_1(\omega) &= \frac{i\omega - b + \sqrt{(i\omega-b)^2 - 4a^2}}{2a} \\ &= \frac{i\omega + (2+\epsilon)a + \sqrt{\epsilon^2a^2 - \omega^2 + 4\epsilon a^2 + i2(2+\epsilon)\omega a}}{2a} \\ &= \frac{i\omega + (2+\epsilon)a + \sqrt{r_1 + ir_2}}{2a},\end{aligned}$$

where $r_1 := \epsilon^2a^2 - \omega^2 + 4\epsilon a^2$ and $r_2 := 2(2+\epsilon)\omega a$. Further, let $z_1 + iz_2 := \sqrt{r_1 + ir_2}$ with $z_1, z_2 \in \mathbb{R}$ and hence $\lambda_1(\omega) = \frac{(2+\epsilon)a+z_1}{2a} + i\frac{\omega+z_2}{2a}$. Similarly, we show $\lambda_1(-\omega) = \frac{-i\omega+(2+\epsilon)a+\sqrt{r_1-ir_2}}{2a}$. Using some techniques of complex analysis one can show that if $\sqrt{r_1+ir_2} = z_1+iz_2$ then $\sqrt{r_1-ir_2} = z_1-iz_2$. Therefore, $\lambda_1(-\omega) = \frac{(2+\epsilon)a+z_1}{2a} - i\frac{\omega+z_2}{2a}$ which shows that $\overline{\lambda_1(-\omega)} = \lambda_1(\omega)$. Now,

$$\begin{aligned}|\rho_n(-\omega,\alpha,\beta)| &= \left|\left(\frac{1}{(\lambda_1(-\omega))^2}\right)^n \left(\frac{\alpha+1-\lambda_1(-\omega)}{(\lambda_1(-\omega))(1+\alpha)-1}\right)\left(\frac{\lambda_1(-\omega)+\beta-1}{1+(\beta-1)(\lambda_1(-\omega))}\right)\right| \\ &= \left|\left(\frac{1}{\left(\overline{\lambda_1(\omega)}\right)^2}\right)^n\right|\left|\left(\frac{\alpha+1-\overline{\lambda_1(\omega)}}{\left(\overline{\lambda_1(\omega)}\right)(1+\alpha)-1}\right)\right|\left|\left(\frac{\overline{\lambda_1(\omega)}+\beta-1}{1+(\beta-1)\left(\overline{\lambda_1(\omega)}\right)}\right)\right| \\ &= \left|\left(\frac{1}{\left(\overline{\lambda_1(\omega)}\right)^2}\right)^n\right|\left|\left(\frac{\overline{\alpha+1-\lambda_1(\omega)}}{(\lambda_1(\omega))(1+\alpha)-1}\right)\right|\left|\left(\frac{\overline{\lambda_1(\omega)+\beta-1}}{1+(\beta-1)(\lambda_1(\omega))}\right)\right| \\ &= \left|\left(\frac{1}{(\lambda_1(\omega))^2}\right)^n\right|\left|\left(\frac{\alpha+1-\lambda_1(\omega)}{(\lambda_1(\omega))(1+\alpha)-1}\right)\right|\left|\left(\frac{\lambda_1(\omega)+\beta-1}{1+(\beta-1)(\lambda_1(\omega))}\right)\right| \\ &= |\rho_n(\omega,\alpha,\beta)|,\end{aligned}$$

that is, $|\rho_n(\omega,\alpha,\beta)|$ is an even function in ω. □

From Theorem 2.3.2, we observe that α_{opt} and β_{opt} are related to each other via the relation $\beta_{opt} = -\alpha_{opt}$, which suggests the natural assumption $\beta = -\alpha$. In our RC circuit of infinite length, this would mean that at the interface (where the circuit is split into two), the current flowing in both sub-circuits is equal but into opposite direction. This interpretation is easy to see for the nonoverlapping case $n = 0$ (see Figure 2.3). Recall that the terms $\frac{u_{n+1}^{k+1}-u_n^{k+1}}{\alpha}$ and $\frac{w_1^{k+1}-w_0^{k+1}}{\beta}$ are viewed as currents. Thus for $n = 0$ with $\beta = -\alpha$, their values are same but their sign is opposite.

Lemma 2.4.1 and Lemma 2.4.2 state that the min-max problem (2.24) needs to be solved for $s = i\omega$, $\omega \geq 0$. However, for numerical simulation, we consider a time $t \in (0, T]$, and its discretization with Δt as the discretization parameter. Hence $\omega_{\min} \leq \omega \leq \omega_{\max}$, where we can estimate $\omega_{\min} = \frac{\pi}{T}$ and $\omega_{\max} = \frac{\pi}{\Delta t}$. Therefore, our

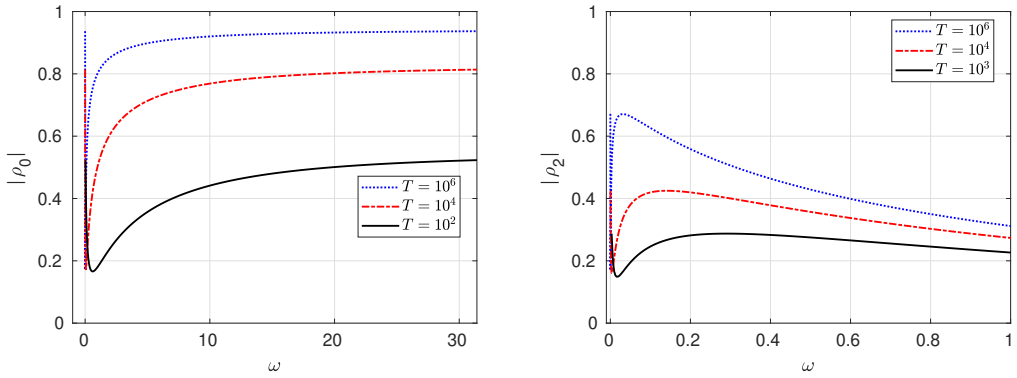

Figure 2.8: Equioscillation for different values of final time T for $n = 0$ (left) and for $n = 2$ (right).

min-max problem (2.24) reduces to

$$\min_{\alpha>0} \left(\max_{\omega_{\min} \le \omega \le \omega_{\max}} |\rho_n(\omega, \alpha, -\alpha)| \right). \tag{2.25}$$

Note that the min-max problem is already too complicated to be solved analytically using available complex analysis tools and optimization techniques. We therefore employ asymptotic analysis. We had already observed in Sections 2.2 and 2.3 that under the conditions $\omega = 0$ and $\epsilon = 0$, we have $|\lambda_1| = 1$ and hence the convergence factors $|\rho_{n,cla}(0)| = 1$ and $|\rho_n(0, \alpha, \beta)| = 1$, for any values of α and β. We therefore consider two asymptotics, $\omega_{\min} \to 0$ with $\epsilon = 0$, and $\epsilon \to 0$ with $\omega_{\min} = 0$.

2.4.1 Asymptotic analysis with respect to time.

In this section, we assume $b = -2a$, that is, $\epsilon = 0$. Further, we consider the minimum frequency $\omega_{\min} \to 0$. This corresponds to considering large time intervals $(0, T]$ with $T \to \infty$. We shall study two different types of overlapping: the nonoverlapping OWR and overlapping OWR with n nodes overlap.

Numerically, we observe from both the plots of Figure 2.8, that a solution for the min-max problem (2.25) is given by equioscillation. However the behavior of equioscillation is different for the nonoverlapping and the overlapping case. We first analyze the nonoverlapping case, that is, $n = 0$, where the equioscillation occurs for $\omega = \omega_{\min}$ and $\omega = \omega_{\max}$ (see the left plot of Figure 2.8). This means the optimized α denoted by $\alpha^*_{T,0}$ satisfies

$$|\rho_0(\omega_{\min}, \alpha^*_{T,0})| = |\rho_0(\omega_{\max}, \alpha^*_{T,0})|,$$

where we have dropped the parameter $-\alpha$ for simplicity, $\rho_n(\omega, \alpha) \equiv \rho_n(\omega, \alpha, -\alpha)$.

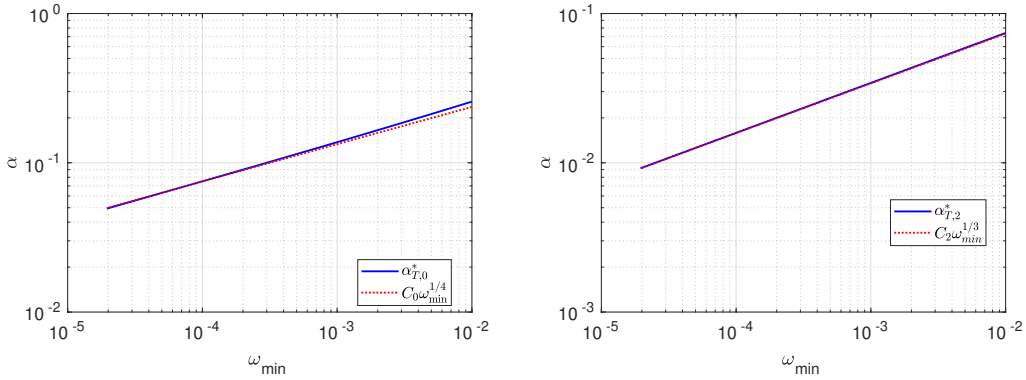

Figure 2.9: Dependence of $\alpha^*_{T,0}$ on $\omega_{\min}$ with $C_0 := \left(\frac{2}{a}\right)^{1/4}$ for $n = 0$ (left) and with $C_2 := \left(\frac{1}{2an}\right)^{1/3}$ for $n = 2$ (right).

To start with, we find an explicit expression for $|\rho_0(\omega, \alpha)|$. In the proof of Lemma 2.4.2, we set $\lambda_1 = x + iy$, where $x = \frac{(2+\epsilon)a+z_1}{2a} = 1 + \frac{z_1}{2a}$ and $y = \frac{\omega+z_2}{2a}$, and hence

$$|\rho_0(\omega, \alpha)| = \frac{|\alpha + 1 - \lambda_1|^2}{|(1+\alpha)\lambda_1 - 1|^2} =: \frac{A(\omega, \alpha)}{B(\omega, \alpha)}, \tag{2.26}$$

where

$$\begin{aligned} A(\omega, \alpha) &:= |\alpha + 1 - \lambda_1|^2 = |(\alpha + 1 - x) - iy|^2 = (\alpha + 1 - x)^2 + y^2 \\ &= \alpha^2 + x^2 + 1 - 2x - 2x\alpha + 2\alpha + y^2, \\ B(\omega, \alpha) &:= |(1+\alpha)\lambda_1 - 1|^2 = |(1+\alpha)x - 1 + iy(1+\alpha)|^2 \\ &= ((1+\alpha)x - 1)^2 + y^2(1+\alpha)^2 \\ &= x^2 + x^2\alpha^2 + 2\alpha x^2 + 1 - 2x - 2x\alpha + y^2 + y^2\alpha^2 + 2\alpha y^2. \end{aligned} \tag{2.27}$$

$A(\omega, \alpha)$ and $B(\omega, \alpha)$ are complicated functions of ω and α which makes the analysis difficult. To simplify, we use asymptotic analysis to find an explicit expression for $\alpha^*_{T,0}$. Let us denote the asymptotic parameter by $\xi = \omega_{\min}$ such that $\xi \to 0$. We first express $|\rho_0(\omega_{\min}, \alpha)|$ and $|\rho_0(\omega_{\max}, \alpha)|$ as polynomials in ξ using the ansatz $\alpha = C_0\xi^\delta$, where $C_0, \delta > 0$. The dependence of $\alpha^*_{T,0}$ on $\omega_{\min}$ for $n = 0$ is illustrated numerically in the left plot of Figure 2.9.

Lemma 2.4.3. *For the nonoverlapping OWR method, that is, with $n = 0$ node overlap and with the assumption $\omega_{\max} > 4a$, the modulus of the convergence factors $|\rho_0(\omega_{\min}, \alpha)|$ and $|\rho_0(\omega_{\max}, \alpha)|$ are given by*

$$|\rho_0(\omega_{\min}, \alpha)| = 1 - \frac{2\sqrt{2}}{C_0\sqrt{a}}\omega_{\min}^{1/2-\delta} + \mathcal{O}(\omega_{\min}^{1/2}), \tag{2.28}$$

and

$$|\rho_0(\omega_{\max}, \alpha)| = 1 - 2C_0\omega_{\min}^{\delta} + \mathcal{O}(\omega_{\min}^{2\delta}). \tag{2.29}$$

Proof. To start with, we first derive asymptotic expressions for $\lambda_1(\omega_{\min})$ and hence for their corresponding x_1 and y_1, where $\lambda_1(\xi) = x_1 + iy_1 = 1 + \frac{z_1}{2a} + i\frac{\xi+z_2}{2a}$. Note that from Lemma 2.4.2, we have $z_1 + iz_2 = \sqrt{-\xi^2 + 4\xi a i}$ and hence squaring both sides and comparing real and imaginary terms leads to $z_1^2 - z_2^2 = -\xi^2$ and $z_1 z_2 = 2a\xi$. The second equation simplifies to $z_2 = \frac{2a\xi}{z_1}$ which on substituting in the first equation produces $z_1^4 + \xi^2 z_1^2 - 4a^2\xi^2 = 0$. The positive root of this equation is given by

$$\begin{aligned} z_1^2 &= \frac{-\xi^2 + \sqrt{\xi^4 + 16a^2\xi^2}}{2} = \frac{-\xi^2 + 4a\xi\sqrt{\frac{\xi^2}{16a^2} + 1}}{2} \\ &= \frac{-\xi^2 + 4a\xi\left(1 + \frac{\xi^2}{32a^2} - \frac{\xi^4}{2048a^4} + \mathcal{O}(\xi^5)\right)}{2} \\ &= 2a\xi - \frac{\xi^2}{2} + \frac{\xi^3}{16a} + \mathcal{O}(\xi^5). \end{aligned}$$

Taking a square root using the asymptotic relation $\sqrt{1+z} = 1 + \frac{z}{2} - \frac{z^2}{8} + \mathcal{O}(z^3)$, leads to

$$\begin{aligned} z_1 &= \sqrt{z_1^2} = \sqrt{2a\xi - \frac{\xi^2}{2} + \frac{\xi^3}{16a} + \mathcal{O}(\xi^5)} = \sqrt{2a\xi}\sqrt{1 - \frac{\xi}{4a} + \frac{\xi^2}{32a^2} + \mathcal{O}(\xi^4)} \\ &= \sqrt{2a\xi}\left(1 - \frac{\xi}{8a} + \frac{\xi^2}{128a^2} + \mathcal{O}(\xi^3)\right) = \sqrt{2a\xi} - \frac{\sqrt{2}\xi^{3/2}}{8\sqrt{a}} + \frac{\sqrt{2}\xi^{5/2}}{128a^{3/2}} + \mathcal{O}(\xi^{7/2}). \end{aligned}$$

Since $z_2 = \frac{2a\xi}{z_1}$, we have

$$\begin{aligned} z_2 &= \frac{2a\xi}{\sqrt{2a\xi}\left(1 - \frac{\xi}{8a} + \frac{\xi^2}{128a^2} + \mathcal{O}(\xi^3)\right)} = \sqrt{2a\xi}\left(1 + \frac{\xi}{8a} + \mathcal{O}(\xi^3)\right) \\ &= \sqrt{2a\xi} + \frac{\sqrt{2}\xi^{3/2}}{8\sqrt{a}} + \mathcal{O}(\xi^{5/2}). \end{aligned}$$

Substituting z_1 and z_2 into the expressions of x_1 and y_1 gives $x_1 = 1 + \frac{z_1}{2a} = 1 + \frac{\sqrt{2\xi}}{2\sqrt{a}} - \frac{\sqrt{2}\xi^{3/2}}{16a^{3/2}} + \mathcal{O}(\xi^{5/2})$ and $y_1 = \frac{\xi+z_2}{2a} = \frac{\sqrt{2\xi}}{2\sqrt{a}} + \frac{\xi}{2a} + \frac{\sqrt{2}\xi^{3/2}}{16a^{3/2}} + \mathcal{O}(\xi^{5/2})$. Further, substituting these expressions of x_1, y_1 and the asymptotic ansatz of α, that is, $\alpha = C_0\xi^\delta$ into $A(\omega, \alpha)$ and $B(\omega, \alpha)$ given by (2.27) leads to

$$A(\omega_{\min}, \alpha) = C_0^2\xi^{2\delta} - \frac{\sqrt{2}C_0\xi^{1/2+\delta}}{\sqrt{a}} + \mathcal{O}(\xi),$$

and

$$B(\omega_{\min}, \alpha) = C_0^2\xi^{2\delta} + \frac{\sqrt{2}C_0\xi^{1/2+\delta}}{\sqrt{a}} + \frac{\sqrt{2}C_0^2\xi^{1/2+2\delta}}{\sqrt{a}} + \mathcal{O}(\xi).$$

Since $\xi \to 0$, the dominating term in both these expressions is $C_0^2\xi^{2\delta}$, and hence the asymptotic formula $\frac{1}{1+z} = 1 - z + \frac{z^2}{2} + \mathcal{O}(z^3)$, for $|z| < 1$ leads to

$$\begin{aligned}
|\rho_0(\omega_{\min}, \alpha)| &= \frac{A(\omega_{\min}, \alpha)}{B(\omega_{\min}, \alpha)} = \frac{1 - \frac{\sqrt{2}\xi^{1/2-\delta}}{C_0\sqrt{a}} + \mathcal{O}(\xi^{1-2\delta})}{1 + \frac{\sqrt{2}\xi^{1/2-\delta}}{C_0\sqrt{a}} + \frac{\sqrt{2}\xi^{1/2}}{\sqrt{a}} + \mathcal{O}(\xi^{1-2\delta})} \\
&= \left(1 - \frac{\sqrt{2}\xi^{1/2-\delta}}{C_0\sqrt{a}} + \mathcal{O}(\xi^{1-2\delta})\right)\left(1 - \frac{\sqrt{2}\xi^{1/2-\delta}}{C_0\sqrt{a}} - \frac{\sqrt{2}\xi^{1/2}}{\sqrt{a}} + \mathcal{O}(\xi^{1-2\delta})\right) \\
&= 1 - \frac{2\sqrt{2}\xi^{1/2-\delta}}{C_0\sqrt{a}} + \mathcal{O}(\xi^{1/2}).
\end{aligned}$$

We now perform a similar analysis to find an expression for $|\rho_0(\omega_{\max}, \alpha)|$. We go to the expression of $\lambda_1(\omega_{\max}) = \tilde{x} + i\tilde{y} = 1 + \frac{\tilde{z}_1}{2a} + i\left(\frac{\omega_{\max}+\tilde{z}_2}{2a}\right)$, where $\tilde{z}_1 + \tilde{z}_2 = \sqrt{-\omega_{\max}^2 + 4a\omega_{\max}i}$. Squaring both sides and comparing the real and imaginary parts leads to $\tilde{z}_2 = \frac{2a\omega_{\max}}{\tilde{z}_1}$ which on substituting in $\tilde{z}_1^2 - \tilde{z}_2^2 = -\omega_{\max}^2$ produces $\tilde{z}_1^4 + \tilde{z}_1^2\omega_{\max}^2 - 4a^2\omega_{\max}^2 = 0$. Using the asymptotic expressions for $\sqrt{1+z}$, for $|z| < 1$, and assuming $\omega_{\max} > 4a$, we find

$$\begin{aligned}
\tilde{z}_1 &= \sqrt{\tilde{z}_1^2} = \sqrt{\frac{-\omega_{\max}^2 + \sqrt{\omega_{\max}^4 + 16a^2\omega_{\max}^2}}{2}} \\
&= \sqrt{\frac{-\omega_{\max}^2 + \omega_{\max}^2\sqrt{1 + \frac{16a^2}{\omega_{\max}^2}}}{2}} \\
&= \sqrt{\frac{-\omega_{\max}^2 + \omega_{\max}^2\left(1 + \frac{8a^2}{\omega_{\max}^2} - \frac{32a^4}{\omega_{\max}^4} + \mathcal{O}(\omega_{\max}^{-6})\right)}{2}} \\
&= \sqrt{4a^2 - \frac{16a^4}{\omega_{\max}^2} + \mathcal{O}(\omega_{\max}^{-4})} = 2a\sqrt{1 - \frac{4a^2}{\omega_{\max}^2} + \mathcal{O}(\omega_{\max}^{-4})} \\
&= 2a\left(1 - \frac{2a^2}{\omega_{\max}^2} + \mathcal{O}(\omega_{\max}^{-4})\right) = 2a - \frac{4a^3}{\omega_{\max}^2} + \mathcal{O}(\omega_{\max}^{-4}).
\end{aligned}$$

Substituting into the expression of $\tilde{z}_2$, we get

$$\begin{aligned}
\tilde{z}_2 &= \frac{2a\omega_{\max}}{\tilde{z}_1} = \frac{2a\omega_{\max}}{2a - \frac{4a^3}{\omega_{\max}^2} + \mathcal{O}(\omega_{\max}^{-4})} = \frac{2a\omega_{\max}}{2a\left(1 - \frac{2a^2}{\omega_{\max}^2} + \mathcal{O}(\omega_{\max}^{-4})\right)} \\
&= \omega_{\max}\left(1 + \frac{2a^2}{\omega_{\max}^2} + \mathcal{O}(\omega_{\max}^{-4})\right) = \omega_{\max} + \frac{2a^2}{\omega_{\max}} + \mathcal{O}(\omega_{\max}^{-3}).
\end{aligned}$$

These give the expressions for $\tilde{x}$ and $\tilde{y}$:

$$\begin{aligned}
\tilde{x} &= 1 + \frac{\tilde{z}_1}{2a} = 2 - \frac{2a^2}{\omega_{\max}^2} + \mathcal{O}(\omega_{\max}^{-4}), \\
\tilde{y} &= \frac{\omega_{\max} + \tilde{z}_2}{2a} = \frac{\omega_{\max}}{a} + \frac{a}{\omega_{\max}} + \mathcal{O}(\omega_{\max}^{-3}).
\end{aligned}$$

Substituting the expressions of $\tilde{x}$, $\tilde{y}$ and α into equation (2.27), we obtain

$$A(\omega_{\max}, \alpha) = 3 + \frac{\omega_{\max}^2}{a^2} - 2C_0\xi^\delta + C_0^2\xi^{2\delta} + \mathcal{O}(\omega_{\max}^{-2}),$$

and

$$B(\omega_{\max}, \alpha) = 3 + \frac{\omega_{\max}^2}{a^2} + \frac{2C_0\xi^\delta\omega_{\max}^2}{a^2} + \frac{C_0^2\xi^{2\delta}\omega_{\max}^2}{a^2} + 8C_0\xi^\delta + 6C_0^2\xi^{2\delta} + \mathcal{O}(\omega_{\max}^{-2}).$$

Since we have assumed $\omega_{\max} > 4a$, the dominating term in both expressions of $A(\omega_{\max}, \alpha)$ and $B(\omega_{\max}, \alpha)$ is $\frac{\omega_{\max}^2}{a^2}$, and hence

$$\begin{aligned}
|\rho_0(\omega_{\max}, \alpha)| &= \frac{A(\omega_{\max}, \alpha)}{B(\omega_{\max}, \alpha)} \\
&= \frac{3 + \frac{\omega_{\max}^2}{a^2} - 2C_0\xi^\delta + C_0^2\xi^{2\delta} + \mathcal{O}(\omega_{\max}^{-2})}{3 + \frac{\omega_{\max}^2}{a^2} + \frac{2C_0\xi^\delta\omega_{\max}^2}{a^2} + \frac{C_0^2\xi^{2\delta}\omega_{\max}^2}{a^2} + 8C_0\xi^\delta + 6C_0^2\xi^{2\delta} + \mathcal{O}(\omega_{\max}^{-2})} \\
&= \frac{\frac{\omega_{\max}^2}{a^2}\left(1 + \frac{3a^2}{\omega_{\max}^2} - \frac{2C_0a^2\xi^\delta}{\omega_{\max}^2} + \frac{C_0^2a^2\xi^{2\delta}}{\omega_{\max}^2} + \mathcal{O}(\omega_{\max}^{-4})\right)}{\frac{\omega_{\max}^2}{a^2}\left(1 + 2C_0\xi^\delta + C_0^2\xi^{2\delta} + \frac{3a^2}{\omega_{\max}^2} + \frac{8C_0a^2\xi^\delta}{\omega_{\max}^2} + \frac{6C_0^2a^2\xi^{2\delta}}{\omega_{\max}^2} + \mathcal{O}(\omega_{\max}^{-4})\right)} \\
&= \left(1 + \frac{3a^2}{\omega_{\max}^2} - \frac{2C_0a^2\xi^\delta}{\omega_{\max}^2} + \frac{C_0^2a^2\xi^{2\delta}}{\omega_{\max}^2} + \mathcal{O}(\omega_{\max}^{-4})\right) \\
&\qquad \left(1 - 2C_0\xi^\delta + 2C_0^2\xi^{2\delta} + \mathcal{O}(\omega_{\max}^{-2}\right) \\
&= 1 - 2C_0\xi^\delta + \mathcal{O}(\omega_{\max}^{-2}),
\end{aligned}$$

which completes the proof. □

Theorem 2.4.1. *For the nonoverlapping OWR algorithm, that is, with $n = 0$ node overlap, and large time intervals $(0, T)$ with $T \to \infty$, if $\alpha_{T,0}^* = \left(\frac{2}{a}\right)^{1/4}\omega_{\min}^{1/4}$, then the convergence factor ρ_0 satisfies*

$$|\rho_0(\omega, \alpha)| \le |\rho_0(\omega_{\min}, \alpha_{T,0}^*)| = 1 - 2\left(\frac{2}{a}\right)^{1/4}\omega_{\min}^{1/4} + \mathcal{O}(\omega_{\min}^{1/2}). \tag{2.30}$$

Proof. For the nonoverlapping case $n = 0$, we observe from the left plot of Figure 2.8, that a solution of the min-max problem (2.25) is given by the equioscillation at $\omega_{\min}$ and $\omega_{\max}$. Comparing the dominating terms in expressions (2.28) and (2.29), we obtain $2C_0\xi^\delta = \frac{2\sqrt{2}}{C_0\sqrt{a}}\xi^{1/2-\delta}$. Equating the exponents of these terms leads to $\delta = 1/2 - \delta$, that is, $\delta = 1/4$. Similarly, equating their coefficients simplifies to $C_0^2\sqrt{a} = \sqrt{2}$, and hence $C_0 = \left(\frac{2}{a}\right)^{1/4}$. Substituting these expressions into (2.29) results in

$$|\rho_0(\omega_{\min}, \alpha_{T,0}^*)| = 1 - 2\left(\frac{2}{a}\right)^{1/4}\omega_{\min}^{1/4} + \mathcal{O}(\omega_{\min}^{1/2}),$$

and this completes the proof. □

We now consider the overlapping case, with n nodes overlap. The right plot of Figure 2.8 depicts that a solution of the min max problem (2.25) is given by the equioscillation between $\omega_{\min}$ and $\bar{\omega}$, where $\omega_{\min} < \bar{\omega} < \omega_{\max}$ with $\bar{\omega} \to 0$ as $\omega_{\min} \to 0$. We therefore use the ansatz $\alpha = C_n \xi^\delta$ and $\bar{\omega} := k\xi^\eta$, where the constants $C_n, \delta, k, \eta > 0$ and $\xi = \omega_{\min}$. Further, solving the min-max problem (2.25) is equivalent to solving the coupled equations:

$$|\rho_n(\omega_{\min}, \alpha^*_{T,n})| = |\rho_n(\bar{\omega}, \alpha^*_{T,n})|, \quad \text{and} \quad \frac{\partial}{\partial \omega}|\rho_n(\bar{\omega}, \alpha^*_{T,n})| = 0, \tag{2.31}$$

where $\alpha^*_{T,n}$ denotes the optimized α for an overlap of size n. We first find the relation between δ and η, and C_n and k in the following lemma.

Lemma 2.4.4. *For the overlapping OWR method with $n > 0$ nodes overlap, solving the equation $\frac{\partial}{\partial \omega}|\rho_n(\bar{\omega}, \alpha^*_{T,n})| = 0$ produces the relations*

$$\eta = \delta, \qquad \text{and} \qquad k = \frac{2aC_n}{n}. \tag{2.32}$$

Proof. We first find the expression for $|\rho_n(\omega, \alpha)|$ using the asymptotic relations and ansatz for α, then derive it with respect to ω and finally substitute the ansatz for $\bar{\omega}$. Recall that from Lemma 2.4.2, $\lambda_1(\omega) = x + iy = 1 + \frac{z_1}{2a} + i\frac{\omega + z_2}{2a}$, where $z_1 + iz_2 = \sqrt{-\omega^2 + 4a\omega i}$. Simplification of this equation by squaring leads to $z_2 = \frac{2a\omega}{z_1}$ and $z_1^4 + z_1^2\omega^2 - 4a^2\omega^2 = 0$. Solving for z_1^2 and using the asymptotic expressions for $\sqrt{1+z}$ and $\frac{1}{1+z}$, where $|z| < 1$ gives

$$\begin{aligned}
z_1 &= \sqrt{z_1^2} = \sqrt{\frac{-\omega^2 + \sqrt{\omega^4 + 16a^2\omega^2}}{2}} \\
&= \sqrt{\frac{-\omega^2 + 4a\omega\sqrt{\frac{\omega^2}{16a^2} + 1}}{2}} \qquad \text{since } 16a^2 > \omega^2 \\
&= \sqrt{\frac{-\omega^2 + 4a\omega\left(1 + \frac{\omega^2}{32a^2} + \mathcal{O}(\omega^4)\right)}{2}} \\
&= \sqrt{2a\omega - \frac{\omega^2}{2} + \frac{\omega^3}{16a} + \mathcal{O}(\omega^5)} = \sqrt{2a\omega}\sqrt{1 - \frac{\omega}{4a} + \frac{\omega^2}{32a^2} + \mathcal{O}(\omega^4)} \\
&= \sqrt{2a\omega}\left(1 - \frac{\omega}{8a} + \frac{\omega^2}{128a^2} + \mathcal{O}(\omega^3)\right) \\
&= \sqrt{2a\omega} - \frac{\sqrt{2}\omega^{3/2}}{8\sqrt{a}} + \frac{\sqrt{2}\omega^{5/2}}{128a^{3/2}} + \mathcal{O}(\omega^{7/2}),
\end{aligned}$$

and thus $z_2 = \sqrt{2a\omega} + \frac{\sqrt{2}\omega^{3/2}}{8\sqrt{a}} + \frac{\sqrt{2}\omega^{5/2}}{128a^{3/2}} + \mathcal{O}(\omega^{7/2})$. Substituting these expressions into x and y yields

$$x = 1 + \frac{z_1}{2a} = 1 + \frac{\sqrt{2}\sqrt{\omega}}{2\sqrt{a}} - \frac{\sqrt{2}\omega^{3/2}}{16a^{3/2}} + \frac{\sqrt{2}\omega^{5/2}}{256a^{5/2}} + \mathcal{O}(\omega^{7/2}), \tag{2.33}$$

$$y = \frac{\omega + z_2}{2a} = \frac{\sqrt{2}\sqrt{\omega}}{2\sqrt{a}} + \frac{\omega}{2a} + \frac{\sqrt{2}\omega^{3/2}}{16a^{3/2}} + \frac{\sqrt{2}\omega^{5/2}}{256a^{5/2}} + \mathcal{O}(\omega^{7/2}). \tag{2.34}$$

Recall that the convergence factor for n nodes overlap (2.20) is

$$\begin{aligned} |\rho_n(\omega,\alpha)| &= \left| \left(\frac{\alpha + 1 - \lambda_1}{\lambda_1(1+\alpha) - 1} \right) \left(\frac{\lambda_1 + \beta - 1}{1 + (\beta - 1)\lambda_1} \right) \left(\frac{1}{\lambda_1^2} \right)^n \right| \\ &= |\rho_0(\omega,\alpha)| \left| \left(\frac{1}{\lambda_1^2} \right)^n \right| = \frac{A(\omega,\alpha)}{B(\omega,\alpha)} L(\omega,\alpha), \end{aligned} \tag{2.35}$$

where $\lambda_1(\omega) = x + iy$ and hence

$$\begin{aligned} A(\omega,\alpha) &= |\alpha + 1 - \lambda_1|^2 = |(\alpha + 1 - x) + iy|^2 \\ &= \alpha^2 + x^2 + 1 + y^2 - 2x - 2x\alpha + 2\alpha, \end{aligned} \tag{2.36}$$

$$\begin{aligned} B(\omega,\alpha) &= |(1+\alpha)\lambda_1 - 1|^2 = |(1+\alpha)x - 1 + iy(1+\alpha)|^2 \\ &= x^2 + x^2\alpha^2 + 2\alpha x^2 + 1 - 2x - 2x\alpha + y^2 + y^2\alpha^2 + 2\alpha y^2, \end{aligned} \tag{2.37}$$

$$L(\omega,\alpha) = \left| \left(\frac{1}{\lambda_1^2} \right)^n \right| = \frac{1}{(x^2 + y^2)^n}. \tag{2.38}$$

A simple substitution of the ansatz $\alpha = C_n \xi^\delta$ and expressions for x and y derived in (2.33) and (2.34) into the above equations (2.36)-(2.37):

$$\begin{aligned} A(\omega,\alpha) &= \tfrac{\omega}{a} - \tfrac{C_n \xi^\delta \sqrt{2}\sqrt{\omega}}{\sqrt{a}} + \tfrac{\sqrt{2}\omega^{3/2}}{2a^{3/2}} + \mathcal{O}(\omega^2), \\ B(\omega,\alpha) &= \tfrac{\omega}{a} + \tfrac{C_n \xi^\delta \sqrt{2}\sqrt{\omega}}{\sqrt{a}} + \tfrac{\sqrt{2}\omega^{3/2}}{2a^{3/2}} + \mathcal{O}(\omega^2). \end{aligned} \tag{2.39}$$

Further, the effect of overlap is given by $L(\omega,\alpha) = \left| \left(\frac{1}{\lambda_1^2} \right)^n \right|$. Using equations (2.33)-(2.34) and the asymptotic formula, $(1+z)^{-n} = 1 - nz + \frac{n^2 z^2}{2} + \mathcal{O}(z^3)$, for $|z| < 1$, we arrive at

$$\begin{aligned} L(\omega,\alpha) &= = \frac{1}{(x^2 + y^2)^n} = \frac{1}{\left(1 + \frac{\sqrt{2}\sqrt{\omega}}{\sqrt{a}} + \frac{\omega}{a} + \frac{3\sqrt{2}\omega^{3/2}}{8a^{3/2}} + \mathcal{O}(\omega^2)\right)^n} \\ &= 1 - \frac{n\sqrt{2}\sqrt{\omega}}{\sqrt{a}} - \frac{n\omega}{a} + \frac{n^2\omega}{a} + \mathcal{O}(\omega^{3/2}). \end{aligned} \tag{2.40}$$

Finally, we derive $|\rho_n(\omega,\alpha)|$ with respect to ω and obtain

$$\begin{aligned} \frac{\partial}{\partial\omega}|\rho_n(\omega,\alpha)| &= \frac{\partial}{\partial\omega}\left(\frac{A(\omega,\alpha)}{B(\omega,\alpha)} L(\omega,\alpha) \right) \\ &= \frac{B(\omega,\alpha)\left[A(\omega,\alpha)L_\omega(\omega,\alpha) + A_\omega(\omega,\alpha)L(\omega,\alpha)\right] - A(\omega,\alpha)L(\omega,\alpha)B_\omega(\omega,\alpha)}{B^2(\omega,\alpha)}, \end{aligned}$$

where $Z_\omega(\omega,\alpha)$ denotes the derivative of $Z(\omega,\alpha)$ with respect to ω. Equating $\frac{\partial}{\partial\omega}|\rho_n(\omega,\alpha)|$ to zero results in solving $F_1(\omega,\alpha)-F_2(\omega,\alpha)=0$, where

$$\begin{aligned} F_1(\omega,\alpha) &:= B(\omega,\alpha)\left[A(\omega,\alpha)L_\omega(\omega,\alpha)+A_\omega(\omega,\alpha)L(\omega,\alpha)\right], \\ F_2(\omega,\alpha) &:= A(\omega,\alpha)L(\omega,\alpha)B_\omega(\omega,\alpha). \end{aligned} \tag{2.41}$$

Since $A(\omega,\alpha)$, $B(\omega,\alpha)$ and $L(\omega,\alpha)$ are polynomial expressions in ω (see (2.39) and (2.40)), differentiating them is not complicated and we obtain

$$\begin{aligned} A_\omega(\omega,\alpha) &= \tfrac{1}{a}-\tfrac{C_n\xi^\delta\sqrt{2}}{2\sqrt{a}\sqrt{\omega}}+\mathcal{O}(\omega^{1/2}), \\ B_\omega(\omega,\alpha) &= \tfrac{1}{a}+\tfrac{C_n\xi^\delta\sqrt{2}}{2\sqrt{a}\sqrt{\omega}}+\mathcal{O}(\omega^{1/2}), \\ L_\omega(\omega,\alpha) &= -\tfrac{n\sqrt{2}}{2\sqrt{\omega}\sqrt{a}}-\tfrac{n}{a}+\tfrac{n^2}{a}+\mathcal{O}(\omega^{1/2}). \end{aligned}$$

Substituting these expressions into (2.41), leads to

$$\begin{aligned} F_1(\omega,\alpha) &= \left(\frac{\omega}{a}+\frac{C_n\xi^\delta\sqrt{2}\sqrt{\omega}}{\sqrt{a}}+\mathcal{O}(\omega^{3/2})\right)\left(A(\omega,\alpha)L_\omega(\omega,\alpha)+A_\omega(\omega,\alpha)L(\omega,\alpha)\right) \\ &= \left(\frac{\omega}{a}+\frac{C_n\xi^\delta\sqrt{2}\sqrt{\omega}}{\sqrt{a}}+\mathcal{O}(\omega^{3/2})\right)\left(\frac{2C_n\xi^\delta n}{a}+\frac{1}{a}-\frac{C_n\xi^\delta\sqrt{2}}{2\sqrt{a}\sqrt{\omega}}-\frac{3n\sqrt{2}\sqrt{\omega}}{2a^{3/2}}+\mathcal{O}(\omega)\right) \\ &= \frac{C_n\xi^\delta\sqrt{2}\sqrt{\omega}}{2a^{3/2}}+\frac{\omega}{a^2}-\frac{3n\sqrt{2}\omega^{3/2}}{2a^{5/2}}+\mathcal{O}(\omega^2). \end{aligned}$$

Similarly,

$$\begin{aligned} F_2(\omega,\alpha) &= \left(A(\omega,\alpha)L(\omega,\alpha)\right)\left(\frac{1}{a}+\frac{C_n\xi^\delta\sqrt{2}}{2\sqrt{a}\sqrt{\omega}}+\mathcal{O}(\omega^{1/2})\right) \\ &= \left(\frac{\omega}{a}-\frac{\omega^2 n}{a^2}+\frac{\omega^2 n^2}{a^2}-\frac{C_n\xi^\delta\sqrt{2}\sqrt{\omega}}{\sqrt{a}}+\mathcal{O}(\omega^{3/2})\right)\left(\frac{1}{a}+\frac{C_n\xi^\delta\sqrt{2}}{2\sqrt{a}\sqrt{\omega}}+\mathcal{O}(\omega^{1/2})\right) \\ &= -\frac{C_n\xi^\delta\sqrt{2}\sqrt{\omega}}{2a^{3/2}}+\frac{\omega}{a^2}-\frac{n\sqrt{2}\omega^{3/2}}{2a^{5/2}}+\mathcal{O}(\omega^2), \end{aligned}$$

and therefore, $F_1(\omega,\alpha)=F_2(\omega,\alpha)$ results in $\frac{C_n\xi^\delta\sqrt{2}\sqrt{\omega}}{2a^{3/2}}=\frac{n\sqrt{2}\omega^{3/2}}{2a^{5/2}}$. Now we substitute the ansatz $\bar{\omega}=k\xi^\eta$ into the above equation. First comparing the exponent of ξ and then the coefficients gives us the required relations (2.32), and this completes the proof. □

The solution of the first equation of (2.31), along with Lemma 2.4.4 will give us the values of constants δ, η, C_n, and k and hence, explicit asymptotic expressions for $\bar{\omega}$ and $\alpha^*_{T,n}$.

Lemma 2.4.5. *For the overlapping OWR, with $n > 0$ nodes overlap, the modulus of the convergence factor $\rho_n(\omega_{\min}, \alpha)$ and $\rho_n(\bar{\omega}, \alpha)$ are given by*

$$|\rho_n(\omega_{\min}, \alpha)| = 1 - \frac{2\sqrt{2}}{C_n\sqrt{a}}\omega_{\min}^{1/2-\delta} + \mathcal{O}(\omega_{\min}^{1/2}), \tag{2.42}$$

and

$$|\rho_n(\bar{\omega}, \alpha)| = 1 - \frac{n\sqrt{2}\sqrt{k}}{\sqrt{a}}\omega_{\min}^{\delta/2} - \frac{2\sqrt{2}\sqrt{a}C_n}{\sqrt{k}}\omega_{\min}^{\delta/2} + \mathcal{O}(\omega_{\min}^{1/2}), \tag{2.43}$$

Proof. Note that the modulus of the convergence factor for the overlapping case is related to the modulus of the convergence factor for the nonoverlapping case by

$$|\rho_n(\omega, \alpha)| = |\rho_0(\omega, \alpha)| \left| \left(\frac{1}{\lambda_1^2} \right)^n \right|,$$

and hence we will use some expressions derived in the proof of Lemma 2.4.3. The polynomial expression for $|\rho_0(\omega_{\min}, \alpha)|$ is given by (2.28). Further, in Lemma 2.4.3 we have also expressed $\lambda_1(\omega_{\min})$ as $x_1 + iy_1$, where $x_1 = 1 + \frac{\sqrt{2\xi}}{2\sqrt{a}} - \frac{\sqrt{2}\xi^{3/2}}{16a^{3/2}} + \mathcal{O}(\xi^2)$ and $y_1 = \frac{\sqrt{2\xi}}{2\sqrt{a}} + \frac{\xi}{2a} + \frac{\sqrt{2}\xi^{3/2}}{16a^{3/2}} + \mathcal{O}(\xi^2)$, and the modulus of the effect of the overlap at $\omega_{\min} = \xi$ has the polynomial expression

$$\begin{aligned} L(\omega_{\min}, \alpha) &:= \left| \left(\frac{1}{\lambda_1^2(\omega_{\min})} \right)^n \right| = \left(\frac{1}{x_1^2 + y_1^2} \right)^n = \left(\frac{1}{1 + \frac{\sqrt{2}\sqrt{\xi}}{\sqrt{a}} + \frac{\xi}{a} + \frac{3\sqrt{2}\xi^{3/2}}{8a^{3/2}} + \mathcal{O}(\xi^2)} \right)^n \\ &= 1 - \frac{n\sqrt{2}\sqrt{\xi}}{\sqrt{a}} - \frac{n\xi}{a} + \frac{n^2\xi}{a} + \mathcal{O}(\xi^{3/2}). \end{aligned}$$

Multiplying the above polynomial with (2.28) gives

$$\begin{aligned} |\rho_n(\omega_{\min}, \alpha)| &= \left(1 - \frac{2\sqrt{2}}{C_n\sqrt{a}}\xi^{1/2-\delta} + \mathcal{O}(\xi^{1/2}) \right) \left(1 - \frac{n\sqrt{2}\sqrt{\xi}}{\sqrt{a}} - \frac{n\xi}{a} + \frac{n^2\xi}{a} + \mathcal{O}(\xi^{3/2}) \right) \\ &= 1 - \frac{2\sqrt{2}\xi^{1/2-\delta}}{C_n\sqrt{a}} + \mathcal{O}(\xi^{1/2}). \end{aligned}$$

We now derive the polynomial expression for $|\rho_n(\bar{\omega}, \alpha)|$. In Lemma 2.4.4, we derived a simplified expression for the modulus of $\rho_n(\bar{\omega}, \alpha)$, namely

$$|\rho_n(\omega, \alpha)| = \frac{A(\omega, \alpha)}{B(\omega, \alpha)} L(\omega, \alpha),$$

where $A(\omega,\alpha)$, $B(\omega,\alpha)$ and $L(\omega,\alpha)$ are expressed in polynomials of ξ in equations (2.39) and (2.40). Substituting the ansatz $\bar{\omega} = k\xi^\delta$ into these equations yields

$$\begin{aligned}
A(\bar{\omega},\alpha) &= \frac{k}{a}\xi^\delta - \frac{C_n\sqrt{2}\sqrt{k}}{\sqrt{a}}\xi^{3\delta/2} + \frac{\sqrt{2}k^{3/2}}{2a^{3/2}}\xi^{3\delta/2} + \mathcal{O}(\xi^{2\delta}),\\
B(\bar{\omega},\alpha) &= \frac{k}{a}\xi^\delta + \frac{C_n\sqrt{2}\sqrt{k}}{\sqrt{a}}\xi^{3\delta/2} + \frac{\sqrt{2}k^{3/2}}{2a^{3/2}}\xi^{3\delta/2} + \mathcal{O}(\xi^{2\delta}),\\
L(\bar{\omega},\alpha) &= 1 - \frac{n\sqrt{2}\sqrt{k}}{\sqrt{a}}\xi^{\delta/2} - \frac{nk}{a}\xi^\delta + \frac{n^2k}{a}\xi^\delta + \mathcal{O}(\xi^{3\delta/2}).
\end{aligned}$$

Since $\xi \to 0$, the dominating term in $A(\bar{\omega},\alpha)$ and $B(\bar{\omega},\alpha)$ is $\frac{k}{a}\xi^\delta$. Collecting the dominating terms and using asymptotic formulas, we obtain

$$\begin{aligned}
|\rho_n(\bar{\omega},\alpha)| &= \frac{A(\bar{\omega},\alpha)}{B(\bar{\omega},\alpha)}L(\bar{\omega},\alpha)\\
&= \left(\frac{\frac{k}{a}\xi^\delta - \frac{C_n\sqrt{2}\sqrt{k}}{\sqrt{a}}\xi^{3\delta/2} + \frac{\sqrt{2}k^{3/2}}{2a^{3/2}}\xi^{3\delta/2} + \mathcal{O}(\xi^{2\delta})}{\frac{k}{a}\xi^\delta + \frac{C_n\sqrt{2}\sqrt{k}}{\sqrt{a}}\xi^{3\delta/2} + \frac{\sqrt{2}k^{3/2}}{2a^{3/2}}\xi^{3\delta/2} + \mathcal{O}(\xi^{2\delta})}\right)\left(1 - \frac{n\sqrt{2}\sqrt{k}}{\sqrt{a}}\xi^{\delta/2} + \mathcal{O}(\xi^\delta)\right)\\
&= \left(\frac{1 - \frac{C_n\sqrt{2}\sqrt{a}}{\sqrt{k}}\xi^{\delta/2} + \frac{\sqrt{2}\sqrt{k}}{2\sqrt{a}}\xi^{\delta/2} + \mathcal{O}(\xi^\delta)}{1 + \frac{C_n\sqrt{2}\sqrt{a}}{\sqrt{k}}\xi^{\delta/2} + \frac{\sqrt{2}\sqrt{k}}{2\sqrt{a}}\xi^{\delta/2} + \mathcal{O}(\xi^\delta)}\right)\left(1 - \frac{n\sqrt{2}\sqrt{k}}{\sqrt{a}}\xi^{\delta/2} + \mathcal{O}(\xi^\delta)\right)\\
&= \left(1 - \frac{C_n\sqrt{2}\sqrt{a}}{\sqrt{k}}\xi^{\delta/2} + \frac{\sqrt{2}\sqrt{k}}{2\sqrt{a}}\xi^{\delta/2} + \mathcal{O}(\xi^\delta)\right)\left(1 - \frac{n\sqrt{2}\sqrt{k}}{\sqrt{a}}\xi^{\delta/2} + \mathcal{O}(\xi^\delta)\right)\\
&\qquad \left(1 - \frac{C_n\sqrt{2}\sqrt{a}}{\sqrt{k}}\xi^{\delta/2} - \frac{\sqrt{2}\sqrt{k}}{2\sqrt{a}}\xi^{\delta/2} + \mathcal{O}(\xi^\delta)\right)\\
&= \left(1 - \frac{2C_n\sqrt{2}\sqrt{a}}{\sqrt{k}}\xi^{\delta/2} + \mathcal{O}(\xi^\delta)\right)\left(1 - \frac{n\sqrt{2}\sqrt{k}}{\sqrt{a}}\xi^{\delta/2} + \mathcal{O}(\xi^\delta)\right)\\
&= 1 - \frac{2C_n\sqrt{2}\sqrt{a}}{\sqrt{k}}\xi^{\delta/2} - \frac{n\sqrt{2}\sqrt{k}}{\sqrt{a}}\xi^{\delta/2} + \mathcal{O}(\xi^\delta).
\end{aligned}$$

This completes the proof. □

Theorem 2.4.2. *For the overlapping OWR algorithm with $n \geq 1$ nodes overlap and large time interval $(0,T)$ with $T \to \infty$, if $\alpha^*_{T,n} = \left(\frac{1}{2an}\right)^{1/3}\omega_{\min}^{1/3}$, then the convergence factor ρ_n satisfies*

$$|\rho_n(\omega,\alpha)| \leq |\rho_n(\omega_{\min},\alpha^*_{T,n})| \sim 1 - 2^{11/6}\left(\frac{n^2}{a}\right)^{1/6}\omega_{\min}^{1/6} + \mathcal{O}(\omega_{\min}^{1/3}). \tag{2.44}$$

Proof. The right plot of Figure 2.8 shows that a solution of the min-max problem (2.25) is given by equioscillation between the two frequencies $\omega_{\min}$ and $\bar{\omega}$, where

$\omega_{\min} < \bar{\omega} < \omega_{\max}$ with $\bar{\omega} \to 0$ as $\omega_{\min} \to 0$. Hence a solution of the min-max problem (2.25) can be found by solving equations (2.31). Lemmas 2.4.4 and 2.4.5 provide us with relations between $\bar{\omega}$ and the optimized $\alpha^*_{T,n}$, and with the polynomial expressions for $|\rho_n(\omega_{\min}, \alpha)|$ and $|\rho_n(\bar{\omega}, \alpha)|$ respectively. Thus equating the exponents of the dominating terms of these polynomials (2.42) and (2.43) leads to $\delta/2 = 1/2 - \delta$, that is, $\delta = 1/3$, while equating their coefficients gives $\frac{2C_n\sqrt{2}\sqrt{a}}{\sqrt{k}} + \frac{n\sqrt{2}\sqrt{k}}{\sqrt{a}} = \frac{2\sqrt{2}}{C_n\sqrt{a}}$. Substituting $k = \frac{2aC_n}{n}$ obtained from Lemma 2.4.4 produces

$$\begin{aligned}
& \frac{2\sqrt{2}}{C_n\sqrt{a}} = \frac{2C_n\sqrt{2}\sqrt{a}}{\sqrt{k}} + \frac{n\sqrt{2}\sqrt{k}}{\sqrt{a}} \\
\implies & \frac{2}{C_n\sqrt{a}} = \frac{2C_n a + nk}{\sqrt{k}\sqrt{a}} \\
\implies & \frac{2\sqrt{2}\sqrt{a}\sqrt{C_n}}{C_n\sqrt{n}} = 2C_n a + 2C_n a \\
\implies & \frac{\sqrt{2}\sqrt{a}}{\sqrt{n}} = 2C_n^{3/2} a \\
\implies & C_n^{3/2} = \frac{1}{\sqrt{2}\sqrt{a}\sqrt{n}},
\end{aligned}$$

which on squaring both sides leads to $C_n = \left(\frac{1}{2an}\right)^{1/3}$.

Finally, substituting $\delta = 1/3$ and $C_n = \left(\frac{1}{2an}\right)^{1/3}$ into equation (2.42) results in

$$\begin{aligned}
|\rho_{\min}(\omega_{\min}, \alpha^*_{T,n})| &= 1 - \frac{2^{3/2}}{\sqrt{a}}(2an)^{1/3}\omega_{\min}^{1/6} + \mathcal{O}(\omega_{\min}^{1/3}) \\
&= 1 - 2^{11/6}\left(\frac{n^2}{a}\right)^{1/6}\omega_{\min}^{1/6} + \mathcal{O}(\omega_{\min}^{1/3}).
\end{aligned}$$

This completes the proof. □

2.4.2 Asymptotic analysis with respect to the reaction term

In this section, we assume that $\epsilon \to 0$, where $b = -(2+\epsilon)a$. The main task to be accomplished in this section is to find a solution of the min-max problem (2.25) using asymptotic analysis with respect to $\epsilon \to 0$. As explained earlier, this analysis corresponds to the case when the reaction terms $\epsilon a\hat{\mathbf{u}}$ and $\epsilon a\hat{\mathbf{w}}$ tends to zero. Note that the minimum frequency $\omega_{\min}$ is $\omega_{\min} = \pi/T$, but to further simplify our analysis, we consider a wider range for ω, that is, $\omega \in [0, \omega_{\max}]$. Therefore, our min-max problem (2.25) further changes to

$$\min_{\alpha>0}\left(\max_{0\le\omega\le\omega_{\max}} |\rho_n(\omega, \alpha)|\right). \tag{2.45}$$

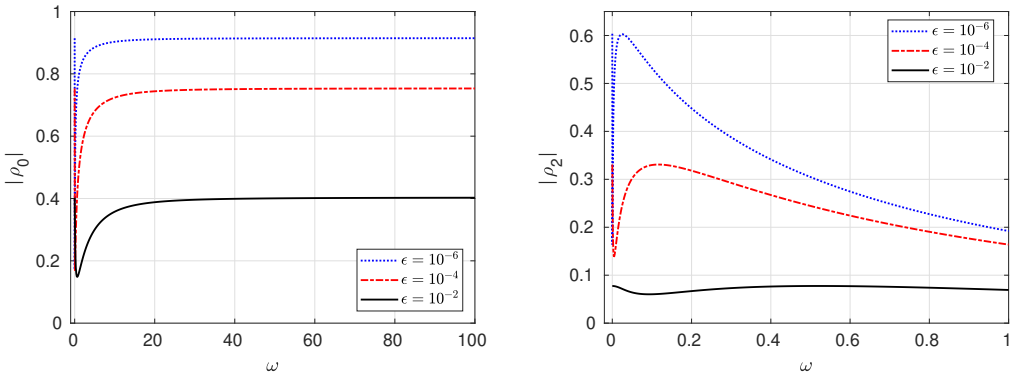

Figure 2.10: Equioscillation for different values of ϵ for $n = 0$ (left) and for $n = 2$ (right).

Note that the frequency range $0 \leq \omega \leq \omega_{\max}$ corresponds to an infinite time interval and hence the results for this asymptotic analysis will hold for infinitely large time intervals. Under the asymtotic $\epsilon \to 0$, we observe numerically, see Figure 2.10, that a solution for the min-max problem (2.45) is given by equioscillation. Moreover, the behavior of equioscillation is different for the nonoverlapping and the overlapping case. We first analyze the nonoverlapping case, that is, $n = 0$, where the equioscillation occurs for $\omega = 0$ and $\omega = \omega_{\max}$ (see the left plot of Figure 2.10). This means the optimized α denoted by $\alpha^*_{R,0}$ satisfies

$$|\rho_0(0, \alpha^*_{R,0})| = |\rho_0(\omega_{\max}, \alpha^*_{R,0})|, \tag{2.46}$$

To start with, we find the explicit expression for $|\rho_0(\omega, \alpha)|$. Next, similar to the analysis in Section 2.4.1, we use the ansatz $\alpha = P_0\epsilon^\gamma$, where $\epsilon = -\frac{b}{a} - 2$ and $P_0, \gamma > 0$. The dependence of $\alpha^*_{R,0}$ on ϵ for $n = 0$ is illustrated numerically in the left plot of Figure 2.11.

Lemma 2.4.6. *For the nonoverlapping OWR method, that is, with $n = 0$ node overlap and for small $\epsilon > 0$, the modulus of the convergence factor $\rho_0(\omega, \alpha)$ for $\omega = 0$ and large $\omega_{\max}$ is given by*

$$|\rho_0(0, \alpha)| = 1 - \frac{4}{P_0}\epsilon^{\frac{1}{2}-\gamma} + \mathcal{O}(\epsilon^{1-2\gamma}) \tag{2.47}$$

and

$$|\rho_0(\omega_{\max}, \alpha)| = 1 - 2P_0\epsilon^\gamma + \mathcal{O}(\epsilon^{2\gamma}). \tag{2.48}$$

Proof. We first find the asymptotic expression for $\lambda_1(0) = x + iy$, where x and y are functions of ϵ. From the expression of $\lambda_1(\omega)$ given in (2.10), and using a Taylor

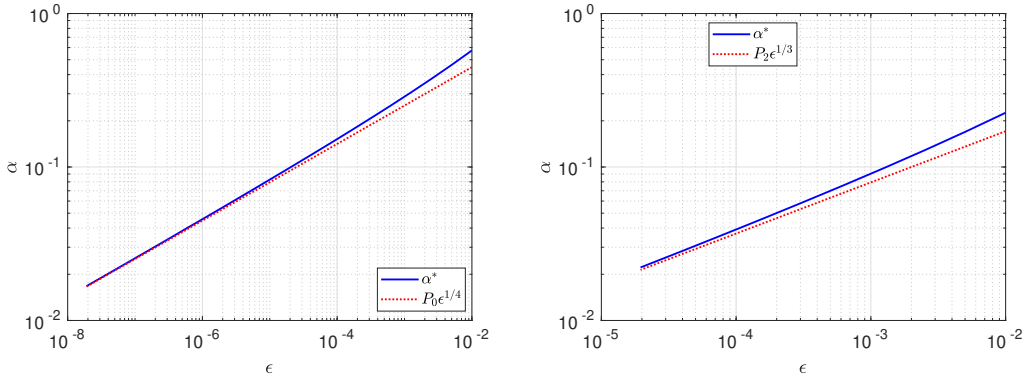

Figure 2.11: Dependence of α^* on ϵ with $P_0 = \sqrt{2}$ for $n = 0$ (left) and with $P_2 = \left(\frac{1}{n}\right)^{1/3}$ for $n = 2$ (right).

expansion for $(1+\epsilon)^{1/2} = 1 + \frac{\epsilon}{2} - \frac{\epsilon^2}{8} + \mathcal{O}(\epsilon^3)$ leads to

$$\begin{aligned}\lambda_1(0) &= \frac{2+\epsilon}{2} + \frac{\sqrt{4\epsilon+\epsilon^2}}{2} = 1 + \frac{\epsilon}{2} + \epsilon^{1/2}\sqrt{1+\frac{\epsilon}{4}} = 1 + \frac{\epsilon}{2} + \epsilon^{1/2}\left(1 + \frac{\epsilon}{8} + \mathcal{O}(\epsilon^2)\right) \\ &= 1 + \epsilon^{1/2} + \frac{\epsilon}{2} + \mathcal{O}(\epsilon^{3/2}).\end{aligned}$$

Thus we have $x = 1 + \epsilon^{1/2} + \frac{\epsilon}{2} + \mathcal{O}(\epsilon^{3/2})$ and $y = 0$. Recall from (2.26),

$$|\rho_0(\omega,\alpha)| = \frac{|\alpha + 1 - \lambda_1|^2}{|(1+\alpha)\lambda_1 - 1|^2} =: \frac{A(\omega,\alpha)}{B(\omega,\alpha)}.$$

Substituting the ansatz $\alpha = P_0\epsilon^\gamma$, we arrive at

$$A(0,\alpha) = \alpha^2 + x^2 + 1 + y^2 - 2x - 2x\alpha + 2\alpha = P_0^2\epsilon^{2\gamma} - 2P_0\epsilon^{\gamma+1/2} + \mathcal{O}(\epsilon),$$

and

$$\begin{aligned}B(0,\alpha) &= x^2 + x^2\alpha^2 + 2\alpha x^2 + 1 - 2x - 2x\alpha + y^2 + y^2\alpha^2 + 2\alpha y^2 \\ &= P_0^2\epsilon^{2\gamma} + 2P_0\epsilon^{\gamma+1/2} + 2P_0^2\epsilon^{2\gamma+1/2} + \mathcal{O}(\epsilon).\end{aligned}$$

Since $\epsilon \to 0$, the term with lowest power of ϵ is the dominating term in these asymptotic expressions, and hence $P_0^2\epsilon^{2\gamma}$ is the dominating term in $A(0,\alpha)$ and $B(0,\alpha)$. The convergence factor at $\omega = 0$ simplifies to

$$\begin{aligned}|\rho_0(0,\alpha)| &= \frac{A(0,\alpha)}{B(0,\alpha)} = \frac{P_0^2\epsilon^{2\gamma}\left(1 - \frac{2}{P_0}\epsilon^{1/2-\gamma} + \mathcal{O}(\epsilon^{1-2\gamma})\right)}{P_0^2\epsilon^{2\gamma}\left(1 + \frac{2}{P_0}\epsilon^{1/2-\gamma} + 2\epsilon^{1/2} + \mathcal{O}(\epsilon^{1-2\gamma})\right)} \\ &= \left(1 - \frac{2}{P_0}\epsilon^{1/2-\gamma} + \mathcal{O}(\epsilon^{1-\gamma})\right)\left(1 - \frac{2}{P_0}\epsilon^{1/2-\gamma} + \mathcal{O}(\epsilon^{1/2})\right) \\ &= 1 - \frac{4}{P_0}\epsilon^{1/2-\gamma} + \mathcal{O}(\epsilon^{1/2}).\end{aligned}$$

For large ω, we have large $|\lambda(\omega)|$, and hence it is easier to find an expression for $|\rho_0(\omega_{\max}, \alpha)|$ with the assumption $\omega_{\max} \to \infty$,

$$\begin{aligned} |\rho_0(\omega_{\max}, \alpha)| &= \lim_{\omega\to\infty} \frac{A(\omega,\alpha)}{B(\omega,\alpha)} = \lim_{\omega\to\infty} \left| \frac{\frac{\alpha+1}{\lambda_1(\omega)} - 1}{1+\alpha-\frac{1}{\lambda_1(\omega)}} \right|^2 = \left| \frac{1}{1+\alpha} \right|^2 = \frac{1}{1+2P_0\epsilon^\gamma + P_0^2\epsilon^{2\gamma}} \\ &= 1 - 2P_0\epsilon^\gamma + \mathcal{O}(\epsilon^{2\gamma}), \end{aligned}$$

which concludes the proof. □

Theorem 2.4.3. *For the nonoverlapping OWR, that is, for $n = 0$ and small $\epsilon > 0$, if $\alpha^*_{R,0} = \sqrt{2}\epsilon^{1/4}$, then the convergence factor ρ_0 satisfies*

$$|\rho_0(\omega, \alpha)| \le |\rho_0(0, \alpha^*_{R,0})| \sim 1 - 2\sqrt{2}\epsilon^{1/4} + \mathcal{O}(\epsilon^{1/2}). \tag{2.49}$$

Proof. For the nonoverlapping case, the solution of the min-max problem (2.45) is given by equioscillation for $\omega = 0$ and $\omega = \omega_{\max}$, see the left plot of Figure 2.10. Further, in Lemma 2.4.6 we have derived the asymptotic polynomial expressions for $|\rho_0(0, \alpha)|$ and $|\rho_0(\omega_{\max}, \alpha)|$ which are equal for $\alpha^*_{R,0}$. Thus, comparing the powers of the dominating terms of these expressions results in $\frac{1}{2} - \gamma = \gamma$ which implies $\gamma = \frac{1}{4}$. Now, equating the coefficients of these dominating terms gives $P_0 = \sqrt{2}$ and this completes the proof. □

Similar to the analysis in Section 2.4.1, the analysis is different for the overlapping case $n > 0$. Numerically, we observe that the solution of the min-max problem (2.45) is also given by equioscillation, see the right plot of Figure 2.10. But in this case, equioscillation for $|\rho_n(\omega, \alpha)|$ occurs for $\omega = 0$ and $\omega = \bar{\omega}$, where $\omega_{\min} < \bar{\omega} < \omega_{\max}$ with $\bar{\omega} \to 0$ as $\epsilon \to 0$. The dependence of the optimized α^* and $\bar{\omega}$ on ϵ for $n = 2$ can be seen in the right plot of Figure 2.11 and in Figure 2.12. We therefore use the ansatz $\alpha = P_n\epsilon^\delta$ and $\bar{\omega} = d_n\epsilon^\eta$, for some constants $P_n, \delta, d_n, \eta > 0$. The constants P_n and d_n depends on number of overlapping circuit elements n. Solving the min-max problem (2.45) by equioscillation is equivalent to solving the system of equations

$$|\rho_n(0, \alpha^*_{R,n})| = |\rho_n(\bar{\omega}, \alpha^*_{R,n})| \quad \text{and} \quad \frac{\partial}{\partial\omega}|\rho(\bar{\omega}, \alpha^*_{R,n})| = 0, \tag{2.50}$$

where $\alpha^*_{R,n}$ is the optimized α for an overlap of size n. The approach of solving these coupled equations is similar to that used in Section 2.4.1. However, one needs to be careful since the dominating terms will change.

We first solve the equation $\frac{\partial}{\partial\omega}|\rho(\bar{\omega}, \alpha^*_n)| = 0$ and find a relation between $\bar{\omega}$ and $\alpha^*_{R,n}$.

Lemma 2.4.7. *For the overlapping case, $n > 0$, solving $\frac{\partial}{\partial\omega}|\rho(\bar{\omega}, \alpha^*_{R,n})| = 0$ gives us the relation*

$$\eta = \gamma \quad \text{and} \quad d_n = \frac{2a}{n} P_n, \tag{2.51}$$

where $\bar{\omega} = d_n\epsilon^\eta$ and $\alpha^*_{R,n} = P_n\epsilon^\gamma$.

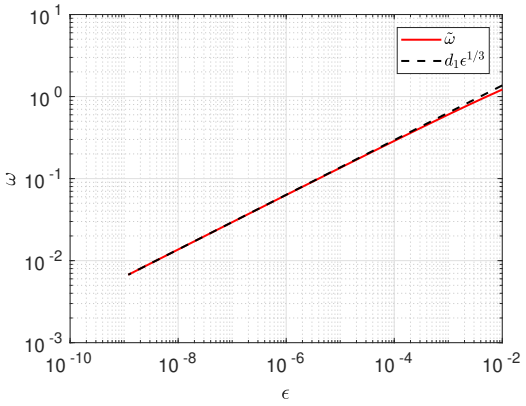

Figure 2.12: Dependence of $\bar{\omega}$ on ϵ with $d_1 = 2a$ for $n = 1$.

Proof. We recall the expression for the convergence factor (2.35) for the OWR algorithm with n overlap,

$$|\rho_n(\omega,\alpha)| = \left|\left(\frac{\alpha+1-\lambda_1}{(1+\alpha)\lambda_1-1}\right)^2\left(\frac{1}{\lambda_1^2}\right)^n\right| = |\rho_0(\omega,\alpha)|\left|\left(\frac{1}{\lambda_1^2}\right)^n\right| = \frac{A(\omega,\alpha)}{B(\omega,\alpha)}L(\omega,\alpha),$$

where $\lambda_1 = x + iy$ and the expressions of $A(\omega,\alpha)$, $B(\omega,\alpha)$ and $L(\omega,\alpha)$ are given by equations (2.36)-(2.38). We now derive polynomial expressions for x and y in terms of ϵ. Recall from the proof of Lemma 2.4.2, we defined $x = \frac{(2+\epsilon)a+z_1}{2a}$ and $y = \frac{\omega+z_2}{2a}$, where $z_1 + iz_2 = \sqrt{(\epsilon^2a^2 - \omega^2 + 4\epsilon a^2) + i[2(2+\epsilon)\omega a]}$. Squaring both sides and comparing the real and imaginary parts yields

$$z_1^2 - z_2^2 = r_1 \quad \text{and} \quad 2z_1z_2 = r_2,$$

where $r_1 := \epsilon^2a^2 - \omega^2 + 4\epsilon a^2$ and $r_2 := 2(2+\epsilon)\omega a$. The second equation simplifies to $z_2 = \frac{r_2}{2z_1}$, which on substitution into the first equation results in $4z_1^4 - 4z_1^2r_1 - r_2^2 = 0$. The positive root of this equation is given by $z_1^2 = \frac{r_1+\sqrt{r_1^2+r_2^2}}{2}$. A Taylor expansion for $(1+y)^{1/2}$, with $|y| < 1$, leads to

$$\begin{aligned}
\sqrt{r_1^2+r_2^2} &= \sqrt{(-\omega^2+4a^2\epsilon+a^2\epsilon^2)^2 + 4\omega^2a^2(2+\epsilon)^2} \\
&= \sqrt{16a^2\omega^2+\omega^4+8\omega^2a^2\epsilon+\mathcal{O}(\epsilon^2)} = 4\omega a\sqrt{1+\left(\frac{\omega^2}{16a^2}+\frac{\epsilon}{2}+\mathcal{O}(\epsilon^2\omega^{-2})\right)} \\
&= 4\omega a\left(1+\frac{\omega^2}{32a^2}+\frac{\epsilon}{4}+\mathcal{O}(\omega^4)\right) = 4\omega a + \frac{\omega^3}{8a} + \omega a\epsilon + \mathcal{O}(\omega^5).
\end{aligned}$$

Similarly, we obtain expressions for z_1 and z_2,

$$\begin{aligned} z_1 &= \sqrt{\frac{r_1+\sqrt{r_1^2+r_2^2}}{2}} = \sqrt{\frac{a^2\epsilon^2+4a^2\epsilon-\omega^2+4\omega a+\frac{\omega^3}{8a}+a\omega\epsilon+\mathcal{O}(\omega^5)}{2}} \\ &= \sqrt{2\omega a-\frac{\omega^2}{2}+\frac{\omega^3}{16a}+2a^2\epsilon+\frac{a\omega\epsilon}{2}+\mathcal{O}(\omega^5)} \\ &= \sqrt{2a\omega}\sqrt{1-\frac{\omega}{4a}+\frac{\omega^2}{32a^2}+\frac{a\epsilon}{\omega}+\frac{\epsilon}{4}+\mathcal{O}(\omega^4)} \\ &= \sqrt{2a\omega}\left(1-\frac{\omega}{8a}+\frac{\omega^2}{128a^2}+\mathcal{O}(\omega^3)\right) \\ &= \sqrt{2a\omega}-\frac{\sqrt{2}\omega^{3/2}}{8\sqrt{a}}+\frac{\sqrt{2}\omega^{5/2}}{128a^{3/2}}+\mathcal{O}(\omega^{7/2}), \end{aligned}$$

and

$$\begin{aligned} z_2 &= \frac{r_2}{2z_1} = \frac{2(2+\epsilon)\omega a}{2\sqrt{2a\omega}\left(1-\frac{\omega}{8a}+\frac{\omega^2}{128a^2}+\mathcal{O}(\omega^3)\right)} \\ &= (\sqrt{2}\sqrt{\omega}\sqrt{a}+\frac{\epsilon\sqrt{\omega}\sqrt{a}}{\sqrt{2}})\left(1+\frac{\omega}{8a}+\mathcal{O}(\omega^3)\right) \\ &= \sqrt{2a\omega}+\frac{\sqrt{2}\omega^{3/2}}{8\sqrt{a}}+\frac{\epsilon\sqrt{\omega}\sqrt{a}}{\sqrt{2}}+\mathcal{O}(\omega^{7/2}). \end{aligned}$$

Substituting these into the expressions for x and y leads to

$$\begin{aligned} x &= 1+\frac{\epsilon}{2}+\frac{z_1}{2a} = 1+\frac{\sqrt{2}\sqrt{\omega}}{2\sqrt{a}}-\frac{\sqrt{2}\omega^{3/2}}{16a^{3/2}}+\mathcal{O}(\omega^{5/2}), \\ y &= \frac{\omega+z_2}{2a} = \frac{\sqrt{2}\sqrt{\omega}}{2\sqrt{a}}+\frac{\omega}{2a}+\frac{\sqrt{2}\omega^{3/2}}{16a^{3/2}}+\mathcal{O}(\omega^{5/2}). \end{aligned}$$

We substitute these expressions for x, y and the ansatz $\alpha = P_n\epsilon^\gamma$ into equations (2.36)-(2.38),

$$\begin{aligned} A(\omega,\alpha) &= \tfrac{\omega}{a}-\tfrac{\sqrt{2}P_n\epsilon^\gamma\sqrt{\omega}}{\sqrt{a}}+\tfrac{\sqrt{2}\omega^{3/2}}{2a^{3/2}}+\mathcal{O}(\omega^2), \\ B(\omega,\alpha) &= \tfrac{\omega}{a}+\tfrac{\sqrt{2}P_n\epsilon^\gamma\sqrt{\omega}}{\sqrt{a}}+\tfrac{\sqrt{2}\omega^{3/2}}{2a^{3/2}}+\mathcal{O}(\omega^2), \end{aligned} \tag{2.52}$$

and

$$\begin{aligned} L(\omega,\alpha) &= \left(\frac{1}{x^2+y^2}\right)^n = \left(\frac{1}{1+\frac{\sqrt{2}\sqrt{\omega}}{\sqrt{a}}+\frac{\omega}{a}+\frac{3\sqrt{2}\omega^{3/2}}{8a^{3/2}}+\mathcal{O}(\omega^2)}\right)^n \\ &= 1-\frac{n\sqrt{2}\sqrt{\omega}}{\sqrt{a}}-\frac{n\omega}{a}+\frac{n^2\omega}{a}+\mathcal{O}(\omega^{3/2}). \end{aligned} \tag{2.53}$$

Further, differentiating $|\rho_n(\omega,\alpha)| = \frac{A(\omega,\alpha)}{B(\omega,\alpha)}L(\omega,\alpha)$ with respect to ω gives

$$\frac{\partial}{\partial\omega}|\rho_n(\omega,\alpha)| = \frac{B(\omega,\alpha)[A(\omega,\alpha)L_\omega(\omega,\alpha) + A_\omega(\omega,\alpha)L(\omega,\alpha)] - A(\omega,\alpha)L(\omega,\alpha)B_\omega(\omega,\alpha)}{B^2(\omega,\alpha)},$$

where $Z_\omega(\omega,\alpha)$ denotes the partial derivative of $Z(\omega,\alpha)$ with respect to ω. Let

$$F_1(\omega,\alpha) := B(\omega,\alpha)[A(\omega,\alpha)L_\omega(\omega,\alpha) + A_\omega(\omega,\alpha)L(\omega,\alpha)]$$

and

$$F_2(\omega,\alpha) := A(\omega,\alpha)L(\omega,\alpha)B_\omega(\omega,\alpha).$$

Differentiating these terms given in equations (2.52)-(2.53) with respect to ω gives

$$\begin{aligned} A_\omega(\omega,\alpha) &= \tfrac{1}{a} - \tfrac{\sqrt{2}P_n\epsilon^\gamma}{2\sqrt{a}\sqrt{\omega}} + \mathcal{O}(\omega^{1/2}),\\ B_\omega(\omega,\alpha) &= \tfrac{1}{a} + \tfrac{\sqrt{2}P_n\epsilon^\gamma}{2\sqrt{a}\sqrt{\omega}} + \mathcal{O}(\omega^{1/2}),\\ L_\omega(\omega,\alpha) &= 1 - \tfrac{n\sqrt{2}}{2\sqrt{a}\sqrt{\omega}} - \tfrac{n}{a} + \tfrac{n^2}{a} + \mathcal{O}(\omega^{1/2}). \end{aligned} \tag{2.54}$$

Substituting these expressions into $F_1(\omega,\alpha)$ and $F_2(\omega,\alpha)$, we arrive at

$$\begin{aligned} F_1(\omega,\alpha) &= \left(\frac{\omega}{a} + \frac{\sqrt{2}P_n\epsilon^\gamma\sqrt{\omega}}{\sqrt{a}} + \mathcal{O}(\omega^{3/2})\right)(A(\omega,\alpha)L_\omega(\omega,\alpha) + A_\omega(\omega,\alpha)L(\omega,\alpha))\\ &= \left(\frac{\omega}{a} + \frac{\sqrt{2}P_n\epsilon^\gamma\sqrt{\omega}}{\sqrt{a}} + \mathcal{O}(\omega^{3/2})\right)\left(\frac{1}{a} - \frac{3n\sqrt{2}\sqrt{\omega}}{2a^{3/2}} - \frac{P_n\epsilon^\gamma\sqrt{2}}{2\sqrt{a}\sqrt{\omega}} + \mathcal{O}(\omega)\right)\\ &= \frac{P_n\epsilon^\gamma\sqrt{2}\sqrt{\omega}}{2a^{3/2}} + \frac{\omega}{a^2} - \frac{3n\sqrt{2}\omega^{3/2}}{2a^{5/2}} + \mathcal{O}(\omega^2), \end{aligned}$$

and

$$\begin{aligned} F_2(\omega,\alpha) &= (A(\omega,\alpha)L(\omega,\alpha)\left(\frac{1}{a} + \frac{\sqrt{2}P_n\epsilon^\gamma}{2\sqrt{a}\sqrt{\omega}} + \mathcal{O}(\omega^{1/2})\right)\\ &= \left(-\frac{P_n\epsilon^\gamma\sqrt{2}\sqrt{a\omega}}{a} + \frac{\omega}{a} - \frac{n\sqrt{2}\omega^{3/2}}{a^{3/2}} + \mathcal{O}(\omega^2)\right)\left(\frac{1}{a} + \frac{\sqrt{2}P_n\epsilon^\gamma}{2\sqrt{a}\sqrt{\omega}} + \mathcal{O}(\omega^{1/2})\right)\\ &= -\frac{P_n\epsilon^\gamma\sqrt{2}\sqrt{\omega}}{a^{3/2}} + \frac{\omega}{a^2} - \frac{n\sqrt{2}\omega^{3/2}}{a^{5/2}} + \mathcal{O}(\omega^2). \end{aligned}$$

Finally, we equate $F_1(\bar{\omega},\alpha) = F_2(\bar{\omega},\alpha)$ to obtain $\frac{P_n\epsilon^\gamma\sqrt{2}\bar{\omega}^{1/2}}{a^{3/2}} = \frac{n\sqrt{2}\bar{\omega}^{3/2}}{2a^{5/2}}$. Since we use the ansatz $\bar{\omega} = d_n\epsilon^\eta$, comparing the exponents of the above terms simplifies to $\gamma + \eta/2 = 3\gamma/2$, that is, $\gamma = \eta$. Similarly, a comparison of their coefficients leads to

$$\frac{P_n\sqrt{2}d_n^{1/2}}{a^{3/2}} = \frac{n\sqrt{2}d_n^{3/2}}{2a^{5/2}},$$

which results in $d_n = \frac{2a}{n}P_n$. This completes the proof. □

Now we need to solve the first equation of (2.50), $|\rho_n(0,\alpha^*_{R,n})| = |\rho_n(\bar{\omega},\alpha^*_{R,n})|$. We do this in a similar way as for the nonoverlapping case, $n = 0$. We express $|\rho_n(0,\alpha^*_{R,n})|$ and $|\rho_n(\bar{\omega},\alpha^*_{R,n})|$ as asymptotic expansions in ϵ.

Lemma 2.4.8. *For the overlapping case, $n > 0$, the modulus of the convergence factor $|\rho_n(\omega,\alpha)|$ for the OWR algorithm for $\omega = 0$ and $\omega = \bar{\omega}$ is for small ϵ given by*

$$|\rho_n(0,\alpha)| = 1 - \frac{4}{P_n}\epsilon^{\frac{1}{2}-\gamma} + \mathcal{O}(\epsilon^{1-2\gamma}), \tag{2.55}$$

and

$$|\rho_n(\bar{\omega},\alpha)| = 1 - \frac{2\sqrt{2}P_n\sqrt{a}\epsilon^{\gamma/2}}{\sqrt{d_n}} - \frac{n\sqrt{2}\sqrt{d_n}\epsilon^{\gamma/2}}{\sqrt{a}} + \mathcal{O}(\epsilon^{\gamma}). \tag{2.56}$$

Proof. From the polynomial expansion of $L(\omega,\alpha)$ given in (2.53), we observe that $L(0,\alpha) = \left|\left(\frac{1}{\lambda_1^2(0)}\right)^n\right| = 1$. Substituting this into the formula for the convergence factor (2.35) for OWR with n overlap leads to $|\rho_n(0,\alpha)| = |\rho_0(0,\alpha)|\left|\left(\frac{1}{\lambda_1^2(0)}\right)^n\right| = |\rho_0(0,\alpha)|$ and equation (2.47) results in

$$|\rho_n(0,\alpha)| = 1 - \frac{4}{P_n}\epsilon^{\frac{1}{2}-\gamma} + \mathcal{O}(\epsilon^{1-2\gamma}).$$

The analysis to find the expression for $|\rho_n(\bar{\omega},\alpha)|$ is similar. Substituting $\bar{\omega} = d_n\epsilon^{\gamma}$ into the expressions for $A(\omega,\alpha)$ and $B(\omega,\alpha)$ given in (2.52) leads to

$$\begin{aligned}
A(\bar{\omega},\alpha) &= \frac{\bar{\omega}}{a} - \frac{\sqrt{2}P_n\epsilon^{\gamma}\sqrt{\bar{\omega}}}{\sqrt{a}} + \frac{\sqrt{2}\bar{\omega}^{3/2}}{2a^{3/2}} + \mathcal{O}(\bar{\omega}^2)\\
&= \frac{d_n\epsilon^{\gamma}}{a} - \frac{\sqrt{2}P_n\sqrt{d_n}\epsilon^{3\gamma/2}}{\sqrt{a}} + \frac{d_n^{3/2}\epsilon^{3\gamma/2}}{\sqrt{2}a^{3/2}} + \mathcal{O}(\epsilon^{2\gamma})\\
&= \frac{d_n\epsilon^{\gamma}}{a}\left(1 - \frac{\sqrt{2}P_n\sqrt{a}\epsilon^{\gamma/2}}{\sqrt{d_n}} + \frac{\sqrt{d_n}\epsilon^{\gamma/2}}{\sqrt{2}\sqrt{a}} + \mathcal{O}(\epsilon^{\gamma})\right),\\
B(\bar{\omega},\alpha) &= \frac{\bar{\omega}}{a} + \frac{\sqrt{2}P_n\epsilon^{\gamma}\sqrt{\bar{\omega}}}{\sqrt{a}} + \frac{\sqrt{2}\bar{\omega}^{3/2}}{2a^{3/2}} + \mathcal{O}(\bar{\omega}^2)\\
&= \frac{d_n\epsilon^{\gamma}}{a} + \frac{\sqrt{2}P_n\sqrt{d_n}\epsilon^{3\gamma/2}}{\sqrt{a}} + \frac{d_n^{3/2}\epsilon^{3\gamma/2}}{\sqrt{2}a^{3/2}} + \mathcal{O}(\epsilon^{5\gamma/2})\\
&= \frac{d_n\epsilon^{\gamma}}{a}\left(1 + \frac{\sqrt{2}P_n\sqrt{a}\epsilon^{\gamma/2}}{\sqrt{d_n}} + \frac{\sqrt{d_n}\epsilon^{\gamma/2}}{\sqrt{2}\sqrt{a}} + \mathcal{O}(\epsilon^{\gamma})\right).
\end{aligned}$$

Dividing $A(\bar{\omega},\alpha)$ by $B(\bar{\omega},\alpha)$ and using the Taylor expansion $\frac{1}{1+z} = 1 - z + \frac{z^2}{2} + \mathcal{O}(z^3)$ gives us

$$\begin{aligned}\frac{A(\bar{\omega},\alpha)}{B(\bar{\omega},\alpha)} &= \left(1 - \frac{\sqrt{2}P_n\sqrt{a}\epsilon^{\gamma/2}}{\sqrt{d_n}} + \frac{\sqrt{d_n}\epsilon^{\gamma/2}}{\sqrt{2}\sqrt{a}} + +\mathcal{O}(\epsilon^{\gamma})\right) \\ &\qquad \left(1 - \frac{\sqrt{2}P_n\sqrt{a}\epsilon^{\gamma/2}}{\sqrt{d_n}} - \frac{\sqrt{d_n}\epsilon^{\gamma/2}}{\sqrt{2}\sqrt{a}} + +\mathcal{O}(\epsilon^{\gamma})\right) \\ &= 1 - \frac{2\sqrt{2}P_n\sqrt{a}\epsilon^{\gamma/2}}{\sqrt{d_n}} + \mathcal{O}(\epsilon^{\gamma}).\end{aligned}$$

Similarly, from the equation (2.53) we obtain the expression for $L(\bar{\omega},\alpha)$; namely

$$L(\bar{\omega},\alpha) = 1 - \frac{n\sqrt{2}\bar{\omega}^{1/2}}{\sqrt{a}} - \frac{n\bar{\omega}}{a} + \frac{n^2\bar{\omega}}{a} + \mathcal{O}(\bar{\omega}^{3/2}) = 1 - \frac{n\sqrt{2}\sqrt{d_n}\epsilon^{\gamma/2}}{\sqrt{a}} + \mathcal{O}(\epsilon^{\gamma}).$$

Multiplying the above expression by the expansion for $\frac{A(\bar{\omega},\alpha)}{B(\bar{\omega},\alpha)}$, we find

$$\begin{aligned}|\rho_n(\bar{\omega},\alpha)| &= \left(1 - \frac{2\sqrt{2}P_n\sqrt{a}\epsilon^{\gamma/2}}{\sqrt{d_n}} + \mathcal{O}(\epsilon^{\gamma})\right)\left(1 - \frac{n\sqrt{2}\sqrt{d_n}\epsilon^{\gamma/2}}{\sqrt{a}} + \mathcal{O}(\epsilon^{\gamma})\right) \\ &= 1 - \frac{2\sqrt{2}P_n\sqrt{a}\epsilon^{\gamma/2}}{\sqrt{d_n}} - \frac{n\sqrt{2}\sqrt{d_n}\epsilon^{\gamma/2}}{\sqrt{a}} + \mathcal{O}(\epsilon^{\gamma}),\end{aligned}$$

which completes the proof. □

We are now ready to prove a remarkably simple formula for the optimized parameter depending on the overlap $n > 0$ which is quite different from the nonoverlapping case:

Theorem 2.4.4. *For the OWR algorithm in the overlapping case, $n > 0$, and for small $\epsilon > 0$, if $\alpha^*_{R,n} = \left(\frac{\epsilon}{n}\right)^{1/3}$, then the convergence factor ρ_n satisfies*

$$|\rho_n(\omega,\alpha)| \leq |\rho_n(0,\alpha^*_{R,n})| \sim 1 - 4n^{1/3}\epsilon^{1/6} + \mathcal{O}(\epsilon^{1/3}). \tag{2.57}$$

Proof. Since the solution of our min-max problem (2.45) is obtained numerically by equioscillation for $\omega = 0$ and $\omega = \bar{\omega}$, we equate the expansions for $|\rho_n(0,\alpha)|$ and $|\rho_n(\bar{\omega},\alpha)|$ given by (2.55) and (2.56). Comparing the exponents and coefficients of their dominating terms, we obtain

$$\frac{\gamma}{2} = \frac{1}{2} - \gamma \quad \text{and} \quad \frac{4}{P_n} = \frac{2\sqrt{2}P_n\sqrt{a}}{\sqrt{d_n}} + \frac{n\sqrt{2}\sqrt{d_n}}{\sqrt{a}}.$$

The first equation implies that $\gamma = 1/3$, and substituting the expression for d_n given by (2.51) results in

$$\begin{aligned}\frac{4}{P_n} &= \frac{2\sqrt{2}P_n a + n\sqrt{2}d_n}{\sqrt{a}\sqrt{d_n}} = \frac{2\sqrt{2}P_n a + 2\sqrt{2}P_n a}{\sqrt{2}\sqrt{P_n a}}\sqrt{n} \\ &= 4\sqrt{n}\sqrt{P_n},\end{aligned}$$

that is, $P_n = \left(\frac{1}{n}\right)^{1/3}$. Substituting $Pn = \left(\frac{1}{n}\right)^{1/3}$ and $\gamma = 1/3$ in (2.55) gives us (2.57) and this completes the proof. □

2.5 Multiple Sub-circuits

We studied so far only the decomposition of the system of equations (2.1) into only two sub-systems. However, for the practical use on parallel computers, we need to split the system into many subsystems and apply the WR or OWR algorithm to them. We thus split the RC circuit of infinite length in Figure 2.2 into N_s subcircuits which are denoted by $\mathbf{v}_r$, $r = 1, 2, \ldots, N_s$. Assume that each sub-circuit $\mathbf{v}_r$ contains M_r nodes. Applying the OWR algorithm (with α, β as the optimization parameters) with n nodes overlap leads to

$$\begin{aligned}
\tfrac{d}{dt}\mathbf{v}_1^{k+1}(t) &= \begin{bmatrix} \ddots & \ddots & \ddots & \\ & a & b & a \\ & & a & b + \frac{a}{\alpha+1} \end{bmatrix} \mathbf{v}_1^{k+1}(t) + \begin{bmatrix} \vdots \\ 0 \\ a v_{2,n+1}^k(t) - \frac{a}{\alpha+1} v_{2,n}^k(t) \end{bmatrix}, \\
\tfrac{d}{dt}\mathbf{v}_r^{k+1}(t) &= \begin{bmatrix} b - \frac{a}{\beta-1} & a & & \\ a & b & a & \\ & \ddots & \ddots & \ddots \\ & & a & b + \frac{a}{\alpha+1} \end{bmatrix} \mathbf{v}_r^{k+1}(t) + \begin{bmatrix} a v_{r-1,M_r}^k(t) + \frac{a}{\beta-1} v_{r-1,M_r+1}^k(t) \\ 0 \\ \vdots \\ 0 \\ a v_{r+1,n+1}^k(t) - \frac{a}{\alpha+1} v_{r+1,n}^k(t) \end{bmatrix}, \\
\tfrac{d}{dt}\mathbf{v}_{N_s}^{k+1}(t) &= \begin{bmatrix} b - \frac{a}{\beta-1} & a & & \\ a & b & a & \\ & \ddots & \ddots & \ddots \end{bmatrix} \mathbf{v}_{N_s}^{k+1}(t) + \begin{bmatrix} a v_{N_s-1,M_r}^k(t) + \frac{a}{\beta-1} v_{N_s-1,M_r+1}^k(t) \\ 0 \\ \vdots \end{bmatrix},
\end{aligned} \tag{2.58}$$

where $r = 2, 3, \ldots, N_s - 1$ and we have considered the source term $\mathbf{f} = 0$ for simplicity. For $\alpha = \infty$, $\beta = -\infty$, we obtain the classical WR algorithm. Note that one can use different sets of α_i and β_i at different interfaces, but this will make the analysis complicated and hence we stick to the same α and β.

In the case of OWR for two subdomains, we saw that with the optimal transmission conditions (2.23), convergence is achieved in 2 iterations and the parameters α, β represent non-local operators in time. In the case of N_s sub-circuits, with the use of optimal transmission conditions, one can show that convergence can be achieved in N_s iterations [37], and this result still holds in the overlapping case. Again these

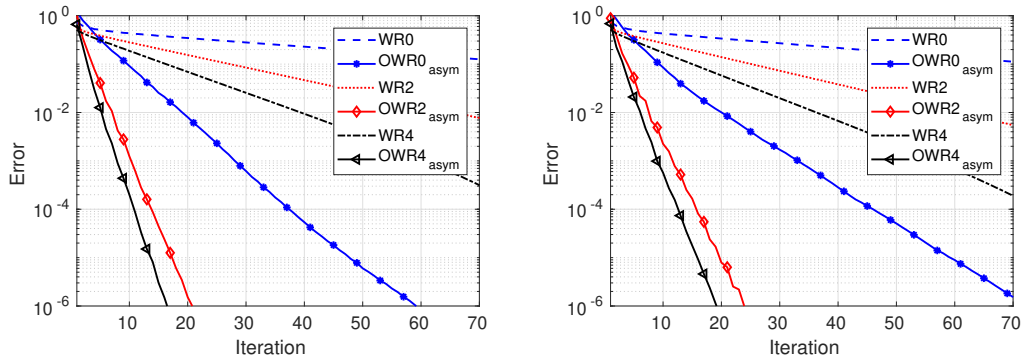

Figure 2.13: Effect of overlap for time $T = 2000$ with $\omega_{\min} \to 0$ and $\epsilon = 0$ (left) and with $\epsilon = 10^{-4}$ (right)

parameters α, β are non-local operators in time and the analysis becomes very complicated. Depending on the choice of asymptotic analysis, we will either use $\alpha^*_{T,0}$ and $\alpha^*_{T,n}$ given in Theorem 2.4.1 and Theorem 2.4.2 respectively or $\alpha^*_{R,0}$ and $\alpha^*_{R,n}$ given in Theorem 2.4.3 and Theorem 2.4.4 respectively, from our two sub-circuit analysis and test their performance numerically for the multiple sub-circuit case.

2.6 Numerical Results

We support now our theoretical and asymptotic results with numerical experiments. Throughout these experiments, we shall consider $R = 0.5k\Omega$, $C = 0.63pF$ and $a = \frac{1}{RC}$. Note that our analysis is for infinitely long RC circuits, but due to the computational cost and processor memory limitations, we consider the length of the circuit $N = 100$ or $N = 200$, depending on the numerical test to be performed. Further, in all these numerical experiments, we consider homogeneous source terms, zero initial conditions and random initial guess for both WR and OWR algorithms, and thus simulate directly for the error equations. We consider both WR and OWR algorithms for the two subdomain case, that is, the circuit is split into only two subcircuits. For time integration, we consider the backward Euler scheme with $\Delta t = 0.1$ and final time $T = 2000$. In both plots of Figure 2.13 we clearly observe the effect of optimized transmission conditions (2.16) on the WR algorithm. The thick lines depict the error plots of the OWR algorithm for different overlaps, $n = 0, 2, 4$, while the other lines depict the error for the classical WR algorithm. For the OWR algorithm, we use the optimized α^* derived by both asymptotic analyses, that is, $\omega_{\min} \to 0$ and $\epsilon \to 0$. We observe numerically that the OWR algorithm is faster than the classical WR algorithm. These plots also show that increasing the number of overlapping circuit elements increases the rate of convergence.

We next compare the numerically and asymptotically optimized values of α^*_n. The numerically optimized α^*_n is found by two different approaches: for $n = 0$, we fix the

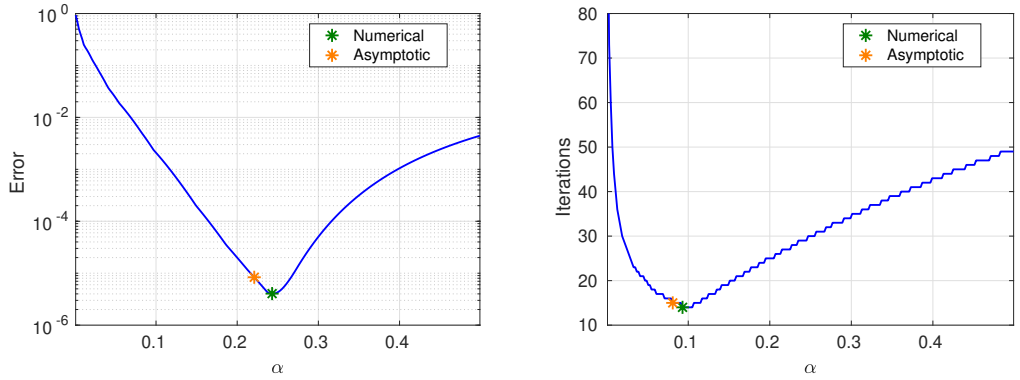

Figure 2.14: Comparison of optimized $\alpha^*_{T,n}$ with $T = 1000$ for $n = 0$ (left) and $n = 1$ (right)

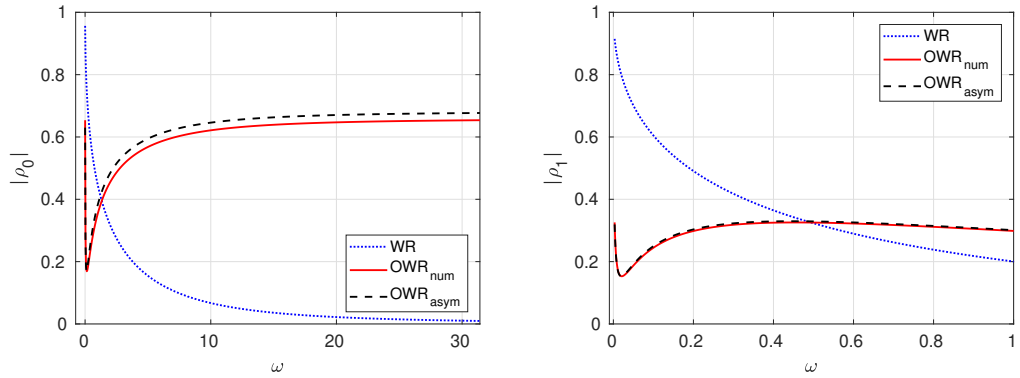

Figure 2.15: Convergence factor in the Laplace space for optimal $\alpha^*_{T,n}$ for $n = 0$ (left) and $n = 1$ (right) for asymptotic analysis with respect to $\omega_{\min} \to 0$.

number of iterations to 50 and find the error of the OWR algorithm for different values of α at the end of 50 iterations. The left plot of Figure 2.14 illustrates this approach, while the right plot depicts the other approach for $n = 1$. In this second approach, for each value of α, we note down the number of iterations required to reach the error to 10^{-4}. In this approach, since the number of iterations is discrete, we observe that the plot has step functions, while it is continuous in the case of the first approach. The asymptotic values of α^* are found by using the asymptotic expressions for $\alpha^*_{T,n}$ derived in Theorem 2.4.1 and 2.4.2 respectively, which are derived for asymptotic analysis with respect to $\omega_{\min} \to 0$ with $\epsilon = 0$. Next, we plot the modulus of the convergence factor $|\rho_n(\omega, \alpha^*_{T,n})|$ in the Laplace space. Both plots of Figure 2.15 show the improvement in the convergence factor by using the optimized transmission conditions. They also show that the convergence plots are very close to each other when the optimized $\alpha^*_{T,n}$ is found numerically or by asymptotic expressions. In the left plot of Figure 2.16, we compare the number of iterations by OWR to reach

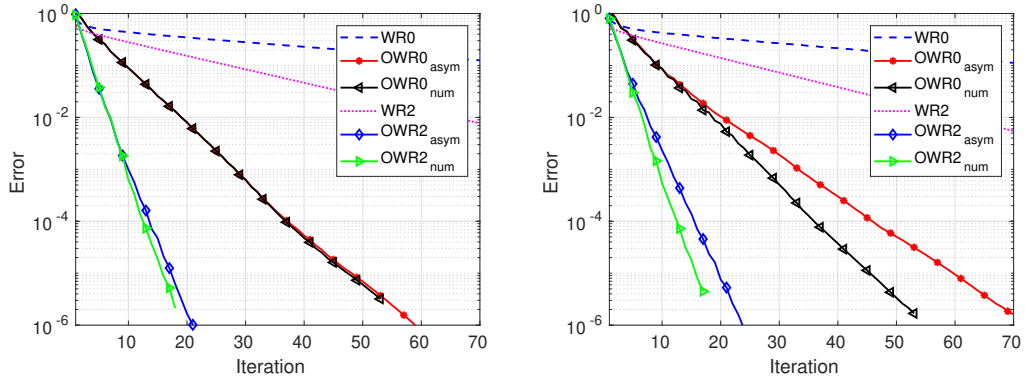

Figure 2.16: Convergence for $T = 2000$ for numerically and asymptotically optimized α_n^* using asymptotes $\omega_{\min} \to 0$ with $\epsilon = 0$ (left) and $\epsilon \to 0$ with $\epsilon = 10^{-4}$ (right)

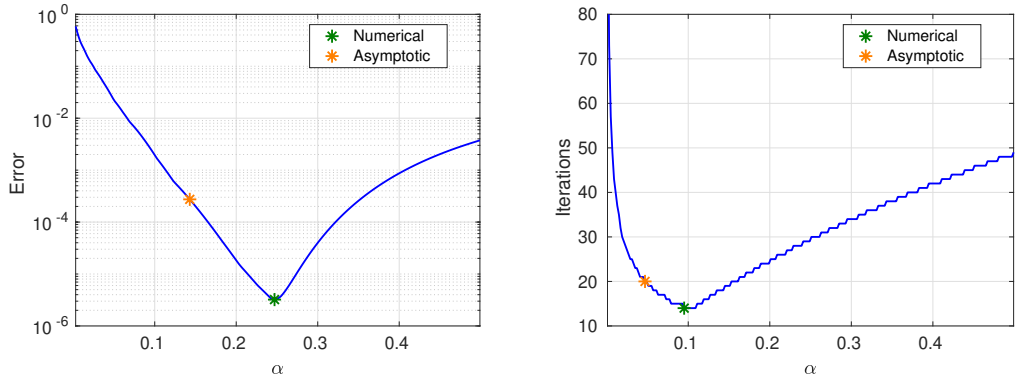

Figure 2.17: Comparison of optimized $\alpha_{R,n}^*$ for $T = 1000$ with $\epsilon = 10^{-4}$ and $n = 0$ (left) and for $n = 1$ (right)

an error of 10^{-6} using the values of the optimized $\alpha_{T,n}^*$ found numerically and by asymptotic expressions given in Theorem 2.4.1 and 2.4.2 respectively. We observe that almost the same number of iterations are required in both cases. From Figures 2.14, 2.15 and 2.16, we conclude that the optimized $\alpha_{T,n}^*$ found asymptotically with respect to $\omega_{\min} \to 0$ are very close to that found numerically.

Similar numerical experiments have also been performed to support the results for the asymptotic analysis with respect to $\epsilon \to 0$. The left plot of Figure 2.17 shows that our asymptotic formula for $\alpha_{R,0}^*$ from Theorem 2.4.3 underestimates the optimal choice a bit, while for $n = 1$, these values are close (see the right plot of Figure 2.17). However, when we plot the convergence factor in the Laplace space using these different values of $\alpha_{R,n}^*$, they are very close to each other. This behavior is clearly visible in both plots of Figure 2.18. In both plots of Figure 2.17, the small difference in the values of optimized α^* for OWR using the numerically and asymptotically optimized $\alpha_{R,n}^*$

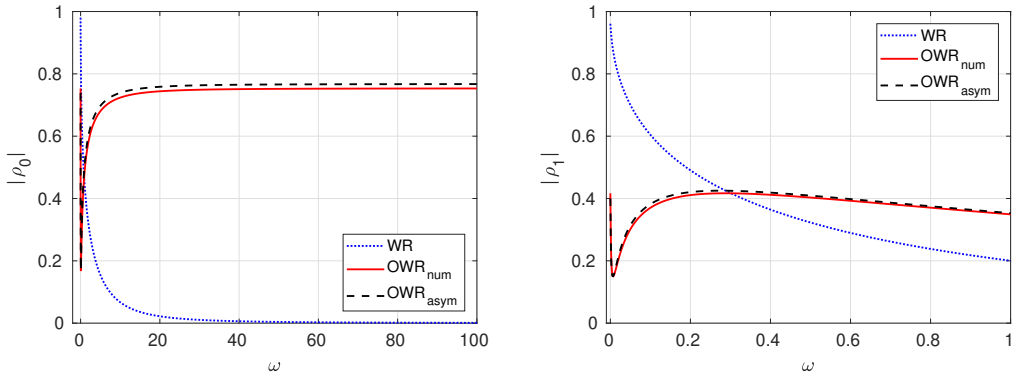

Figure 2.18: Convergence factor in the Laplace space for optimal $\alpha^*_{R,n}$ for $n = 0$ on (left) and $n = 1$ on (right) for asymptotic analysis with respect to $\epsilon \to 0$.

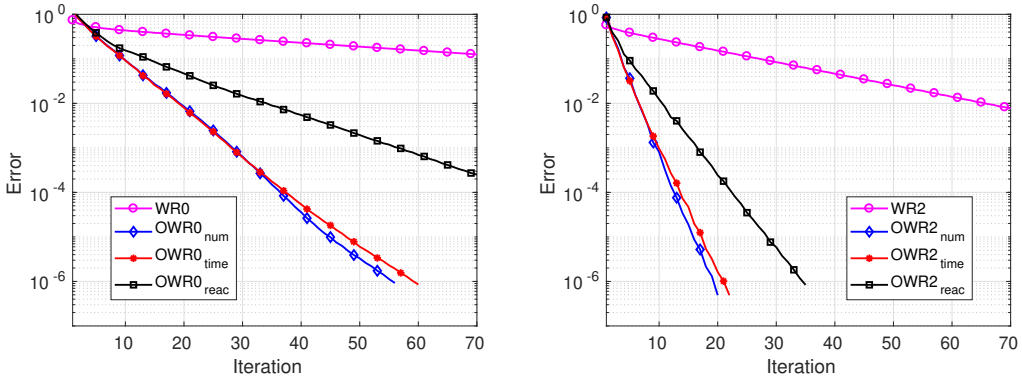

Figure 2.19: Convergence for the heat equation for $T = 2000$ for numerically and asymptotically optimized α^*_n using asymptotes $\omega_{\min} \to 0$ (left) and $\epsilon \to 0$ (right)

is due to the fact that the asymptotic analysis has been done for $\omega_{\min} = 0$, that is, for an infinite time interval, while for the numerical experiments we use a finite time $t \in (0, 1000]$.

In Section 2.1.1, we have seen that for $\epsilon \to 0$, the RC circuit of infinite length is an approximation of the one dimensional heat equation. We now apply the WR and OWR algorithm for different overlaps $n = 0$ and $n = 2$ to the heat equation (2.2). For the OWR algorithm, we have used the values of the optimized α^* found by solving the min-max problem numerically and by using the asymptotic expressions for $\alpha^*_{T,n}$ and $\alpha^*_{R,n}$. The left plot of Figure 2.19 shows the convergence for the non-overlapping case using $\alpha^*_{T,0}$ and $\alpha^*_{R,0}$ from Theorem 2.4.1 and 2.4.3 respectively. Note that "$\text{OWR2}_{\text{time}}$" and "$\text{OWR2}_{\text{reac}}$" denotes the convergence for OWR using $\alpha^*_{T,n}$ and $\alpha^*_{R,n}$ respectively. The convergence for the overlapping case $n = 2$ is illustrated in the right plot of Figure 2.19. From these plots, we conclude that the optimized

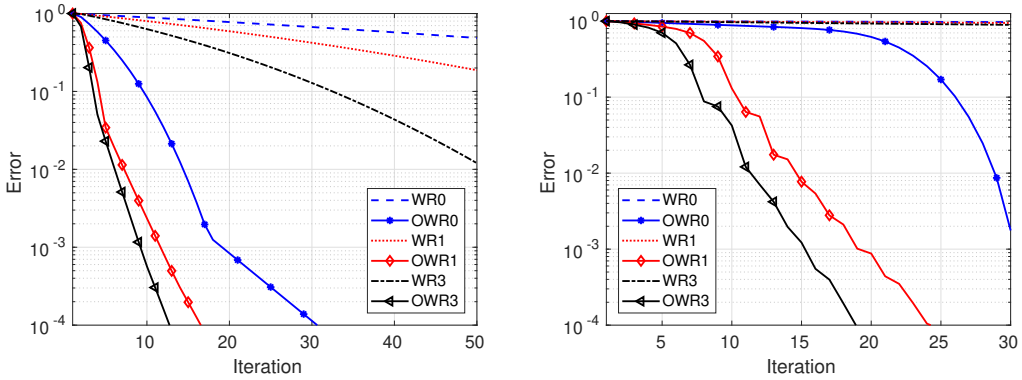

Figure 2.20: Convergence for $T = 1000$ for multiple sub-circuits $N_s = 5$ (left) and for $N_s = 50$ (right) using our asymptotic analysis with respect to $\epsilon \to 0$.

α^* found by asymptotic analysis with respect to $\omega_{\min} \to 0$ and $\epsilon = 0$ can be used for the simulation of the heat equation.

Finally, we consider the case when we split our RC circuit with size $N_s = 1000$ into multiple sub-circuits. We choose $\epsilon = 10^{-5}$ and $T = 1000$, with zero initial condition, homogeneous source and random initial guesses. We use our optimized α in Theorem 2.4.3 and 2.4.4 from the two sub-circuit analysis. We first consider $N_s = 5$ and then $N_s = 50$ sub-circuits. We see in Figure 2.20 that our asymptotically optimized parameters from the two sub-circuits work extremely well for the many sub-circuit case, and make the OWR solver into a rather effective method for solving many sub-circuit problems.

2.7 Conclusion

We presented a first analysis for the influence of overlap on the convergence factor for both the WR and OWR methods applied to infinitely long RC circuits. We found that increasing the overlap increases the convergence rate for both WR and OWR, but the impact of optimized transmission conditions is far more important than the impact of overlap. An important task of finding the explicit expressions for the optimizing parameters in the transmission conditions has been achieved.

The asymptotic analysis has been performed in two ways: first by letting $\epsilon = 0$ and $\omega_{\min} \to 0$ and the other by letting $\omega_{\min} = 0$ and $\epsilon \to 0$, where $b = -(2+\epsilon)a$ and $\omega_{\min}$ denotes the minimum frequency in the numerical simulation. Both cases are quite interesting and physically relevant. The first case, $\omega_{\min} \to 0$ with $\epsilon = 0$ corresponds to the simulation of the given infinite RC circuit for very large time intervals, since $\omega_{\min} = \pi/T$ and hence $\omega_{\min} \to 0$ implies $T \to \infty$. Since $\epsilon = 0$, it means that there is no leakage of current in the dielectric. The second case; $\epsilon \to 0$ with $\omega_{\min} = 0$

corresponds to the simulation on the infinitely large time interval. This analysis can be used when there is small leakage of current in the dielectric.

From both analyses, we conclude that the overlap changes the optimized parameters, and we provided closed form asymptotic formulas for them. Using OWR with these parameters leads to much lower iteration counts, also when OWR is used for many sub-circuits. We also showed that our optimized parameters can be used when solving heat equations with waveform relaxation techniques. A final important contribution is our interpretation of these optimized transmission conditions as circuit elements, which should help circuit designers to better understand and embrace this new technology.

Chapter 3

Waveform Relaxation Methods Applied to infinitely long RLCG Transmission Lines

In this chapter, we study the application of both WR and OWR methods to infinitely long RLCG transmission lines. RLCG Transmission Lines are conductors designed to carry electricity or an electrical signal over large distances with minimum losses and distortion (see the left image of Figure 3.1). These lines are used for purposes such as connecting radio transmitters and receivers with their antennas, distributing cable television signals, computer network connections, etc.

Transmission lines have four different structures namely coaxial cable, parallel wire, micro strip line and strip line (see the image on the right of Figure 3.1). The common

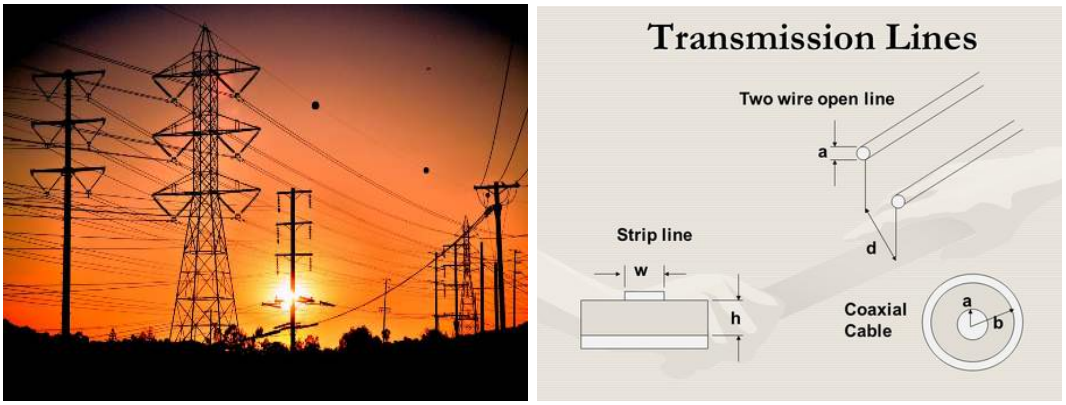

Figure 3.1: Transmission lines carrying electricity (left) and types of transmission lines (right).

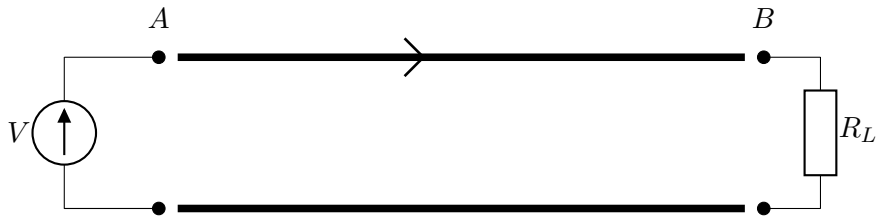

Figure 3.2: Two conductor system of transmission line.

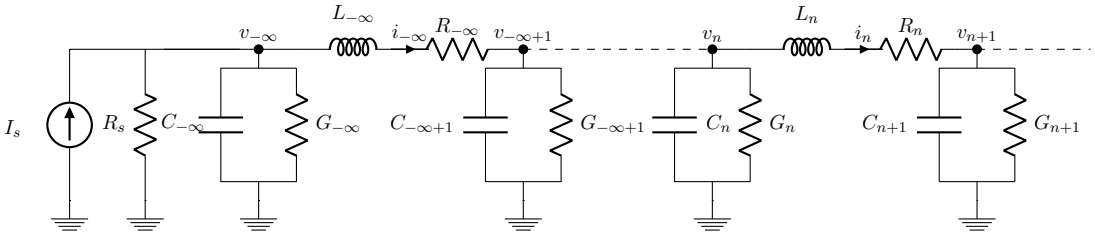

Figure 3.3: Infinite RLCG transmission line.

feature among all of them is that they are two conductor systems across which time varying voltage is applied at one end and load resistance at the other end (as shown in Figure 3.2).

For an ideal conductor, since its resistance is zero, the potential difference across its ends is zero, that is, the voltage at points A and B is the same. However when we apply a time varying voltage or current source, then at high frequency a potential difference is created between the points A and B. This results in development of magnetic fields around both the conductors, and the electric field between them. Further, the linkage of the magnetic field with the current gives us an inductance (L) while the separation of these two conductors by the dielectric material gives us a capacitance (C). Thus, the inductance is created along the conductors and the capacitance between them. As the frequency increases, the presence of inductance and capacitance creates a resistance (R) along the conductors. Also, the conductors may have small resistance since they are not ideal. The conductance (G) appears because of the small leakage of current in the dielectric. This conductance is in parallel to the capacitance. However these parameters are not located at any particular point but are equally distributed, that is, the elements R, L, C, and G represent resistance, inductance, capacitance, and conductance per unit length respectively. Therefore, the two conductor transmission line (depicted in Figure 3.2) can be viewed as an RLCG circuit as shown in Figure 3.3.

The ultimate aim of this chapter is to find optimized parameters involved in transmission conditions when the OWR method is applied to this infinitely long RLCG transmission line. In Section 3.1, we use the MNA formulation to develop a math-

ematical model of this circuit and then define WR and OWR methods in Sections 3.2-3.3. We consider both nonoverlapping and overlapping WR methods and study their convergence. Further, we explore different types of splittings for both WR and OWR methods. Finally, we support our theoretical results with numerical experiments.

3.1 Mathematical Model

For the infinitely long RLCG transmission line shown in Figure 3.3, we are interested in determining both the voltages v_j at the nodes and currents i_j in the circuit branches. Using the MNA formulation explained in Section 1.2, we develop a mathematical model of this circuit, which is an infinite system of differential equations in time,

$$\frac{d\mathbf{x}}{dt} = \begin{bmatrix} \ddots & \ddots & \ddots & & & & & \\ & a & b & -a & & & & \\ & & -c & \tilde{b} & c & & & \\ & & & a & b & -a & & \\ & & & & -c & \tilde{b} & c & \\ & & & & & \ddots & \ddots & \ddots \end{bmatrix} \mathbf{x} + \mathbf{f}, \tag{3.1}$$

where

$$a := \frac{1}{L}, \quad b := -\frac{R}{L}, \quad c := -\frac{1}{C}, \quad \tilde{b} := -\frac{G}{C}, \tag{3.2}$$

and $\mathbf{f} = (I_s/C, 0, 0, \ldots, 0)^\top$. The unknown vector $\mathbf{x}$ contains the voltages $v(t)$ and currents $i(t)$ which are arranged in a systematic manner: $\mathbf{x}(t) := (\ldots, x_{-1}(t), x_0(t), x_1(t), \ldots)^\top$, such that $x_{2j}(t) = i_j(t)$ and $x_{2j-1}(t) = v_j(t)$ for all $j \in \mathbb{Z}$. The odd index rows, which have c and $\tilde{b}$ elements correspond to voltage unknowns while the even rows correspond to current unknowns.

Assumption 3.1.1. We assume that all R, L, C, and G are bounded in order to have a well posed problem.

Before applying and analyzing WR methods to this circuit, we show its relation with the well known Maxwell's equations in 1D.

3.1.1 Relation with Maxwell's equations

Electromagnetism is the study of electromagnetic forces present in nature, which are carried by electromagnetic fields. The electromagnetic field is composed of the electric field $\mathbf{E}$ and the magnetic field $\mathbf{H}$ which are dependent on each other. These coupled fields are mathematically expressed by the well-known Maxwell's equations [61], and are represented as

$$\nabla \times \mathbf{E} = -\frac{\partial \mathbf{B}}{\partial t}, \quad \nabla \times \mathbf{H} = -\frac{\partial \mathbf{D}}{\partial t} + \mathbf{J}, \quad \nabla \cdot \mathbf{D} = \rho, \quad \nabla \cdot \mathbf{B} = 0, \tag{3.3}$$

where $\mathbf{B}$ and $\mathbf{D}$ are the electric and the magnetic flux density, ρ is the electric charge density and $\mathbf{J}$ is the electric current density. All these physical quantities depend on the space variable $\mathbf{r} \in \Omega$ and the time $t \in (t_0, T]$, for some initial time t_0 and final time T. Further, these equations (3.3) are related to each other via additional constitutive relations,

$$\mathbf{D} = \epsilon \mathbf{E}, \qquad \mathbf{B} = \mu \mathbf{H}, \quad \mathbf{J} = \sigma \mathbf{E} + \mathbf{J}_s,$$

where the permittivity ϵ, the permeability μ, and the conductivity σ depend on $\mathbf{r}$ and $\mathbf{J}_s$ is the electric source density. Substituting these relations into (3.3) leads to

$$\nabla \times \mathbf{E} = -\mu \frac{\partial \mathbf{H}}{\partial t}, \quad \text{and} \quad \nabla \times \mathbf{H} = -\epsilon \frac{\partial \mathbf{E}}{\partial t} + \sigma \mathbf{E} + \mathbf{J}_s, \tag{3.4}$$

where we have not considered the last two equations $\nabla \cdot \mathbf{D} = \rho$ and $\nabla \cdot \mathbf{B} = 0$ since one can show that if these conditions are satisfied at initial time $t = t_0$, that is, $\nabla \cdot (\epsilon \mathbf{E}_0) = \rho(0)$ and $\nabla \cdot (\mu \mathbf{H}_0) = 0$, then they remain satisfied for all time t. Here, $\mathbf{E}_0$ and $\mathbf{H}_0$ denote the electric field and magnetic field intensity at initial time t_0. The Maxwell's equations (3.4) in 1D take the form

$$\frac{\partial H}{\partial t} + \frac{1}{\mu}\frac{\partial E}{\partial x} = 0, \quad \text{and} \quad \frac{\partial E}{\partial t} + \frac{1}{\epsilon}\frac{\partial H}{\partial x} = -\frac{\sigma}{\epsilon} E, \tag{3.5}$$

where we have considered the electric source density $\mathbf{J}_s = 0$.

The coupled differential equations of system (3.1) for the RLCG circuit can be explicitly written as

$$\frac{\partial x_{2j}}{\partial t} = a x_{2j-1} + b x_{2j} - a x_{2j+1}, \quad \text{and} \quad \frac{\partial x_{2j+1}}{\partial t} = -c x_{2j} + \tilde{b} x_{2j+1} + c x_{2j+2}, \quad \text{for} \quad j \in \mathbb{Z}.$$

The odd index rows correspond to voltage unknowns and the even index rows correspond to current unknowns and hence the above equations reduces for $j \in \mathbb{Z}$ to,

$$\begin{aligned} \frac{\partial i_j}{\partial t} &= \frac{1}{L} v_j - \frac{R}{L} i_j - \frac{1}{L} v_{j+1}, \\ \frac{\partial v_{j+1}}{\partial t} &= \frac{1}{C} i_j - \frac{G}{C} v_{j+1} - \frac{1}{C} i_{j+1}. \end{aligned}$$

The parameters R, L, C, G are defined per unit length, that is, $R = R_T \Delta x$, $L = L_T \Delta x$, $C = C_T \Delta x$ and $G = G_T \Delta x$; where R_T, L_T, C_T and G_T represent the total quantities in the circuit. Interpreting these differences as derivatives, we arrive at

$$\frac{\partial i}{\partial t} + \frac{1}{L_T}\frac{\partial v}{\partial x} = -\frac{R_T}{L_T} i, \qquad \text{and} \qquad \frac{\partial v}{\partial t} + \frac{1}{C_T}\frac{\partial i}{\partial x} = -\frac{G_T}{C_T} v. \tag{3.6}$$

Under the condition $G_T = 0$, which means that there is no leakage of current in the dielectic, equation (3.6) can be compared with the Maxwell's equations in 1D (3.5) and we arrive at $i \sim E$, $v \sim H$, $L_T \sim \epsilon$, $C_T \sim \mu$ and $R_T \sim \sigma$. We can also consider

the other case, $R_T = 0$, which means that that the conductors of the transmission lines are ideal and have no reactance. Comparing again (3.6) with Maxwell's equation in 1D, we see $i \sim H$, $v \sim E$, $L_T \sim \mu$, $C_T \sim \epsilon$ and $G_T \sim \sigma$. Therefore, both RLC and LCG transmission lines can be viewed as approximations of Maxwell's equations in 1D.

3.2 Waveform Relaxation Methods

In this section, we analyze the application of the classical WR methods to the RLCG transmission line presented in Figure 3.3.

We consider two main cases: nonoverlapping and overlapping nodes. In the overlapping case, since the infinite system (3.1) consists of two different equations, one for current and the other for voltage, the type of partitioning is interesting and we will study whether the type of partitioning effects the convergence. In general, WR methods decompose the system (3.1) into multiple subsystems, but then the convergence analysis becomes complicated, and to understand the key features of this method, we decompose the system (3.1) into two subsystems with unknowns $\mathbf{x}(s_1)$ and $\mathbf{x}(s_2)$, where both unknowns depend on time t but for simplicity, we have removed t from the notation.

3.2.1 Nonoverlapping WR

We first study the nonoverlapping WR method. To start with this method, we divide system (3.1) at node x_0 into two subsystems with unknowns $\mathbf{x}(s_1) := (\dots, x_{-2}(t), x_{-1}(t), x_0(t))^\top$ and $\mathbf{x}(s_2) := (x_1(t), x_2(t), \dots)^\top$. Both subsystems have equal length and their differential equations are

$$\begin{aligned}
\tfrac{d}{dt}\mathbf{x}^{k+1}(s_1) &= \begin{bmatrix} \ddots & \ddots & \ddots & \\ & -c & \tilde{b} & c \\ & & a & b \end{bmatrix} \mathbf{x}^{k+1}(s_1) + \begin{bmatrix} \vdots \\ 0 \\ -a x_1^{k+1}(s_1) \end{bmatrix} + \begin{bmatrix} \vdots \\ f_{-1} \\ f_0 \end{bmatrix}, \\
\tfrac{d}{dt}\mathbf{x}^{k+1}(s_2) &= \begin{bmatrix} \tilde{b} & c & & \\ a & b & -a & \\ & \ddots & \ddots & \ddots \end{bmatrix} \mathbf{x}^{k+1}(s_2) + \begin{bmatrix} -c x_0^{k+1}(s_2) \\ 0 \\ \vdots \end{bmatrix} + \begin{bmatrix} f_1 \\ f_2 \\ \vdots \end{bmatrix},
\end{aligned} \tag{3.7}$$

where k is the iteration index and the unknowns $x_1^{k+1}(s_1)$ and $x_0^{k+1}(s_2)$ are given by transmission conditions,

$$x_1^{k+1}(s_1) = x_1^k(s_2), \quad \text{and} \quad x_0^{k+1}(s_2) = x_0^k(s_1). \tag{3.8}$$

These transmission conditions exchange either current or voltage at the interface. For the convergence study, we consider the homogeneous problem $\mathbf{f} = 0$ and zero initial conditions $\mathbf{x}(0) = 0$. The analysis of these two subsystems in the time domain is very

difficult and hence using the Laplace transformation defined in (2.2.1), we transform these systems of differential equations into an algebraic system of equations. The Laplace transformation with $s \in \mathbb{C}^+$ for the subsystems (3.7) yields

$$\begin{aligned} s\hat{\mathbf{x}}^{k+1}(s_1) &= \begin{bmatrix} \ddots & \ddots & \ddots & \\ & -c & \tilde{b} & c \\ & & a & b \end{bmatrix} \begin{bmatrix} \vdots \\ \hat{x}_{-1}^{k+1}(s_1) \\ \hat{x}_0^{k+1}(s_1) \end{bmatrix} + \begin{bmatrix} \vdots \\ 0 \\ -a\hat{x}_1^k(s_2) \end{bmatrix}, \\ s\hat{\mathbf{x}}^{k+1}(s_2) &= \begin{bmatrix} \tilde{b} & c & & \\ a & b & -a & \\ & \ddots & \ddots & \ddots \end{bmatrix} \begin{bmatrix} \hat{x}_1^{k+1}(s_2) \\ \hat{x}_2^{k+1}(s_2) \\ \vdots \end{bmatrix} + \begin{bmatrix} -c\hat{x}_0^k(s_1) \\ 0 \\ \vdots \end{bmatrix}, \end{aligned} \tag{3.9}$$

where we have already included the transmission conditions (3.8).

Note that the circuit elements R, L, C, and G are fixed and hence we denote the convergence factor $\rho_{cla}(s) \equiv \rho_{cla}(s, a, b, \tilde{b}, c)$.

Theorem 3.2.1. *The convergence factor of the classical nonoverlapping WR algorithm for an RLCG transmission line of infinite length is*

$$\rho_{cla}(s) := \begin{cases} -\lambda_1 & , \quad |\lambda_1| < 1, \\ -\lambda_2 & , \quad |\lambda_1| > 1, \end{cases} \tag{3.10}$$

where $\lambda_{1,2} := \frac{2ac-(s-\tilde{b})(s-b)\pm\sqrt{(2ac-(s-\tilde{b})(s-b))^2-4a^2c^2}}{2ac}$ *with the property* $\lambda_1\lambda_2 = 1$.

Proof. Solving the first subsystem of (3.9) corresponds to solving coupled recurrence equations, for $j = \ldots, -2, -1, 0$,

$$\begin{aligned} -a\hat{x}_{2j-1}^{k+1}(s_1) + (s-b)\hat{x}_{2j}^{k+1}(s_1) + a\hat{x}_{2j+1}^{k+1}(s_1) &= 0, \\ c\hat{x}_{2j-2}^{k+1}(s_1) + (s-\tilde{b})\hat{x}_{2j-1}^{k+1}(s_1) - c\hat{x}_{2j}^{k+1}(s_1) &= 0. \end{aligned}$$

To simplify, we introduce the new notation $\hat{p}_j^{k+1} := \hat{x}_{2j}^{k+1}(s_1)$ and $\hat{q}_j^{k+1} := \hat{x}_{2j-1}^{k+1}(s_1)$ for $j = \ldots, -2, -1, 0$ to get

$$-a\hat{q}_j^{k+1} + (s-b)\hat{p}_j^{k+1} + a\hat{q}_{j+1}^{k+1} = 0, \quad \text{and} \quad c\hat{p}_{j-1}^{k+1} + (s-\tilde{b})\hat{q}_j^{k+1} - c\hat{p}_j^{k+1} = 0. \tag{3.11}$$

Solving the first equation for $\hat{p}_j^{k+1}$ and substituting it into the second equation yields $ac\hat{q}_{j-1}^{k+1} + \Big((s-\tilde{b})(s-b) - 2ac\Big)\hat{q}_j^{k+1} + ac\hat{q}_{j+1}^{k+1} = 0$. The general solution of this recurrence equation is

$$\hat{q}_j^{k+1} = A^{k+1}\lambda_1^j + B^{k+1}\lambda_2^j,$$

where $\lambda_{1,2} := \frac{2ac-(s-\tilde{b})(s-b)\pm\sqrt{(2ac-(s-\tilde{b})(s-b))^2-4a^2c^2}}{2ac}$ are the roots of the characteristic equation and the constants A^{k+1}, B^{k+1} need to be determined. We first consider the

case $|\lambda_1| < 1$. Since $\left|\lambda_1^{2j-1}\right| \to \infty$ as $j \to -\infty$ and $\hat{q}_j^{k+1}$ are bounded, we have $A^{k+1} = 0$. The coupled equations (3.11) give

$$\hat{q}_j^{k+1} = B^{k+1}\lambda_2^j, \quad \text{and} \quad \hat{p}_j^{k+1} = \frac{aB^{k+1}}{s-b}\left(\lambda_2^j - \lambda_2^{j+1}\right). \tag{3.12}$$

Similarly, from the second subsystem of (3.9), for $j \in \mathbb{N}$ we define $\hat{u}_j^{k+1} := \hat{x}_{2j}^{k+1}(s_2)$ and $\hat{w}_j^{k+1} := \hat{x}_{2j-1}^{k+1}(s_2)$ to arrive at

$$\hat{w}_j^{k+1} = D^{k+1}\lambda_1^j, \quad \text{and} \quad \hat{u}_j^{k+1} = \frac{aD^{k+1}}{s-b}\left(\lambda_1^j - \lambda_1^{j+1}\right). \tag{3.13}$$

Finally, to determine the constants B^{k+1} and D^{k+1}, we use the transmission conditions (3.8) and the relations between λ_1 and λ_2. Since λ_1 and λ_2 are roots of the characteristic equation $ac + \Big((s-\tilde{b})(s-b) - 2ac\Big)\lambda + ac\lambda^2 = 0$, they satisfy $\lambda_1\lambda_2 = 1$ and $\lambda_1 + \lambda_2 = 2 - \frac{(s-\tilde{b})(s-b)}{ac}$. Further, the last equation of the first subsystem of (3.9) gives $-a\hat{q}_0^{k+1} + (s-b)\hat{p}_0^{k+1} = -a\hat{w}_1^k$ which simplifies to

$$\begin{aligned}
& -aB^{k+1} + (s-b)\frac{a}{(s-b)}B^{k+1}(1-\lambda_2) = -aD^k\lambda_1 \\
\implies \quad & B^{k+1}(-1+1-\lambda_2) = -D^k\lambda_1 \\
\implies \quad & B^{k+1} = D^k\frac{\lambda_1}{\lambda_2} = D^k\lambda_1^2.
\end{aligned}$$

Similarly, the first equation of the second subsystem of (3.9) gives $(s-\tilde{b})\hat{x}_1^{k+1}(s_2) - c\hat{x}_2^{k+1}(s_2) = -c\hat{x}_0^k(s_1)$ which simplifies to

$$\begin{aligned}
& (s-\tilde{b})w_1^{k+1} - c\hat{u}_1^{k+1} = -cp_0^k \\
\implies \quad & (s-\tilde{b})D^{k+1}\lambda_1 - \frac{acD^{k+1}}{s-b}\left(\lambda_1 - \lambda_1^2\right) = -\frac{acB^k}{s-b}(1-\lambda_2) \\
\implies \quad & D^{k+1}\lambda_1\left(\frac{(s-b)(s-\tilde{b})}{ac} - (1-\lambda_1)\right) = -B^k(1-\lambda_2) \\
\implies \quad & D^{k+1}\lambda_1\left(2-\lambda_1-\lambda_2-1+\lambda_1\right) = -B^k(1-\lambda_2) \\
\implies \quad & D^{k+1}\lambda_1(1-\lambda_2) = -B^k(1-\lambda_2) \\
\implies \quad & D^{k+1} = -B^k\lambda_2.
\end{aligned}$$

Therefore, we have $B^{k+1} = -\lambda_1^2\lambda_2 B^{k-1} = -\lambda_1 B^{k-1}$ and $D^{k+1} = -\lambda_1 D^{k-1}$ which implies $\hat{x}_j^{k+1}(s_1) = \rho_{cla}(s)\hat{x}_j^{k-1}(s_1)$, and $\hat{x}_j^{k+1}(s_2) = \rho_{cla}(s)\hat{x}_j^{k-1}(s_2)$, where $\rho_{cla}(s)$ is defined in (3.10). Similarly, we derive the convergence factor when $|\lambda_1| > 1$. □

Remark 3.2.1. We observe that the convergence factor ρ_{cla} is the same for all the nodes irrespective of which subsystem they belong to. Further, we observe that

$|\lambda_1| \to 1$ as $s \to 0$, which implies $|\rho_{cla}(s)| \to 1$. This means that the convergence of this WR method slows down when we consider large time intervals since large time intervals correspond to small frequency ω in s, where $s = \sigma + i\omega$.

To overcome this issue of slow convergence, we consider the overlapping case, where some nodes of both subsystems of (3.7) are overlapped.

3.2.2 Overlapping WR

We have analyzed the effect of overlapping nodes on the convergence rate of the classical WR methods when applied to infinitely long RC circuits in Section 2.2 of Chapter 2, and proved that overlapping nodes increases the rate of convergence. In this section, we will study the effect of convergence for WR methods applied to RLCG transmission lines which are infinitely long. However now since the system (3.1) contains two different types of equations, one for the current unknown and the other for the voltage unknowns, analyzing the type of partitioning of the RLCG circuit and then overlapping nodes will be interesting.

We first consider splitting the circuit at a voltage node unknown and add overlap. To start with this algorithm, we divide system (3.1) at an odd row, say at $x_{-1}(t)$ into two subsystems with unknowns $\mathbf{x}(s_1)$ and $\mathbf{x}(s_2)$, and overlap n nodes of the circuit (which corresponds to an overlap of $2n$ nodes of the two subsystems in (3.14) below). Thus, initially, both the subsystems have equal length and then we increase the size of $\mathbf{x}(s_1)$ by $2n-1$ to include the overlap while the size of $\mathbf{x}(s_2)$ remains unchanged. This leads to two new subsystems of differential equations: for $\mathbf{x}(s_1) := (\dots, x_{-1}, x_0, \dots, x_{2n-3})^\top$ and $\mathbf{x}(s_2) := (x_{-1}, x_0, \dots)^\top$,

$$\begin{aligned}
\tfrac{d}{dt}\mathbf{x}^{k+1}(s_1) &= \begin{bmatrix} \ddots & \ddots & \ddots & \\ & a & b & -a \\ & & -c & \tilde{b} \end{bmatrix} \mathbf{x}^{k+1}(s_1) + \begin{bmatrix} \vdots \\ 0 \\ c x^{k+1}_{2n-2}(s_1) \end{bmatrix} + \begin{bmatrix} \vdots \\ f_{2n-4} \\ f_{2n-3} \end{bmatrix}, \\
\tfrac{d}{dt}\mathbf{x}^{k+1}(s_2) &= \begin{bmatrix} \tilde{b} & c & & \\ a & b & -a & \\ & \ddots & \ddots & \ddots \end{bmatrix} \mathbf{x}^{k+1}(s_2) + \begin{bmatrix} -c x^{k+1}_{-2}(s_2) \\ 0 \\ \vdots \end{bmatrix} + \begin{bmatrix} f_{-1} \\ f_0 \\ \vdots \end{bmatrix},
\end{aligned} \tag{3.14}$$

where k is the iteration index and the unknowns $x^{k+1}_{2n-2}(s_1)$ and $x^{k+1}_{-2}(s_2)$ are given by the transmission conditions,

$$x^{k+1}_{2n-2}(s_1) = x^k_{2n-2}(s_2), \quad \text{and} \quad x^{k+1}_{-2}(s_2) = x^k_{-2}(s_1), \tag{3.15}$$

which now exchange only current at the interfaces. For the convergence study, we consider the homogeneous problem $\mathbf{f} = 0$ and zero initial conditions $\mathbf{x}(0) = 0$. The

Laplace transformation with $s \in \mathbb{C}^+$ for the subsystems (3.14) yields

$$\begin{aligned} s\hat{\mathbf{x}}^{k+1}(s_1) &= \begin{bmatrix} \ddots & \ddots & \ddots & \\ & a & b & -a \\ & & -c & \tilde{b} \end{bmatrix} \begin{bmatrix} \vdots \\ \hat{x}^{k+1}_{2n-4}(s_1) \\ \hat{x}^{k+1}_{2n-3}(s_1) \end{bmatrix} + \begin{bmatrix} \vdots \\ 0 \\ c\hat{x}^{k}_{2n-2}(s_2) \end{bmatrix}, \\ s\hat{\mathbf{x}}^{k+1}(s_2) &= \begin{bmatrix} \tilde{b} & c & & \\ a & b & -a & \\ & \ddots & \ddots & \ddots \end{bmatrix} \begin{bmatrix} \hat{x}^{k+1}_{-1}(s_2) \\ \hat{x}^{k+1}_{0}(s_2) \\ \vdots \end{bmatrix} + \begin{bmatrix} -c\hat{x}^{k}_{-2}(s_1) \\ 0 \\ \vdots \end{bmatrix}. \end{aligned} \tag{3.16}$$

Theorem 3.2.2. *The convergence factor of the classical overlapping WR algorithm for an RLCG transmission line of infinite length with splitting at a voltage node and with $n \geq 1$ circuit nodes overlap is given by*

$$\rho^{v}_{n,cla}(s) = \begin{cases} (\lambda_1)^{2n} & , \quad |\lambda_1| < 1, \\ (\lambda_2)^{2n} & , \quad |\lambda_1| > 1, \end{cases}$$

where λ_1 and λ_2 are defined in Theorem 3.2.1.

Proof. The proof of this theorem is similar to the proof of Theorem 3.2.1. Let us assume $|\lambda_1| < 1$, and define $\hat{p}^{k+1}_j := \hat{x}^{k+1}_{2j}(s_1)$ and $\hat{q}^{k+1}_j := \hat{x}^{k+1}_{2j+1}(s_1)$, for $j = -\infty, \ldots, -1, 0, \ldots, n-1$. With these new notations, the system of equations (3.16) reduces to

$$-a\hat{q}^{k+1}_{j-1} + (s-b)\hat{p}^{k+1}_j + a\hat{q}^{k+1}_j = 0, \quad \text{and} \quad c\hat{p}^{k+1}_j + (s-\tilde{b})\hat{q}^{k+1}_j - c\hat{p}^{k+1}_{j+1} = 0,$$

which results in

$$\hat{q}^{k+1}_j = B^{k+1}\lambda_2^j, \quad \text{and} \quad \hat{p}^{k+1}_j = \frac{aB^{k+1}}{s-b}\left(\lambda_2^{j-1} - \lambda_2^j\right).$$

Similarly, for the second subsystem of (3.16), we define $\hat{u}^{k+1}_j := \hat{x}^{k+1}_{2j}(s_2)$ and $\hat{w}^{k+1}_j := \hat{x}^{k+1}_{2j-1}(s_2)$ for for $j = 0, 1, 2, \ldots$ to arrive at

$$\hat{w}^{k+1}_j = D^{k+1}\lambda_1^j \quad \text{and} \quad \hat{u}^{k+1}_j = \frac{aD^{k+1}}{s-b}\left(\lambda_1^j - \lambda_1^{j+1}\right).$$

The constants B^{k+1} and D^{k+1} are determined using the transmission conditions defined in (3.15). The last equation of the first subsystem of (3.16) simplifies to $B^{k+1} = -D^k(\lambda_1^2)^{n-1}$, while the the first equation of the second subsystem gives $D^{k+1} = -B^k\lambda_1^2$. Combining these two equations results in $\hat{x}^{k+1}_j(s_1) = (\lambda_1)^{2n}\hat{x}^{k-1}_j(s_1)$ and $\hat{x}^{k+1}_j(s_2) = (\lambda_1)^{2n}\hat{x}^{k-1}_j(s_2)$. Similarly, we derive the convergence factor when $|\lambda_1| > 1$. □

We now consider the other splitting, that is, at a current node, and study whether it produces better convergence for the overlapping WR method. This is done in a similar way as discussed above. We split the system (3.1) at an even row, say at $x_0(t)$ into two subsystems and then add overlap. Let $\mathbf{x}(s_1) := (\dots, x_{2n-3}, x_{2n-2})^\top$ and $\mathbf{x}(s_2) := (x_0, x_1, \dots)^\top$ be the two subsystems. We then transform these subsystems into the Laplace space to arrive for $s \in \mathbb{C}^+$ at,

$$\begin{aligned} s\hat{\mathbf{x}}^{k+1}(s_1) &= \begin{bmatrix} \ddots & \ddots & \ddots & \\ & -c & \tilde{b} & c \\ & & a & b \end{bmatrix} \begin{bmatrix} \vdots \\ \hat{x}^{k+1}_{2n-3}(s_1) \\ \hat{x}^{k+1}_{2n-2}(s_1) \end{bmatrix} + \begin{bmatrix} \vdots \\ 0 \\ -a\hat{x}^{k+1}_{2n-1}(s_1) \end{bmatrix}, \\ s\hat{\mathbf{x}}^{k+1}(s_2) &= \begin{bmatrix} b & -a & & \\ -c & \tilde{b} & c & \\ & \ddots & \ddots & \ddots \end{bmatrix} \begin{bmatrix} \hat{x}^{k+1}_0(s_2) \\ \hat{x}^{k+1}_1(s_2) \\ \vdots \end{bmatrix} + \begin{bmatrix} a\hat{x}^{k+1}_{-1}(s_2) \\ 0 \\ \vdots \end{bmatrix}, \end{aligned} \tag{3.17}$$

where the unknowns $\hat{x}^{k+1}_{2n-1}(s_1)$ and $\hat{x}^{k+1}_{-1}(s_2)$ are given by the classical transmission conditions

$$x^{k+1}_{2n-1}(s_1) = x^k_{2n-1}(s_2), \quad \text{and} \quad x^{k+1}_{-1}(s_2) = x^k_{-1}(s_1), \tag{3.18}$$

with k as the iteration number. Note that in this splitting, only voltages at the interface nodes are transferred via the transmission conditions.

Theorem 3.2.3. *The convergence factor of the classical overlapping WR algorithm for an RLCG transmission line of infinite length with splitting at a current node and with $n \geq 1$ circuit nodes overlap is given by*

$$\rho^c_{n,cla}(s) = \begin{cases} (\lambda_1)^{2n} & , \quad |\lambda_1| < 1, \\ (\lambda_2)^{2n} & , \quad |\lambda_1| \geq 1, \end{cases}$$

where λ_1 and λ_2 are defined in Theorem 3.2.1.

Proof. The proof is almost the same as the proof of Theorems 3.2.1 and 3.2.2. Hence we will mention only the important steps. We first assume $|\lambda_1| < 1$, and define $\hat{p}^{k+1}_j := \hat{x}^{k+1}_{2j}(s_1)$ and $\hat{q}^{k+1}_j := \hat{x}^{k+1}_{2j-1}(s_1)$ for $j = -\infty, \dots, n-1$. With these new notations, the first subsystem of equation (3.17) results in

$$\hat{q}^{k+1}_j = B^{k+1}\lambda_2^j, \quad \text{and} \quad \hat{p}^{k+1}_j = \frac{aB^{k+1}}{s-b}\left(\lambda_2^j - \lambda_2^{j+1}\right).$$

Similarly, for the second subsystem, we define $\hat{u}^{k+1}_j = \hat{x}^{k+1}_{2j}(s_2)$ and $\hat{w}^{k+1}_j = \hat{x}^{k+1}_{2j+1}(s_2)$ for $j = 0, 1, 2, \dots$. The second subsystem of (3.17) reduces to

$$\hat{w}^{k+1}_j = D^{k+1}\lambda_1^j, \quad \text{and} \quad \hat{u}^{k+1}_j = \frac{aD^{k+1}}{s-b}\left(\lambda_1^{j-1} - \lambda_1^j\right).$$

The transmission conditions (3.18) along with the last and first equations of the first and second subsystems of (3.17) produces

$$B^{k+1} = \lambda_1^{2n}\lambda_2 D^k, \quad \text{and} \quad D^{k+1} = \lambda_1 B^k.$$

Combining these two equations results in $\hat{x}_j^{k+1}(s_1) = (\lambda_1)^{2n}\hat{x}_j^{k-1}(s_1)$ and $\hat{x}_j^{k+1}(s_2) = (\lambda_1)^{2n}\hat{x}_j^{k-1}(s_2)$. This completes the proof. □

Remark 3.2.2. We observe that the convergence factor for the WR method is the same for all the nodes irrespective of which subsystem they belong to. The convergence becomes faster by increasing the number of nodes in the overlap. Further, the convergence factor of the overlapping WR method does not depend on the type of partitioning employed.

Remark 3.2.3. Note that λ_1, λ_2 satisfy the relation $\lambda_1 = \lambda_2 = 1$ under the condition $s = b$ or $s = \tilde{b}$, and hence the convergence factors $\rho_{cla}(s)$, $\rho^v_{n,cla}(s)$, and $\rho^c_{n,cla}(s)$, defined in Theorems 3.2.1, 3.2.2 and 3.2.3 satisfy $\rho_{cla}(s) = \rho^v_{n,cla}(s) = \rho^c_{n,cla}(s) = 1$. Substituting the expressions for b and $\tilde{b}$ given in (3.2) states that these WR algorithms do not converge if s lies on the negative real axis of the complex plane.

Moreover the expressions of λ_1 and λ_2 defined in Theorem 3.2.1 state that $|\lambda_1|,|\lambda_2| \to 1$ as $s \to 0$. Let $s = \sigma + i\omega$, with $\sigma \geq 0$. Then large time $T \to \infty$ corresponds to small frequency $\omega \to 0$ in s. This shows the typical behavior of the classical WR method, that is, its slow convergence when large time windows are used. We observed and proved in Chapter 2, that the slow convergence of WR method can be overcome by using better transmission conditions. In next section, we define new transmission conditions for RLCG transmission lines and analyze its effect on convergence.

3.3 Optimized Waveform Relaxation Method

Motivated by the previous work on RLCG transmission lines by M. D. Khaleel and el [1, 25], we introduce new transmission conditions for all three cases: nonoverlapping OWR, overlapping OWR with splitting at a voltage node, and overlapping OWR with splitting at a current node. The effect of new transmission conditions on the convergence of the WR algorithm will be studied in this section. We start by considering the nonoverlapping case.

3.3.1 Nonoverlapping OWR

In the classical WR algorithm, either voltage or current at the interface was transferred from one subcircuit to the other. However, this leads to slow convergence. Hence we introduce new transmission conditions which are a particular combination of voltage and current at the interface. This leads to a new algorithm, which we call Optimized Waveform Relaxation (OWR). The optimized transmission conditions for

the nonoverlapping splitting are

$$\begin{aligned} x_1^{k+1}(s_1) + \alpha x_0^{k+1}(s_1) &= x_1^k(s_2) + \alpha x_0^k(s_2), \\ x_3^{k+1}(s_2) + \beta x_0^{k+1}(s_2) &= x_{-1}^k(s_1) + \beta x_0^k(s_1), \end{aligned} \tag{3.19}$$

where $\alpha,\ \beta \in \mathbb{R}$ are the optimizing parameters, and $x_j(s_1)$ and $x_j(s_2)$ denotes the unknowns in the first and second subsystems of (3.7).

Remark 3.3.1. Under the conditions $\alpha = 0$ and $\beta = 0$, the optimized transmission conditions (3.19) reduce to the classical transmission conditions (3.8).

For the analysis of the convergence of OWR methods, we move to the Laplace space. For this, we reorient the transmission conditions (3.19) and take their Laplace transformation to arrive for $\beta \neq 0$ at,

$$\begin{aligned} \hat{x}_1^{k+1}(s_1) &= -\alpha \hat{x}_0^{k+1}(s_1) + \hat{x}_1^k(s_2) + \alpha \hat{x}_0^k(s_2), \\ \hat{x}_0^{k+1}(s_2) &= -\frac{\hat{x}_3^{k+1}(s_2)}{\beta} + \frac{\hat{x}_{-1}^k(s_1)}{\beta} + \hat{x}_0^k(s_1). \end{aligned}$$

Substituting these optimized transmission conditions changes both subsystems in (3.9) leads to

$$\begin{aligned} s\hat{\mathbf{x}}^{k+1}(s_1) &= \begin{bmatrix} \ddots & \ddots & \ddots & \\ & -c & \tilde{b} & c \\ & & a & (b+a\alpha) \end{bmatrix} \begin{bmatrix} \vdots \\ \hat{x}_{-1}^{k+1}(s_1) \\ \hat{x}_0^{k+1}(s_1) \end{bmatrix} + \begin{bmatrix} \vdots \\ 0 \\ -a\hat{x}_1^k(s_2) - a\alpha\hat{x}_0^k(s_2) \end{bmatrix}, \\ s\hat{\mathbf{x}}^{k+1}(s_2) &= \begin{bmatrix} \tilde{b} & c & \frac{c}{\beta} & \\ a & b & -a & \\ & \ddots & \ddots & \ddots \end{bmatrix} \begin{bmatrix} \hat{x}_1^{k+1}(s_2) \\ \hat{x}_2^{k+1}(s_2) \\ \vdots \end{bmatrix} + \begin{bmatrix} -c\hat{x}_0^k(s_1) - \frac{c}{\beta}\hat{x}_{-1}^k(s_1) \\ 0 \\ \vdots \end{bmatrix}. \end{aligned} \tag{3.20}$$

We now find an expression for the convergence factor of this nonoverlapping OWR method.

Theorem 3.3.1. *The convergence factor of the nonoverlapping optimized waveform relaxation algorithm for an RLCG transmission line of infinite length is*

$$\rho(s,\alpha,\beta) := \begin{cases} \left(\frac{(s-b)+a\alpha(\lambda_2-1)}{(s-b)\lambda_2+a\alpha(1-\lambda_2)}\right)\left(\frac{(s-b)+a\beta(1-\lambda_2)}{(s-b)\lambda_1-a\beta(1-\lambda_2)}\right) & , \quad |\lambda_1| < 1, \\ \left(\frac{(s-b)+a\alpha(\lambda_1-1)}{(s-b)\lambda_1+a\alpha(1-\lambda_1)}\right)\left(\frac{(s-b)+a\beta(1-\lambda_1)}{(s-b)\lambda_2-a\beta(1-\lambda_1)}\right) & , \quad |\lambda_1| > 1. \end{cases} \tag{3.21}$$

Proof. The proof of this theorem is very similar to the proof of Theorem 3.2.1. Due to the presence of the optimized transmission conditions (3.19), the constants B^{k+1} and D^{k+1} change. For the case $|\lambda_1| < 1$, referring back to equations (3.12) and (3.13), we have for the subsystem $\mathbf{x}(s_1)$,

$$\hat{q}_j^{k+1} = B^{k+1}\lambda_2^j, \quad \text{and} \quad \hat{p}_j^{k+1} = \frac{aB^{k+1}}{s-b}\left(\lambda_2^j - \lambda_2^{j+1}\right),$$

and for the subsystem $\mathbf{x}(s_2)$,

$$\hat{w}_j^{k+1} = D^{k+1}\lambda_1^j, \quad \text{and} \quad \hat{u}_j^{k+1} = \frac{aD^{k+1}}{s-b}\left(\lambda_1^j - \lambda_1^{j+1}\right),$$

where $\hat{q}_j^{k+1} := \hat{x}_{2j-1}^{k+1}(s_1)$, $\hat{p}_j := \hat{x}_{2j}^{k+1}(s_1)$, $\hat{u}_j := \hat{x}_{2j}^{k+1}(s_2)$ and $\hat{w}_j^{k+1} := \hat{x}_{2j-1}^{k+1}(s_2)$. The last equation of the first subsystem of (3.20) leads to $-a\hat{x}_{-1}^{k+1}(s_1) + (s-b-a\alpha)\hat{x}_0^{k+1}(s_1) = -a\alpha\hat{x}_0^k(s_2) - a\hat{x}_1^k(s_2)$, which simplifies to

$$\begin{aligned}
& -a\hat{q}_0^{k+1} + (s-b-a\alpha)\hat{p}_0^{k+1} = -a\alpha\hat{u}_0^k - a\hat{w}_1^k \\
\implies & -B^{k+1} + \frac{(s-b-a\alpha)}{s-b}B^{k+1}(1-\lambda_2) = -\frac{a\alpha}{s-b}D^k(1-\lambda_1) - D^k\lambda_1 \\
\implies & B^{k+1}\left(-1 + \left(1 - \frac{a\alpha}{s-b}\right)(1-\lambda_2)\right) = D^k\left(-\frac{a\alpha}{s-b}(1-\lambda_1) - \lambda_1\right) \\
\implies & B^{k+1}\left(-(s-b)\lambda_2 - a\alpha(1-\lambda_2)\right) = D^k\left(-(s-b)\lambda_1 - a\alpha(1-\lambda_1)\right) \\
\implies & B^{k+1} = D^k\left(\frac{(s-b)\lambda_1 + a\alpha(1-\lambda_1)}{(s-b)\lambda_2 + a\alpha(1-\lambda_2)}\right). \qquad (3.22)
\end{aligned}$$

Similarly the first equation of the second subsystem of (3.20) produces

$$\begin{aligned}
& (s-\tilde{b})\hat{x}_1^{k+1}(s_2) - c\hat{x}_2^{k+1}(s_2) - \frac{c}{\beta}\hat{x}_3^{k+1}(s_2) = \frac{-c}{\beta}\hat{x}_{-1}^k(s_1) - c\hat{x}_0^k(s_1) \\
\implies & (s-\tilde{b})\hat{w}_1^{k+1} - c\hat{u}_1^{k+1} - \frac{c}{\beta}\hat{w}_2^{k+1} = -\frac{c}{\beta}\hat{q}_0^k - c\hat{p}_0^k \\
\implies & (s-\tilde{b})D^{k+1}\lambda_1 - \frac{ac}{s-b}D^{k+1}\lambda_1(1-\lambda_1) - \frac{c}{\beta}D^{k+1}\lambda_1^2 = -\frac{c}{\beta}B^k - \frac{ac}{s-b}B^k(1-\lambda_2) \\
\implies & \lambda_1 D^{k+1}\left((s-\tilde{b}) - \frac{ac(1-\lambda_1)}{s-b} - \frac{c\lambda_1}{\beta}\right) = B^k\left(-\frac{c}{\beta} - \frac{ac(1-\lambda_2)}{s-b}\right) \\
\implies & D^{k+1}\lambda_1\left(1 - \lambda_2 + \lambda_1\left(-\frac{s-b}{a\beta}\right)\right) = B^k\left(-\frac{s-b}{a\beta} - (1-\lambda_2)\right),
\end{aligned}$$

which reduces to

$$D^{k+1} = B^k\left(\frac{s-b+a\beta(1-\lambda_2)}{(s-b)\lambda_1 - a\beta(1-\lambda_2)}\right)\left(\frac{1}{\lambda_1}\right). \qquad (3.23)$$

The combination of (3.22) and (3.23) leads to

$$\begin{aligned}
B^{k+1} &= D^k\left(\frac{(s-b)\lambda_1 + a\alpha(1-\lambda_1)}{(s-b)\lambda_2 + a\alpha(1-\lambda_2)}\right) \\
&= \left(\frac{(s-b)\lambda_1 + a\alpha(1-\lambda_1)}{(s-b)\lambda_2 + a\alpha(1-\lambda_2)}\right)\left(\frac{s-b+a\beta(1-\lambda_2)}{(s-b)\lambda_1 - a\beta(1-\lambda_2)}\right)\left(\frac{1}{\lambda_1}\right) \\
&= \left(\frac{(s-b) + a\alpha(\lambda_2-1)}{(s-b)\lambda_2 + a\alpha(1-\lambda_2)}\right)\left(\frac{(s-b) + a\beta(1-\lambda_2)}{(s-b)\lambda_1 - a\beta(1-\lambda_2)}\right)B^{k-1} \\
&=: \rho(s,\alpha,\beta)B^{k-1},
\end{aligned}$$

and similarly, we get $D^{k+1} = \rho(s,\alpha,\beta)D^{k-1}$, where $\rho(s,\alpha,\beta)$ is defined by (3.21). We do similar calculations for the other case $|\lambda_1| > 1$. □

Corollary 1. The optimal α and β for the nonoverlapping OWR applied to RLCG transmission lines are given by

$$\begin{cases} \alpha_{opt} := \frac{s-b}{a(1-\lambda_2)}, & \text{and} \quad \beta_{opt} := -\frac{s-b}{a(1-\lambda_2)} \quad , \quad |\lambda_1| < 1, \\ \alpha_{opt} := \frac{s-b}{a(1-\lambda_1)}, & \text{and} \quad \beta_{opt} := -\frac{s-b}{a(1-\lambda_1)} \quad , \quad |\lambda_1| > 1, \end{cases}$$

and hence satisfy the relation $\beta_{opt} = -\alpha_{opt}$.

Proof. Equating the numerator of the convergence factor $\rho(s,\alpha,\beta)$ to zero results in these expressions for α_{opt} and β_{opt}. □

Remark 3.3.2. For the special choice of $\alpha = \alpha_{opt}$ and $\beta = \beta_{opt}$, we have $\rho(s,\alpha_{opt},\beta_{opt}) = 0$, which states that the nonoverlapping OWR algorithm converges in two iterations independently of the choice of initial guess required to start this algorithm. However, α_{opt} and β_{opt} are functions of s. Their inverse Laplace transformation leads to non-local operators in time which are expensive to calculate, and hence we approximate them by constants and find their expressions. This optimization will be performed in Section 3.4.

3.3.2 Overlapping OWR

In this section, we consider the overlapping OWR method. In Section 3.2.2, we considered the splitting of the infinite system (3.1) representing an infinitely long RLCG transmission line in two ways: one with splitting at a voltage node and the other with splitting at a current node, and proved that different splittings do not effect the convergence of the classical overlapping WR algorithm. We will define new transmission conditions for both splittings and study how they affect the convergence rate of the OWR algorithm. We further analyze the effect of splitting on the convergence. We start with splitting at a voltage node.

We refer to Section 3.2.2 for the detailed description of the process of splitting the system of equations (3.1), and adding n node overlap. For the splitting at a voltage node, say at x_{-1}, the new transmission conditions are defined as

$$\begin{aligned} x^{k+1}_{2n-2}(s_1) + \alpha^v x^{k+1}_{2n-3}(s_1) &= x^k_{2n-2}(s_2) + \alpha^v x^k_{2n-3}(s_2), \\ x^{k+1}_{-1}(s_2) + \beta^v x^{k+1}_{-2}(s_2) &= x^k_{-1}(s_1) + \beta^v x^k_{-2}(s_1), \end{aligned} \tag{3.24}$$

where α^v, $\beta^v \in \mathbb{R}$ are optimizing parameters. These transmission conditions are rewritten for $\beta^v \neq 0$ as,

$$\begin{aligned} x^{k+1}_{2n-2}(s_1) &= -\alpha^v x^{k+1}_{2n-3}(s_1) + x^k_{2n-2}(s_2) + \alpha^v x^k_{2n-3}(s_2), \\ x^{k+1}_{-2}(s_2) &= -\frac{x^{k+1}_{-1}(s_2)}{\beta^v} + \frac{x^k_{-1}(s_1)}{\beta^v} + x^k_{-2}(s_1). \end{aligned}$$

Substituting the Laplace transformation of the above equations into system (3.16) leads to

$$s\hat{\mathbf{x}}^{k+1}(s_1) = \begin{bmatrix} \ddots & \ddots & \ddots & \\ & a & b & -a \\ & & -c & (\tilde{b}-c\alpha^v) \end{bmatrix} \begin{bmatrix} \vdots \\ \hat{x}^{k+1}_{2n-4}(s_1) \\ \hat{x}^{k+1}_{2n-3}(s_1) \end{bmatrix} + \begin{bmatrix} \vdots \\ 0 \\ c\hat{x}^{k}_{2n-2}(s_2) + c\alpha^v \hat{x}^{k}_{2n-3}(s_2) \end{bmatrix},$$

$$s\hat{\mathbf{x}}^{k+1}(s_2) = \begin{bmatrix} \left(\tilde{b}+\frac{c}{\beta^v}\right) & c & \\ a & b & -a \\ & \ddots & \ddots & \ddots \end{bmatrix} \begin{bmatrix} \hat{x}^{k+1}_{-1}(s_2) \\ \hat{x}^{k+1}_{0}(s_2) \\ \vdots \end{bmatrix} + \begin{bmatrix} -c\hat{x}^{k}_{-2}(s_1) - \frac{c}{\beta^v}\hat{x}^{k}_{-1}(s_1) \\ 0 \\ \vdots \end{bmatrix}. \tag{3.25}$$

Theorem 3.3.2. *The convergence factor of the overlapping OWR algorithm with n nodes overlap and for a splitting at a voltage node for an infinitely long RLCG transmission line is*

$$\rho^v_n(s,\alpha^v,\beta^v) := \begin{cases} \left(\frac{(s-b)\alpha^v+a(1-\lambda_1)}{(s-b)\alpha^v\lambda_1+a(\lambda_1-1)}\right)\left(\frac{(s-b)-a\beta^v(1-\lambda_1)}{(s-b)\lambda_1-a\beta^v(\lambda_1-1)}\right)\left(\lambda_1^2\right)^n & ,|\lambda_1|<1, \\ \left(\frac{(s-b)\alpha^v+a(1-\lambda_2)}{(s-b)\alpha^v\lambda_2+a(\lambda_2-1)}\right)\left(\frac{(s-b)-a\beta^v(1-\lambda_2)}{(s-b)\lambda_2-a\beta^v(\lambda_2-1)}\right)\left(\lambda_2^2\right)^n & ,|\lambda_1|>1. \end{cases} \tag{3.26}$$

Proof. The proof is similar to the proof of Theorem 3.2.2, but the constants B^{k+1} and D^{k+1} change due to the presence of the optimized transmission conditions (3.24). Under the condition $|\lambda_1|<1$, tracing back to the proof of Theorem 3.2.2, we have

$$\hat{q}^{k+1}_j = B^{k+1}\lambda_2^j, \quad \text{and} \quad \hat{p}^{k+1}_j = \frac{aB^{k+1}}{s-b}\left(\lambda_2^{j-1}-\lambda_2^j\right),$$
$$\hat{w}^{k+1}_j = D^{k+1}\lambda_1^j, \quad \text{and} \quad \hat{u}^{k+1}_j = \frac{aD^{k+1}}{s-b}\left(\lambda_1^{j}-\lambda_1^{j+1}\right).$$

Substituting these equations into the last equation of first subsystem of (3.25) results in

$$\begin{aligned} & (s-\tilde{b}+c\alpha^v)\hat{x}^{k+1}_{2n-3}(s_1) + c\hat{x}^{k+1}_{2n-4}(s_1) = c\hat{x}^{k}_{2n-2}(s_2) + c\alpha^v\hat{x}^{k}_{2n-3}(s_2) \\ \Longrightarrow \quad & (s-\tilde{b}+c\alpha^v)\hat{q}^{k+1}_{n-2} + c\hat{p}^{k+1}_{n-2} = c\hat{u}^{k}_{n-1} + c\alpha^v\hat{w}^{k}_{n-1} \\ \Longrightarrow \quad & B^{k+1}\lambda_2^{n-2}\left((s-\tilde{b}+c\alpha^v) + \frac{ac}{s-b}\left(\lambda_2^{-1}-1\right)\right) = D^k\lambda_1^{n-1}\left(\frac{ac}{s-b}(1-\lambda_1)+c\alpha^v\right) \\ \Longrightarrow \quad & B^{k+1}\lambda_2^{n-2}\left(1-\lambda_2+\frac{\alpha^v}{a}(s-b)\right) = D^k\lambda_1^{n-1}\left(1-\lambda_1+\frac{\alpha^v}{a}(s-b)\right) \\ \Longrightarrow \quad & B^{k+1} = D^k\frac{(\lambda_1^2)^{n-1}}{\lambda_1}\left(\frac{(s-b)\alpha^v+a(1-\lambda_1)}{(s-b)\alpha^v+a(1-\lambda_2)}\right). \end{aligned} \tag{3.27}$$

Similarly, the first equation of the second subsystem of (3.25) leads to

$$\begin{aligned}
&\left(s-\tilde{b}-\frac{c}{\beta^v}\right)\hat{x}_{-1}^{k+1}(s_2)-c\hat{x}_0^{k+1}(s_2)=-c\hat{x}_{-2}^{k}(s_1)-\frac{c}{\beta^v}\hat{x}_{-1}^{k}(s_1)\\
\Longrightarrow\quad &\left(s-\tilde{b}-\frac{c}{\beta^v}\right)\hat{w}_0^{k+1}-c\hat{u}_0^{k+1}=-c\hat{p}_{-1}^{k}-\frac{c}{\beta^v}\hat{q}_{-1}^{k}\\
\Longrightarrow\quad &D^{k+1}\left(1-\lambda_2-\frac{(s-b)}{a\beta^v}\right)=B^k\lambda_1\left(1-\lambda_1-\frac{(s-b)}{a\beta^v}\right)\\
\Longrightarrow\quad &D^{k+1}=B^k\lambda_1\left(\frac{(s-b)-a\beta^v(1-\lambda_1)}{(s-b)-a\beta^v(1-\lambda_2)}\right). \qquad (3.28)
\end{aligned}$$

Combining (3.27) and (3.28) produces

$$\begin{aligned}
B^{k+1} &= \frac{\left(\lambda_1^2\right)^{n-1}}{\lambda_1}\left(\frac{(s-b)\alpha^v+a(1-\lambda_1)}{(s-b)\alpha^v+a(1-\lambda_2)}\right)\lambda_1\left(\frac{(s-b)-a\beta^v(1-\lambda_1)}{(s-b)-a\beta^v(1-\lambda_2)}\right)B^{k-1}\\
&= \left(\lambda_1^2\right)^n\left(\frac{(s-b)\alpha^v+a(1-\lambda_1)}{(s-b)\alpha^v\lambda_1+a(\lambda_1-1)}\right)\left(\frac{(s-b)-a\beta^v(1-\lambda_1)}{(s-b)\lambda_1-a\beta^v(\lambda_1-1)}\right)B^{k-1},
\end{aligned}$$

that is, $B^{k+1}=\rho_n^v(s,\alpha^v,\beta^v)B^{k-1}$ and in a similar way, we get $D^{k+1}=\rho_n^v(s,\alpha^v,\beta^v)D^{k-1}$. This completes the proof. □

Corollary 2. The optimal α^v and β^v for the overlapping OWR with n nodes overlap and splitting at a voltage node are given by

$$\begin{cases}
\alpha_{opt}^v := \frac{a(\lambda_1-1)}{s-b}, \quad \text{and} \quad \beta_{opt}^v := -\frac{s-b}{a(\lambda_1-1)}, \quad , \quad |\lambda_1|<1,\\
\alpha_{opt}^v := \frac{a(\lambda_2-1)}{s-b}, \quad \text{and} \quad \beta_{opt}^v := -\frac{s-b}{a(\lambda_2-1)} \quad , \quad |\lambda_1|>1,
\end{cases}$$

and hence satisfy the relation $\beta_{opt}^v=-\frac{1}{\alpha_{opt}^v}$ for both cases.

We now consider the other splitting, that is, splitting at an even row (say at x_0) corresponding to a current node. Results for this splitting are similar to the splitting at a voltage node, but for completeness, we show the required calculations. For this splitting, the optimized transmission conditions are defined as

$$\begin{aligned}
x_{2n-1}^{k+1}(s_1)+\alpha^c x_{2n-2}^{k+1}(s_1) &= x_{2n-1}^{k}(s_2)+\alpha^c x_{2n-2}^{k}(s_2),\\
x_0^{k+1}(s_2)+\beta^c x_{-1}^{k+1}(s_2) &= x_0^{k}(s_1)+\beta^c x_{-1}^{k}(s_1),
\end{aligned} \qquad (3.29)$$

where α^c, $\beta^c\in\mathbb{R}$ are optimization parameters. These transmission conditions are rewritten for $\beta^c\neq 0$ as,

$$\begin{aligned}
x_{2n-1}^{k+1}(s_1) &= -\alpha^c x_{2n-2}^{k+1}(s_1)+x_{2n-1}^{k}(s_2)+\alpha^c x_{2n-2}^{k}(s_2),\\
x_{-1}^{k+1}(s_2) &= -\frac{x_0^{k+1}(s_2)}{\beta^c}+\frac{x_0^{k}(s_1)}{\beta^c}+x_{-1}^{k}(s_1).
\end{aligned}$$

Substituting the above Laplace transformed transmission conditions into (3.17) leads to

$$s\hat{\mathbf{x}}^{k+1}(s_1) = \begin{bmatrix} \ddots & \ddots & \ddots & \\ & -c & \tilde{b} & c \\ & & a & (b+a\alpha^c) \end{bmatrix} \begin{bmatrix} \vdots \\ \hat{x}^{k+1}_{2n-3}(s_1) \\ \hat{x}^{k+1}_{2n-2}(s_1) \end{bmatrix} + \begin{bmatrix} \vdots \\ 0 \\ -a\hat{x}^{k}_{2n-1}(s_2) - a\alpha^c\hat{x}^{k}_{2n-2}(s_2) \end{bmatrix},$$

$$s\hat{\mathbf{x}}^{k+1}(s_2) = \begin{bmatrix} (b-\frac{a}{\beta^c}) & -a & & \\ -c & \tilde{b} & c & \\ & \ddots & \ddots & \ddots \end{bmatrix} \begin{bmatrix} \hat{x}^{k+1}_{0}(s_2) \\ \hat{x}^{k+1}_{1}(s_2) \\ \vdots \end{bmatrix} + \begin{bmatrix} a\hat{x}^{k}_{-1}(s_1) + \frac{a}{\beta^c}\hat{x}^{k}_{0}(s_1) \\ 0 \\ \vdots \end{bmatrix}. \tag{3.30}$$

Theorem 3.3.3. *The convergence factor of the overlapping OWR algorithm with n nodes overlap and for a splitting at a current node for an infinitely long RLCG transmission line is*

$$\rho^c_n(s,\alpha^c,\beta^c) := \begin{cases} \left(\frac{(s-b)+a\alpha^c(\lambda_2-1)}{(s-b)+a\alpha^c(\lambda_1-1)}\right)\left(\frac{\beta^c(s-b)+a(1-\lambda_2)}{\beta^c(s-b)+a(1-\lambda_1)}\right)(\lambda_1^2)^n & , \quad |\lambda_1|<1, \\ \left(\frac{(s-b)+a\alpha^c(\lambda_1-1)}{(s-b)+a\alpha^c(\lambda_2-1)}\right)\left(\frac{\beta^c(s-b)+a(1-\lambda_1)}{\beta^c(s-b)+a(1-\lambda_2)}\right)(\lambda_2^2)^n & , \quad |\lambda_1|>1. \end{cases} \tag{3.31}$$

Proof. The proof is similar to the proof of Theorem 3.2.3, but the optimized transmission conditions (3.29) change the constants B^{k+1} and D^{k+1}. For the case $|\lambda_1|<1$, going back to the proof of Theorem 3.2.3, we have

$$\hat{q}^{k+1}_j = B^{k+1}\lambda_2^j, \quad \text{and} \quad \hat{p}^{k+1}_j = \frac{aB^{k+1}}{s-b}\left(\lambda_2^j - \lambda_2^{j+1}\right),$$
$$\hat{w}^{k+1}_j = D^{k+1}\lambda_1^j, \quad \text{and} \quad \hat{u}^{k+1}_j = \frac{aD^{k+1}}{s-b}\left(\lambda_1^{j-1} - \lambda_1^{j}\right).$$

Substituting these equations into the last equation of the first subsystem of (3.30) results in

$$\begin{aligned} & (s-b+a\alpha^c)\hat{x}^{k+1}_{2n-2}(s_1) - a\hat{x}^{k+1}_{2n-3}(s_1) = -a\hat{x}^{k}_{2n-1}(s_2) - a\alpha^c\hat{x}^{k}_{2n-2}(s_2) \\ \Longrightarrow \quad & (s-b-a\alpha^c)\hat{p}^{k+1}_{n-1} - a\hat{q}^{k+1}_{n-1} = -a\hat{w}^{k}_{n-1} - a\alpha^c\hat{u}^{k}_{n-1} \\ \Longrightarrow \quad & B^{k+1}\lambda_2^{n-1}\left(-1+\left(1-\frac{a\alpha^c}{s-b}\right)(1-\lambda_2)\right) = D^k\lambda_1^{n-1}\left(-1-\frac{a\alpha^c}{s-b}(\lambda_2-1)\right) \\ \Longrightarrow \quad & B^{k+1} = D^k(\lambda_1^2)^{n-1}\left(\frac{(s-b)+a\alpha(\lambda_2-1)}{(s-b)\lambda_2+a\alpha(1-\lambda_2)}\right). \end{aligned} \tag{3.32}$$

Similarly, the first equation of the second subsystem of (3.30) leads to

$$\begin{aligned}
&\left(s-b+\frac{a}{\beta^c}\right)\hat{x}_0^{k+1}(s_2)+a\hat{x}_1^{k+1}(s_2)=a\hat{x}_{-1}^{k}(s_1)+\frac{a}{\beta^c}\hat{x}_0^{k}(s_1)\\
\Longrightarrow\quad &\left(s-b+\frac{a}{\beta^c}\right)\hat{u}_0^{k+1}+a\hat{w}_0^{k+1}=a\hat{q}_0^{k}+\frac{a}{\beta^c}\hat{p}_0^{k}\\
\Longrightarrow\quad & D^{k+1}\left(\left(1+\frac{a}{\beta^c(s-b)}\right)(\lambda_2-1)+1\right)=B^k\left(\frac{a}{\beta^c(s-b)}(1-\lambda_2)+1\right)\\
\Longrightarrow\quad & D^{k+1}=B^k\left(\frac{\beta^c(s-b)+a(1-\lambda_2)}{\beta^c(s-b)\lambda_2+a(\lambda_2-1)}\right). \qquad (3.33)
\end{aligned}$$

Combining (3.32) and (3.33) yields

$$\begin{aligned}
B^{k+1} &= (\lambda_1^2)^{n-1}\left(\frac{(s-b)+a\alpha^c(\lambda_2-1)}{(s-b)\lambda_2+a\alpha^c(1-\lambda_2)}\right)\left(\frac{\beta^c(s-b)+a(1-\lambda_2)}{\beta^c(s-b)\lambda_2+a(\lambda_2-1)}\right)B^{k-1}\\
&= (\lambda_1^2)^{n}\left(\frac{(s-b)+a\alpha^c(\lambda_2-1)}{(s-b)+a\alpha^c(\lambda_1-1)}\right)\left(\frac{\beta^c(s-b)+a(1-\lambda_2)}{\beta^c(s-b)+a(1-\lambda_1)}\right)B^{k-1},
\end{aligned}$$

that is, $B^{k+1}=\rho_n^c(s,\alpha^c,\beta^c)B^{k-1}$ and in a similar way, we get $D^{k+1}=\rho_n^c(s,\alpha^c,\beta^c)D^{k-1}$. This completes the proof. □

Corollary 3. The optimal α^c and β^c for the overlapping OWR with n nodes overlap and splitting at a current node are given by

$$\begin{cases}
\alpha_{opt}^c := \frac{s-b}{a(1-\lambda_2)}, \quad \text{and} \quad \beta_{opt}^c := -\frac{a(1-\lambda_2)}{s-b}, \quad , \quad |\lambda_1|<1,\\
\alpha_{opt}^c := \frac{s-b}{a(1-\lambda_1)}, \quad \text{and} \quad \beta_{opt}^c := -\frac{a(1-\lambda_1)}{s-b}, \quad , \quad |\lambda_1|>1,
\end{cases}$$

and hence satisfy the relation $\beta_{opt}^c=-\frac{1}{\alpha_{opt}^c}$ for both cases.

Remark 3.3.3. We observe that for all cases, that is, nonoverlapping OWR, overlapping OWR with splitting at a voltage node and overlapping OWR with splitting at a current node, the convergence factor for each case is the same at all nodes irrespective of which subsystem they belong to.

Remark 3.3.4. For the overlapping OWR, it is interesting to note the relation between α_{opt}^v and α_{opt}^c. Since $\lambda_1\lambda_2=1$, we have

$$\alpha_{opt}^c=\frac{s-b}{a(1-\lambda_2)}=\frac{s-b}{a(\lambda_1-1)\lambda_2}=\frac{\lambda_1}{\alpha_{opt}^v},$$

that is, $\alpha_{opt}^v\alpha_{opt}^c=\lambda_1$. But since λ_1 is a complicated function of s, one cannot find an expression for α_{opt}^c using an expression for α_{opt}^v and vice versa. This forces us to perform an optimization study for both cases separately.

3.4 Optimization

In Section 3.2, we proved that the classical WR methods converge, but their convergence rate is very low. For the OWR methods, the optimized transmission conditions which transfer a specific combination of currents and voltages at the interface are expected to improve the convergence. We need to choose the optimization parameters α and β appropriately to have rapid convergence, that is, we would like to have $|\rho(s,\alpha,\beta)| \ll 1$ for the nonoverlapping OWR method and $|\rho_n^v(s,\alpha^v,\beta^v)| \ll 1$, and $|\rho_n^c(s,\alpha^c,\beta^c)| \ll 1$ for the overlapping OWR methods. This leads to solving a min-max problem of the form

$$\min_{\alpha,\beta\in\mathbb{R}} \left(\max_{\Re(s)\geq 0} |\Gamma(s,\alpha,\beta)| \right), \tag{3.34}$$

where $\Gamma(s,\alpha,\beta)$ refers to $\rho(s,\alpha,\beta)$ or $\rho_n^v(s,\alpha^v,\beta^v)$ or $\rho_n^c(s,\alpha^c,\beta^c)$ defined in equations (3.21), (3.26) and (3.31) respectively. But there are already four unknowns in each min-max problem. We thus reduce this problem to a simplified problem using some assumptions and lemmas.

We start with the nonoverlapping OWR method.

3.4.1 Nonoverlapping OWR

Motivated by the relation between β_{opt} and α_{opt} given in Corollary 1, we assume $\beta = -\alpha$. Thus the convergence factor $\rho(s,\alpha,\beta)$ defined in (3.21) reduces to $\rho(s,\alpha) := \rho(s,\alpha,-\alpha)$ and is given by

$$\rho(s,\alpha) = \begin{cases} \left(\frac{(s-b)+a\alpha(\lambda_2-1)}{(s-b)\lambda_2+a\alpha(1-\lambda_2)}\right)\left(\frac{(s-b)+a\alpha(\lambda_2-1)}{(s-b)\lambda_1+a\alpha(1-\lambda_2)}\right) & , \quad |\lambda_1|<1, \\ \left(\frac{(s-b)+a\alpha(\lambda_1-1)}{(s-b)\lambda_1+a\alpha(1-\lambda_1)}\right)\left(\frac{(s-b)+a\alpha(\lambda_1-1)}{(s-b)\lambda_2+a\alpha(1-\lambda_1)}\right) & , \quad |\lambda_1|>1. \end{cases} \tag{3.35}$$

We further reduce the range of $s \in \mathbb{C}^+$ using the following lemmas.

Lemma 3.4.1. *For $\alpha < 0$, the maximum of the modulus of the convergence factor $|\rho(s,\alpha)|$ lies on the imaginary axis of the complex plane.*

Proof. We prove this lemma by contradiction. We assume that the zeros of the denominator of the convergence factor $\rho(s,\alpha)$ lie on the right half of the complex plane, that is, $\sigma \geq 0$, where $s = \sigma + i\omega$. We first consider the condition $|\lambda_1| < 1$, with $\lambda_1 = l_1 + il_2$. Since $|\lambda_1| < 1$, we have $|l_1| < 1$ and $|l_2| < 1$. Equating the denominator of $\rho(s,\alpha)$ to zero, we get $(s-b)\lambda_2 + a\alpha(1-\lambda_2) = 0$, that is, $s - b = a\alpha(1-\lambda_1)$. Comparing the real part of the last equation leads to $\sigma = b + a\alpha(1-l_1)$, which is a contradiction since $\sigma \geq 0$ while $b < 0$ and $a\alpha(1-l_1) < 0$. A similar analysis can be done for the other case $|\lambda_1| > 1$. Thus $|\rho(s,\alpha)|$ is analytic in the right half of the complex plane. The Maximum Modulus Principle for the analytic functions states that the maximum lies on the boundary, that is, on the imaginary axis of the complex plane. □

Lemma 3.4.1 states that we can restrict the domain of $\Re(s) \geq 0$ to $s = i\omega$, where $\omega \in \mathbb{R}$.

Lemma 3.4.2. *For $s = i\omega$, the functions λ_1 and λ_2 satisfy*

$$\overline{\lambda_1(-\omega)} = \lambda_1(\omega), \quad \textit{and} \quad \overline{\lambda_2(-\omega)} = \lambda_2(\omega).$$

Proof. The proof of this theorem is similar to the proof of Lemma 2.4.2. Recall the definition of λ_1 from Theorem 3.2.1. For $s = i\omega$,

$$\begin{aligned}
\lambda_1(\omega) &= \frac{2ac - (i\omega - \tilde{b})(i\omega - b) + \sqrt{(2ac - (i\omega - \tilde{b})(i\omega - b))^2 - 4a^2c^2}}{2ac} \\
&= \frac{\omega^2 + 2ac - b\tilde{b} + i\omega(b + \tilde{b}) + \sqrt{r_1 + ir_2}}{2ac} = \frac{\omega^2 + 2ac - b\tilde{b} + i\omega(b + \tilde{b}) + (z_1 + iz_2)}{2ac} \\
&= \left(\frac{\omega^2 + 2ac - b\tilde{b} + z_1}{2ac}\right) + i\left(\frac{\omega(b + \tilde{b}) + z_2}{2ac}\right), \qquad (3.36)
\end{aligned}$$

where

$$\begin{aligned}
r_1 &:= \omega^4 + (4ac - b^2 - 4b\tilde{b} - \tilde{b}^2)\omega^2 - 4ac\tilde{b}b + \tilde{b}^2b^2, \\
r_2 &:= 2\omega(b + \tilde{b})(2ac - b\tilde{b} + \omega^2),
\end{aligned}$$

and $z_1 + iz_2 := \sqrt{r_1 + ir_2}$, with $z_1,\ z_2 \in \mathbb{R}$. Further, a similar calculation shows $\lambda_1(-\omega) = \frac{\omega^2 + 2ac - b\tilde{b} - i\omega(b+\tilde{b}) + \sqrt{r_1 - ir_2}}{2ac}$. Using some techniques of complex analysis one can show that if $\sqrt{r_1 + ir_2} = z_1 + iz_2$ then $\sqrt{r_1 - ir_2} = z_1 - iz_2$. Thus,

$$\begin{aligned}
\overline{\lambda_1(-\omega)} &= \overline{\left(\frac{\omega^2 + 2ac - b\tilde{b} + z_1}{2ac}\right) - i\left(\frac{\omega(b + \tilde{b}) + z_2}{2ac}\right)} \\
&= \left(\frac{\omega^2 + 2ac - b\tilde{b} + z_1}{2ac}\right) + i\left(\frac{\omega(b + \tilde{b}) + z_2}{2ac}\right) = \lambda_1(\omega).
\end{aligned}$$

Following these calculations, we can also prove that $\overline{\lambda_2(-\omega)} = \lambda_2(\omega)$, and this completes the proof of this lemma. □

Lemma 3.4.3. *For $s = i\omega$, $|\rho(\omega, \alpha)|$ is an even function of ω.*

Proof. Using Lemma 3.4.2 and the definition of the convergence factor of the nonover-

lapping OWR given in (3.35), for $|\lambda_1| < 1$ and $s = i\omega$,

$$\begin{aligned}
|\rho(-\omega,\alpha)| &= \left|\left(\frac{(-i\omega-b)+a\alpha(\lambda_2(-\omega)-1)}{(-i\omega-b)\lambda_2(-\omega)+a\alpha(1-\lambda_2(-\omega))}\right)\left(\frac{(-i\omega-b)+a\alpha(\lambda_2(-\omega)-1)}{(-i\omega-b)\lambda_1(-\omega)+a\alpha(1-\lambda_2(-\omega))}\right)\right| \\
&= \left|\left(\frac{(\overline{i\omega}-b)+a\alpha(\overline{\lambda_2(\omega)}-1)}{(\overline{i\omega}-b)\overline{\lambda_2(\omega)}+a\alpha(1-\overline{\lambda_2(\omega)})}\right)\left(\frac{(\overline{i\omega}-b)+a\alpha(\overline{\lambda_2(\omega)}-1)}{(\overline{i\omega}-b)\overline{\lambda_1(\omega)}+a\alpha(1-\overline{\lambda_2(\omega)})}\right)\right| \\
&= \left|\left(\frac{\overline{(i\omega-b)+a\alpha(\lambda_2(\omega)-1)}}{\overline{(i\omega-b)\lambda_2(\omega)+a\alpha(1-\lambda_2(\omega))}}\right)\left(\frac{\overline{(i\omega-b)+a\alpha(\lambda_2(\omega)-1)}}{\overline{(i\omega-b)\lambda_1(\omega)+a\alpha(1-\lambda_2(\omega))}}\right)\right| \\
&= \left|\left(\frac{(i\omega-b)+a\alpha(\lambda_2(\omega)-1)}{(i\omega-b)\lambda_2(\omega)+a\alpha(1-\lambda_2(\omega))}\right)\left(\frac{(i\omega-b)+a\alpha(\lambda_2(\omega)-1)}{(i\omega-b)\lambda_1(\omega)+a\alpha(1-\lambda_2(\omega))}\right)\right| \\
&= |\rho(\omega,\alpha)|\,.
\end{aligned}$$

□

Lemmas 3.4.1 and 3.4.3, reduce the min-max problem (3.34) for the nonoverlapping OWR to

$$\min_{\alpha<0}\left(\max_{\omega_{\min}\le\omega\le\omega_{max}}|\rho(\omega,\alpha)|\right), \tag{3.37}$$

where we have restricted the range of ω to $[\omega_{\min},\omega_{\max}]$, where $\omega_{\min} := \frac{\pi}{T}$ and $\omega_{\max} := \frac{\pi}{\Delta t}$, with T as the final time and Δt as the time discretization parameter. This restriction is valid since for numerical simulations, we consider time integration over finite time $t \in (0,T]$. Solving the min-max problem (3.37) in closed form is impossible using the available complex analysis tools. We therefore make some more assumptions and then use asymptotic analysis with respect to $\omega_{\min} \to 0$, which corresponds to final time $T \to \infty$.

Assumption 3.4.1. We assume that $\tilde{b} = 0$. Since $\tilde{b} = -\frac{G}{C}$, assuming $\tilde{b} = 0$ means that the conductance G in the RLCG transmission line is zero. This is the case when there is no leakage of current in the dielectric medium between the two conductors of the transmission line.

Numerically, we observe from the left plot of Figure 3.4 that the solution of the min-max problem (3.37) is given by equioscillation between the frequencies $\omega_{\min}$ and $\omega_{\max}$, that is, the optimized α, denoted by α_0^* satisfies

$$|\rho(\omega_{\min},\alpha_0^*)| = |\rho(\omega_{\max},\alpha_0^*)|. \tag{3.38}$$

Further, we denote the minimum frequency $\omega_{\min}$ by the asymptotic parameter ϵ and study the behavior of the convergence factor as $\epsilon \to 0$. Under this condition, we observe numerically that the optimized α_0^* satisfy the relation $\alpha_0^* = -C_0\epsilon^{-\delta}$, for some $\delta, C_0 > 0$. We determine these constants using the equioscillation relation (3.38).

We first evaluate λ_1 and λ_2 at $\omega_{\min} = \epsilon$.

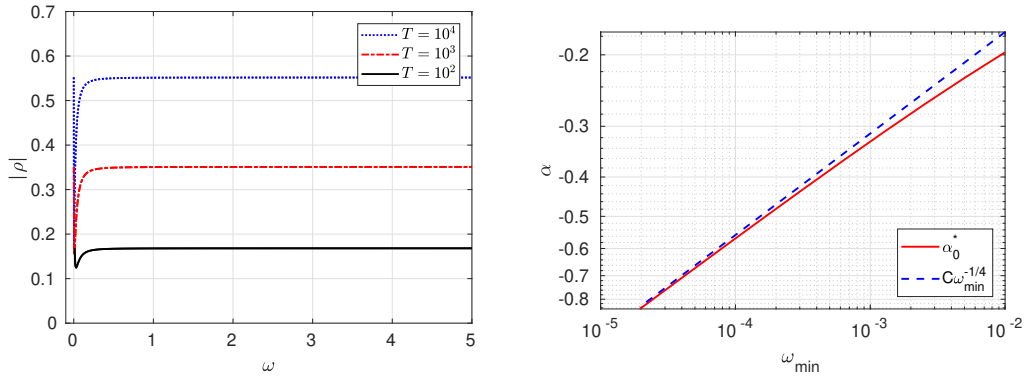

Figure 3.4: Equioscillation for nonoverlapping OWR for different values of T (left) and dependence of α_0^* on $\omega_{\min}$ (right).

Lemma 3.4.4. *For small ω such that $\omega \to 0$, the functions λ_1 and λ_2 satisfy the asymptotic relation*

$$\begin{aligned}
\lambda_1(\omega) &= \left(1 + \frac{\sqrt{2}\sqrt{acb}\omega^{1/2}}{2ac} + \left(\frac{\sqrt{2}\sqrt{acb}}{4acb} - \frac{b\sqrt{2}\sqrt{acb}}{16a^2c^2}\right)\omega^{3/2}\right) \\
&\quad + i\left(\frac{\sqrt{2}b\omega^{1/2}}{2\sqrt{acb}} + \frac{b\omega}{2ac} + \left(\frac{\sqrt{2}b^2}{16ac\sqrt{acb}} - \frac{\sqrt{2}}{4\sqrt{acb}}\right)\omega^{3/2}\right) + \mathcal{O}(\omega^{5/2}), \\
\lambda_2(\omega) &= \left(1 - \frac{\sqrt{2}\sqrt{acb}\omega^{1/2}}{2ac} - \left(\frac{\sqrt{2}\sqrt{acb}}{4acb} - \frac{b\sqrt{2}\sqrt{acb}}{16a^2c^2}\right)\omega^{3/2}\right) \\
&\quad + i\left(-\frac{\sqrt{2}b\omega^{1/2}}{2\sqrt{acb}} + \frac{b\omega}{2ac} + \left(\frac{\sqrt{2}}{4\sqrt{acb}} - \frac{\sqrt{2}b^2}{16ac\sqrt{acb}}\right)\omega^{3/2}\right) + \mathcal{O}(\omega^{5/2}),
\end{aligned}$$

with $|\lambda_1| < 1 < |\lambda_2|$.

Proof. We go back to the proof of Lemma 3.4.2, and note that for $\tilde{b} = 0$,

$$r_1 = \omega^2(4ac - b^2 + \omega^2), \quad \text{and} \quad r_2 = 2b\omega(2ac + \omega^2).$$

Since $z_1 + iz_2 = \sqrt{r_1 + ir_2}$, squaring both sides and comparing real and imaginary parts leads to $z_1^2 - z_2^2 = r_1$ and $2z_1z_2 = r_2$. Further, z_2 can be written in terms of z_1 as $z_2 = \frac{r_2}{2z_1}$, which on substituting into first equation yields

$$z_1^4 - r_1z_1^2 - \frac{r_2^2}{4} = 0.$$

Taking the positive root of this equation, since $\omega \to 0$ gives

$$\begin{aligned} z_1^2 &= \frac{r_1 + \sqrt{r_1^2 + r_2^2}}{2} = \frac{\omega^2(4ac - b^2 + \omega^2) + \sqrt{(\omega^2(4ac - b^2 + \omega^2))^2 + (2b\omega(2ac + \omega^2))^2}}{2} \\ &= 2acb\omega + \left(\frac{4ac - b^2 + \omega^2}{2}\right)\omega^2 + \left(\frac{ac}{b} + \frac{b}{2} + \frac{b^3}{16ac}\right)\omega^3 + \mathcal{O}(\omega^5). \end{aligned}$$

Taking the square root leads to

$$\begin{aligned} z_1 &= \sqrt{2acb\omega + \left(\frac{4ac - b^2 + \omega^2}{2}\right)\omega^2 + \left(\frac{ac}{b} + \frac{b}{2} + \frac{b^3}{16ac}\right)\omega^3 + \mathcal{O}(\omega^5)} \\ &= \sqrt{2}\sqrt{acb}\omega^{1/2} + \left(\frac{\sqrt{2}\sqrt{acb}}{2b} - \frac{\sqrt{2}\sqrt{acbb}}{8ac}\right)\omega^{3/2} + \mathcal{O}(\omega^{5/2}). \end{aligned}$$

Since $z_2 = \frac{r_2}{z_1}$,

$$\begin{aligned} z_2 &= \frac{2b\omega(2ac + \omega^2)}{\sqrt{2}\sqrt{acb}\omega^{1/2} + \left(\frac{\sqrt{2}\sqrt{acb}}{2b} - \frac{\sqrt{2}\sqrt{acbb}}{8ac}\right)\omega^{3/2} + \mathcal{O}(\omega^{5/2})} \\ &= \sqrt{2}\sqrt{acb}\omega^{1/2} - \left(\frac{\sqrt{2}ac}{2\sqrt{acb}} - \frac{\sqrt{2}b^2}{8\sqrt{acb}}\right)\omega^{3/2} + \mathcal{O}(\omega^{5/2}). \end{aligned}$$

From (3.36), we get

$$\begin{aligned} \lambda_1(\omega) = &\left(1 + \frac{\sqrt{2}\sqrt{acb}\omega^{1/2}}{2ac} + \left(\frac{\sqrt{2}\sqrt{acb}}{4acb} - \frac{b\sqrt{2}\sqrt{acb}}{16a^2c^2}\right)\omega^{3/2}\right) \\ &+ i\left(\frac{\sqrt{2}b\omega^{1/2}}{2\sqrt{acb}} + \frac{b\omega}{2ac} - \left(\frac{\sqrt{2}}{4\sqrt{acb}} - \frac{\sqrt{2}b^2}{16ac\sqrt{acb}}\right)\omega^{3/2}\right) + \mathcal{O}(\omega^{5/2}) \end{aligned}$$

and

$$\begin{aligned} \lambda_2(\omega) &= \left(\frac{\omega^2 + 2ac - z_1}{2ac}\right) + i\left(\frac{b\omega - z_2}{2ac}\right) \\ &= \left(1 - \frac{\sqrt{2}\sqrt{acb}\omega^{1/2}}{2ac} - \left(\frac{\sqrt{2}\sqrt{acb}}{4acb} - \frac{b\sqrt{2}\sqrt{acb}}{16a^2c^2}\right)\omega^{3/2}\right) \\ &\quad + i\left(-\frac{\sqrt{2}b\omega^{1/2}}{2\sqrt{acb}} + \frac{b\omega}{2ac} + \left(\frac{\sqrt{2}}{4\sqrt{acb}} - \frac{\sqrt{2}b^2}{16ac\sqrt{acb}}\right)\omega^{3/2}\right) + \mathcal{O}(\omega^{5/2}). \end{aligned}$$

This completes the proof. □

Lemma 3.4.5. *For the nonoverlapping OWR, the modulus of the convergence factor* $|\rho(\omega, \alpha)|$ *at* $\omega_{\min}$ *and* $\omega_{\max}$ *is given by*

$$|\rho(\omega_{\min}, \alpha)| = 1 - \frac{2C_0\sqrt{2}\sqrt{acb}\omega_{\min}^{1/2-\delta}}{bc} + \mathcal{O}\left(\omega_{\min}^{1-2\delta}\right), \tag{3.39}$$

and,

$$|\rho(\omega_{\max},\alpha)| = 1 - \frac{g_r}{aC_0}\omega_{\min}^{\delta} + \mathcal{O}(\omega_{\min}^{2\delta}), \tag{3.40}$$

where $g_r := \Re\left(\frac{(i\omega_{\max}-b)(2+\lambda_1(\omega_{\max})+\lambda_2(\omega_{\max}))}{\lambda_2(\omega_{\max})-1}\right)$ *and* $\omega_{\min}\to 0$.

Proof. We first derive an asymptotic expression for $|\rho(\omega,\alpha)|$ at $\omega_{\min}=\epsilon$. The dependence of α on ϵ is given by $\alpha = -C_0\epsilon^{-\delta}$, for some $C_0,\delta>0$. Let $A(\epsilon)$ and $B(\epsilon)$ denote the modulus of numerator and denominator of $\rho(\omega_{\min},\alpha)$. Using the asymptotic expansions and Lemma 3.4.4, we have

$$\begin{aligned}
A(\epsilon) &:= \left|((s-b)+a\alpha(\lambda_2-1))^2\right| \\
&= \left|\left(-b+\frac{C_0\sqrt{2}\sqrt{acb}\sqrt{\epsilon}}{2\epsilon^{\delta}c}\right)+i\left(\frac{aC_0b\sqrt{2}b\sqrt{\epsilon}}{2\epsilon^{\delta}\sqrt{acb}}+\epsilon-\frac{C_0b\epsilon}{2e^{\delta}c}\right)+\mathcal{O}\left(\epsilon^{3/2-\delta}\right)\right|^2 \\
&= b^2-\frac{bC_0\sqrt{2}\sqrt{acb}\epsilon^{1/2-\delta}}{c}+\frac{C_0^2ab\epsilon^{1-2\delta}}{c}+\mathcal{O}\left(\epsilon^{3/2-\delta}\right),
\end{aligned}$$

and

$$\begin{aligned}
B(\epsilon) &:= |((s-b)\lambda_2+a\alpha(1-\lambda_2))\,((s-b)\lambda_1+a\alpha(1-\lambda_2))| \\
&= \left|\left(b^2+\frac{bC_0\sqrt{2}\sqrt{acb}\sqrt{\epsilon}}{\epsilon^{\delta}c}\right)+i\left(\frac{aC_0\sqrt{2}b^2\sqrt{\epsilon}}{\epsilon^{\delta}\sqrt{acb}}+\frac{C_0^2ab\epsilon}{\epsilon^{2\delta}c}-2b\epsilon\right)+\mathcal{O}\left(\epsilon^{3/2-\delta}\right)\right| \\
&= \left(b^4+\frac{2b^3C_0\sqrt{2}\sqrt{acb}\epsilon^{1/2-\delta}}{c}+\frac{4b^3C_0^2a\epsilon^{1-2\delta}}{c}+\mathcal{O}\left(\epsilon^{3/2-\delta}\right)\right)^{1/2} \\
&= b^2\left(1+\frac{2C_0\sqrt{2}\sqrt{acb}\epsilon^{1/2-\delta}}{bc}+\frac{4C_0^2a\epsilon^{1-2\delta}}{bc}+\mathcal{O}\left(\epsilon^{3/2-\delta}\right)\right)^{1/2} \\
&= b^2+\frac{bC_0\sqrt{2}\sqrt{acb}\epsilon^{1/2-\delta}}{c}+\frac{C_0^2ab\epsilon^{1-2\delta}}{c}+\mathcal{O}\left(\epsilon^{3/2-\delta}\right).
\end{aligned}$$

The expression for $|\rho(\omega_{\min},\alpha)|$ is thus reduced to

$$\begin{aligned}
|\rho(\omega_{\min},\alpha)| &= \frac{A(\epsilon)}{B(\epsilon)} = \frac{b^2-\frac{bC_0\sqrt{2}\sqrt{acb}\epsilon^{1/2-\delta}}{c}+\frac{C_0^2ab\epsilon^{1-2\delta}}{c}+\mathcal{O}\left(\epsilon^{3/2-\delta}\right)}{b^2+\frac{bC_0\sqrt{2}\sqrt{acb}\epsilon^{1/2-\delta}}{c}+\frac{C_0^2ab\epsilon^{1-2\delta}}{c}+\mathcal{O}\left(\epsilon^{3/2-\delta}\right)} \\
&= \frac{1-\frac{C_0\sqrt{2}\sqrt{acb}\epsilon^{1/2-\delta}}{bc}+\frac{C_0^2a\epsilon^{1-2\delta}}{bc}+\mathcal{O}\left(\epsilon^{3/2-\delta}\right)}{1+\frac{C_0\sqrt{2}\sqrt{acb}\epsilon^{1/2-\delta}}{bc}+\frac{C_0^2a\epsilon^{1-2\delta}}{bc}+\mathcal{O}\left(\epsilon^{3/2-\delta}\right)} \\
&= \left(1-\frac{C_0\sqrt{2}\sqrt{acb}\epsilon^{1/2-\delta}}{bc}+\mathcal{O}\left(\epsilon^{1-2\delta}\right)\right)\left(1-\frac{C_0\sqrt{2}\sqrt{acb}\epsilon^{1/2-\delta}}{bc}+\mathcal{O}\left(\epsilon^{1-2\delta}\right)\right) \\
&= 1-\frac{2C_0\sqrt{2}\sqrt{acb}\epsilon^{1/2-\delta}}{bc}+\mathcal{O}\left(\epsilon^{1-2\delta}\right),
\end{aligned}$$

that is, we arrive at (3.39). Further, since $\omega_{\max}$ is fixed, the asymptotic expansion in $|\rho(\omega_{\max},\alpha)|$ is only because of the presence of $\alpha = -C_0\epsilon^{-\delta}$ which satisfies $\alpha \to \infty$ as $\epsilon \to 0$. Recall from (3.35), at $\omega = \omega_{\max}$,

$$\begin{aligned}
|\rho(\omega_{\max},\alpha)| &= \left|\frac{((i\omega_{\max}-b)+a\alpha(\lambda_2-1))^2}{((i\omega_{\max}-b)\lambda_2+a\alpha(1-\lambda_2))((i\omega_{\max}-b)\lambda_1+a\alpha(1-\lambda_2))}\right| \\
&= \left|\frac{a^2\alpha^2(\lambda_2-1)^2\left(1+\frac{i\omega_{\max}-b}{a\alpha(\lambda_2-1)}\right)^2}{a^2\alpha^2(\lambda_2-1)^2\left(\frac{(i\omega_{\max}-b)\lambda_2}{a\alpha(\lambda_2-1)}-1\right)\left(\frac{(i\omega_{\max}-b)\lambda_1}{a\alpha(\lambda_2-1)}-1\right)}\right| \\
&= \left|\frac{\left(1+\frac{i\omega_{\max}-b}{a\alpha(\lambda_2-1)}\right)^2}{1-\frac{(i\omega_{\max}-b)(\lambda_1+\lambda_2)}{a\alpha(\lambda_2-1)}+\frac{(i\omega_{\max}-b)^2}{a^2\alpha^2(\lambda_2-1)^2}}\right| \\
&= \left|\left(1-\frac{(i\omega_{\max}-b)}{aC_0(\lambda_2-1)}\epsilon^{\delta}\right)^2\left(1-\frac{(i\omega_{\max}-b)(\lambda_1+\lambda_2)}{aC_0(\lambda_2-1)}\epsilon^{\delta}+\mathcal{O}(\epsilon^{2\delta})\right)\right| \\
&= \left|\left(1-\frac{2(i\omega_{\max}-b)}{aC_0(\lambda_2-1)}\epsilon^{\delta}+\mathcal{O}(\epsilon^{2\delta})\right)\left(1-\frac{(i\omega_{\max}-b)(\lambda_1+\lambda_2)}{aC_0(\lambda_2-1)}\epsilon^{\delta}+\mathcal{O}(\epsilon^{2\delta})\right)\right| \\
&= \left|1-\frac{(i\omega_{\max}-b)(2+\lambda_1+\lambda_2)}{aC_0(\lambda_2-1)}\epsilon^{\delta}+\mathcal{O}(\epsilon^{2\delta})\right|,
\end{aligned}$$

where λ_1 and λ_2 are evaluated at $\omega = \omega_{\max}$. It is complicated to separate the real and imaginary part, and hence we define the real and imaginary part by $g_r := \Re\left(\frac{(i\omega_{\max}-b)(2+\lambda_1(\omega_{\max})+\lambda_2(\omega_{\max}))}{\lambda_2(\omega_{\max})-1}\right)$ and $g_i := \Im\left(\frac{(i\omega_{\max}-b)(2+\lambda_1(\omega_{\max})+\lambda_2(\omega_{\max}))}{\lambda_2(\omega_{\max})-1}\right)$. The asymptotic expression for $|\rho(\omega_{\max},\alpha)|$ simplifies to

$$\begin{aligned}
|\rho(\omega_{\max},\alpha)| &= \left|1-\frac{(g_r+ig_i)}{aC_0}\epsilon^{\delta}+\mathcal{O}(\epsilon^{2\delta})\right| = \left(1-\frac{2g_r}{aC_0}\epsilon^{\delta}+\mathcal{O}(\epsilon^{2\delta})\right)^{1/2} \\
&= 1-\frac{g_r}{aC_0}\epsilon^{\delta}+\mathcal{O}(\epsilon^{2\delta}),
\end{aligned}$$

and this completes the proof. □

Theorem 3.4.1. *For the nonoverlapping OWR when applied to an infinitely long RLC transmission line, and for small $\omega_{\min} > 0$, if $\alpha_0^* = -C_0\omega_{\min}^{-1/4}$, then the convergence factor $\rho(\omega,\alpha)$ is bounded from above by*

$$|\rho(\omega,\alpha)| \le |\rho(\omega_{\min},\alpha_0^*)| = 1 - \frac{2C_0\sqrt{2}\sqrt{acb}\,\omega_{\min}^{1/4}}{bc} + \mathcal{O}\left(\omega_{\min}^{1/2}\right),$$

where

$$C_0 = \left(\frac{g_r bc}{2\sqrt{2}a\sqrt{abc}}\right)^{1/2}, \quad \text{and} \quad g_r = \Re\left(\frac{(i\omega_{\max}-b)(2+\lambda_1(\omega_{\max})+\lambda_2(\omega_{\max}))}{\lambda_2(\omega_{\max})-1}\right).$$

Proof. The left plot of Figure 3.4 shows that the solution of the min-max problem (3.37) is found by equioscillation between $\omega_{\min}$ and $\omega_{\max}$. The constants C_0 and δ in the expression of $\alpha = -C_0\epsilon^{-\delta}$ are determined by comparing the exponents and coefficients of the dominating terms in the asymptotic expressions of $|\rho(\omega_{\min}, \alpha)|$ and $|\rho(\omega_{\max}, \alpha)|$ which are given by (3.39) and (3.40) respectively. We thus obtain

$$\frac{1}{2} - \delta = \delta, \quad \text{and} \quad \frac{2C_0\sqrt{2}\sqrt{abc}}{bc} = \frac{g_r}{aC_0},$$

which leads to $\delta = \frac{1}{4}$ and $C_0 = \left(\frac{g_r bc}{2\sqrt{2}a\sqrt{abc}}\right)^{1/2}$. This completes the proof. □

3.4.2 Overlapping OWR

We now consider the overlapping OWR, and first consider partitioning at a voltage node. Corollary 2 motivates us to assume $\beta^v = -\frac{1}{\alpha^v}$. The convergence factor (3.26) reduces to

$$\rho_n^v(s, \alpha^v) := \begin{cases} \left(\frac{(s-b)\alpha^v + a(1-\lambda_1)}{(s-b)\alpha^v\lambda_1 + a(\lambda_1 - 1)}\right)^2 (\lambda_1^2)^n & , \quad |\lambda_1| < 1, \\ \left(\frac{(s-b)\alpha^v + a(1-\lambda_2)}{(s-b)\alpha^v\lambda_2 + a(\lambda_2 - 1)}\right)^2 (\lambda_2^2)^n & , \quad |\lambda_1| > 1. \end{cases} \tag{3.41}$$

The process of finding the optimized α^v is similar to the one followed for the nonoverlapping OWR method described in Section 3.4.1.

Lemma 3.4.6. *For $\alpha^v < 0$ the maximum of the modulus of the convergence factor $|\rho_n^v(s, \alpha^v)|$ lies on the imaginary axis of the complex plane.*

Proof. The proof is very similar to the proof of Lemma 3.4.1, and we do not repeat the calculations. □

Lemmas 3.4.6 and 3.4.2 simplify the min-max problem (3.34) to

$$\min_{\alpha^v < 0} \left(\max_{\omega_{\min} \le \omega \le \omega_{\max}} |\rho_n^v(\omega, \alpha^v)| \right). \tag{3.42}$$

Recall that $\omega_{\min} = \frac{\pi}{T}$ and $\omega_{\max} = \frac{\pi}{\Delta t}$. We solve the above min-max problem by using asymptotic analysis with respect to $\omega_{\min} \to 0$. The left plot of Figure 3.5 illustrates that the solution of the min-max solution (3.42) is numerically given by equioscillation between $\omega_{\min}$ and $\overline{\omega}$ where $\omega_{\min} < \overline{\omega} < \omega_{\max}$. We thus need to find expressions for $\overline{\omega}$ and the optimized α^v, denoted by α_n^{v*}. They satisfy the coupled equations

$$|\rho_n^v(\omega_{\min}, \alpha_n^{v*})| = |\rho_n^v(\overline{\omega}, \alpha_n^{v*})|, \quad \text{and} \quad \frac{\partial}{\partial\omega}|\rho_n^v(\overline{\omega}, \alpha_n^{v*})| = 0. \tag{3.43}$$

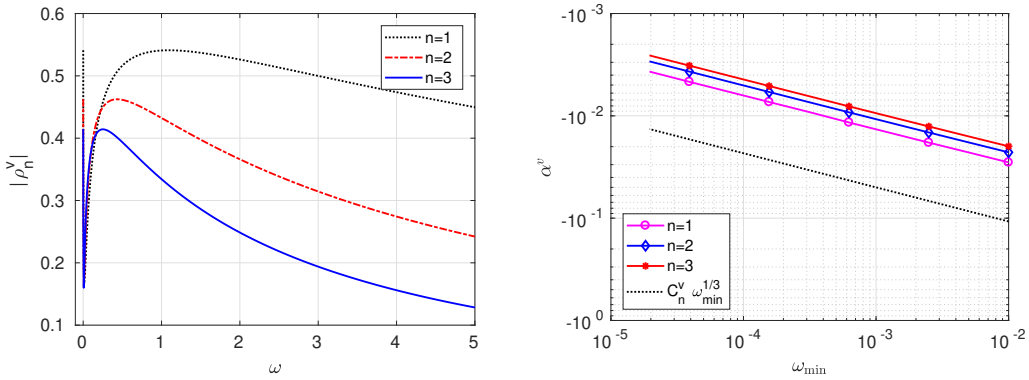

Figure 3.5: Equioscillation for overlapping OWR for partitioning at a voltage node and for different values of overlap n with $\omega_{\min} = 6.25 \times 10^{-4}$ (left) and dependence of α_n^{v*} on $\omega_{\min}$ (right).

Further, the right plot of Figure 3.5 shows the relation between α_n^{v*} and $\omega_{\min}$, which is given by $\alpha_n^{v*} = -C_n^v \epsilon^\delta$, where $\epsilon = \omega_{\min} \to 0$ and $C_n^v, \delta > 0$. Moreover, $\overline{\omega} \to 0$ as $\omega_{\min} \to 0$ (see the left plot of Figure 3.6). We thus assume $\overline{\omega} = d_n^v \epsilon^\eta$ for some constants d_n^v, $\eta > 0$.

Lemma 3.4.7. *For the overlapping OWR with partitioning at a voltage node, solving* $\frac{\partial}{\partial \omega}|\rho_n^v(\overline{\omega}, \alpha_n^{v*})| = 0$ *yields the relation*

$$\eta = \delta, \quad \text{and} \quad d_n^v = -\frac{2cC_n^v}{n}. \tag{3.44}$$

Proof. For small ω, Lemma 3.4.4 states that $|\lambda_1| < 1$. Recalling the expression for $\rho_n^v(\omega, \alpha)$ given in (3.41), we have

$$\begin{aligned} |\rho_n^v(\omega, \alpha^v)| &= \left| \left(\frac{(i\omega - b)\alpha^v + a(1-\lambda_1)}{(i\omega - b)\alpha^v \lambda_1 + a(\lambda_1 - 1)} \right)^2 \left(\lambda_1^2\right)^n \right| \\ &= \left| \left(\frac{(i\omega - b)\alpha^v + a(1-\lambda_1)}{(i\omega - b)\alpha^v \lambda_1 + a(\lambda_1 - 1)} \right) \right|^2 \left(|\lambda_1|^2 \right)^n \\ &= \frac{A(\omega, \epsilon)}{B(\omega, \epsilon)} L(\omega), \end{aligned} \tag{3.45}$$

where $A(\omega, \epsilon) := |(i\omega - b)\alpha^v + a(1-\lambda_1)|^2$, $B(\omega, \epsilon) := |(i\omega - b)\alpha^v \lambda_1 + a(\lambda_1 - 1)|^2$ and $L(\omega) = \left(|\lambda_1|^2 \right)^n$. Using the asymptotic expressions for λ_1 derived in Lemma

3.4.4, for small ω, we obtain

$$\begin{aligned} A(\omega,\epsilon) &= \Bigg| \left(C_n^v b\omega^\delta - \frac{\sqrt{2}\sqrt{acb}\sqrt{\omega}}{2c} - \left(\frac{\sqrt{2}\sqrt{acb}}{4cb} - \frac{b\sqrt{2}\sqrt{acb}}{16ac^2} \right) \omega^{3/2} \right) \\ &\quad + i \left(-\frac{a\sqrt{2}b\sqrt{\omega}}{2\sqrt{acb}} - \frac{b\omega}{2c} + \left(\frac{a\sqrt{2}}{4\sqrt{acb}} - \frac{\sqrt{2}b^2}{16c\sqrt{acb}} \right) \omega^{3/2} \right) + \mathcal{O}(\omega^{5/2}) \Bigg| \\ &= \frac{ab\omega}{c} - \frac{C_n^v b\epsilon^\delta \sqrt{2}\sqrt{acb}\sqrt{\omega}}{c} + \frac{a\sqrt{2}b^2\omega^{3/2}}{2c\sqrt{acb}} + \mathcal{O}(\omega^{3/2}\epsilon^\delta), \end{aligned} \tag{3.46}$$

$$\begin{aligned} B(\omega,\epsilon) &= \left(C_n^v b\epsilon^\delta + \frac{C_n^v b\sqrt{2}\sqrt{acb}\sqrt{\omega}\epsilon^\delta}{2ac} + \frac{\sqrt{2}\sqrt{acb}\sqrt{\omega}}{2c} + \left(\frac{\sqrt{2}\sqrt{acb}}{4cb} - \frac{b\sqrt{2}\sqrt{acb}}{16ac^2} \right) \omega^{3/2} \right)^2 \\ &\quad + \left(\frac{a\sqrt{2}b\sqrt{\omega}}{2\sqrt{acb}} + \frac{C_n^v\sqrt{2}b^2\sqrt{\omega}\epsilon^\delta}{2\sqrt{acb}} + \frac{b\omega}{2c} - \left(\frac{a\sqrt{2}}{4\sqrt{acb}} - \frac{\sqrt{2}b^2}{16c\sqrt{acb}} \right) \omega^{3/2} \right)^2 + \mathcal{O}(\omega^{5/2}) \\ &= \frac{ab\omega}{c} + \frac{C_n^v b\sqrt{2}\sqrt{acb}\sqrt{\omega}\epsilon^\delta}{c} + \frac{a\sqrt{2}b^2\omega^{3/2}}{2c\sqrt{acb}} + \mathcal{O}(\omega^{3/2}\epsilon^\delta), \end{aligned} \tag{3.47}$$

and

$$\begin{aligned} L(\omega) &= \left(\left(1 + \frac{\sqrt{2}\sqrt{acb}\omega^{1/2}}{2ac} \right)^2 + \left(\frac{\sqrt{2}b\omega^{1/2}}{2\sqrt{acb}} + \frac{b\omega}{2ac} \right)^2 + \mathcal{O}(\omega^{3/2}) \right)^n, \\ &= \left(1 + \frac{\sqrt{2}\sqrt{acb}\sqrt{\omega}}{ac} + \frac{b\omega}{ac} + \mathcal{O}(\omega^{3/2}) \right)^n, \\ &= 1 + \frac{n\sqrt{2}\sqrt{acb}\sqrt{\omega}}{ac} + \frac{nb(1-n)\omega}{ac} + \mathcal{O}(\omega^{3/2}). \end{aligned} \tag{3.48}$$

Further, differentiating these expressions with respect to ω produces

$$\begin{aligned} \frac{\partial}{\partial\omega}A(\omega,\epsilon) &= \frac{ab}{c} - \frac{C_n^v b\sqrt{2}\sqrt{acb}\epsilon^\delta}{2c\sqrt{\omega}} + \frac{3a\sqrt{2}b^2\sqrt{\omega}}{4c\sqrt{acb}} + \mathcal{O}(\omega^{1/2}\epsilon^\delta), \\ \frac{\partial}{\partial\omega}B(\omega,\epsilon) &= \frac{ab}{c} + \frac{C_n^v b\sqrt{2}\sqrt{acb}\epsilon^\delta}{2c\sqrt{\omega}} + \frac{3a\sqrt{2}b^2\sqrt{\omega}}{4c\sqrt{acb}} + \mathcal{O}(\omega^{1/2}\epsilon^\delta), \\ \frac{\partial}{\partial\omega}L(\omega) &= \frac{n\sqrt{2}\sqrt{acb}}{2\sqrt{\omega}ac} + \frac{nb(1-n)}{ac} + \mathcal{O}(\omega^{1/2}). \end{aligned} \tag{3.49}$$

Finally, solving $\frac{\partial}{\partial\omega}|\rho_n^v(\omega,\alpha^v)| = 0$, is equivalent to equating $F_1 = F_2$, where

$$\begin{aligned} F_1 &:= B(\omega,\epsilon)\left(A(\omega,\epsilon)\frac{\partial}{\partial\omega}L(\omega) + L(\omega)\frac{\partial}{\partial\omega}A(\omega,\epsilon) \right) \\ &= \frac{a^2b^2\omega}{c^2} - \frac{ab^2C_n^v\sqrt{2}\sqrt{acb}\sqrt{\omega}\epsilon^\delta}{2c^2} + \left(\frac{3ab^2n\sqrt{2}\sqrt{acb}}{2c^3} + \frac{5a^2b^4\sqrt{2}}{4c^2\sqrt{acb}} \right)\omega^{3/2} + \mathcal{O}(\omega\epsilon^\delta), \end{aligned}$$

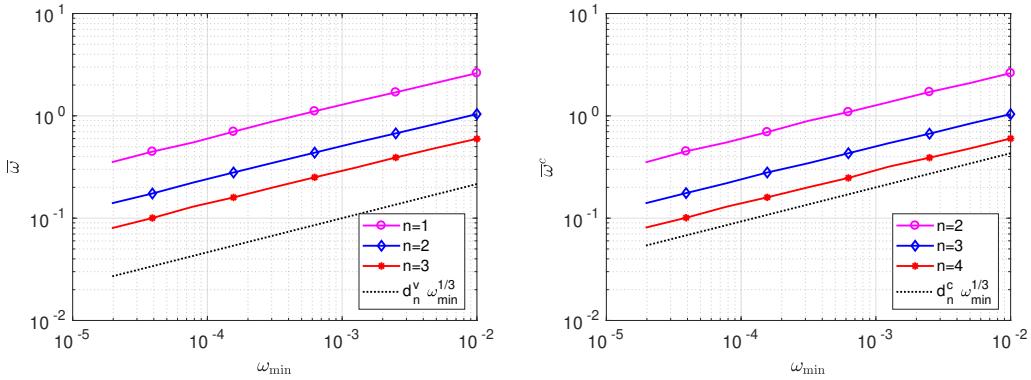

Figure 3.6: Relation between $\overline{\omega}$ and $\omega_{\min}$ for overlapping OWR with partitioning at a voltage node (left) and at a current node (right).

and

$$\begin{aligned} F_2 &:= A(\omega,\epsilon)L(\omega)\frac{\partial}{\partial\omega}B(\omega,\epsilon) \\ &= \frac{a^2b^2\omega}{c^2} + \frac{ab^2C_n^v\sqrt{2}\sqrt{acb}\sqrt{\omega}\epsilon^\delta}{2c^2} + \left(\frac{ab^2n\sqrt{2}\sqrt{acb}}{c^3} + \frac{5a^2b^3\sqrt{2}}{4c^2\sqrt{acb}}\right)\omega^{3/2} + \mathcal{O}(\omega\epsilon^\delta). \end{aligned}$$

Thus, $F_1 = F_2$ leads to $\overline{\omega} = -\frac{2C_n^v c\epsilon^\delta}{n}$. Since $\overline{\omega}$ is asymptotically represented as $\overline{\omega} = d_n^v\epsilon^\eta$, comparing the exponents and coefficients yield the relation (3.44). □

Lemma 3.4.8. *For the overlapping OWR with splitting at a voltage node, the modulus of the convergence factor $|\rho_n^v(\omega,\alpha^v)|$ evaluated at $\omega_{\min}$ and $\overline{\omega}$ are given by*

$$|\rho_n^v(\omega_{\min},\alpha^v) = 1 - \frac{2\sqrt{2}\sqrt{abc}\,\omega_{\min}^{1/2-\delta}}{C_n^v bc} + \mathcal{O}(\omega_{\min}^{1-2\delta}), \tag{3.50}$$

and

$$|\rho_n^v(\overline{\omega}),\alpha^v| = 1 + \left(\frac{n\sqrt{2}\sqrt{abc}\sqrt{d_n^v}}{ac} - \frac{2C_n^v\sqrt{2}\sqrt{acb}}{a\sqrt{d_n^v}}\right)\omega_{\min}^{\delta/2} + \mathcal{O}(\omega_{\min}^{\delta}), \tag{3.51}$$

where we have already substituted the asymptotic relations $\alpha^v = -C_n^v\epsilon^\delta$ and $\overline{\omega} = d_n^v\epsilon^\delta$, with $\epsilon = \omega_{\min}$.

Proof. We first find an expression for $|\rho(\overline{\omega},\alpha)|$ by substituting $\omega = d_n^v\epsilon^\delta$ in the asymptotic expressions $A(\omega,\epsilon)$ and $B(\omega,\epsilon)$ calculated in (3.46) and (3.47) . From Lemma

3.4.4 we have $|\lambda_1| < 1$ and hence

$$\begin{aligned}
\frac{A(\overline{\omega},\epsilon)}{B(\overline{\omega},\epsilon)} &= \frac{\frac{abd_n^v\epsilon^\delta}{c} + \left(-\frac{C_n^v b\sqrt{2}\sqrt{abc}\sqrt{d_n^v}}{c} + \frac{a\sqrt{2}b^2(d_n^v)^{3/2}}{2c\sqrt{abc}}\right)\epsilon^{3\delta/2} + \mathcal{O}(\epsilon^{2\delta})}{\frac{abd_n^v\epsilon^\delta}{c} + \left(\frac{C_n^v b\sqrt{2}\sqrt{abc}\sqrt{d_n^v}}{c} + \frac{a\sqrt{2}b^2(d_n^v)^{3/2}}{2c\sqrt{abc}}\right)\epsilon^{3\delta/2} + \mathcal{O}(\epsilon^{2\delta})} \\
&= \frac{1 + \left(-\frac{C_n^v\sqrt{2}\sqrt{abc}}{a\sqrt{d_n^v}} + \frac{b\sqrt{d_n^v}\sqrt{2}}{2\sqrt{abc}}\right)\epsilon^{\delta/2} + \mathcal{O}(\epsilon^\delta)}{1 + \left(\frac{C_n^v\sqrt{2}\sqrt{abc}}{a\sqrt{d_n^v}} + \frac{b\sqrt{d_n^v}\sqrt{2}}{2\sqrt{abc}}\right)\epsilon^{\delta/2} + \mathcal{O}(\epsilon^\delta)} \\
&= \left(1 + \left(-\frac{C_n^v\sqrt{2}\sqrt{abc}}{a\sqrt{d_n^v}} + \frac{b\sqrt{d_n^v}\sqrt{2}}{2\sqrt{abc}}\right)\epsilon^{\delta/2} + \mathcal{O}(\epsilon^\delta)\right) \\
&\quad \left(1 - \left(\frac{C_n^v\sqrt{2}\sqrt{abc}}{a\sqrt{d_n^v}} + \frac{b\sqrt{d_n^v}\sqrt{2}}{2\sqrt{abc}}\right)\epsilon^{\delta/2} + \mathcal{O}(\epsilon^\delta)\right) \\
&= 1 - \frac{2C_n^v\sqrt{2}\sqrt{abc}}{a\sqrt{d_n^v}}\epsilon^{\delta/2} + \mathcal{O}(\epsilon^\delta), \qquad (3.52)
\end{aligned}$$

which on multiplication with $L(\omega)$ given in (3.48) yeilds

$$\begin{aligned}
|\rho_n^v(\overline{\omega},\alpha)| &= \left(\frac{A(\overline{\omega},\epsilon)}{B(\overline{\omega},\epsilon)}\right)L(\overline{\omega}) \\
&= \left(1 - \frac{2C_n^v\sqrt{2}\sqrt{abc}}{a\sqrt{d_n^v}}\epsilon^{\delta/2} + \mathcal{O}(\epsilon^\delta)\right)\left(1 + \frac{n\sqrt{2}\sqrt{abc}\sqrt{d_n^v}}{ac}\epsilon^{\delta/2} + \mathcal{O}(\epsilon^\delta)\right) \\
&= 1 + \left(-\frac{2C_n^v\sqrt{2}\sqrt{abc}}{a\sqrt{d_n^v}} + \frac{n\sqrt{2}\sqrt{abc}\sqrt{d_n^v}}{ac}\right)\epsilon^{\delta/2} + \mathcal{O}(\epsilon^\delta).
\end{aligned}$$

For $\omega = \omega_{\min}$, we go back to Lemmas 3.4.4 and 3.4.7, and substitute $\omega = \epsilon$ in the expressions of $A(\omega,\epsilon)$ and $B(\omega,\epsilon)$ defined in (3.45) to arrive at

$$\begin{aligned}
\frac{A(\omega_{\min},\epsilon)}{B(\omega_{\min},\epsilon)} &= \frac{\left|-(i\epsilon - b)C_n^v\epsilon^\delta + a\left(-\frac{\sqrt{2}\sqrt{acb}\sqrt{\epsilon}}{2ac} - \frac{i\sqrt{2}b\sqrt{\epsilon}}{2\sqrt{abc}} + \mathcal{O}(\epsilon)\right)\right|^2}{\left|-(i\epsilon - b)C_n^v\epsilon^\delta\left(1 + \frac{\sqrt{2}\sqrt{acb}\sqrt{\epsilon}}{2ac} + \frac{i\sqrt{2}b\sqrt{\epsilon}}{2\sqrt{abc}}\right) + a\left(\frac{\sqrt{2}\sqrt{acb}\sqrt{\epsilon}}{2ac} + \frac{i\sqrt{2}b\sqrt{\epsilon}}{2\sqrt{abc}}\right) + \mathcal{O}(\epsilon)\right|^2} \\
&= \frac{\left|\left(C_n^v b\epsilon^\delta - \frac{\sqrt{2}\sqrt{abc}\epsilon^{1/2}}{2c}\right) - i\left(\frac{a\sqrt{2}b\epsilon^{1/2}}{2\sqrt{abc}}\right) + \mathcal{O}(\epsilon)\right|^2}{\left|\left(C_n^v b\epsilon^\delta + \frac{C_n^v b\sqrt{2}\sqrt{abc}\epsilon^{1/2+\delta}}{2ac} + \frac{\sqrt{2}\sqrt{abc}\sqrt{\epsilon}}{2c}\right) + i\left(\frac{C_n^v\sqrt{2}b^2\epsilon^{1/2+\delta}}{2\sqrt{abc}} + \frac{a\sqrt{2}b\sqrt{\epsilon}}{2\sqrt{abc}}\right) + \mathcal{O}(\epsilon)\right|^2} \\
&= \frac{(C_n^v)^2b^2\epsilon^{2\delta} - \frac{C_n^v b\sqrt{2}\sqrt{abc}\epsilon^{1/2+\delta}}{c} + \mathcal{O}(\epsilon)}{(C_n^v)^2b^2\epsilon^{2\delta} + \frac{C_n^v b\sqrt{2}\sqrt{abc}\epsilon^{1/2+\delta}}{c} + \mathcal{O}(\epsilon)}.
\end{aligned}$$

Dividing the numerator and denominator by the dominating term $(C_n^v)^2\, b^2\epsilon^{2\delta}$ further simplifies it to

$$\begin{aligned}\frac{A(\omega_{\min},\epsilon)}{B(\omega_{\min},\epsilon)} &= \left(1-\frac{\sqrt{2}\sqrt{acb}}{C_n^v bc}\epsilon^{1/2-\delta}+\mathcal{O}(\epsilon^{1-2\delta})\right)\left(1-\frac{\sqrt{2}\sqrt{acb}}{C_n^v bc}\epsilon^{1/2-\delta}+\mathcal{O}(\epsilon^{1-2\delta})\right)\\ &= 1-\frac{2\sqrt{2}\sqrt{acb}}{C_n^v bc}\epsilon^{1/2-\delta}+\mathcal{O}(\epsilon^{1-2\delta}),\end{aligned} \tag{3.53}$$

which on multiplication with $L(\omega_{\min})$ given in (3.48) leads to

$$\begin{aligned}|\rho_n^v(\omega_{\min},\alpha^v)| &= \left(1-\frac{2\sqrt{2}\sqrt{acb}}{C_n^v bc}\epsilon^{1/2-\delta}+\mathcal{O}(\epsilon^{1-2\delta})\right)\left(1+\frac{n\sqrt{2}\sqrt{abc}}{ac}\epsilon^{1/2}+\mathcal{O}(\epsilon)\right)\\ &= \left(1-\frac{2\sqrt{2}\sqrt{acb}}{C_n^v bc}\epsilon^{1/2-\delta}+\mathcal{O}(\epsilon^{1-2\delta})\right).\end{aligned}$$

This completes the proof. □

Theorem 3.4.2. *For the overlapping OWR with partitioning at a voltage node and with n node overlap, if $\alpha_n^{v*} = -C_n^v\omega_{\min}^{1/3}$, then the convergence factor $\rho_n^v(\omega,\alpha^v)$ is bounded above by*

$$|\rho_n^v(\omega,\alpha^v)| \le |\rho_n^v(\omega_{\min},\alpha_n^{v*})| = 1-\frac{2\sqrt{2}\sqrt{abc}\,\omega_{\min}^{1/6}}{C_n^v bc}+\mathcal{O}(\omega_{\min}^{1/3}),$$

where $C_n^v = \left(\frac{-a^2}{2nb^2c}\right)^{1/3}$.

Proof. For the overlapping OWR with $n \ge 1$ node overlap, the left plot of Figure 3.5 numerically shows that the solution of the min-max problem (3.42) is given by equioscillation between $\omega_{\min}$ and $\overline{\omega}$. Using the relation (3.44), and equating the expressions of the modulus of the convergence factor $|\rho_n^v(\omega_{\min},\alpha^v)|$ and $|\rho_n^v(\overline{\omega},\alpha^v)|$ leads to

$$\delta/2 = 1/2-\delta, \quad \text{and} \quad \frac{2\sqrt{2}\sqrt{acb}}{C_n^v bc} = \frac{n\sqrt{2}\sqrt{abc}\sqrt{d_n^v}}{ac}-\frac{2C_n^v\sqrt{2}\sqrt{abc}}{a\sqrt{d_n^v}},$$

which simplifies to

$$\delta = 1/3, \quad \text{and} \quad C_n^v = \left(\frac{-a^2}{2nb^2c}\right)^{1/3}.$$

Substituting these constants into (3.50) completes the proof. □

We now consider the other type of partitioning, that is, splitting at a current node. For this partitioning, β_{opt}^c and α_{opt}^c are related via the relation $\beta_{opt}^c = -\frac{1}{\alpha_{opt}^c}$ (see

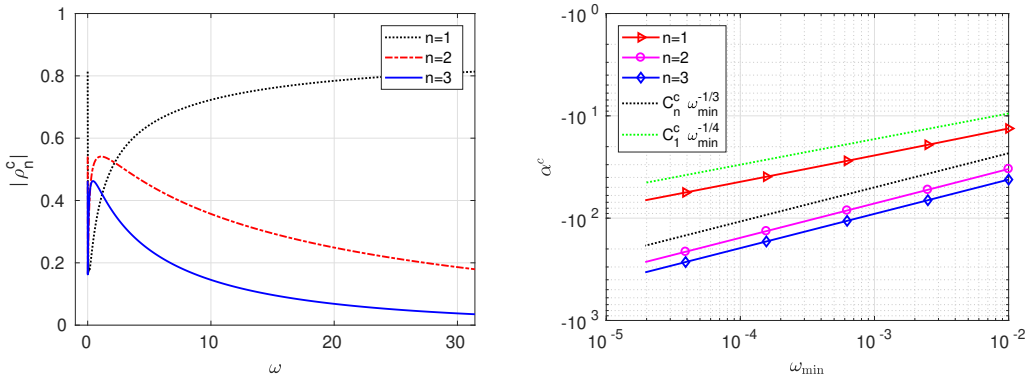

Figure 3.7: Equioscillation for overlapping OWR for partitioning at a current node and for different values of overlap n with $\omega_{\min} = 6.25 \times 10^{-4}$ (left) and dependence of α_n^{c*} on $\omega_{\min}$ for $n > 1$ (right).

Corollary 3). Thus assuming $\beta^c = -\frac{1}{\alpha^c}$ simplifies the convergence factor $\rho_n^c(s, \alpha^c)$ defined in (3.31) to

$$\rho_n^c(s,\alpha^c) := \begin{cases} \left(\frac{(s-b)+a\alpha^c(\lambda_2-1)}{(s-b)+a\alpha^c(\lambda_1-1)}\right)^2 (\lambda_1^2)^n & , \quad |\lambda_1| < 1, \\ \left(\frac{(s-b)+a\alpha^c(\lambda_1-1)}{(s-b)+a\alpha^c(\lambda_2-1)}\right)^2 (\lambda_2^2)^n & , \quad |\lambda_1| > 1, \end{cases} \tag{3.54}$$

Lemma 3.4.9. *For $\alpha^c < 0$ the maximum of the modulus of the convergence factor $|\rho_n^c(s, \alpha^c)|$ lies on the imaginary axis of the complex plane.*

Proof. The idea is to use the method of contradiction. The proof is very similar to the proof of Lemma 3.4.1, and hence we do not repeat the calculations. □

Lemmas 3.4.2 and 3.4.9 reduce the min-max problem (3.34) to

$$\min_{\alpha^c<0} \left(\max_{\omega_{\min}\le\omega\le\omega_{\max}} |\rho_n^c(\omega, \alpha^c)| \right). \tag{3.55}$$

We solve this min-max problem using asymptotic analysis with respect to $\omega_{\min} \to 0$. The left plot of Figure 3.7 shows that for $n = 1$, the solution of the min-max problem is numerically given by equioscillation between $\omega_{\min}$ and $\omega_{\max}$, while for $n > 1$, the equioscillation takes place between $\omega_{\min}$ and $\overline{\omega}^c$, where $\omega_{\min} < \overline{\omega}^c < \omega_{\max}$. Solving (3.55) is equivalent to solve

$$|\rho_1^c(\omega_{\min}, \alpha_1^{c*})| = |\rho_1^c(\omega_{\max}, \alpha_1^{c*})|, \quad \text{for} \quad n = 1, \tag{3.56}$$

and

$$|\rho_n^c(\omega_{\min}, \alpha_n^{c*})| = |\rho_n^c(\overline{\omega}^c, \alpha_n^{c*})|, \quad \text{and} \quad \frac{\partial}{\partial\omega} |\rho_n^c(\overline{\omega}^c, \alpha_n^{c*})| = 0, \quad \text{for} \quad n > 1, \tag{3.57}$$

Further, from the right plot of Figure 3.7, we observe that the optimized α^c, denoted by α_n^{c*} is given by $\alpha_n^{c*} = -C_n^c \epsilon^{-\delta}$, with $C_n^c, \delta > 0$ and $\epsilon = \omega_{\min} \to 0$. Moreover, the right plot of Figure 3.6 illustrates that for $n > 1$, $\overline{\omega}^c \to 0$ as $\omega_{\min} \to 0$. Thus, we assume that $\overline{\omega}^c = d_n^c \epsilon^\eta$, where $d_n^c > 0$ and $\eta > 0$.

Note that $\alpha_n^{c*} \to -\infty$ as $\epsilon \to 0$. We therefore introduce the new notation $\gamma := -\frac{1}{\alpha^c}$, and hence $\gamma = h_n^c \epsilon^\delta$, where $h_n^c := \frac{1}{C_n^c}$. With this new notation, the convergence factor (3.54) can be rewritten as

$$\Gamma_n^c(s,\gamma) := \begin{cases} \left(\frac{(s-b)\lambda_1\gamma + a(\lambda_1-1)}{(s-b)\gamma + a(1-\lambda_1)}\right)^2 (\lambda_1^2)^{n-1} & , \quad |\lambda_1| < 1, \\ \left(\frac{(s-b)\lambda_2\gamma + a(\lambda_2-1)}{(s-b)\gamma + a(1-\lambda_2)}\right)^2 (\lambda_2^2)^{n-1} & , \quad |\lambda_1| > 1. \end{cases} \tag{3.58}$$

We show the calculations for the case $|\lambda_1| < 1$,

$$\begin{aligned} \rho_n^c(s,\alpha^c) &= \left(\frac{(s-b) + a\alpha^c(\lambda_2 - 1)}{(s-b) + a\alpha^c(\lambda_1 - 1)}\right)^2 (\lambda_1^2)^n \\ &= \left(\frac{(s-b)\lambda_1\gamma - a(1-\lambda_1)}{(s-b)\gamma - a(\lambda_1 - 1)}\right)^2 (\lambda_2^2)\,(\lambda_1^2)^n \\ &= \left(\frac{(s-b)\lambda_1\gamma + a(\lambda_1 - 1)}{(s-b)\gamma + a(1-\lambda_1)}\right)^2 (\lambda_1^2)^{n-1} = \Gamma_n^c(s,\gamma). \end{aligned}$$

Remark 3.4.1. Comparing $\Gamma_n^c(s,\gamma)$ with $\rho_n^v(s,\alpha^v)$ defined in (3.41), we observe that the numerator of $\Gamma_n^c(s,\gamma)$ is similar to the denominator of $\rho_n^v(s,\alpha^v)$ and vice versa. Therefore, we can use the asymptotic expressions for $\rho_n^v(s,\alpha^v)$ and avoid doing the same calculations again. Since $\alpha_n^v = -C_n^v \epsilon^\delta$ and $\gamma = h_n^c \epsilon^\delta$, the constants C_n^c in these expressions will be replaced by h_n^c.

We first find the optimized α^c for $n = 1$ by solving (3.56).

Theorem 3.4.3. *For the overlapping OWR with splitting at a current node and with $n = 1$ node overlap, if $\alpha_1^{c*} = -C_1^c \epsilon^{-1/4}$, then the convergence factor ρ_1^c satisfies*

$$|\rho_1^c(\omega,\alpha)| \le |\rho_1^c(\omega_{\min},\alpha_1^{c*})| = 1 - \frac{2\sqrt{2}\sqrt{acb}C_1^c}{bc}\omega_{\min}^{1/4} + \mathcal{O}(\omega_{\min}^{1/2}),$$

where

$$C_1^c = \left(\frac{g_r bc}{2\sqrt{2}\sqrt{abc}}\right)^{1/2}, \quad \textit{and} \quad g_r := \Re\left(\frac{2(i\omega_{\max} - b)(1 + \lambda_2(\omega_{\max}))}{\lambda_2(\omega_{\max}) - 1}\right).$$

Proof. We first find an expression for $|\rho_1^c(\omega_{\min},\alpha_1^{c*})|$. For $\omega = \omega_{\min}$, from Lemma 3.4.4, we have $|\lambda_1| < 1$ and hence

$$|\Gamma_1^c(\omega,\gamma)| = \left|\frac{(i\omega_{\min} - b)\lambda_1\gamma + a(\lambda_1 - 1)}{(i\omega_{\min} - b)\gamma + a(1-\lambda_1)}\right|^2 = \frac{B(\omega_{\min},\epsilon)}{A(\omega_{\min},\epsilon)},$$

where $A(\omega_{\min},\epsilon)$ and $B(\omega_{\min},\epsilon)$ are defined in (3.45). However in these expressions, the constants C_n^v will be replaced by h_n^c. Using the expression (3.53), we arrive at

$$\begin{aligned}
|\rho_1^c(\omega_{\min},\alpha^c)| &= |\Gamma_1^c(\omega_{\min},\gamma)| = \frac{B(\omega_{\min},\epsilon)}{A(\omega_{\min},\epsilon)} = \frac{1}{\frac{B(\omega_{\min},\epsilon)}{A(\omega_{\min},\epsilon)}} \\
&= \frac{1}{1+\frac{2\sqrt{2}\sqrt{acb}}{h_1^c bc}\epsilon^{1/2-\delta}+\mathcal{O}(\epsilon^{1-2\delta})} \\
&= 1-\frac{2\sqrt{2}\sqrt{acb}}{h_1^c bc}\epsilon^{1/2-\delta}+\mathcal{O}(\epsilon^{1-2\delta}) \\
&= 1-\frac{2\sqrt{2}\sqrt{acb}C_1^c}{bc}\epsilon^{1/2-\delta}+\mathcal{O}(\epsilon^{1-2\delta}). \qquad (3.59)
\end{aligned}$$

For $\omega=\omega_{\max}$, we use the technique used in the proof of Lemma 3.4.5. Since $\alpha=C_1^c\epsilon^\delta$, we have from (3.54),

$$\begin{aligned}
|\rho_1^c(\omega_{\max},\alpha)| &= \left|\left(\frac{(i\omega_{\max}-b)+a\alpha^c(\lambda_2-1)}{(i\omega_{\max}-b)+a\alpha^c(\lambda_1-1)}\right)^2\lambda_1^2\right| \\
&= \left|\frac{(i\omega_{\max}-b)+a\alpha^c(\lambda_2-1)}{(i\omega_{\max}-b)\lambda_2-a\alpha^c(\lambda_2-1)}\right|^2 = \left|\frac{\left(1+\frac{(i\omega_{\max}-b)}{aC_1^c(\lambda_2-1)}\epsilon^\delta\right)^2}{\left(1-\frac{(i\omega_{\max}-b)\lambda_2}{aC_1^c(\lambda_2-1)}\epsilon^\delta\right)^2}\right| \\
&= \left|\left(1-\frac{2(i\omega_{\max}-b)}{aC_1^c(\lambda_2-1)}\epsilon^\delta+\mathcal{O}(\epsilon^{2\delta})\right)\left(1-\frac{2(i\omega_{\max}-b)\lambda_2}{aC_1^c(\lambda_2-1)}\epsilon^\delta+\mathcal{O}(\epsilon^{2\delta})\right)\right| \\
&= \left|1-\frac{2(i\omega_{\max}-b)(1+\lambda_2)}{aC_1^c(\lambda_2-1)}\epsilon^\delta+\mathcal{O}(\epsilon^{2\delta})\right| = \left|1-\frac{(g_r+ig_i)}{aC_1^c}\epsilon^\delta+\mathcal{O}(\epsilon^\delta)\right| \\
&= \left(1-\frac{2g_r}{aC_1^c}\epsilon^\delta+\mathcal{O}(\epsilon^\delta)\right)^{1/2} = 1-\frac{g_r}{aC_1^c}\epsilon^\delta+\mathcal{O}(\epsilon^\delta),
\end{aligned}$$

where λ_1 and λ_2 are evaluated at $\omega_{\max}$, and $g_r := \Re\left(\frac{2(i\omega_{\max}-b)(1+\lambda_2(\omega_{\max}))}{\lambda_2(\omega_{\max})-1}\right)$ and $g_i := \Im\left(\frac{2(i\omega_{\max}-b)(1+\lambda_2(\omega_{\max}))}{\lambda_2(\omega_{\max})-1}\right)$. For $n=1$, the constants C_1^c and δ can be found by comparing the exponents and coefficients of the dominating terms of $|\rho_1^c(\omega_{\min},\alpha^c)|$ and $|\rho_1^c(\omega_{\max},\alpha^c)|$, which results in $\delta=1/4$ and $C_1^c=\left(\frac{g_r bc}{2\sqrt{2}\sqrt{abc}}\right)^{1/2}$. This completes the proof. □

We now consider the case when $n>1$ nodes are overlapped.

Lemma 3.4.10. *For the overlapping OWR with $n>1$ nodes overlap and partitioning at a current node, solving $\frac{\partial}{\partial\omega}|\rho_n^c(\overline{\omega}^c,\alpha_n^{c*})|=0$ produces the relation*

$$\eta=\delta, \quad \textit{and} \quad d_n^c=\frac{-2c}{(n-1)C_n^c}. \qquad (3.60)$$

Proof. For small ω, $|\lambda_1| < 1$, and hence using (3.58), we have

$$|\rho_n^c(\omega,\alpha^c)| = |\Gamma_n^c(\omega,\gamma)| = \left|\frac{(s-b)\lambda_1\gamma + a(\lambda_1-1)}{(s-b)\gamma + a(1-\lambda_1)}\right|^2 |\lambda_1^2|^{n-1} = \frac{B(\omega,\alpha)}{A(\omega,\alpha)} L_c(\omega), \tag{3.61}$$

where $A(\omega,\alpha)$ and $B(\omega,\alpha)$ are defined in (3.45) and $L_c(\omega) = |\lambda_1^2|^{n-1}$. For small ω, we have already derived expressions for $A(\omega,\alpha)$, $B(\omega,\alpha)$ and $L_c(\omega)$ in (3.46), (3.47) and (3.48). Hence we do not do these calculations again but change the constants to arrive at

$$\begin{aligned}
A(\omega,\epsilon) &= \frac{ab\omega}{c} + \frac{h_n^c b\sqrt{2}\sqrt{acb}\epsilon^\delta\sqrt{\omega}}{c} + \frac{a\sqrt{2}b^2\omega^{3/2}}{2c\sqrt{acb}} + \mathcal{O}(\omega^{3/2}\epsilon^\delta),\\
B(\omega,\epsilon) &= \frac{ab\omega}{c} - \frac{h_n^c b\sqrt{2}\sqrt{acb}\epsilon^\delta\sqrt{\omega}}{c} + \frac{a\sqrt{2}b^2\omega^{3/2}}{2c\sqrt{acb}} + \mathcal{O}(\omega^{3/2}\epsilon^\delta),\\
L_c(\omega) &= 1 + \frac{(n-1)\sqrt{2}\sqrt{acb}\sqrt{\omega}}{ac} + \frac{(n-1)nb\omega}{ac} - \frac{(n-1)^2 b\omega}{ac} + \mathcal{O}(\omega^{3/2}),
\end{aligned} \tag{3.62}$$

which on differentiating with respect to ω leads to

$$\begin{aligned}
\frac{\partial}{\partial\omega}A(\omega,\epsilon) &= \frac{ab}{c} + \frac{h_n^c b\sqrt{2}\sqrt{acb}\epsilon^\delta}{2c\sqrt{\omega}} + \frac{3a\sqrt{2}b^2\sqrt{\omega}}{4c\sqrt{acb}} + \mathcal{O}(\omega^{1/2}\epsilon^\delta),\\
\frac{\partial}{\partial\omega}B(\omega,\epsilon) &= \frac{ab}{c} - \frac{h_n^c b\sqrt{2}\sqrt{acb}\epsilon^\delta}{2c\sqrt{\omega}} + \frac{3a\sqrt{2}b^2\sqrt{\omega}}{4c\sqrt{acb}} + \mathcal{O}(\omega^{1/2}\epsilon^\delta),\\
\frac{\partial}{\partial\omega}L_c(\omega) &= \frac{(n-1)\sqrt{2}\sqrt{acb}}{2\sqrt{\omega}ac} + \frac{(n-1)b}{ac} + \frac{(n-1)^2 b}{ac} + \mathcal{O}(\omega^{1/2}).
\end{aligned}$$

Finally, solving $\frac{\partial}{\partial\omega}|\rho_n^c(\omega,\alpha^c)| = 0$, is equivalent to equating $F_1 - F_2 = 0$, where

$$\begin{aligned}
F_1 &:= A(\omega,\epsilon)\left(B(\omega,\epsilon)\frac{\partial}{\partial\omega}L_c(\omega) + L_c(\omega)\frac{\partial}{\partial\omega}B(\omega,\epsilon)\right)\\
&= \frac{a^2b^2\omega}{c^2} + \frac{ab^2h_n^c\sqrt{2}\sqrt{acb}\epsilon^\delta\sqrt{\omega}}{2c^2} + \left(\frac{5a^2b^3\sqrt{2}}{4c^2\sqrt{acb}} + \frac{3(n-1)ab^2\sqrt{2}\sqrt{acb}}{2c^3}\right)\omega^{3/2} + \mathcal{O}(\omega\epsilon^\delta),
\end{aligned}$$

and

$$\begin{aligned}
F_2 &:= B(\omega,\epsilon)L_c(\omega)\frac{\partial}{\partial\omega}A(\omega,\epsilon)\\
&= \frac{a^2b^2\omega}{c^2} - \frac{ab^2h_n^c\sqrt{2}\sqrt{acb}\epsilon^\delta\sqrt{\omega}}{2c^2} + \left(\frac{5a^2b^3\sqrt{2}}{4c^2\sqrt{acb}} + \frac{(n-1)ab^2\sqrt{2}\sqrt{acb}}{c^3}\right)\omega^{3/2} + \mathcal{O}(\omega\epsilon^\delta).
\end{aligned}$$

Thus, $F_1 - F_2 = 0$ leads to $\overline{\omega}^c = \frac{-2h_n^c c\epsilon^\delta}{n-1}$. Since $h_n^c = \frac{1}{C_n^c}$ and $\overline{\omega}^c$ is asymptotically represented as $\overline{\omega} = d_n^c\epsilon^\eta$, comparing the exponents and coefficients yields the required relation (3.60). □

Lemma 3.4.11. *For the overlapping OWR with splitting at a current node, and with $n > 1$, the modulus of the convergence factor $|\rho_n^c(\omega, \alpha)|$ evaluated at $\omega_{\min}$ and $\overline{\omega}^c$ is given by*

$$|\rho_n^c(\omega_{\min}, \alpha^c)| = 1 - \frac{2\sqrt{2}\sqrt{acb}C_n^c}{bc}\omega_{\min}^{1/2-\delta} + \mathcal{O}(\omega_{min}^{1-2\delta}), \tag{3.63}$$

and

$$|\rho_n^c(\overline{\omega}^c, \alpha^c)| = 1 + \left(\frac{(n-1)\sqrt{2}\sqrt{acb}\sqrt{d_n^c}}{ac} - \frac{2\sqrt{2}\sqrt{abc}}{aC_n^c\sqrt{d_n^c}}\right)\omega_{\min}^{\delta/2} + \mathcal{O}(\omega_{\min}^{\delta}), \tag{3.64}$$

where we have already substituted asymptotic relations $\alpha = -C_n^c\epsilon^\delta$ and $\overline{\omega}^c = d_n^c\epsilon^\delta$, with $\epsilon = \omega_{\min}$.

Proof. For $|\lambda_1| < 1$, using the definition of the convergence factor ρ_n^c and (3.61), we have

$$|\rho_n^c(\omega_{\min}, \alpha^c)| = |\rho_1^c(\omega_{\min}, \alpha^c)||\lambda_1^2|^{n-1} = |\rho_1^c(\omega_{\min}, \alpha^c)|L_c(\omega_{\min}),$$

and using the expressions of $|\rho_1^c(\omega_{\min}, \alpha^c)|$ and $L_c(\omega_{\min})$ given by (3.59) and (3.62), we arrive at

$$\begin{aligned}
|\rho_n^c(\omega_{\min}, \alpha^c)| &= \left(1 - \frac{2\sqrt{2}\sqrt{acb}C_n^c}{bc}\epsilon^{1/2-\delta} + \mathcal{O}(\epsilon^{1-2\delta})\right)\left(1 + \frac{(n-1)\sqrt{2}\sqrt{acb}\sqrt{\epsilon}}{ac} + \mathcal{O}(\epsilon)\right), \\
&= 1 - \frac{2\sqrt{2}\sqrt{acb}C_n^c}{bc}\epsilon^{1/2-\delta} + \mathcal{O}(\epsilon^{1-2\delta}).
\end{aligned}$$

Similarly, for $\omega = \overline{\omega}^c$, the combination of equations (3.61), (3.52) and (3.62) yields

$$\begin{aligned}
|\rho_n^c(\overline{\omega}^c, \alpha)| &= \frac{B(\overline{\omega}^c, \epsilon)}{A(\overline{\omega}^c, \epsilon)}L_c(\overline{\omega}^c) = \frac{1}{\frac{B(\overline{\omega}^c, \epsilon)}{A(\overline{\omega}^c, \epsilon)}}L_c(\overline{\omega}^c) \\
&= \left(\frac{1}{1 + \frac{2h_n^c\sqrt{2}\sqrt{abc}}{a\sqrt{d_n^c}}\epsilon^{\delta/2} + \mathcal{O}(\epsilon^\delta)}\right)\left(1 + \frac{(n-1)\sqrt{2}\sqrt{acb}\sqrt{d_n^c}}{ac}\epsilon^{\delta/2} + \mathcal{O}(\epsilon^\delta)\right) \\
&= \left(1 - \frac{2h_n^c\sqrt{2}\sqrt{abc}}{a\sqrt{d_n^c}}\epsilon^{\delta/2} + \mathcal{O}(\epsilon^\delta)\right)\left(1 + \frac{(n-1)\sqrt{2}\sqrt{acb}\sqrt{d_n^c}}{ac}\epsilon^{\delta/2} + \mathcal{O}(\epsilon^\delta)\right) \\
&= 1 + \left(-\frac{2\sqrt{2}\sqrt{abc}}{aC_n^c\sqrt{d_n^c}} + \frac{(n-1)\sqrt{2}\sqrt{acb}\sqrt{d_n^c}}{ac}\right)\epsilon^{\delta/2} + \mathcal{O}(\epsilon^\delta).
\end{aligned}$$

□

Theorem 3.4.4. *For the overlapping OWR with splitting at a current node and with $n > 1$ overlap, if $\alpha_n^{c*} = -C_n^c\epsilon^{-1/3}$, then the convergence factor ρ_n^c satisfies*

$$|\rho_n^c(\omega, \alpha^c)| \leq |\rho_n^c(\omega_{\min}, \alpha_n^{c*})| = 1 - \frac{2\sqrt{2}\sqrt{acb}C_n^c}{bc}\omega_{\min}^{1/6} + \mathcal{O}(\omega_{\min}^{1/3}), \tag{3.65}$$

where

$$C_n^c = \left(-\frac{2(n-1)b^2c}{a^2}\right)^{1/3}.$$

Proof. The left plot of Figure 3.7 illustrates that for $n > 1$ overlap, the solution of the min-max problem (3.55) is given by equioscillation between $\omega_{\min}$ and $\overline{\omega}^c$. Using the relation (3.60) and comparing the exponents and coefficients of the dominating terms of $|\rho_n^c(\omega_{\min}, \alpha^c)|$ and $|\rho_n^c(\overline{\omega}^c, \alpha^c)|$, we obtain

$$\delta = 1/3, \quad \text{and} \quad C_n^c = \left(\frac{2(n-1)b^2c}{a}\right)^{1/3}.$$

This completes the proof. □

Theorem 3.4.5. *The convergence of the overlapping OWR is faster for the splitting at a voltage node.*

Proof. We substitute the values of C_n^c and C_n^v into the expression of $|\rho_n^c(\omega_{\min}, \alpha_n^{c*})|$ and $|\rho_n^v(\omega_{\min}, \alpha_n^{v*})|$ which for $n > 1$ leads to,

$$\begin{aligned}
|\rho_n^c(\omega_{\min}, \alpha_n^{c*})| \;-\; & |\rho_n^v(\omega_{\min}, \alpha_n^{v*})| \\
= \;& \left(1 - \frac{2\sqrt{2}\sqrt{abc}C_n^c}{bc}\omega_{\min}^{1/6} + \mathcal{O}(\omega^{1/3})\right) \\
& - \left(1 - \frac{2\sqrt{2}\sqrt{abc}}{C_n^v bc}\omega_{\min}^{1/6} + \mathcal{O}(\omega^{1/3})\right) \\
= \;& \left(\frac{2\sqrt{2}\sqrt{abc}}{bc}\omega_{\min}^{1/6}\right)\left(\frac{1}{C_n^v} - C_n^c\right) + \mathcal{O}(\omega^{1/3}) \\
= \;& \left(\frac{2\sqrt{2}\sqrt{abc}}{bc}\omega_{\min}^{1/6}\right)\left(\left(-\frac{2nb^2c}{a^2}\right)^{1/3} - \left(-\frac{2(n-1)b^2c}{a^2}\right)^{1/3}\right) + \mathcal{O}(\omega^{1/3}) \\
> \;& 0,
\end{aligned}$$

where the last inequality follows since $c < 0$ and this completes the proof. □

3.5 Numerical Results

We consider an RLC transmission line of length $N = 149$ with $R = 2K\Omega/cm$, $L = 4.95 \times 10^{-3}\mu H/cm$ and $C = 0.021pF/cm$. For the time discretization, we use backward Euler with $\Delta t = T/5000$, where T is the total time. We first compare the classical WR and OWR algorithm for large time $T = 100$. The left plot in Figure 3.8 clearly shows the improvement in the convergence factor when optimized transmission conditions are used. The dashed and dotted lines show the results for

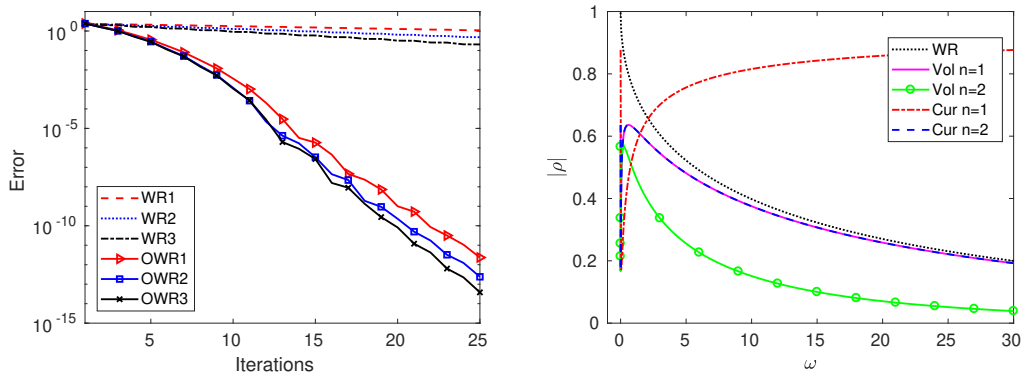

Figure 3.8: Convergence for long time $T = 100$ (left) and convergence factor in Laplace space (right).

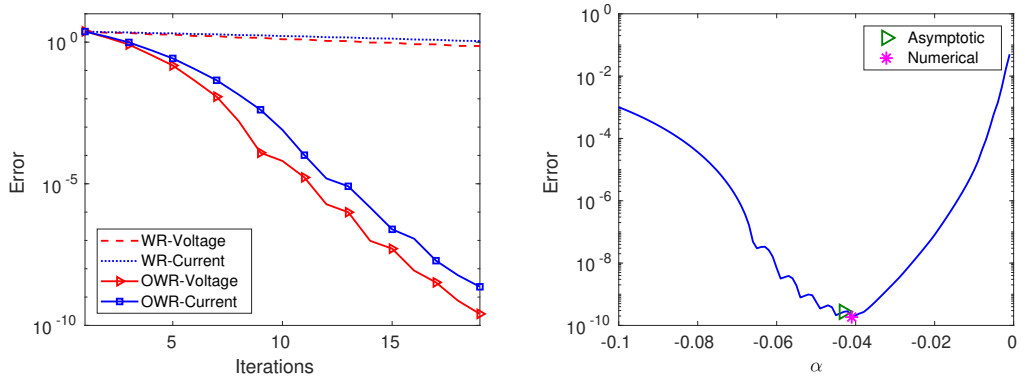

Figure 3.9: Comparison of different splittings in time (left) and of values of the optimized alpha for the overlapping OWR with splitting at a voltage node (right).

classical WR while solid lines represent the OWR algorithm. We also see the effect of overlapping nodes (e.g. WR1 denotes the WR algorithm with one node overlap). Increasing the overlap increases the convergence speed. However, the gain is very small. The right plot of Figure 3.8 compares the convergence factor for OWR in Laplace space for both splittings, at a current node and a voltage node. The dotted black line is for WR with single node overlap while the other lines are for OWR. For OWR, the splitting at a voltage node leads to faster convergence. This is also true in the time domain, see the left plot of Figure 3.9. But for classical WR, splitting does not matter in the Laplace space, see Theorems 3.2.2 and 3.2.2, while there is small difference in time domain. Finally, the right plot of Figure 3.9 validates our asymptotic result in Theorem 3.4.2. Both numerically computed and asymptotically derived values of the optimal α for splitting at a voltage node are very close.

3.6 Conclusion

For an infinitely long RLC transmission line, we presented a first analysis of all three cases: nonoverlapping WR and OWR, and overlapping WR and OWR with splitting either at a current or voltage node. We showed that using optimized transmission conditions, we can achieve a drastic improvement in the convergence rate. Note that our analysis is in the Laplace domain since the analysis is easier and the convergence in the Laplace domain implies convergence in the time domain, see Lemma 2.2.1. We also see that overlapping nodes increase the convergence rate for both WR and OWR algorithms but the improvement (by the factor of $(\lambda_1)^{2n}$) is not large. Further, for OWR, the splitting at a voltage node leads to a little faster convergence than the splitting at a current node, while this splitting does not effect the convergence of WR. We finally compared the values of the optimized α found numerically and by asymptotic analysis and they are very close.

Chapter 4

Approximation of a large RC circuit by a small RC circuit

In general, the analysis of the application of OWR methods to large electric circuits is complicated. In previous chapters, we saw that RC circuits and RLCG transmission lines are an integral part of many circuits and hence their quick simulation is important. We considered infinitely long RC circuits and found that the analysis to find the optimization parameters in OWR is impossible without the use of asymptotic analysis. The same happens with infinitely long RLCG transmission lines (refer to Chapter 3). We therefore search for a better way to find the optimization parameters of the OWR method.

The complexity of the min-max problem of the type

$$\min_{\alpha,\beta\in\mathbb{R}} \left(\max_{\Re(s)>0} |\rho(s,\alpha,\beta)| \right)$$

can be reduced if we consider a smaller circuit, say with two or four nodes. In such cases, the expression of the convergence factor $\rho(s,\alpha,\beta)$ for the OWR algorithm is less complicated and hence the above mentioned min-max problem can be solved using available complex analysis tools.

In this chapter, we therefore first reduce the infinitely long RC circuit shown in Figure 2.2 to a smaller RC circuit with two nodes and four nodes respectively. We then apply the WR and OWR methods to these reduced circuits, and find explicit expressions for the optimization parameters in the OWR method. Finally, we show that under special conditions for the reduced RC circuits, we can derive expressions for $\alpha^*_{T,0}$ and $\alpha^*_{R,0}$ from Theorems 2.4.1 and 2.4.3 for the infinitely long RC circuits. We then perform some numerical experiments and conclude this chapter. Note that we consider only the nonoverlapping WR and OWR methods in this chapter; the study of overlapping WR and OWR for these reduced circuits is in progress.

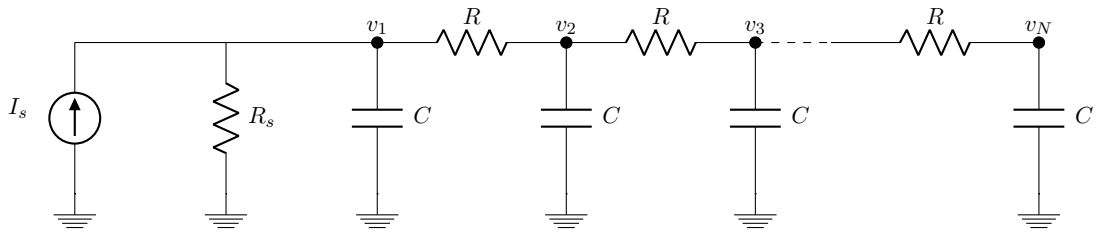

Figure 4.1: An RC circuit of length N.

4.1 RC circuit with two nodes

We would first like to reduce an infinitely long RC circuit to a small RC circuit of two nodes. We have shown in Chapter 2 that the MNA formulation of an infinitely long RC circuit leads to a large system of differential equations. Further, we analyzed the convergence of WR and OWR in the Laplace space. In this section, we shall again use the Laplace transformation to reduce these large circuits into smaller ones.

Consider an RC circuit of length N as shown in Figure 4.1. For convenience in the analysis that will follow, we assume N to be even, and we renumber the nodes: instead of using the numbering from 1 to N, we use the numbering from -$N/2+1$ to $N/2$. We split this circuit into two sub-circuits of equal length at node 0 and do not add any overlap. Let $\mathbf{u}$ and $\mathbf{w}$ denote the unknowns in the first and second sub-circuit respectively. Application of the Laplace transformation to the WR system of differential equations for these two sub-circuits leads to

$$\begin{aligned} s\hat{\mathbf{u}}^{k+1} &= \begin{bmatrix} b & a & & \\ \ddots & \ddots & \ddots & \\ & a & b & a \\ & & a & b \end{bmatrix} \begin{bmatrix} \hat{u}_{-\frac{N}{2}+1} \\ \vdots \\ \hat{u}_{-1} \\ \hat{u}_0 \end{bmatrix}^{k+1} + \begin{bmatrix} 0 \\ \vdots \\ 0 \\ a\hat{u}_1^{k+1} \end{bmatrix}, \\ s\hat{\mathbf{w}}^{k+1} &= \begin{bmatrix} b & a & & \\ a & b & a & \\ & \ddots & \ddots & \ddots \\ & & a & b \end{bmatrix} \begin{bmatrix} \hat{w}_1 \\ \hat{w}_2 \\ \vdots \\ \hat{w}_{\frac{N}{2}} \end{bmatrix}^{k+1} + \begin{bmatrix} a\hat{w}_0^{k+1} \\ 0 \\ \vdots \\ 0 \end{bmatrix}, \end{aligned} \tag{4.1}$$

where we have considered the source term $\mathbf{f} = 0$. One can refer to Sections 2.1 and 2.2 for more details.

Our goal is to reduce these two subsystems to smaller subsystems by eliminating $\hat{u}_j$ where $j \in \{-N/2+1, -1\}$ and $\hat{w}_j$ for $j \in \{2, N/2\}$. We start with the second subsystem corresponding to $\hat{\mathbf{w}}^{k+1}$. Backward elimination leads to $\hat{w}_{N/2}^{k+1} = \hat{h}_1 \hat{w}_{N/2-1}^{k+1}$ and $\hat{w}_{N/2-j}^{k+1} = \hat{h}_{j+1} \hat{w}_{N/2-j-1}^{k+1}$ where $\hat{h}_1 := \frac{a}{s-b}$ and $\hat{h}_{j+1} := \frac{a}{s-b-a\hat{h}_j}$, for $j = 1, 2, \ldots, N/2-2$. Thus, eliminating all $\hat{w}_j^{k+1}$ except $\hat{w}_1^{k+1}$ leaves us with only

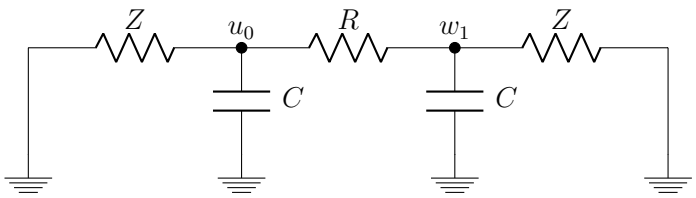

Figure 4.2: Reduced RC Circuit into 2 nodes with impedance $Z = R/(1-h)$.

one equation $s\hat{w}_1^{k+1} = (b + a\hat{h}_{N/2-1})\hat{w}_1^{k+1} + a\hat{w}_0^{k+1}$. Similarly, for the first subsystem corresponding to $\hat{\mathbf{u}}$, we are left with $s\hat{u}_0^{k+1} = (b + a\hat{h}_{N/2-1})\hat{u}_0^{k+1} + a\hat{u}_1^{k+1}$.

We now find an expression for $\hat{h}_j$. If the length of the circuit is infinite, that is, $N \to \infty$, then we can write $\hat{h}_\infty = \frac{a}{s-b-a\hat{h}_\infty}$ which on solving leads to $\hat{h}_\infty = \frac{s-b\pm\sqrt{(s-b)^2-4a^2}}{2a}$, which are the same as λ_1 and λ_2 defined in (2.10) for the infinite RC circuit. A careful calculation shows that for $\Re(s) > 0$ or $b = -(2+\epsilon)a$, where $\epsilon > 0$, $|\hat{h}_j| < 1$. From Lemma 2.2.2 and Remark 2.2.2, we have $|\lambda_2| < 1 < |\lambda_1|$ and hence we consider $h := \hat{h}_\infty$ that represents λ_2 at a certain frequency ω, where $s = \sigma + i\omega$ with $\sigma \geq 0$.

Therefore, the two subsystems of equations (4.1) reduces to

$$s\begin{bmatrix}\hat{u}_0\\ \hat{w}_1\end{bmatrix}^{k+1} = \begin{bmatrix}b+ah & a\\ a & b+ah\end{bmatrix}\begin{bmatrix}\hat{u}_0\\ \hat{w}_1\end{bmatrix}^{k+1}, \tag{4.2}$$

where h is the value of $\lambda_2(s)$ for some $s \in \mathbb{C}^+$ and is given by

$$h := h_1 + ih_2 \approx \lambda_2(s) = \frac{s-b-\sqrt{(s-b)^2-4a^2}}{2a}. \tag{4.3}$$

Using Kirchoff's current law and Kirchoff's voltage law as explained in the book [63], we present the circuit interpretation of this reduced system (4.2) in Figure 4.2. We see that two resistors with impedance $R/(1-h)$ are added on both sides of the circuit. Note that we have considered homogeneous source terms since the system (4.1) represents error equations. Further, $h \approx \lambda_2(s)$ and $0 < |\lambda_2| < 1$, and hence $|R/(1-h)| > 0$. Also, if the value of h is very close to 1, then we need to add huge resistors on both sides.

In the next section, we analyze the WR algorithm applied to the reduced system (4.2), and find the convergence factor as a function of h.

4.1.1 Classical Waveform Relaxation Method

We decompose the reduced RC circuit in Figure 4.2 into two smaller RC circuits with one node each. We do not introduce any overlap. The circuit interpretation of

Figure 4.3: Application of the classical WR to the reduced RC circuit of 2 nodes with impedance $Z = R/(1-h)$.

WR can be seen in Figure 4.3. We have already seen in Chapter 2 that the classical WR methods transfers only the voltages at the interfaces. In the PDE sense, these transmission conditions are interpreted as Dirichlet transmission conditions.

We now find an explicit formulation of the convergence factor (in the Laplace space) for the classical WR method, when applied to the reduced circuit of two nodes (see Figure 4.2).

Theorem 4.1.1. *The convergence factor of the classical nonoverlapping WR method when applied to the reduced system of equations (4.2) is given by*

$$\Gamma^{[2]}_{cla}(s,h) := \frac{1}{\phi^2(s,h)} = \frac{a^2}{(s-b-ah)(s-b-ah)}, \tag{4.4}$$

where

$$\phi(s,h) := \frac{s-b}{a} - h. \tag{4.5}$$

Proof. The application of WR method to the system of equations (4.2) leads to solving two coupled equations,

$$s\hat{u}_0^{k+1} = (b+ah)\hat{u}_0^{k+1} + a\hat{u}_1^{k+1}, \tag{4.6}$$
$$s\hat{w}_1^{k+1} = (b+ah)\hat{w}_1^{k+1} + a\hat{w}_0^{k+1}, \tag{4.7}$$

where the unknowns $\hat{u}_1^{k+1}$ and $\hat{w}_0^{k+1}$ are given by the transmission conditions

$$u_1^{k+1} = w_1^k, \qquad \text{and} \qquad w_0^{k+1} = u_0^k. \tag{4.8}$$

These transmission conditions are interpreted as voltages and are transferred at the start of each iteration. Substituting the transmission conditions (4.8) into (4.6)-(4.7) leads to

$$\hat{u}_0^{k+1} = \frac{a}{s-b-ah}\hat{w}_1^k = \frac{1}{\phi}\hat{w}_1^k, \quad \text{and} \quad \hat{w}_1^{k+1} = \frac{a}{s-b-ah}\hat{u}_0^k = \frac{1}{\phi}\hat{u}_0^k,$$

where $\phi = \frac{s-b}{a} - h$. These coupled equations simplify to $\hat{u}_0^{k+1} = \Gamma^{[2]}_{cla}(s,h)\hat{u}_0^{k-1}$ and $\hat{w}_1^{k+1} = \Gamma^{[2]}_{cla}(s,h)\hat{w}_1^{k-1}$, where the convergence factor $\Gamma^{[2]}_{cla}(s,h)$ is defined by (4.4), and this completes the proof. □

From now onwards, we will denote $\phi := \phi(s,h)$ to simplify the notations and will show its dependence on s and h whenever necessary.

Remark 4.1.1. Note that if $h = \lambda_2(s)$, then $\phi = \frac{s-b}{a} - h = \frac{s-b}{a} - \lambda_2$ and since $\lambda_1+\lambda_2 = (s-b)/a$, we have $\phi = \lambda_1$, which means $\Gamma^{[2]}_{cla}(s,\lambda_2) = \frac{1}{\lambda_1^2}$. Thus, substituting $h = \lambda_2$ in the convergence factor of the reduced RC circuit with two nodes gives us the convergence factor of infinitely long RC circuit.

Further, from the expression of the convergence factor (4.4), we can clearly observe that for fixed h, $\left|\Gamma^{[2]}_{cla}\right|$ decreases as frequency ω, where $s = i\omega$, increases. Thus, $\left|\Gamma^{[2]}_{cla}\right|$ is inversely proportional to ω.

4.1.2 Optimized Waveform Relaxation Method

We had already seen in Chapters 2 and 3, that the classical WR method has an extremely slow convergence factor especially when large time windows are used. Hence we use more efficient transmission conditions to increase its convergence. Similarly, we define new transmission conditions for this reduced RC circuit:

$$\begin{aligned}(u_1^{k+1} - u_0^{k+1}) + \alpha u_1^{k+1} &= (w_1^k - w_0^k) + \alpha w_1^k,\\ (w_1^{k+1} - w_0^{k+1}) + \beta w_0^{k+1} &= (u_1^k - u_0^k) + \beta u_0^k,\end{aligned} \tag{4.9}$$

where the parameters α, $\beta \in \mathbb{R}$. We rewrite the above transmission conditions as:

$$\begin{aligned}u_1^{k+1} &= \tfrac{u_0^{k+1}}{1+\alpha} + w_1^k - \tfrac{w_0^k}{1+\alpha},\\ w_0^{k+1} &= -\tfrac{w_1^{k+1}}{\beta-1} + \tfrac{u_1^k}{\beta-1} + u_0^k.\end{aligned} \tag{4.10}$$

Theorem 4.1.2. *The convergence factor of the nonoverlapping OWR method for the reduced RC circuit with two nodes is given by*

$$\Gamma^{[2]}(s,h,\alpha,\beta) := \left(\frac{\alpha+1-\phi}{(\alpha+1)\phi-1}\right)\left(\frac{\beta-1+\phi}{(\beta-1)\phi+1}\right). \tag{4.11}$$

Proof. Substituting the Laplace transformed transmission conditions (4.10) into the equation (4.6) yields

$$(s-b-ah)\hat{u}_0^{k+1} = \frac{a\hat{u}_0^{k+1}}{1+\alpha} + a\hat{w}_1^k - \frac{a\hat{w}_0^k}{1+\alpha}.$$

Further, $\hat{w}_0^k$ can be expressed in terms of $\hat{w}_1^k$ using (4.7) as $a\hat{w}_0^k = (s-b-ah)\hat{w}_1^k$, which on substituting in the above equation gives

$$\left(s-b-ah-\frac{a}{1+\alpha}\right)\hat{u}_0^{k+1} = \left(a - \frac{s-b-ah}{1+\alpha}\right)\hat{w}_1^k,$$

which on simplification leads to

$$\hat{u}_0^{k+1} = \left(\frac{\alpha + 1 - \phi}{(\alpha+1)\phi - 1}\right)\hat{w}_1^k, \tag{4.12}$$

where ϕ is defined in (4.5). Proceeding in a similar way for the other sub-system $\hat{w}_1$, we arrive at

$$\hat{w}_1^{k+1} = \left(\frac{\beta - 1 + \phi}{(\beta-1)\phi + 1}\right)\hat{u}_0^k. \tag{4.13}$$

Combining (4.12) and (4.13), we obtain $\hat{u}_0^{k+1} = \Gamma^{[2]}(s,h,\alpha,\beta)\hat{u}_0^{k-1}$ and $\hat{w}_1^{k+1} = \Gamma^{[2]}(s,h,\alpha,\beta)\hat{w}_1^{k-1}$, where $\Gamma^{[2]}(s,h,\alpha,\beta)$ is given by (4.11) and this completes the proof. □

Remark 4.1.2. If we choose $h = \lambda_2(s)$, then we get $\phi = \frac{s-b}{a} - \lambda_2$. Further, using the property $\lambda_1 + \lambda_2 = \frac{s-b}{a}$, the expression for ϕ simplifies to $\phi = \lambda_1$, and substituting this in the definition (4.11) results in

$$\Gamma^{[2]}(s,\lambda_2,\alpha,\beta) = \left(\frac{\alpha + 1 - \lambda_1}{(\alpha+1)\lambda_1 - 1}\right)\left(\frac{\beta - 1 + \lambda_1}{(\beta-1)\lambda_1 + 1}\right) = \rho_0(s,\alpha,\beta),$$

where $\rho_0(s,\alpha,\beta)$ is the convergence factor of the nonoverlapping OWR when applied to infinitely long RC circuits and is given in (2.20).

We would now like to make the modulus of the convergence factor $\Gamma^{[2]}$ as small as possible, which means we need to choose appropriate α and β. This leads to solving the min-max problem

$$\min_{\alpha,\beta\in\mathbb{R}}\left(\max_{\Re(s)\geq 0}\left|\Gamma^{[2]}(s,h,\alpha,\beta)\right|\right). \tag{4.14}$$

Circuit elements are fixed and hence the parameters a and b cannot be changed. Also, we still do not know what value of h should be taken, since h is somehow considered as the approximation of $\lambda_2(s)$ at some $s \in \mathbb{C}^+$. Therefore we are left with the parameters α and β to optimize. We assume $\beta = -\alpha$. This choice comes from the optimal values of α and β which are given as

$$\alpha_{opt} := \phi - 1, \qquad \text{and} \qquad \beta_{opt} := 1 - \phi.$$

Lemma 4.1.1. *For $0 < |h| < 1$, with $0 < h_1 < 1$, $-b \geq 2a$ and $\alpha > 0$, the convergence factor $\Gamma^{[2]}$ is analytic in the right half of the complex plane. Further, $\left|\Gamma^{[2]}\right|$ attains its maximum on the imaginary axis of the complex plane.*

Proof. We first show that under the conditions, $-b \geq 2a$ and $0 < |h| < 1$, with $0 < h_1 < 1$, we have $|\phi| > 1$. Let $b = -(2+\epsilon)a$, where $\epsilon \geq 0$. Since s lies in the right

half of the complex plane, we can express $s = \sigma + i\omega$, where $\sigma \geq 0$ and $-\infty < \omega < \infty$. From the definition of ϕ in (4.5), for $\epsilon \geq 0$,

$$\begin{aligned} |\phi|^2 &= \left|\frac{s-b}{a} - h\right|^2 = \left|\frac{\sigma + i\omega + (2+\epsilon)a}{a} - h_1 - ih_2\right|^2 \\ &= \left|\frac{\sigma}{a} + 2 + \epsilon - h_1 + i\left(\frac{\omega}{a} - h_2\right)\right|^2 = \left(\frac{\sigma}{a} + 2 + \epsilon - h_1\right)^2 + \left(\frac{\omega}{a} - h_2\right)^2 \\ &> 1, \end{aligned}$$

where the last inequality holds since σ, $a \geq 0$ and $2 + \epsilon - h_1 > 1$. We now show that the denominator of $\Gamma^{[2]}$ defined in (4.11) does not have a root in the right half of the complex plane. This can be proved by contradiction using the same arguments used in the proof of Theorem 2.4.1. Finally, the maximum modulus principle for analytic functions states that its maximum is attained on the imaginary axis of the complex plane and this completes the proof. □

Lemma 4.1.2. *The modulus of the convergence factor* $\left|\Gamma^{[2]}\right|$ *is an even function with respect to the frequency* ω *where* $s = i\omega$.

Proof. We first prove that for $s = i\omega$, if $h(\omega) = h_1 + ih_2$, then $h(-\omega) = h_1 - ih_2$. From the proof of Lemma 2.4.2, we observe that $h(\omega) = \frac{(2+\epsilon)a - z_1}{2a} + i\frac{\omega - z_2}{2a} = h_1 + ih_2$. Using the same analysis we note that $h(-\omega) = \frac{(2+\epsilon)a - z_1}{2a} + i\frac{-\omega + z_2}{2a} = h_1 - ih_2$, and hence

$$\begin{aligned} |\phi(-\omega)| &= \left|\frac{-i\omega - b}{a} - h(-\omega)\right| = \left|\frac{-i\omega - b}{a} - h_1 + ih_2\right| \\ &= \left|\left(\frac{-b}{a} - h_1\right) + i\left(\frac{-\omega}{a} + h_2\right)\right| = \sqrt{\left(\frac{-b}{a} - h_1\right)^2 + \left(\frac{-\omega}{a} + h_2\right)^2} \\ &= \sqrt{\left(\frac{-b}{a} - h_1\right)^2 + \left(\frac{\omega}{a} - h_2\right)^2} \\ &= \left|\frac{i\omega - b}{a} - h_1 - ih_2\right| = \left|\frac{i\omega - b}{a} - h(\omega)\right| \\ &= |\phi(\omega)|. \end{aligned}$$

□

As a result of Lemmas 4.1.1 and 4.1.2, our minimization problem (4.14) reduces to

$$\min_{\alpha > 0} \left(\max_{\omega_{\min} \leq \omega \leq \omega_{\max}} \left|\Gamma^{[2]}(\omega, h, \alpha)\right| \right), \tag{4.15}$$

where we have restricted ω between $\omega_{\min} := \frac{\pi}{T}$ and $\omega_{\max} := \frac{\pi}{\Delta t}$ with T as the final simulation time and Δt as the time discretization parameter. The restriction holds since we solve the problem on a finite time interval $[0, T]$ and with time discretization Δt.

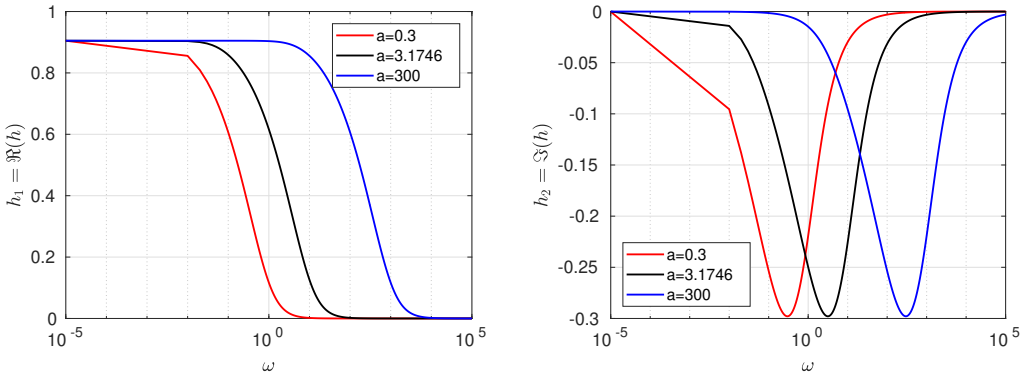

Figure 4.4: Dependence of h_1 (left) and h_2 (right) on ω for different values of a.

Remark 4.1.3. Since $h = \lambda_2(s)$, for some $s \in \mathbb{C}^+$, Lemma 2.2.2 states that $0 < |h| < 1$. Further, for $\omega \geq 0$, where $s = i\omega$, the left plot of Figure 4.4 shows that the real part of h, that is, h_1 satisfies $0 < h_1 < 1$, while the right plot shows that the imaginary part of h, that is, h_2 satisfies $-1 < h_2 \leq 0$.

We now solve the min-max problem (4.15) using the available complex analysis tools. We observed in Chapter 2 that a solution of the min-max problem is given by equioscillation. Since we apply the nonoverlapping OWR to the reduced RC circuit, the equioscillation occurs between $\omega = \omega_{\min}$ and $\omega = \omega_{\max}$, when the asymptotic analysis is carried out with respect to the final time $T \to 0$ along with $\epsilon = 0$ (see Section 2.4.1), while the equioscillation occurs between $\omega = 0$ and $\omega = \omega_{\max}$, when the asymptotic analysis is carried out with respect to the reaction term $\epsilon \to 0$ (see Section 2.4.2). We thus solve the min-max problem (4.15) using equioscillation such that both these asymptotic analysis results are valid.

We simplify the expression of $\left|\Gamma^{[2]}\right|$ by defining

$$x := \frac{\omega}{a}, \quad p := \alpha + 1, \quad 2c^2 := -\frac{b}{a}, \quad d := 2c^2 - h_1. \tag{4.16}$$

Since $\alpha > 0$, $b \geq 2a$ and $0 < h_1 < 1$, we have $x \geq 0$, $p > 1$, $c^2 \geq 1$ and $d > 1$. The modulus of the convergence factor of the OWR given in (4.11) in these new variables

simplifies to

$$\begin{aligned} R(x,p,d) &:= \left|\Gamma^{[2]}(\omega,h,\alpha)\right| = \left|\left(\frac{\alpha+1-\left(\frac{i\omega-b}{a}-(h_1+ih_2)\right)}{(\alpha+1)\left(\frac{i\omega-b}{a}-(h_1+ih_2)\right)-1}\right)^2\right| \\ &= \left|\left(\frac{p-\left(ix+2c^2-h_1-ih_2\right)}{p\left(ix+2c^2-h_1-ih_2\right)-1}\right)\right|^2 \\ &= \frac{(p-d)^2+(x-h_2)^2}{(pd-1)^2+(x-h_2)^2p^2}. \end{aligned} \tag{4.17}$$

Our min-max problem (4.15) thus reduces to: Find for fixed $d>1$ and h, the

$$\min_{p>1}\left(\max_{0\le x_{\min}\le x\le x_{\max}} R(x,p,d,h_2)\right), \tag{4.18}$$

where $x_{\min} := \frac{\omega_{\min}}{a}$ and $x_{\max} := \frac{\omega_{\max}}{a}$.

Lemma 4.1.3. *$R(x,p,d,h_2)$ has only one critical point $x=0$ with respect to x. Further, $x=0$ is a local minimum if $d-\sqrt{d^2-1} < p < d+\sqrt{d^2-1}$ and a local maximum if $p\in(-\infty,d-\sqrt{d^2-1})\cup(d+\sqrt{d^2-1},\infty)$.*

Proof. Differentiating $R(x,p,d,h_2)$ with respect to x yields

$$\begin{aligned} \frac{\partial R(x,p,d,h_2)}{\partial x} &= \frac{\partial}{\partial x}\left(\frac{p^2+d^2-2pd+x^2+h_2^2-2xh_2}{p^2(x^2+d^2)+1-2pd}\right) \\ &= \frac{2(x-h_2)\left(2dp^3-p^4-2pd+1\right)}{\left(d^2p^2+p^2(x-h_2)^2-2pd+1\right)^2}. \end{aligned} \tag{4.19}$$

Equating the numerator with 0 states that $R(x,p,d,h_2)$ has only one critical point with respect to x at $x=h_2$. Remark 4.1.3 states that for $s=i\omega$, with $\omega\ge 0$, the imaginary part of h, that is, h_2 satisfies $-1<h_2\le 0$. Since $x\ge 0$, the equality $x=h_2$ holds only when $x=h_2=0$. We now check whether the critical point $x=0$ is a local maximum or local minimum by checking the sign of $\frac{\partial^2 R(x,p,d,h_2)}{\partial x^2}$ at $x=0$. Differentiating (4.19) with respect to x and evaluating at $h_2=0$ leads to

$$\frac{\partial^2 R(x,p,d,0)}{\partial x^2} = \frac{2(p-1)(p+1)(2dp-p^2-1)(d^2p^2-3p^2x^2-2dp+1)}{\left(d^2p^2+p^2x^2-2dp+1\right)^3},$$

which on evaluation at $x=0$ simplifies to

$$\left.\frac{\partial^2 R(x,p,d,0)}{\partial x^2}\right|_{x=0} = \frac{2(p-1)(p+1)(2dp-p^2-1)}{(dp-1)^4}.$$

Since $p>1$, the polynomial $2dp-p^2-1$ determines the sign of $\frac{\partial^2 R(x,p,d)}{\partial x^2}|_{x=0}$. Simplifying the polynomial $-p^2+2dp-1=-(p-p_1)(p-p_2)$, where $p_1=d-\sqrt{d^2-1}$ and $p_2=d+\sqrt{d^2-1}$, we observe that $2dp-p^2-1>0$ if $p\in(p_1,p_2)$ and $2dp-p^2-1<0$ if $p\in(-\infty,p_1)\cup(p_2,\infty)$. □

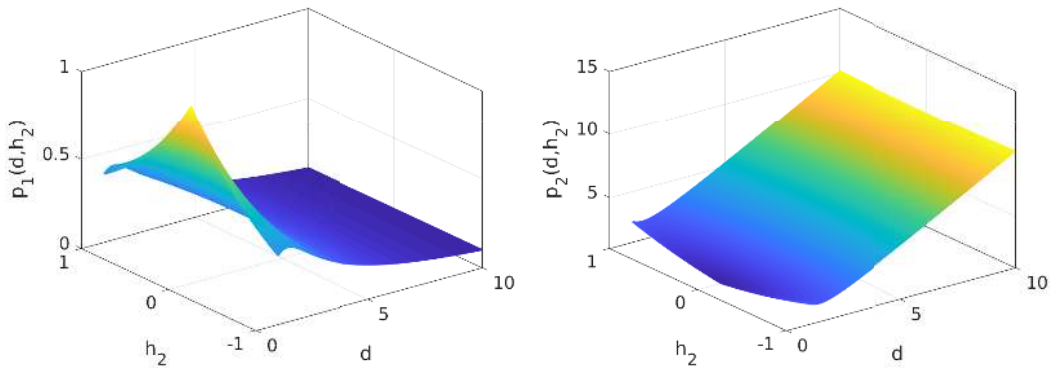

Figure 4.5: Plots of $p_1(d, h_2)$ and $p_2(d, h_2)$ for different values of d and h_2.

Lemma 4.1.3 states that $R(x, p, d, h_2)$ has two extrema with respect to x at $x_{\min}$ and $x_{\max}$, where $x_{\min} \geq 0$ and hence the min-max problem (4.18) reduces to

$$\min_{p>1} \left(\max \left\{ R(x_{\min}, p, d, h_2), R(x_{\max}, p, d, h_2) \right\} \right).$$

In order to find the solution p^* of the above problem, we will first consider $x_{\min} \to 0$ and sufficiently large $x_{\max}$. Then we will show that with this solution p^*, the modulus of the convergence factor $R(x, p^*, d, h_2)$ does not depend on x for $0 \leq x_{\min} \leq x \leq x_{\max}$. These two steps will thus infer that the optimized p^* is the solution of the min-max problem (4.18).

Theorem 4.1.3. *For the reduced RC circuit with two nodes, the optimized α^* for the nonoverlapping OWR method is given by*

$$\alpha^{[2]*} := 2c^2 - h_1 - 1 + \sqrt{(2c^2 - h_1)^2 - 1}. \tag{4.20}$$

Proof. We will study the behavior of the polynomials $R(x_{\min}, p, d, h_2)$ and $R(x_{\max}, p, d, h_2)$ with respect to p. Recall from (4.17), for $x_{\min} \to 0$,

$$R(x_{\min}, p, d, h_2) = \lim_{x_{\min} \to 0} \left(\frac{(p-d)^2 + (x_{\min} - h_2)^2}{(pd-1)^2 + (x_{\min} - h_2)^2 p^2} \right) = \frac{(p-d)^2 + h_2^2}{(pd-1)^2 + p^2 h_2^2}.$$

At $p = 1$, $R(x_{\min}, 1, d, h_2) = 1$ and for large values of p, $R(x_{\min}, p, d, h_2) = \frac{1}{d^2 + h_2^2}$. Differentiating $R(x_{\min}, p, d, h_2)$ with respect to p leads to

$$\frac{\partial R(x_{\min}, p, d, h_2)}{\partial p} = \frac{2(d^2 + h_2^2 - 1)(-d^2 p + dp^2 - h_2^2 p + d - p)}{(d^2 p^2 + h_2^2 p^2 - 2dp + 1)^2}. \tag{4.21}$$

Since $d > 1$, we have $(d^2 + h_2^2 - 1) > 0$. The sign of $\frac{\partial R(x_{\min}, p, d, h_2)}{\partial p}$ is thus determined by the polynomial $Q(p) := (-d^2 p + dp^2 - h_2^2 p + d - p)$. Let p_1 and p_2 be the roots of

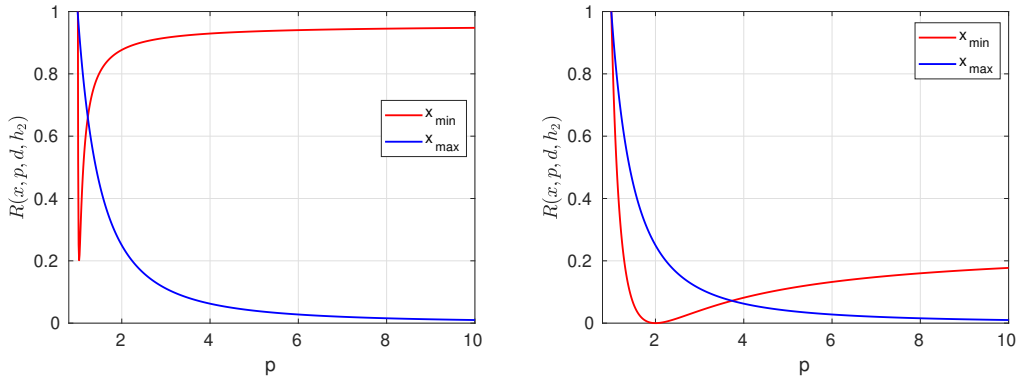

Figure 4.6: Dependence of $R(x, p, d, h_2)$ on p under the condition $x_{\min} \to 0$ and $x_{\max} \to \infty$ for $d = 1.022$ (left) and $d = 2$ (right).

this polynomial, given by

$$\begin{aligned} p_1 &:= \frac{d^2 + h_2^2 + 1 - \sqrt{d^4 + 2d^2h_2^2 + h_2^4 - 2d^2 + 2h_2^2 + 1}}{2d}, \\ p_2 &:= \frac{d^2 + h_2^2 + 1 + \sqrt{d^4 + 2d^2h_2^2 + h_2^4 - 2d^2 + 2h_2^2 + 1}}{2d}. \end{aligned}$$

Both plots of Figure 4.5 numerically illustrate that $p_1 < 1 < p_2$ for $d > 1$ and $-1 < h_2 < 1$. Moreover, the sign of p^2 in the polynomial $Q(p)$ is d, which is greater than zero. Thus, we can conclude that $Q(p) \geq 0$ for $p \in (-\infty, p_1] \cup [p_2, \infty)$, while $Q(p) < 0$ for $p \in (p_1, p_2)$. Equation (4.21) states that at $p = 1$, $R(x_{\min}, 1, d, h_2) = 1$ and it initially decreases on increasing p till p reaches p_2. For $p > p_2$, it starts increasing monotonically to reach $R(x_{\min}, p, d, h_2) = \frac{1}{d^2+h_2^2}$. This behavior can be seen numerically in the plots of Figure 4.6. We now consider $x_{\max} \to \infty$. From (4.18), we have

$$R(x_{\max}, p, d, h_2) = \lim_{x_{\max}\to\infty} \left(\frac{(p-d)^2 + (x_{\max} - h_2)^2}{(pd-1)^2 + (x_{\max} - h_2)^2 p^2} \right) = \frac{1}{p^2}. \tag{4.22}$$

Further, differentiating $R(x_{\max}, p, d, h_2)$ with respect to p leads to

$$\frac{\partial R(x_{\max}, p, d, h_2)}{\partial p} = -\frac{2}{p^3},$$

which states that $R(x_{\max}, p, d, h_2)$ is a decreasing function with respect to p. Starting at $p = 1$, the function $R(x_{\max}, 1, d, h_2) = 1$ and it monotonically decreases till its value reaches 0 (see Figure 4.6). The behavior of $R(x_{\min}, p, d, h_2)$ and $R(x_{\max}, p, d, h_2)$ with respect to p thus shows that the solution of the min-max problem (4.18) is

given uniquely by equating $R(x_{\min}, p^*, d, h_2) = R(x_{\max}, p^*, d, h_2)$. This value is optimal since perturbing p^* will increase the maximum value of R over x. Equating $R(x_{\min}, p^*, d, h_2) = R(x_{\max}, p^*, d, h_2)$ gives $\frac{(p-d)^2+h_2^2}{(pd-1)^2+p^2h_2^2} = \frac{1}{p^2}$ which simplifies to $p^* = d \pm \sqrt{d^2-1}$. We observe that $d - \sqrt{d^2-1} < 1$ while p ranges from 1 to ∞ and hence, we infer that the optimized $p^* = d + \sqrt{d^2-1}$. Substituting these expressions into $\alpha^{[2]*} = p^* - 1$ gives the expression for the optimized $\alpha^{[2]*}$ given in (4.20).

Finally, we prove that at this optimal value of p^*, the value of $R(x, p^*, d, h_2)$ is the same for all $0 \le x_{\min} \le x \le x_{\max}$. For $p = p^* = d + \sqrt{d^2-1}$,

$$
\begin{aligned}
R(x, p^*, d, h_2) &= \frac{(p^*-d)^2 + (x-h_2)^2}{(p^*d-1)^2 + (x-h_2)^2(p^*)^2} \\
&= \frac{d^2 - 1 + (x-h_2)^2}{(d^2 + d\sqrt{d^2-1} - 1)^2 + (x-h_2)^2(d^2 + d^2 - 1 + 2d\sqrt{d^2-1})} \\
&= \frac{d^2 - 1 + (x-h_2)^2}{(2d^4 + 2d^3\sqrt{d^2-1} - 3d^2 - 2d\sqrt{d^2-1} + 1) + (x-h_2)^2(2d^2 - 1 + 2d\sqrt{d^2-1})} \\
&= \frac{d^2 - 1 + (x-h_2)^2}{(d^2-1)(2d^2 + 2d\sqrt{d^2-1} - 1) + (x-h_2)^2(2d^2 - 1 + 2d\sqrt{d^2-1})} \\
&= \frac{d^2 - 1 + (x-h_2)^2}{(d^2 - 1 + (x-h_2)^2)(2d^2 + 2d\sqrt{d^2-1} - 1)} \\
&= \frac{1}{2d^2 + 2d\sqrt{d^2-1} - 1},
\end{aligned}
$$

that is, for $p = p^*$, the modulus of the convergence factor $R(x, p^*, d, h_2)$ does not depend on x and hence not on ω. This shows that to make the analysis easy, we could consider the assumption $x_{\min} \to 0$ and $x_{\max} \to \infty$ instead of evaluating R at $x_{\min}$ and $x_{\max}$ and this completes the proof. □

4.1.3 Relation with the infinitely long RC circuit

In this section, we will relate the reduced RC circuit with two nodes shown in Figure 4.2 to the infinitely long RC circuit as shown in Figure 2.2. We will then verify if the expression of the optimized $\alpha^{[2]*}$ for the RC circuit with two nodes given by (4.20) is the same for the optimized α^* for the infinitely long RC circuit.

For the reduced RC circuit, the value of h is given by $h = \lambda_2(\omega)$ for some $\omega_{\min} \le \omega \le \omega_{\max}$. Remark 4.1.2 states that for the particular choice of $h = \lambda_2$, we have $\Gamma^{[2]}(\omega, \lambda_2, \alpha, \beta) = \rho_0(\omega, \alpha, \beta)$, where $\Gamma^{[2]}$ and ρ_0 are the convergence factor of OWR applied to the RC circuit of two nodes and infinitely long RC circuit respectively. But h is fixed and we cannot vary it with ω. Moreover for the nonoverlapping OWR applied to the RC circuit, we proved that the optimized α^* is found by equating the modulus of the convergence factor at $\omega_{\min}$ and $\omega_{\max}$. This reduces the choice of range of h and we can choose either $h = \lambda_2(\omega_{\min})$ or $h = \lambda_2(\omega_{\max})$. But for $\omega = \omega_{\max}$,

equation (4.22) proves that $\Gamma^{[2]}(\omega_{\max}, h, \alpha) = \frac{1}{\alpha+1}$, that is, the convergence factor is independent of h and ω. This allows us to choose $h = \lambda_2(\omega_{\min})$.

With this choice of h, we find an expression for the optimized α^* for the infinitely long RC circuits.

4.1.3.1 Asymptotics with respect to time $T \to \infty$

In Section 2.4.1 of Chapter 2, we proved that for the nonoverlapping OWR, the optimized $\alpha^*_{T,0}$ is given by (2.30), that is, $\alpha^*_{T,0} = \left(\frac{2}{a}\right)^{1/4} \omega_{\min}^{1/4}$, where $\omega_{\min} = \frac{\pi}{T}$. In this section, we will see that we can arrive at the same expression for the optimized α^* using Theorem 4.1.3.

When we use asymptotics with respect to large time, we consider $b = -2a$ and $\xi = \omega_{\min} \to 0$. Under this condition, we proceed in the same manner as in the proof of Lemma 2.4.3 to arrive at $\lambda_2(\omega_{\min}) = 1 - \frac{z_1}{2a} + i\frac{\xi - z_2}{2a}$, where $z_1 + iz_2 := \sqrt{-\xi^2 + 4\xi a i}$. Using the asymptotic expressions for z_1 and z_2 derived in the proof of Lemma 2.4.3, we get

$$h = \lambda_2(\omega_{\min}) = \left(1 - \frac{\sqrt{2}\sqrt{\xi}}{2\sqrt{a}} + \frac{\sqrt{2}\xi^{3/2}}{16a^{3/2}}\right) + i\left(-\frac{\sqrt{2}\sqrt{\xi}}{2\sqrt{a}} + \frac{\xi}{2a} - \frac{\sqrt{2}\xi^{3/2}}{16a^{3/2}}\right) + \mathcal{O}(\xi^{5/2}),$$

and thus separating real and imaginary parts of $h = h_1 + ih_2$ leads to

$$h_1 = 1 - \frac{\sqrt{2}\sqrt{\xi}}{2\sqrt{a}} + \mathcal{O}(\xi^{3/2}), \quad \text{and} \quad h_2 = -\frac{\sqrt{2}\sqrt{\xi}}{2\sqrt{a}} + \frac{\xi}{2a} + \mathcal{O}(\xi^{3/2}).$$

Further, we had defined $c^2 = -\frac{b}{2a}$ and since $b = -2a$, we have $c^2 = 1$ and

$$d = 2c^2 - h_1 = 2 - \left(1 - \frac{\sqrt{\xi}}{\sqrt{2}\sqrt{a}} + \mathcal{O}(\xi^{3/2})\right) = 1 + \frac{\sqrt{\xi}}{\sqrt{2}\sqrt{a}} + \mathcal{O}(\xi^{3/2}).$$

Now

$$\begin{aligned}\sqrt{d^2 - 1} &= \sqrt{\left(1 + \frac{\sqrt{\xi}}{\sqrt{2}\sqrt{a}} + \mathcal{O}(\xi^{3/2})\right)^2 - 1} = \sqrt{1 + \frac{\sqrt{2}\sqrt{\xi}}{\sqrt{a}} + \mathcal{O}(\xi) - 1} \\ &= \left(\frac{2}{a}\right)^{1/4} \xi^{1/4} + \mathcal{O}(\xi^{1/2}).\end{aligned}$$

Substituting the expansions for d and $\sqrt{d^2 - 1}$ into the expression for the optimized $\alpha^{[2]*}$ for the reduced RC circuit (4.20), we arrive at

$$\begin{aligned}\alpha^{[2]*} &= d + \sqrt{d^2 - 1} = \left(\frac{2}{a}\right)^{1/4} \xi^{1/4} + \mathcal{O}(\xi^{1/2}), \\ &= \left(\frac{2}{a}\right)^{1/4} \omega_{\min}^{1/4} + \mathcal{O}(\omega_{\min}^{1/2}),\end{aligned}$$

which is the same expression for the optimized $\alpha^*_{T,0}$ given in Theorem 2.4.1 for the infinitely long RC circuit.

4.1.3.2 Asymptotics with respect to $\epsilon \to 0$

In Section 2.4.2 of Chapter 2, we proved that for the nonoverlapping OWR, the optimized α^* is given by (2.49), that is, $\alpha^*_{R,0} = \sqrt{2}\epsilon^{1/4}$, where $b = -(2+\epsilon)a$. In this section, we will see that we can arrive at the same expression for the optimized α^* using Theorem 4.1.3.

We used asymptotics with respect to the reaction term $\epsilon \to 0$, where $b = -(2+\epsilon)a$ and considered $\omega_{\min} = 0$. Under these conditions,

$$\begin{aligned} h &= \lambda_2(0) = \frac{-b - \sqrt{b^2 - 4a^2}}{2a} = \frac{(2+\epsilon)a - \sqrt{\epsilon^2 a^2 + 4\epsilon a^2}}{2a} = \frac{2 + \epsilon - 2\sqrt{\epsilon}\sqrt{1+\frac{\epsilon}{4}}}{2} \\ &= \frac{2 + \epsilon - 2\sqrt{\epsilon}\left(1 + \frac{\epsilon}{8} + \mathcal{O}(\epsilon^2)\right)}{2} = 1 - \sqrt{\epsilon} + \frac{\epsilon}{2} + \mathcal{O}(\epsilon^{3/2}). \end{aligned}$$

Since h in general is complex with $h = h_1 + ih_2$, we have $h_1 = 1 - \sqrt{\epsilon} + \frac{\epsilon}{2} + \mathcal{O}(\epsilon^{3/2})$. Now, we had defined $c^2 = -\frac{b}{2a}$ and since $b = -(2+\epsilon)a$, we have $c^2 = 1 + \frac{\epsilon}{2}$. This simplifies d to

$$d = 2c^2 - h_1 = 2 + \epsilon - \left(1 - \sqrt{\epsilon} + \frac{\epsilon}{2} + \mathcal{O}(\epsilon^{3/2})\right) = 1 + \sqrt{\epsilon} - \frac{\epsilon}{2} + \mathcal{O}(\epsilon^{3/2}),$$

and therefore,

$$\sqrt{d^2 - 1} = \sqrt{\left(1 + \sqrt{\epsilon} - \frac{\epsilon}{2} + \mathcal{O}(\epsilon^{3/2})\right)^2 - 1} = \sqrt{2\sqrt{\epsilon} + \mathcal{O}(\epsilon)} = \sqrt{2}\epsilon^{1/4} + \mathcal{O}(\epsilon^{1/2}).$$

Substituting the expansions for d and $\sqrt{d^2-1}$ into the expression for the optimized $\alpha^{[2]*}$ for the reduced RC circuit (4.20), we arrive at

$$\alpha^{[2]*} = d + \sqrt{d^2 - 1} = \sqrt{2}\epsilon^{1/4} + \mathcal{O}(\epsilon^{1/2}) = \alpha^*_{R,0},$$

which is the same expression for the optimized $\alpha^*_{R,0}$ given in Theorem 2.4.3 for the infinitely long RC circuit.

We thus conclude that in order to find the optimized $\alpha^*_{T,0}$ and $\alpha^*_{R,0}$ for the nonoverlapping WR method applied to the infinitely long RC circuit, we can first reduce it to a smaller equivalent RC circuit with two nodes and then use the expression for $\alpha^{[2]*}$ given by (4.20). Further, we could not prove in Chapter 2 that the solution of the min-max problem (2.25) obtained by equioscillation is unique. But using the technique of reducing the large circuit into a smaller circuit, we could prove the uniqueness of the solution obtained by equioscillation.

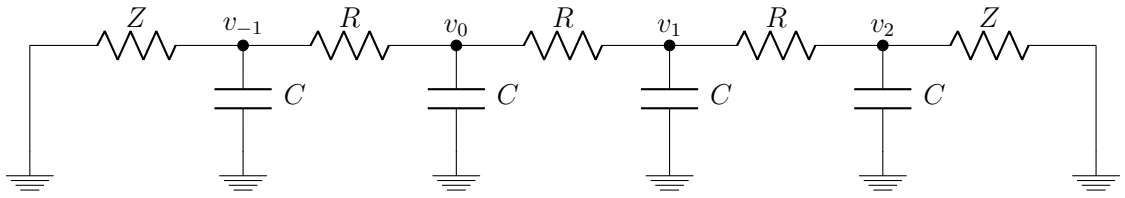

Figure 4.7: Reduced RC Circuit with four nodes and impedance $Z = R/(1-h)$.

4.2 RC circuit with four nodes

In this section, we do a similar but quite more complicated analysis for the reduction of the infinitely long RC circuit (as shown in Figure 2.2) into a smaller RC circuit with four nodes (see Figure 4.7). The process of reduction to the smaller circuit is the same as discussed in Section 4.1, and we arrive at the smaller system of equations

$$s\begin{bmatrix}\hat{u}_{-1}\\ \hat{u}_0\\ \hat{u}_1\\ \hat{u}_2\end{bmatrix}^{k+1} = \begin{bmatrix} b+ah & a & & \\ a & b & a & \\ & a & b & a \\ & & a & b+ah\end{bmatrix}\begin{bmatrix}\hat{u}_{-1}\\ \hat{u}_0\\ \hat{u}_1\\ \hat{u}_2\end{bmatrix}^{k+1}, \tag{4.23}$$

where $a > 0$, $-b \geq 2a$ and

$$h = \lambda_2(s) = \frac{s-b-\sqrt{(s-b)^2-4a^2}}{2a}, \quad \text{with} \quad s \in \mathbb{C}^+.$$

4.2.1 Classical Waveform Relaxation Method

When the nonoverlapping classical WR algorithm is applied to an RC Circuit with four nodes, the system of equations (4.23) is split into two equal subsystems at node 0;

$$\begin{aligned} s\begin{bmatrix}\hat{u}_{-1}\\ \hat{u}_0\end{bmatrix}^{k+1} &= \begin{bmatrix} b+ah & a \\ a & b\end{bmatrix}\begin{bmatrix}\hat{u}_{-1}\\ \hat{u}_0\end{bmatrix}^{k+1} + \begin{bmatrix}0\\ a\hat{u}_1^{k+1}\end{bmatrix}, \\ s\begin{bmatrix}\hat{w}_1\\ \hat{w}_2\end{bmatrix}^{k+1} &= \begin{bmatrix} b & a \\ a & b+ah\end{bmatrix}\begin{bmatrix}\hat{w}_1\\ \hat{w}_2\end{bmatrix}^{k+1} + \begin{bmatrix}a\hat{w}_0^{k+1}\\ 0\end{bmatrix}, \end{aligned} \tag{4.24}$$

with the classical transmission conditions given by

$$\hat{u}_1^{k+1} = \hat{w}_1^k, \quad \text{and} \quad \hat{w}_0^{k+1} = \hat{u}_0^k. \tag{4.25}$$

We now find the expression for the convergence factor of this WR method.

Theorem 4.2.1. *For the reduced RC circuit with four nodes, the convergence factor of the nonoverlapping waveform relaxation method is given by*

$$\Gamma_{cla}^{[4]}(s,h) := \frac{1}{\psi^2} = \left(\frac{a(s-b-ah)}{(s-b)(s-b-ah)-a^2}\right)^2, \tag{4.26}$$

where

$$\psi := \left(\frac{(s-b)(s-b-ah) - a^2}{a(s-b-ah)} \right). \tag{4.27}$$

Proof. We solve the coupled equations (4.24) using the transmission conditions (4.25). Solving the first subsystem $\hat{\mathbf{u}}$ for $\hat{u}_{-1}$ and $\hat{u}_0$ leads to

$$\hat{u}_{-1}^{k+1} = \left(\frac{a}{s-b-ah} \right) \hat{u}_0^{k+1}, \quad \text{and} \quad (s-b)\hat{u}_0^{k+1} = a\hat{u}_{-1}^{k+1} + a\hat{u}_1^{k+1}.$$

Substituting the first equation into the second simplifies it to

$$\begin{aligned}
(s-b)\hat{u}_0^{k+1} &= \frac{a^2}{(s-b-ah)}\hat{u}_0^{k+1} + a\hat{u}_1^{k+1} \\
\implies \left((s-b) - \frac{a^2}{s-b-ah} \right) \hat{u}_0^{k+1} &= a\hat{u}_1^{k+1} \\
\implies \hat{u}_0^{k+1} &= \left(\frac{a(s-b-ah)}{(s-b)(s-b-ah) - a^2} \right) \hat{u}_1^{k+1} \\
\implies \hat{u}_0^{k+1} &= \frac{1}{\psi}\hat{u}_1^{k+1} = \frac{1}{\psi}\hat{w}_1^{k}.
\end{aligned} \tag{4.28}$$

Similarly, from the second sub-system for $\hat{\mathbf{w}}$, we have

$$\hat{w}_1^{k+1} = \left(\frac{a(s-b-ah)}{(s-b)(s-b-ah) - a^2} \right) \hat{w}_0^{k+1} = \frac{1}{\psi}\hat{w}_0^{k+1} = \frac{1}{\psi}\hat{u}_0^{k}. \tag{4.29}$$

Combining equations (4.28) and (4.29) results in $\hat{\mathbf{u}}^{k+1} = \Gamma_{cla}^{[4]}(s,h)\hat{\mathbf{u}}^{k-1}$ and $\hat{\mathbf{w}}^{k+1} = \Gamma_{cla}^{[4]}(s,h)\hat{\mathbf{w}}^{k-1}$, and this completes the proof. □

Remark 4.2.1. For the special choice of $h = \lambda_2(s)$, using the properties of λ_1 and λ_2 defined in Lemma 2.2.2, the convergence factor $\Gamma_{cla}^{[4]}$ reduces to $\rho_{0,cla}(s)$, where $\rho_{0,cla}(s)$ is the convergence factor (2.11) for the nonoverlapping WR method applied to the infinitely long RC circuit. To prove this, we first simplify the expression of ψ given by (4.27). For $h = \lambda_2$,

$$\begin{aligned}
\psi &= \left(\frac{(s-b)(s-b-a\lambda_2) - a^2}{a(s-b-a\lambda_2)} \right) = \left(\frac{\left(\frac{s-b}{a}\right)\left(\frac{s-b}{a} - \lambda_2\right) - 1}{\frac{s-b}{a} - \lambda_2} \right) \\
&= \left(\frac{(\lambda_1+\lambda_2)(\lambda_1+\lambda_2-\lambda_2) - 1}{\lambda_1+\lambda_2-\lambda_2} \right) = \left(\frac{(\lambda_1+\lambda_2)(\lambda_1) - 1}{\lambda_1} \right) \\
&= \left(\frac{\lambda_1^2 + 1 - 1}{\lambda_1} \right) = \lambda_1.
\end{aligned} \tag{4.30}$$

The convergence factor thus reduces to $\Gamma_{cla}^{[4]}(s,\lambda_2(s)) = \frac{1}{\psi^2} = \frac{1}{\lambda_1^2} = \rho_{0,cla}(s)$. We would thus like to choose h such that analyzing the convergence factor $\Gamma_{cla}^{[4]}$ will be sufficient to understand the convergence behavior of the infinitely long RC circuit.

4.2.2 Optimized Waveform Relaxation Method

We now deal with the usual problem of the classical WR methods, that is, the slow convergence when a large time interval is used. To improve its convergence, we use the same optimized transmission conditions (2.16) defined in Section 2.3,

$$\begin{aligned}(u_1^{k+1} - u_0^{k+1}) + \alpha u_1^{k+1} &= (w_1^k - w_0^k) + \alpha w_1^k,\\ (w_1^{k+1} - w_0^{k+1}) + \beta w_0^{k+1} &= (u_1^k - u_0^k) + \beta u_0^k,\end{aligned} \tag{4.31}$$

with α, $\beta \in \mathbb{R}$. These transmission conditions can be rewritten as

$$\begin{aligned}u_1^{k+1} &= \tfrac{u_0^{k+1}}{1+\alpha} + w_1^k - \tfrac{w_0^k}{1+\alpha},\\ w_0^{k+1} &= -\tfrac{w_1^{k+1}}{\beta-1} + \tfrac{u_1^k}{\beta-1} + u_0^k.\end{aligned} \tag{4.32}$$

These transmission conditions are same as the one considered by Khaleel et al [2], where the analysis was carried for the application of OWR to an RC circuit of length four.

Theorem 4.2.2. *The convergence factor of the nonoverlapping OWR method for the reduced RC circuit with four nodes is given by*

$$\Gamma^{[4]}(s,h,\alpha,\beta) := \left(\frac{\alpha+1-\psi}{(\alpha+1)\psi-1}\right)\left(\frac{\beta-1+\psi}{(\beta-1)\psi+1}\right). \tag{4.33}$$

Proof. We solve the two subsystems (4.24) with these new transmission conditions (4.31). We go back to the proof of Theorem 4.2.1, and substitute the Laplace transformed transmission conditions (4.32) into equation (4.28) to obtain

$$\hat{u}_0^{k+1} = \frac{1}{\psi}\hat{u}_1^{k+1} = \frac{1}{\psi}\left(\frac{\hat{u}_0^{k+1}}{1+\alpha} + \hat{w}_1^k - \frac{\hat{w}_0^k}{1+\alpha}\right).$$

From (4.29), we have $\hat{w}_1^{k+1} = \frac{1}{\psi}\hat{w}_0^{k+1}$. Substituting this into the above equation simplifies it to

$$\begin{aligned}&\left(1 - \frac{1}{(\alpha+1)\psi}\right)\hat{u}_0^{k+1} = \left(\frac{1}{\psi} - \frac{1}{1+\alpha}\right)\hat{w}_1^k\\ \Longrightarrow\ &\left(\frac{\psi(\alpha+1)-1}{\psi(\alpha+1)}\right)\hat{u}_0^{k+1} = \left(\frac{\alpha+1-\psi}{\psi(1+\alpha)}\right)\hat{w}_1^k\\ \Longrightarrow\ &\hat{u}_0^{k+1} = \left(\frac{\alpha+1-\psi}{\psi(1+\alpha)-1}\right)\hat{w}_1^k.\end{aligned} \tag{4.34}$$

Similarly, from the other subsystem for $\hat{\mathbf{w}}$, we obtain

$$\hat{w}_1^{k+1} = \left(\frac{\beta-1+\psi}{\psi(\beta-1)+1}\right)\hat{u}_0^k. \tag{4.35}$$

Combining relations (4.34)-(4.35) yields

$$\begin{aligned} \hat{u}_j^{k+1} &= \Gamma^{[4]}\hat{u}_j^{k-1}, \quad \text{for} \quad j=-1,0, \\ \hat{w}_j^{k+1} &= \Gamma^{[4]}\hat{w}_j^{k-1}, \quad \text{for} \quad j=1,2, \end{aligned}$$

where $\Gamma^{[4]}$ is given by (4.33). This completes the proof. □

Remark 4.2.2. We showed in Remark 4.2.1 that with the special choice of $h=\lambda_2$, the convergence factor $\Gamma_{cla}^{[4]}$ of the WR applied to the reduced RC circuit with four nodes is equal to the convergence factor $\rho_{0,cla}$ of the nonoverlapping WR method when applied to the infinitely long RC circuit. From (4.30), under the condition $h=\lambda_2$, we have $\psi=\lambda_1$, and hence

$$\begin{aligned} \Gamma^{[4]}(s,\lambda_2,\alpha,\beta) &= \left(\frac{\alpha+1-\psi}{(\alpha+1)\psi-1}\right)\left(\frac{\beta-1+\psi}{(\beta-1)\psi+1}\right) = \left(\frac{\alpha+1-\lambda_1}{(\alpha+1)\lambda_1-1}\right)\left(\frac{\beta-1+\lambda_1}{(\beta-1)\lambda_1+1}\right) \\ &= \rho_0(s,\alpha,\beta), \end{aligned}$$

where $\rho_0(s,\alpha,\beta)$ is the convergence factor of the non-overlapping OWR when applied to an infinitely long RC circuit and is given by (2.20).

Remark 4.2.3. For $h=0$, the convergence factor $\Gamma^{[4]}$ reduces to the convergence factor of OWR applied to RC circuit with exactly four nodes. This case has been considered in [2].

For a particular choice of h, we would now like to choose α and β such that the modulus of the convergence factor $\left|\Gamma^{[4]}\right|$ is as small as possible.

4.2.3 Optimization

We observed in Section 2.4 that the best choice of α and β comes by solving a min-max problem. For the reduced RC circuit with four nodes we need to solve for a fixed h with $|h|<1$,

$$\min_{\alpha,\beta\in\mathbb{R}}\left(\max_{\Re(s)\geq 0}\left|\Gamma^{[4]}(s,h,\alpha,\beta)\right|\right). \tag{4.36}$$

Assumption 4.2.1. The analysis is too complicated when h is complex. Hence in this section, we assume $h\in\mathbb{R}$ with $h\in(0,1)$, that is, $h_1=h$ and $h_2=0$, where $h=h_1+ih_2$.

We simplify this problem using the following lemmas.

Lemma 4.2.1. *For $h\in(0,1)$, with $a>0$, and $b<0$ such that $-b\geq 2a$, the function ψ satisfies $|\psi|>1$ in the right half of the complex plane, that is, for $s=\sigma+i\omega$, with $\sigma\geq 0$.*

Proof. We first separate the real and imaginary part of ψ, which is expressed by (4.27). For $s = \sigma + i\omega$ with $\sigma \geq 0$

$$\begin{aligned}\psi &= \left(\frac{(s-b)(s-b-ah)-a^2}{a(s-b-ah)}\right) = \frac{s-b}{a} - \frac{a^2}{a(s-b-ah)} \\ &= \frac{\sigma+i\omega-b}{a} - \frac{a}{\sigma+i\omega-b-ah}.\end{aligned}$$

Let us define $2c^2 := \frac{-b}{a}$, $d := 2c^2 - h$, $\sigma_1 := \frac{\sigma}{a}$ and $z := \frac{\omega}{a}$. Since $-b \geq 2a$, and $0 < h < 1$, we have $c^2 \geq 1$ and $d > 1$. The above expression thus reduces to

$$\begin{aligned}\psi &= \sigma_1 + iz + 2c^2 - \frac{1}{\sigma_1+d+iz} = \sigma_1 + iz + 2c^2 - \frac{\sigma_1+d-iz}{(\sigma_1+d)^2+z^2} \\ &= \left(\sigma_1 + 2c^2 - \frac{\sigma_1+d}{z^2+(\sigma_1+d)^2}\right) + iz\left(1 + \frac{1}{(\sigma_1+d)^2+z^2}\right) \\ &= x + iy,\end{aligned} \tag{4.37}$$

where $x := \left(\sigma_1 + 2c^2 - \frac{\sigma_1+d}{z^2+(\sigma_1+d)^2}\right)$ and $y := z\left(1 + \frac{1}{(\sigma_1+d)^2+z^2}\right)$. Since σ_1, $d > 0$, we have $\frac{\sigma_1+d}{(\sigma_1+d)^2+z^2} < 1$. Further, $c^2 \geq 1$ and hence $x > 1$, that is, $\Re(\psi) > 1$, which implies $|\psi| > 1$. □

Lemma 4.2.2. *Let $h \in (0,1)$, $\beta < 0 < \alpha$, $a > 0$, and $b < 0$ such that $-b \geq 2a$. Then the convergence factor $\Gamma^{[4]}(s,h,\alpha,\beta)$ is analytic in the right half of the complex plane and the maximum of $\left|\Gamma^{[4]}(s,h,\alpha,\beta)\right|$ lies on the non negative imaginary axis, that is, $s = i\omega$, where $\omega \geq 0$.*

Proof. Since $|\psi| > 1$, we use similar arguments used in the proof of Lemma 2.4.1 to show that $\Gamma^{[4]}$ is analytic in the right half of the complex plane. Further, for $s = i\omega$, with $-\infty < \omega < \infty$, we show that $|\psi(\omega)|$ is even with respect to ω. From (4.37) with $\sigma_1 = 0$,

$$\begin{aligned}|\psi(-\omega)| &= \left|\left(2c^2 - \frac{d}{(-z)^2+d^2}\right) - iz\left(1 + \frac{1}{d^2+(-z)^2}\right)\right| \\ &= \left(\left(2c^2 - \frac{d}{(-z)^2+d^2}\right)^2 + z^2\left(1 + \frac{1}{d^2+(-z)^2}\right)^2\right)^{1/2} \\ &= \left|\left(2c^2 - \frac{d}{z^2+d^2}\right) + iz\left(1 + \frac{1}{d^2+z^2}\right)\right| = |\psi(\omega)|.\end{aligned}$$

Now we use exactly the same steps as we used in the proof of Lemma 2.4.2 to show that $\left|\Gamma^{[4]}(-\omega,h,\alpha,\beta)\right| = \left|\Gamma^{[4]}(\omega,h,\alpha,\beta)\right|$ and this completes the proof. □

Finally, we assume that $\beta = -\alpha$ to simplify our problem (4.36). This choice of β again comes from the fact that the optimal α and β are given by $\alpha_{opt} := \psi - 1$ and

$\beta_{opt} := 1 - \psi$. Thus our min-max problem (4.36) reduces for fixed $h \in (0,1)$ to,

$$\min_{\alpha>0} \left(\max_{0\leq\omega<\infty} \left| \Gamma^{[4]}(\omega, h, \alpha) \right| \right). \tag{4.38}$$

From (4.27), we observe that ψ is a complicated function of ω. We therefore first express ψ in a simplified form which will make the analysis feasible. From the definition of ψ in (4.27), for $s = i\omega$ with $\omega \in [0, \infty)$,

$$\psi = \left(\frac{(i\omega - b)(i\omega - b - ah) - a^2}{a(i\omega - b - ah)} \right) = \frac{-b}{a} + \frac{1}{a}\left(x + iy\right), \tag{4.39}$$

where

$$\begin{aligned} x + iy &= i\omega - \frac{a^2}{i\omega - (b+ah)} = i\omega - \frac{a^2(i\omega + (b+ah))}{(i\omega - (b+ah))(i\omega + (b+ah))} \\ &= i\omega + \frac{a^2(i\omega + (b+ah))}{\omega^2 + (b+ah)^2} = \left(\frac{a^2(b+ah)}{\omega^2 + (b+ah)^2} \right) + i\omega \left(1 + \frac{a^2}{\omega^2 + (b+ah)^2} \right). \end{aligned}$$

Thus we have

$$x = \frac{a^2(b+ah)}{\omega^2 + (b+ah)^2}, \quad \text{and} \quad y = \omega \left(1 + \frac{a^2}{\omega^2 + (b+ah)^2} \right). \tag{4.40}$$

We now express y^2 in terms of x by eliminating its dependence on ω. The expression of x can be rewritten as $\frac{x}{b+ah} = \frac{a^2}{\omega^2 + (b+ah)^2}$ and hence, $\omega^2 = \frac{a^2(b+ah)}{x} - (b+ah)^2$. Squaring the expression for y leads to

$$\begin{aligned} y^2 &= \omega^2 \left(1 + \frac{a^2}{\omega^2 + (b+ah)^2} \right)^2 = \left(\frac{a^2(b+ah)}{x} - (b+ah)^2 \right) \left(1 + \frac{x}{b+ah} \right)^2 \\ &= \left(\frac{a^2}{x} - (b+ah) \right) \left(\frac{(b+ah+x)^2}{b+ah} \right) \\ &= \frac{\left(a^2 - x(b+ah)\right)(b+ah+x)^2}{x(b+ah)}. \end{aligned} \tag{4.41}$$

We now approximate the optimal α_{opt} by a constant. From (4.39),

$$\alpha_{opt} := \psi - 1 = -\frac{b}{a} + \frac{p}{a} - 1, \tag{4.42}$$

where $p \in \mathbb{R}$ is the constant approximation for $p := x + iy$ defined in (4.40). Substi-

tuting the expressions for x and y from (4.40) in the convergence factor $\Gamma^{[4]}$ gives

$$\begin{aligned}
|\Gamma^{[4]}(x,h,p)| &= \left|\left(\frac{\alpha+1-\psi}{(\alpha+1)\psi-1}\right)^2\right| = \left|\frac{\left(\frac{p-b}{a}+\frac{b}{a}-\frac{x}{a}-i\frac{y}{a}\right)^2}{\left(\left(\frac{p-b}{a}\right)\left(\frac{x-b}{a}+i\frac{y}{a}\right)-1\right)^2}\right| \\
&= \frac{a^2\left((p-x)^2+y^2\right)}{\left((p-b)(x-b)-a^2\right)^2+y^2(p-b)^2} \\
&= \frac{a^2\left((p-x)^2+\left(\frac{(a^2-x(b+ah))(b+ah+x)^2}{x(b+ah)}\right)\right)}{\left((p-b)(x-b)-a^2\right)^2+\left(\frac{(a^2-x(b+ah))(b+ah+x)^2}{x(b+ah)}\right)(p-b)^2} \\
&= \frac{a^2(x(x-p)^2(b+ah)+(x+b+ah)^2(a^2-x(b+ah))}{x(b+ah)((p-b)(x-b)-a^2)^2+(x+b+ah)^2(p-b)^2(a^2-x(b+ah))}.
\end{aligned}$$

Since $-b \geq 2a$, we assume $2c^2 := -\frac{b}{a}$ with $c^2 \geq 1$. We divide both numerator and denominator by a^6 to get

$$R(c,h,\tilde{x},\tilde{p}) := \left|\Gamma^{[4]}(x,h,p)\right| = \frac{\tilde{a}_2\tilde{x}^2+\tilde{a}_1\tilde{x}+\tilde{a}_0}{\tilde{b}_2\tilde{x}^2+\tilde{b}_1\tilde{x}+\tilde{b}_0}, \tag{4.43}$$

where

$$\begin{aligned}
&\tilde{x} := \tfrac{x}{a}, \\
&\tilde{p} := \tfrac{p}{a}, \\
&\tilde{a}_2 := 1-2h^2-2h\left(-4c^2+\tilde{p}\right)+4c^2\left(\tilde{p}-2c^2\right), \\
&\tilde{a}_1 := \left(4c^4-4c^2h+h^2-\tilde{p}^2-2\right)\left(2c^2-h\right), \\
&\tilde{a}_0 := \left(h-2c^2\right)^2, \\
&\tilde{b}_2 := -\left(2c^2+\tilde{p}\right)\left(32c^6-24c^4h+16c^4\tilde{p}+4c^2h^2-12c^2h\tilde{p}+2h^2\tilde{p}-6c^2+2h-\tilde{p}\right), \\
&\tilde{b}_1 := \left(16c^6h-4c^4h^2+16c^4h\tilde{p}-4c^2h^2\tilde{p}+4c^2h\tilde{p}^2-h^2\tilde{p}^2+4c^2\tilde{p}+2\tilde{p}^2+1\right)\left(h-2c^2\right) \\
&\tilde{b}_0 := \left(2c^2+p\right)^2\left(h-2c^2\right)^2.
\end{aligned}$$

Since $\omega \in [0,\infty)$, the expression for $x = \frac{a^2(b+ah)}{\omega^2+(b+ah)^2}$ produces $x \in \left[\frac{a^2}{b+ah},0\right)$, which implies $\tilde{x} \in \left[\frac{-1}{2c^2-h},0\right)$. Finally, $\alpha > 0$ and since $\alpha = -2c^2+\tilde{p}-1$, we have $\tilde{p} > 1-2c^2$ and hence our min-max problem (4.38) further reduces to, find for fixed $h \in (0,1)$, and $c^2 \geq 1$,

$$\min_{\tilde{p}>1-2c^2}\left(\max_{\frac{-1}{2c^2-h}\leq\tilde{x}<0} R(c,h,\tilde{x},\tilde{p})\right), \tag{4.44}$$

where $R(c,h,\tilde{x},\tilde{p})$ is defined in (4.43).

Lemma 4.2.3. *For $0<h<1$ and $c^2 \geq 1$, the polynomial L defined by*

$$\begin{aligned}
L(c,h,\tilde{p}) := &\left(16c^4-12c^2h+2h^2-1\right)\tilde{p}^2+\left(16c^4h-12c^2h^2+2h^3+4c^2-2h\right)\tilde{p} \\
&+\left(-64c^8+80c^6h-32c^4h^2+4c^2h^3+28c^4-16c^2h+2h^2-1\right)
\end{aligned}$$

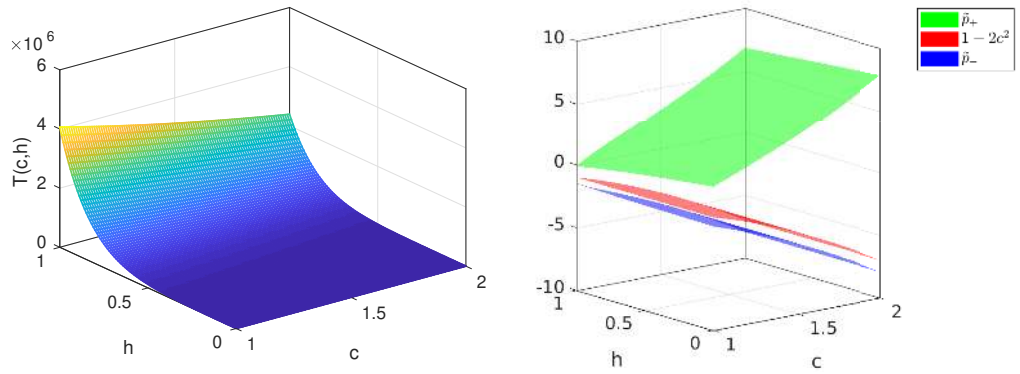

Figure 4.8: The polynomial $T(c,h) > 0$ on (left) and inequality $\tilde{p}_- < 1 - 2c^2 < \tilde{p}_+$ on (right) for all $0 < h < 1$ and $1 \leq c < 2$.

has two roots

$$\tilde{p}_- := \frac{-8c^4h + 6c^2h^2 - h^3 - 2c^2 + h - \sqrt{T(c,h)}}{16c^4 - 12c^2h + 2h^2 - 1}, \tag{4.45}$$

$$\tilde{p}_+ := \frac{-8c^4h + 6c^2h^2 - h^3 - 2c^2 + h + \sqrt{T(c,h)}}{16c^4 - 12c^2h + 2h^2 - 1}, \tag{4.46}$$

with

$$T(c,h) = 1024c^{12} - 2048c^{10}h + \left(1664h^2 - 512\right)c^8 + \left(-704h^3 + 704h\right)c^6 + \left(164h^4 - 352h^2 + 48\right)c^4 + \left(-20h^5 + 76h^3 - 32h\right)c^2 + \left(h^6 - 6h^4 + 5h^2 - 1\right).$$

Moreover, $\tilde{p}_- < 1 - 2c^2 < \tilde{p}_+$, *and*

$$L(c,h,\tilde{p}) = \begin{Bmatrix} > 0, & \text{for } \tilde{p} > \tilde{p}_+ \\ < 0, & \text{for } 1 - 2\,c^2 < \tilde{p} < \tilde{p}_+ \end{Bmatrix}.$$

Proof. Since the polynomial L is quadratic, one can easily check that its roots $\tilde{p}_-$ and $\tilde{p}_+$ are given by (4.45) and (4.46) respectively. For $c^2 \geq 1$, and $h \in (0,1)$, the polynomial $T(c,h)$ is always positive (see the left plot of Figure 4.8). Also, we see numerically $\tilde{p}_- < 1 - 2c^2$ and $\tilde{p}_+ > 1 - 2c^2$ (see the right plot of Figure 4.8). Let $A(c,h) = 16c^4 - 12c^2h + 2h^2 - 1$. The roots of $A(c,h)$ with respect to c^2 are $c^2_\pm(h) := \frac{3h \pm \sqrt{h^2+4}}{8}$. Since $h \in (0,1)$, $8 - 3h > 0$, and hence

$$\begin{aligned} c^2_\pm(h) = \frac{3h \pm \sqrt{h^2+4}}{8} < 1 \quad &\Longleftrightarrow \quad 3h \pm \sqrt{h^2+4} < 8 \\ &\Longleftrightarrow \quad h^2 + 4 < (8 - 3h)^2 = 9h^2 - 48h + 64 \\ &\Longleftrightarrow \quad 0 < 2h^2 - 12h + 15. \end{aligned}$$

The last inequality holds since $h \in (0,1)$. This shows that both real roots of $A(c,h)$ are less than 1 for $h \in (0,1)$. The coefficient of c^4 is positive and therefore $A(c,h) > 0$ for all $c^2 > 1$ and $h \in (0,1)$. Thus we proved that the coefficient of $\tilde{p}$ in the polynomial $L(c,h,\tilde{p})$ is always greater than zero, and hence $L(c,h,\tilde{p})$ is positive for large values of $|\tilde{p}|$, that is, $L(c,h,\tilde{p}) \to \infty$ as $\tilde{p} \to \pm\infty$. Since L is continuous, it should cut the x axis twice, at $\tilde{p} = \tilde{p}_-$ and $\tilde{p} = \tilde{p}_+$. Finally, since $\tilde{p}_- < \tilde{p}_+$, we can conclude that $L(c,h,\tilde{p}) > 0$ for $(\infty, \tilde{p}_-) \cup (\tilde{p}_+, \infty)$ and $L(c,h,\tilde{p}) \le 0$ for $\tilde{p} \in [\tilde{p}_-, \tilde{p}_+]$. □

Lemma 4.2.4. *For $\tilde{p} > 1 - 2c^2$, with $c^2 \ge 1$ and $h \in (0,1)$, the polynomial*

$$\begin{aligned} d(c,h,\tilde{p}) := &\left(-16c^4 + 12c^2h - 2h^2 + 1\right)\tilde{p}^4 + \left(-16c^4h + 12c^2h^2 - 2h^3 - 4c^2 + 2h\right)\tilde{p}^3 \\ &+ \left(128c^8 - 128c^6h + 40c^4h^2 - 4c^2h^3 - 32c^4 + 12c^2h + 2\right)\tilde{p}^2 \\ &+ \left(64c^8h - 48c^6h^2 + 8c^4h^3 + 80c^6 - 88c^4h + 28c^2h^2 - 2h^3 - 4c^2 + 2h\right)\tilde{p} \\ &- 256c^{12} + 320c^{10}h - 128c^8h^2 + 16c^6h^3 + 240c^8 - 208c^6h + 56c^4h^2 \\ &- 4c^2h^3 - 32c^4 + 16c^2h - 2h^2 + 1 \end{aligned}$$

has only two real roots, say $\tilde{p}_1$ and $\tilde{p}_2$, with $1 - 2c^2 < \tilde{p}_1 < \tilde{p}_2$. Moreover $\tilde{p}_2 > 0$ and d satisfies the inequalities

$$d(c,h,\tilde{p}) = \begin{cases} < 0, & \text{for } \tilde{p} \in (1 - 2\,c^2, \tilde{p}_1) \cup (\tilde{p}_2, \infty), \\ > 0, & \text{for } \tilde{p} \in (\tilde{p}_1, \tilde{p}_2) \end{cases}.$$

Proof. In the previous Lemma 4.2.3, we observed that the coefficient of $\tilde{p}^4$ in the polynomial d is negative and hence $d(c,h,\tilde{p})$ is negative for large values of $|\tilde{p}|$. Taking a derivative of $d(c,h,\tilde{p})$ with respect to $\tilde{p}$ leads to

$$\begin{aligned} \frac{\partial d(c,h,\tilde{p})}{\partial \tilde{p}} =& 4\left(-16c^4 + 12c^2h - 2h^2 + 1\right)\tilde{p}^3 + 3\left(-16c^4h + 12c^2h^2 - 2h^3 - 4c^2 + 2h\right)\tilde{p}^2 \\ &+ 2\left(128c^8 - 128c^6h + 40c^4h^2 - 4c^2h^3 - 32c^4 + 12c^2h + 2\right)\tilde{p} \\ &+ \left(64c^8h - 48c^6h^2 + 8c^4h^3 + 80c^6 - 88c^4h + 28c^2h^2 - 2h^3 - 4c^2 + 2h\right). \end{aligned}$$

Further, evaluating the derivative of the polynomial d at different values of $\tilde{p}$ yields

$$\begin{aligned} \left.\frac{\partial d(c,h,\tilde{p})}{\partial \tilde{p}}\right|_{\tilde{p}=-2c^2} &= 128c^6 - 112c^4h + 28c^2h^2 - 2h^3 - 12c^2 + 2h > 0, \\ \left.\frac{\partial d(c,h,\tilde{p})}{\partial \tilde{p}}\right|_{\tilde{p}=1-2c^2} &= -8\left(4c^4 - 2c^2h - 2c^2 + h - 1\right)\left(4c^2 - h - 1\right)^2 < 0, \\ \left.\frac{\partial d(c,h,\tilde{p})}{\partial \tilde{p}}\right|_{\tilde{p}=0} &= 2\left(2c^2 - h\right)\left(16c^6h - 4c^4h^2 + 20c^4 - 12c^2h + h^2 - 1\right) > 0, \\ \left.\frac{\partial d(c,h,\tilde{p})}{\partial \tilde{p}}\right|_{\tilde{p}=2c^2} &= -256c^8h + 192c^6h^2 - 32c^4h^3 - 64c^6 - 16c^4h + 28c^2h^2 - 2h^3 + 4c^2 + 2h < 0. \end{aligned}$$

The above inequalities are illustrated by the plots in Figure 4.9. Using the Interme-

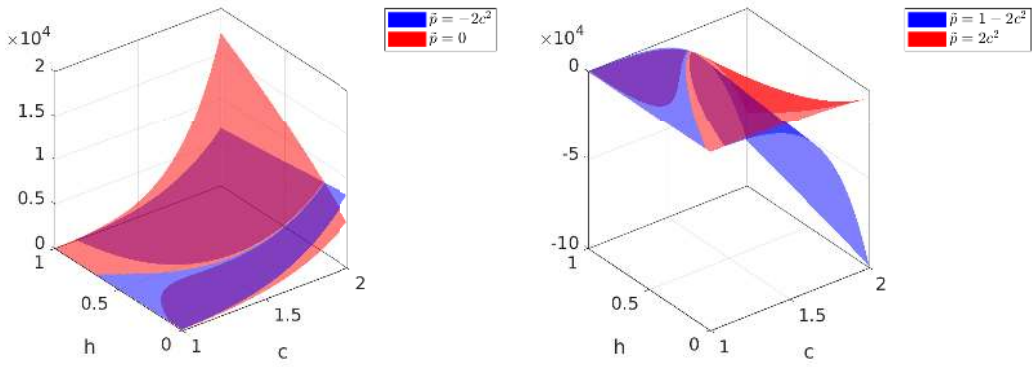

Figure 4.9: Plots of $\frac{\partial d(c,h,\tilde{p})}{\partial \tilde{p}}$ evaluated at different values of $\tilde{p}$.

diate Value Theorem, we infer that the three roots r_1, r_2, and r_3 of the derivative of the polynomial d satisfy the conditions $r_3 \in (-2c^2, 1-2c^2)$, $r_2 \in (1-2c^2, 0)$ and $r_1 \in (0, 2c^2)$. Since we are concerned with $\tilde{p} > 1-2c^2$, we discard r_3.

Since $d(c,h,1-2c^2) = -4\left(4c^4 - 2c^2h - 2c^2 + h - 1\right)\left(4c^2 - h - 1\right)^2 < 0$, looking at the sign of the derivative of the polynomial d at $1-2c^2$, we can infer that by increasing $\tilde{p}$, the polynomial d starts decreasing to reach its minimum at r_2 where it starts increasing to reach its maximum at $r_1 \in (0, 2c^2)$. One can check that $d(c,h,2c^2) = 256c^8 - 320c^6h + 112c^4h^2 - 8c^2h^3 - 32c^4 + 20c^2h - 2h^2 + 1 > 0$ and hence the polynomial d has a root $p_1 \in (1-2c^2, 2c^2)$. Further, d starts decreasing beyond $\tilde{p} > 2c^2$ to become negative. Hence we have the other real root p_2 of d greater than $2c^2$. This proves that d has only two real roots and this completes the proof. □

Lemma 4.2.5. *For $c^2 \geq 1$, and $h \in (0,1)$, the root $\tilde{p}_+$ given by (4.46) lies between $\tilde{p}_1$ and $\tilde{p}_2$, where $\tilde{p}_1$ and $\tilde{p}_2$ are the roots of the polynomial $d(c,h,\tilde{p})$ defined in Lemma 4.2.4.*

Proof. From the left plot of Figure 4.10, we observe that for all $c^2 \geq 1$ and $h \in (0,1)$, the polynomial $d(c,h,\tilde{p})$ defined in Lemma 4.2.4 satisfies $d(c,h,\tilde{p}_+) > 0$ and hence using the same Lemma 4.2.4, we can conclude that $\tilde{p}_+ \in (\tilde{p}_1, \tilde{p}_2)$. □

Lemma 4.2.6. *For $\tilde{p} \in [\tilde{p}_1, \tilde{p}_2]$, with $c^2 \geq 1$ and $h \in (0,1)$, the polynomial $P_2(c,h,\tilde{p})$ defined as*

$$P_2(c,h,\tilde{p}) := (-16c^4 + 12c^2h - 2h^2 + 1)\tilde{p}^2 + (-16c^4h + 12c^2h^2 - 2h^3 - 4c^2 + 2h - 2(2c^2 - h)^3)\tilde{p} + 64c^8 - 80c^6h + 32c^4h^2 - 4c^2h^3 - 28c^4 + 16c^2h - 2h^2 + 1 - 4c^2(2c^2 - h)^3$$

is always negative.

Proof. Let r_- and r_+, with $r_- < r_+$ be the roots (with respect to $\tilde{p}$) of the polynomial $P_2(c,h,\tilde{p})$. From both plots of Figure 4.11, we observe that under the conditions

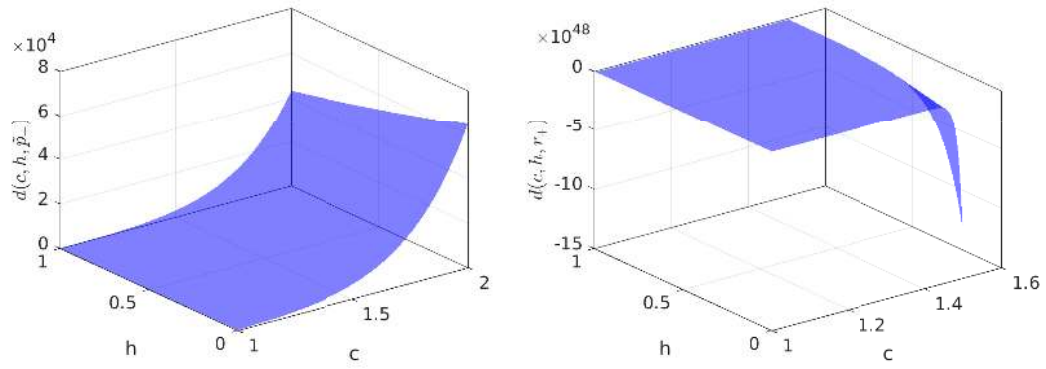

Figure 4.10: Plot of $d(c, h, \tilde{p}_+)$ on (left) and $d(c, h, r_+)$ on (right) for different values of c and h.

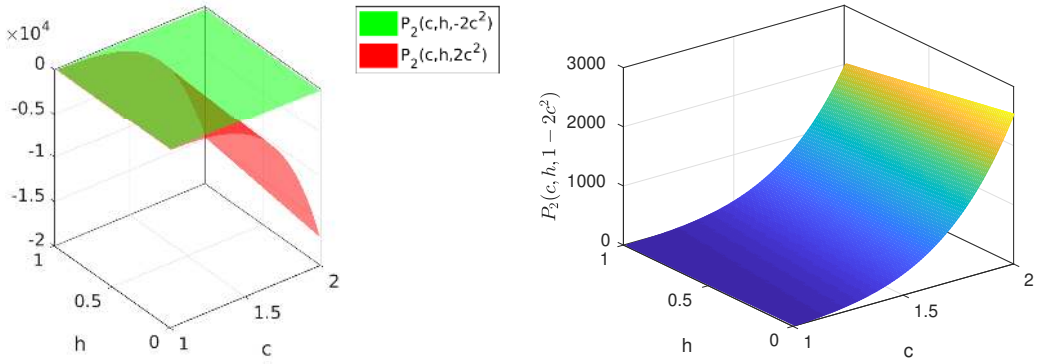

Figure 4.11: Plot of $P_2(c, h, \tilde{p})$ for different values of $\tilde{p}$.

$c^2 \geq 1$ and $h \in (0, 1)$, we have

$$\begin{aligned} P_2(c, h, -2c^2) &= -16c^4 + 12c^2h - 2h^2 + 1 < 0, \\ P_2(c, h, 1 - 2c^2) &= 2\left(4c^4 - 2c^2h - 2c^2 + h - 1\right)\left(6c^2 - 2h - 1\right) > 0, \\ P_2(c, h, 2c^2) &= -64c^8 + 32c^6h - 32c^4 + 20c^2h - 2h^2 + 1 < 0. \end{aligned}$$

Thus by the Intermediate Value Theorem, $r_- \in (-2c^2, 1-2c^2)$ and $r_+ \in (1-2c^2, 2c^2)$. From Lemma 4.2.4, since $d(c, h, r_+) < 0$ (see the right plot of Figure 4.10) , we infer that $r_+ \notin [\tilde{p}_1, \tilde{p}_2]$. Thus $r_- < r_+ < \tilde{p}_1$. Further, the coefficient of $\tilde{p}^2$ in the polynomial P_2 is negative and hence $P_2(c, h, \tilde{p}) \geq 0$ for $\tilde{p} \in [r_-, r_+]$ and $P_2(c, h, \tilde{p}) < 0$ elsewhere. Hence the polynomial $P_2(c, h, \tilde{p})$ is always negative for $\tilde{p} \in [\tilde{p}_1, \tilde{p}_2]$. □

Lemma 4.2.7. *For $\tilde{p} > 1 - 2c^2$ with $c^2 \geq 1$ and $h \in (0, 1)$, we define the polynomial P_4 by*

$$P_4(c, h, \tilde{p}) := L(c, h, \tilde{p})G(c, h, \tilde{p}),$$

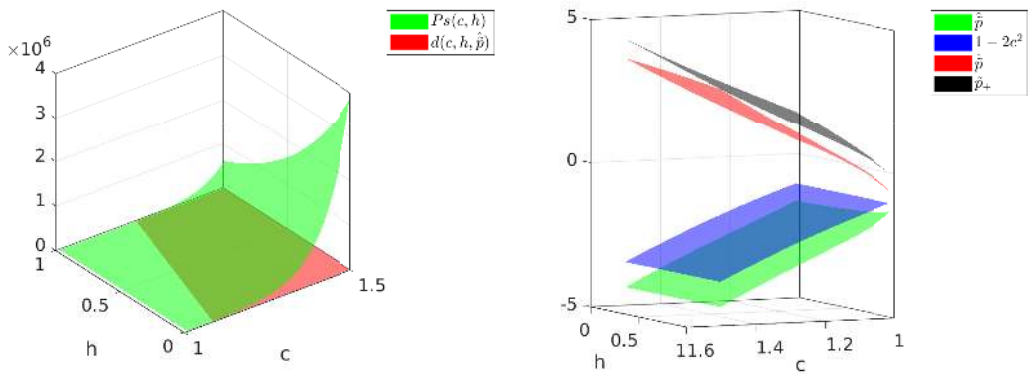

Figure 4.12: Numerical verification of $Ps(c,h) > 0$ and $d(c,h,\hat{\tilde{p}}) > 0$ on (left) and inequality $\hat{\tilde{p}}_- < 1-2c^2 < \hat{\tilde{p}} < \tilde{p}_+$ on (right) for different values of c and h.

where

$$\begin{aligned} G(c,h,\tilde{p}) = &\left(-16c^8+32c^6h-24c^4h^2+8c^2h^3-16c^4-h^4+12c^2h-2h^2+1\right)\tilde{p}^2 \\ &+\left(-32c^6+32c^4h-12c^2h^2+2h^3-4c^2+2h\right)\tilde{p}+64c^{12}-128c^{10}h \\ &+96c^8h^2-32c^6h^3-16c^8+4c^4h^4+48c^6h-40c^4h^2+12c^2h^3 \\ &-28c^4-h^4+16c^2h-2h^2+1. \end{aligned}$$

The polynomial $P_4(c,h,\tilde{p})$ has two real roots $\hat{\tilde{p}}$ and $\tilde{p}_+$ which are both greater than $1-2c^2$. Further, $\hat{\tilde{p}} < \tilde{p}_+$ for $1 \le c < 1.5$. Moreover P_4 is negative for $\tilde{p} \in (1-2c^2, \hat{\tilde{p}}) \cup (\tilde{p}_+, \infty)$ and positive for $\tilde{p} \in (\hat{\tilde{p}}, \tilde{p}_+)$.

Proof. The polynomial P_4 has four roots, two roots of the polynomial L and the two other roots of the polynomial G. We have studied the polynomial L in Lemma 4.2.3 and have shown that L has two real roots $\tilde{p}_-$ and $\tilde{p}_+$ such that $\tilde{p}_- < 1-2c^2 < \tilde{p}_+$. Similarly, one can show that the polynomial G has two real roots,

$$\begin{aligned} \hat{\tilde{p}} &:= \frac{-16c^6+16c^4h-6c^2h^2+h^3-2c^2+h+\sqrt{Ps(c,h)}}{16c^8-32c^6h+24c^4h^2-8c^2h^3+16c^4+h^4-12c^2h+2h^2-1}, \\ \hat{\tilde{p}}_- &:= \frac{-16c^6+16c^4h-6c^2h^2+h^3-2c^2+h-\sqrt{Ps(c,h)}}{16c^8-32c^6h+24c^4h^2-8c^2h^3+16c^4+h^4-12c^2h+2h^2-1}, \end{aligned}$$

where

$$\begin{aligned} Ps(c,h) := &\left(4c^4-2c^2h+2c^2-h-1\right)\left(8c^6-12c^4h+6c^2h^2-h^3+6c^2-2h+1\right) \\ &\left(4c^4-2c^2h-2c^2+h-1\right)\left(8c^6-12c^4h+6c^2h^2-h^3+6c^2-2h-1\right). \end{aligned}$$

From the left plot of Figure 4.12 we observe that $Ps(c,h) > 0$ for $c^2 \ge 1$ and $h \in (0,1)$ and hence the roots $\hat{\tilde{p}}$ and $\hat{\tilde{p}}_-$ are real and $\hat{\tilde{p}}_- < 1-2c^2 < \hat{\tilde{p}}$ (see the right plot of Figure 4.12). The roots $\tilde{p}_-$ and $\tilde{p}_+$ of the polynomial $L(c,h,\tilde{p})$ are well studied in

Lemma 4.2.3. Since $\tilde{p}_-$ and $\hat{\tilde{p}}_-$ are less than $1-2c^2$, we discard them. Further, in general we cannot say if $\hat{\tilde{p}} < \tilde{p}_+$ or $\hat{\tilde{p}} > \tilde{p}_+$, since these inequalities depend on the value of c. But, under the conditions $h \in (0,1)$ and $1 \leq c < 1.5$, we have $\hat{\tilde{p}} < \tilde{p}_+$.

We observe numerically from the left plot of Figure 4.12 that $d(c,h,\hat{\tilde{p}}) > 0$ and hence from Lemma 4.2.4 we conclude that $\hat{\tilde{p}} \in (\tilde{p}_1, \tilde{p}_2)$. The sign of the coefficient of $\tilde{p}^2$ in the polynomial $G(c,h,\tilde{p})$ is negative and hence $G(c,h,\tilde{p}) < 0$ for $\tilde{p} \in (-\infty, \hat{\tilde{p}}_-) \cup (\hat{\tilde{p}}, \infty)$ while $G(c,h,\tilde{p}) \geq 0$ for $\tilde{p} \in [\hat{\tilde{p}}_-, \hat{\tilde{p}}]$. Finally, from Lemma 4.2.3, we have $L(c,h,\tilde{p}) > 0$ for $\tilde{p} > \tilde{p}_+$ and $L(c,h,\tilde{p}) < 0$ for $1-2c^2 < \tilde{p} < \tilde{p}_+$. Summarizing the behavior of the polynomials L and G, we have

$$G(c,h,\tilde{p}) = \begin{cases} > 0, & \text{for } \tilde{p} \in (1-2c^2, \hat{\tilde{p}}), \\ < 0, & \text{for } \tilde{p} \in (\hat{\tilde{p}}, \tilde{p}_+), \\ < 0, & \text{for } \tilde{p} \in (\tilde{p}_+, \infty), \end{cases}, \quad \text{and} \quad L(c,h,\tilde{p}) = \begin{cases} < 0, & \text{for } \tilde{p} \in (1-2c^2, \hat{\tilde{p}}), \\ < 0, & \text{for } \tilde{p} \in (\hat{\tilde{p}}, \tilde{p}_+), \\ > 0, & \text{for } \tilde{p} \in (\tilde{p}_+, \infty), \end{cases}$$

and hence

$$P_4(c,h,\tilde{p}) = \begin{cases} > 0, & \text{for } \tilde{p} \in (\hat{\tilde{p}}, \tilde{p}_+), \\ < 0, & \text{for } \tilde{p} \in (1-2c^2, \hat{\tilde{p}}) \cup (\tilde{p}_+, \infty). \end{cases}$$

This completes the proof. □

Lemma 4.2.8. *For $\tilde{p} > 1-2c^2$, with $c^2 \geq 1$ and $h \in (0,1)$, let $x_1(c,h,\tilde{p})$ be defined as*

$$x_1(c,h,\tilde{p}) := \frac{\left(2\left(2c^2+\tilde{p}\right)\left(2c^2-h\right) + \sqrt{d(c,h,\tilde{p})}\right)\left(2c^2-h\right)}{L(c,h,\tilde{p})}, \tag{4.47}$$

where the polynomials $L(c,h,\tilde{p})$ and $d(c,h,\tilde{p})$ are defined in Lemma 4.2.3 and 4.2.4 respectively. $x_1(c,h,\tilde{p})$ is not defined for $\tilde{p} = \tilde{p}_+$ and is complex for $\tilde{p} \in (1-2c^2, \tilde{p}_1) \cup (\tilde{p}_2, \infty)$. Further, $x_1 < \frac{-1}{2c^2-h}$ for $\tilde{p} \in [\tilde{p}_1, \tilde{p}_+)$ and $x_1 > 0$ for $\tilde{p} \in (\tilde{p}_+, \tilde{p}_2]$.

Proof. Lemma 4.2.3 states that the polynomial $L(c,h,\tilde{p})$ has a unique real root $\tilde{p}_+$ greater than $1-2c^2$. Since $L(c,h,\tilde{p})$ is in the denominator, x_1 is not defined for $\tilde{p} = \tilde{p}_+$. From Lemma 4.2.4, we find that $d(c,h,\tilde{p}) < 0$ for $\tilde{p} \in (1-2c^2, \tilde{p}_1) \cup (\tilde{p}_2, \infty)$ and hence x_1 is complex in this region. Now, consider the case $\tilde{p} \in [\tilde{p}_1, \tilde{p}_+)$. Since $L(c,h,\tilde{p}) < 0$ for $1-2c^2 < \tilde{p} < \tilde{p}_+$, we have

$$\begin{aligned} x_1 < \frac{-1}{2c^2-h} \quad &\iff \quad \frac{(2(2c^2+\tilde{p})(2c^2-h) + \sqrt{d(c,h,\tilde{p})})(2c^2-h)}{L(c,h,\tilde{p})} < \frac{-1}{2c^2-h} \\ &\iff \quad (2(2c^2+\tilde{p})(2c^2-h) + \sqrt{d(c,h,\tilde{p})})(2c^2-h)^2 > -L(c,h,\tilde{p}) \\ &\iff \quad (2c^2-h)^2\sqrt{d(c,h,\tilde{p})} > -L(c,h,\tilde{p}) - 2(2c^2+\tilde{p})(2c^2-h)^3 = P_2(c,h,\tilde{p}). \end{aligned}$$

Lemma 4.2.5 and 4.2.6 state that the right side of the above inequality is negative while the left side is positive and hence $x_1 < \frac{-1}{2c^2-h}$ is true. For the case $\tilde{p} \in (\tilde{p}_+, \tilde{p}_2]$, both the numerators and denominators are positive and hence $x_1 > 0$. □

Lemma 4.2.9. *For $\tilde{p} > 1 - 2c^2$, with $c^2 \geq 1$ and $h \in (0,1)$, we define $x_2(c,h,\tilde{p})$ by*

$$x_2(c,h,\tilde{p}) := \frac{\left(2\left(2c^2+\tilde{p}\right)\left(2c^2-h\right) - \sqrt{d(c,h,\tilde{p})}\right)\left(2c^2-h\right)}{L(c,h,\tilde{p})}, \tag{4.48}$$

where the polynomials $L(c,h,\tilde{p})$ and $d(c,h,\tilde{p})$ are defined in Lemma 4.2.3 and 4.2.4 respectively. $x_2(c,h,\tilde{p})$ is not defined for $\tilde{p} = \tilde{p}_+$ and is complex for $\tilde{p} \in (1-2c^2, \tilde{p}_1) \cup (\tilde{p}_2, \infty)$. Further, under the condition $\tilde{p}_1 < \hat{\tilde{p}} < \tilde{p}_+ < \tilde{p}_2$, we have $x_2 \geq \frac{-1}{2c^2-h}$ for $\tilde{p} \in [\hat{\tilde{p}}, \tilde{p}_+) \cup (\tilde{p}_+, \tilde{p}_2]$, and $x_2 < \frac{-1}{2c^2-h}$ for $\tilde{p} \in [\tilde{p}_1, \hat{\tilde{p}})$. In addition, $x_2 < 0$ for $\tilde{p} \in [\tilde{p}_1, \tilde{p}_+) \cup (\tilde{p}_+, \tilde{\tilde{p}})$, and $x_2 \geq 0$ for $[\tilde{\tilde{p}}, \tilde{p}_2]$ where $\tilde{\tilde{p}} := \sqrt{4c^4-1}$ and $\tilde{p}_+ < \tilde{\tilde{p}} < \tilde{p}_2$.

Proof. The proof is similar to the proof of Lemma 4.2.8. By Lemmas 4.2.3 and 4.2.4, $x_2(c,h,\tilde{p})$ is not defined for $\tilde{p} = \tilde{p}_+$ and complex for $\tilde{p} \in (1-2c^2, \tilde{p}_1) \cup (\tilde{p}_2, \infty)$.

For $\tilde{p} \in [\tilde{p}_1, \tilde{p}_+)$, $L(c,h,\tilde{p}) < 0$ and hence

$$\begin{aligned}
x_2 \geq \frac{-1}{2c^2-h} \quad &\iff \quad \frac{\left(2\left(2c^2+\tilde{p}\right)\left(2c^2-h\right) - \sqrt{d(c,h,\tilde{p})}\right)\left(2c^2-h\right)}{L(c,h,\tilde{p})} \geq \frac{-1}{2c^2-h} \\
&\iff \quad \left(2\left(2c^2+\tilde{p}\right)\left(2c^2-h\right) - \sqrt{d(c,h,\tilde{p})}\right)\left(2c^2-h\right)^2 \leq -L \\
&\iff \quad \left(2c^2-h\right)^2\sqrt{d(c,h,\tilde{p})} \geq L + 2\left(2c^2+\tilde{p}\right)\left(2c^2-h\right)^3 = -P_2(c,h,\tilde{p}).
\end{aligned}$$

By Lemma 4.2.6, $P_2(c,h,\tilde{p})$ is always negative and hence squaring on both sides gives

$$\begin{aligned}
&\iff \quad \left(2c^2-h\right)^4 d(c,h,\tilde{p}) \geq \left(P_2(c,h,\tilde{p})\right)^2 \\
&\iff \quad \left(2c^2-h\right)^4 d(c,h,\tilde{p}) - \left(P_2(c,h,\tilde{p})\right)^2 \geq 0 \\
&\iff \quad P_4(c,h,\tilde{p}) \geq 0.
\end{aligned}$$

Lemma 4.2.7 gives the behavior of the polynomial P_4 and hence we conclude that $x_2 \geq \frac{-1}{2c^2-h}$ for $\tilde{p} \in [\hat{\tilde{p}}, \tilde{p}_+)$ and $x_2 < \frac{-1}{2c^2-h}$ for $\tilde{p} \in [\tilde{p}_1, \hat{\tilde{p}})$.

Similarly, for $\tilde{p} \in (\tilde{p}_+, \tilde{p}_2]$, we follow the steps to arrive at

$$\begin{aligned}
x_2 \geq \frac{-1}{2c^2-h} \quad &\iff \quad \frac{\left(2\left(2c^2+\tilde{p}\right)\left(2c^2-h\right) - \sqrt{d(c,h,\tilde{p})}\right)\left(2c^2-h\right)}{L(c,h,\tilde{p})} \geq \frac{-1}{2c^2-h} \\
&\iff \quad \left(2\left(2c^2+\tilde{p}\right)\left(2c^2-h\right) - \sqrt{d(c,h,\tilde{p})}\right)\left(2c^2-h\right)^2 \geq -L \\
&\iff \quad \left(2c^2-h\right)^2\sqrt{d(c,h,\tilde{p})} \leq L + 2\left(2c^2+\tilde{p}\right)\left(2c^2-h\right)^3 = -P_2(c,h,\tilde{p}) \\
&\iff \quad P_4(c,\tilde{p},h) \leq 0.
\end{aligned}$$

Using Lemma 4.2.7, we conclude $x_2 \geq \frac{-1}{2c^2-h}$ if $\tilde{p} \in [\hat{\tilde{p}}, \tilde{p}_+) \cup (\tilde{p}_+, \tilde{p}_2]$ and $x_2 < \frac{-1}{2c^2-h}$ for $\tilde{p} \in [\tilde{p}_1, \hat{\tilde{p}})$.

Further, for $\tilde{p} \in [\tilde{p}_1, \tilde{p}_+)$, we also have

$$x_2 < 0 \iff \frac{\left(2\left(2c^2+\tilde{p}\right)\left(2c^2-h\right) - \sqrt{d(c,h,\tilde{p})}\right)\left(2c^2-h\right)}{L(c,h,\tilde{p})} < 0.$$

Since $L(c,h,\tilde{p}) < 0$, the above inequality reduces to

$$\begin{aligned}
&\iff \left(2\left(2c^2+\tilde{p}\right)\left(2c^2-h\right) - \sqrt{d(c,h,\tilde{p})}\right)\left(2c^2-h\right) > 0\\
&\iff \left(2\left(2c^2+\tilde{p}\right)\left(2c^2-h\right)\right)^2 - d(c,h,\tilde{p}) > 0\\
&\iff \left(\tilde{p}^2 - 4c^4 + 1\right) L(c,\tilde{p},h) > 0\\
&\iff \left(\tilde{p}-\tilde{\tilde{p}}\right)\left(\tilde{p}+\tilde{\tilde{p}}\right)\left(\tilde{p}-\tilde{p}_+\right)\left(\tilde{p}-\tilde{p}_-\right) > 0\\
&\iff z(c,\tilde{p},h) > 0,
\end{aligned}$$

where $\tilde{p}_+$ and $\tilde{p}_-$ are the roots of $L(c,\tilde{p},h)$ which are defined in Lemma 4.2.3, $\tilde{\tilde{p}} := \sqrt{4c^4-1}$, and $z(c,\tilde{p},h) := \left(\tilde{p}-\tilde{\tilde{p}}\right)\left(\tilde{p}+\tilde{\tilde{p}}\right)\left(\tilde{p}-\tilde{p}_+\right)\left(\tilde{p}-\tilde{p}_-\right)$. Clearly, $\tilde{\tilde{p}} > 1-2c^2$ and hence only two roots of $z(c,\tilde{p},h)$, namely, $\tilde{\tilde{p}}$, $\tilde{p}_+$ are greater than $1-2c^2$. Further, since $L(c,\tilde{\tilde{p}},h) > 0$ and $d(c,\tilde{\tilde{p}},h) > 0$, we infer from Lemmas 4.2.4 and 4.2.3 that $\tilde{p}_1 < \tilde{p}_+ < \tilde{\tilde{p}} < \tilde{p}_2$. Finally, since $\tilde{p} \in [\tilde{p}_1, \tilde{p}_+)$, we have $L(c,\tilde{p},h) > 0$ and $(\tilde{p}-\tilde{\tilde{p}}) < 0$, and thus $z(c,\tilde{p},h) > 0$. Thus we conclude that $x_2 < 0$ for $\tilde{p} \in [\tilde{p}_1, \tilde{p}_+)$.

For $\tilde{p} \in (\tilde{p}_+, \tilde{p}_2]$, we follow similar steps and since $L(c,\tilde{p},h) > 0$, we have

$$\begin{aligned}
x_2 < 0 &\iff \frac{\left(2\left(2c^2+\tilde{p}\right)\left(2c^2-h\right) - \sqrt{d(c,h,\tilde{p})}\right)\left(2c^2-h\right)}{L(c,h,\tilde{p})} < 0\\
&\iff \left(2\left(2c^2+\tilde{p}\right)\left(2c^2-h\right) - \sqrt{d(c,h,\tilde{p})}\right)\left(2c^2-h\right) < 0\\
&\iff \left(\tilde{p}^2 - 4c^4 + 1\right) L(c,\tilde{p},h) < 0\\
&\iff \left(\tilde{p}-\tilde{\tilde{p}}\right)\left(\tilde{p}+\tilde{\tilde{p}}\right)\left(\tilde{p}-\tilde{p}_+\right)\left(\tilde{p}-\tilde{p}_-\right) < 0.
\end{aligned}$$

Since $\tilde{p} \in (\tilde{p}_+, \tilde{p}_2]$ and $\tilde{p}_+ > \tilde{p}_1$, we have $x_2 < 0$ for $\tilde{p} \in (\tilde{p}_+, \tilde{\tilde{p}})$ while $x_2 \geq 0$ for $\tilde{p} \in [\tilde{\tilde{p}}, \tilde{p}_2]$. This completes the proof. □

Lemma 4.2.10. *For $c^2 \geq 1$ and $h \in (0,1)$, the function $\tilde{x} \mapsto R(c,h,\tilde{x},\tilde{p})$ defined in (4.43) has a unique local minimum in $\left[\frac{-1}{2c^2-h}, 0\right)$ located at*

$$\underline{\tilde{x}}(c,h,\tilde{p}) := \frac{\left(2\left(2c^2+\tilde{p}\right)\left(2c^2-h\right) - \sqrt{d(c,h,\tilde{p})}\right)\left(2c^2-h\right)}{L(c,h,\tilde{p})},$$

if $\tilde{p} \in [\hat{\tilde{p}}, \tilde{p}_+) \cup (\tilde{p}_+, \tilde{\tilde{p}})$, where the polynomials $L(c,h,\tilde{p})$, $d(c,h,\tilde{p})$, $\tilde{p}_+$, $\tilde{\tilde{p}}$ are defined in the previous lemmas. For any other value of $\tilde{p} > 1-2c^2$, R has no extrema in $\left[\frac{-1}{2c^2-h}, 0\right)$.

Proof. A partial derivative of $R(c,h,\tilde{x},\tilde{p})$ with respect to $\tilde{x}$ shows that the root of the polynomial

$$Q(\tilde{x}) = \left(2c^2+\tilde{p}+1\right)\left(2c^2+\tilde{p}-1\right)P(\tilde{x})$$

where

$$\begin{aligned}P(\tilde{x}) = \left(2c^2-h\right)\big((&64c^8-80c^6h+32c^4h^2-16c^4h\tilde{p}-16c^4\tilde{p}^2-4c^2h^3+12c^2h^2\tilde{p}+12c^2h\tilde{p}^2\\&-28c^4-2h^3\tilde{p}-2h^2\tilde{p}^2+16c^2h-4c^2\tilde{p}-2h^2+2h\tilde{p}+\tilde{p}^2+1)\tilde{x}^2\\&+(32c^6-32c^4h+16c^4\tilde{p}+8c^2h^2-16c^2h\tilde{p}+4h^2\tilde{p})\tilde{x}\\&+16c^8-16c^6h+4c^4h^2-4c^4\tilde{p}^2+4c^2h\tilde{p}^2-4c^4-h^2\tilde{p}^2+4c^2h-h^2)\end{aligned}$$

determine the extrema of R. Further the roots of the polynomial $P(\tilde{x})$ are

$$\begin{aligned}\bar{\tilde{x}}(c,h,\tilde{p}) &:= \frac{\left(2\left(2c^2+\tilde{p}\right)\left(2c^2-h\right)+\sqrt{d(c,h,\tilde{p})}\right)\left(2c^2-h\right)}{L(c,h,\tilde{p})},\\ \underline{\tilde{x}}(c,h,\tilde{p}) &:= \frac{\left(2\left(2c^2+\tilde{p}\right)\left(2c^2-h\right)-\sqrt{d(c,h,\tilde{p})}\right)\left(2c^2-h\right)}{L(c,h,\tilde{p})}.\end{aligned}$$

Note that $\bar{\tilde{x}}$ and $\underline{\tilde{x}}$ are the same as $\tilde{x}_1$ and $\tilde{x}_2$ defined in (4.47) and (4.48) respectively. By Lemmas 4.2.8 and 4.2.9, both $\bar{\tilde{x}}$ and $\underline{\tilde{x}}$ are not defined for $\tilde{p}=\tilde{p}_+$ and are complex for $\tilde{p}\in(1-2c^2,\tilde{p}_1)\cup(\tilde{p}_2,\infty)$. We therefore analyze for the intervals $[\tilde{p}_1,\tilde{p}_+)$ and $(\tilde{p}_+,\tilde{p}_2]$. Lemmas 4.2.8-4.2.9 state that R has only one extremum in $\left[\frac{-1}{2c^2-h},0\right)$ at $\tilde{x}=\underline{\tilde{x}}$, which is a minimum, if $\tilde{p}\in[\hat{\tilde{p}},\tilde{p}_+)\cup(\tilde{p}_+,\tilde{p}_2]$. For any other value of $\tilde{p}>1-2c^2$, R has no extrema in $\left[\frac{-1}{2c^2-h},0\right)$. □

Lemma 4.2.11. *For fixed $\tilde{x}\in\left[\frac{-1}{2c^2-h},0\right)$ with $h\in(0,1)$, the optimal $\tilde{p}^*$ lies in the interval $\left[\frac{-1}{2c^2-h},\infty\right)$.*

Proof. $R(c,h,\tilde{x},\tilde{p})$ is a complicated function of $\tilde{p}$. Using Maple, we find that the partial derivative of R with respect to $\tilde{p}$ is given by

$$\frac{\partial R(c,h,\tilde{x},\tilde{p})}{\partial\tilde{p}} = -z(\tilde{x},h)P(\tilde{p},h),$$

where the polynomials z and P have the expressions

$$\begin{aligned}z(\tilde{x},h) &:= (16c^4-12c^2h+2h^2-1)\tilde{x}^2+(8c^4h-6c^2h^2+h^3+2c^2-h)\tilde{x}-4c^4+4c^2h-h^2,\\ P(\tilde{p},h) &:= (-8c^4\tilde{x}+4c^2h\tilde{x}-4c^2\tilde{x}^2+2h\tilde{x}^2)\tilde{p}^2+(-32c^6\tilde{x}+32c^4h\tilde{x}+16c^4\tilde{x}^2-12c^2h^2\tilde{x}\\&\quad -16c^2h\tilde{x}^2-8c^4+2h^3\tilde{x}+4h^2\tilde{x}^2+8c^2h+12c^2\tilde{x}-2h^2-6h\tilde{x}-2\tilde{x}^2)\tilde{p}\\&\quad -32c^8\tilde{x}+48c^6h\tilde{x}+48c^6\tilde{x}^2-24c^4h^2\tilde{x}-40c^4h\tilde{x}^2-16c^6+4c^2h^3\tilde{x}+8c^2h^2\tilde{x}^2\\&\quad +16c^4h+16c^4\tilde{x}-4c^2h^2-8c^2h\tilde{x}-8c^2\tilde{x}^2+2h\tilde{x}^2.\end{aligned}$$

Since $z(\tilde{x}, h)$ does not depend on $\tilde{p}$, the extrema of R with respect to $\tilde{p}$ are determined by the roots of the polynomial $P(\tilde{p}, h)$, which are given by

$$\bar{\tilde{p}}(c, h, \tilde{x}) := \frac{Qp(c, h, \tilde{x}) + \sqrt{dp(c, h, \tilde{x})}}{2x(4c^4 - 2c^2h + 2c^2x - hx)}, \tag{4.49}$$

$$\underline{\tilde{p}}(c, h, \tilde{x}) := \frac{Qp(c, h, \tilde{x}) - \sqrt{dp(c, h, \tilde{x})}}{2x(4c^4 - 2c^2h + 2c^2x - hx)}, \tag{4.50}$$

with

$$Qp(c, h, \tilde{x}) = (8c^4 - 8c^2h + 2h^2 - 1)\tilde{x}^2 + (-16c^6 + 16c^4h - 6c^2h^2 + h^3 + 6c^2 - 3h)\tilde{x} - 4c^4 + 4c^2h - h^2,$$

and

$$\begin{aligned} dp(c, h, \tilde{x}) =& ((16c^4 - 12c^2h - 4c^2 + 2h^2 + 2h - 1)\tilde{x}^2 + (8c^4h - 8c^4 - 6c^2h^2 + 4c^2h + h^3 + 6c^2 - 3h)\tilde{x} \\ & - 4c^4 + 4c^2h - h^2)((16c^4 - 12c^2h + 4c^2 + 2h^2 - 2h - 1)\tilde{x}^2 \\ & + (8c^4h + 8c^4 - 6c^2h^2 - 4c^2h + h^3 + 6c^2 - 3h)\tilde{x} - 4c^4 + 4c^2h - h^2). \end{aligned}$$

Using the derivative of $dp(c, h, \tilde{x})$ with respect to $\tilde{x}$, we find the minimum of both factors of the polynomial $dp(c, h, \tilde{x})$, and observe that for $\tilde{x} \in \left[\frac{-1}{2c^2-h}, 0\right)$, $c^2 \geq 1$ and $h \in (0, 1)$,

$$\begin{aligned} &((16c^4 - 12c^2h - 4c^2 + 2h^2 + 2h - 1)\tilde{x}^2 + (8c^4h - 8c^4 - 6c^2h^2 + 4c^2h + h^3 + 6c^2 - 3h)\tilde{x} \\ &-4c^4 + 4c^2h - h^2) < 0, \quad \text{and,} \\ &((16c^4 - 12c^2h + 4c^2 + 2h^2 - 2h - 1)\tilde{x}^2 + (8c^4h + 8c^4 - 6c^2h^2 - 4c^2h + h^3 + 6c^2 - 3h)\tilde{x} \\ &-4c^4 + 4c^2h - h^2) < 0. \end{aligned}$$

Thus, under these conditions, $dp(c, h, \tilde{x}) > 0$.

Further, we also observe that under these conditions, $\bar{\tilde{p}}(c, h, \tilde{x}) < 1 - 2c^2 < \underline{\tilde{p}}(c, h, \tilde{x})$, and hence we discard $\bar{\tilde{p}}(c, h, \tilde{x})$. Moreover, since the coefficient of $\tilde{p}^2$ in the polynomial $P(\tilde{p}, h)$ is always positive when $\tilde{x} \in \left[\frac{-1}{2c^2-h}, 0\right)$, we observe that R attains its minimum at $\underline{\tilde{p}}$. Therefore, for $1 - 2c^2 < \tilde{p} < \underline{\tilde{p}}$, increasing $\tilde{p}$ increases R, while for $\tilde{p} > \underline{\tilde{p}}$, increasing $\tilde{p}$ decreases R. Since the range of $\tilde{x}$ is $\left[\frac{-1}{2c^2-h}, 0\right)$, the optimal $\tilde{p}^*$ will thus be attained at $\underline{\tilde{p}}(c, h, \tilde{x}) \in \left[\frac{-1}{2c^2-h}, \infty\right)$ since with $\tilde{p}$ outside this interval, R can be uniformly decreased by moving $\tilde{p}$ towards this interval. This completes the proof. □

Theorem 4.2.3. *For $1 \leq c < 1.5$ and $h \in (0, 1)$, the optimized $\alpha^{[4]*}$ for the nonoverlapping OWR method applied to the reduced RC circuit with four nodes is given by*

$$\alpha^{[4]*} = 2c^2 - 1 + \tilde{p}^*, \tag{4.51}$$

where $\tilde{p}^*$ is the solution of the min-max problem (4.44)

$$\tilde{p}^* := \frac{-1 + \sqrt{16c^8 - 16c^6h + 4c^4h^2 - 12c^4 + 8c^2h - h^2 + 1}}{2c^2 - h}. \tag{4.52}$$

Proof. We proved in Lemma 4.2.10 that the maximum of the convergence factor R defined in (4.43) can only be attained at the boundaries, that is, $\tilde{x} = \frac{-1}{2c^2-h}$ and $\tilde{x} = 0^-$ since $\tilde{x}$ approaches 0 from the negative axis. Further, Lemma 4.2.11 states that for $\tilde{x} \in \left[\frac{-1}{2c^2-h}, 0\right)$, the optimal $\tilde{p}$ lies in $\left[\frac{-1}{2c^2-h}, \infty\right)$. We thus observe the behavior of R in these intervals. For $\tilde{x} = \frac{-1}{2c^2-h}$, $\tilde{p} = \underline{\tilde{p}}(c, h, \frac{-1}{2c^2-h}) = \frac{-1}{2c^2-h}$, and thus $R(c, h, \tilde{x} = \frac{-1}{2c^2-h}, \tilde{p} = \frac{-1}{2c^2-h}) = 0$. From Lemma 4.2.11, increasing $\tilde{p}$ increases R monotonically. On the other hand, for $\tilde{p} = \frac{-1}{2c^2-h}$, $R(c, h, \tilde{x} = 0^-, \tilde{p} = \frac{-1}{2c^2-h}) = \frac{(2c^2-h)^2}{(4c^4-2c^2h-1)^2} > 0$ and increasing $\tilde{p}$ decreases $R(c, h, 0^-, \tilde{p}) = \frac{1}{(2c^2+\tilde{p})^2}$ to reach the $\lim_{\tilde{p}\to\infty}\left(\frac{1}{(2c^2+\tilde{p})^2}\right) = 0$. Thus by increasing $\tilde{p}$, we can increase $R(c, h, \frac{-1}{2c^2-h}, \tilde{p}) = R(c, h, 0^-, \tilde{p})$. Equating $R\left(c, h, 0, \tilde{p}\right) = R\left(c, h, \frac{-1}{2c^2-h}, \tilde{p}\right)$ results in

$$\begin{aligned}\tilde{p}^* =& 1 - 2c^2, -1 - 2c^2, \frac{-1 - \sqrt{16c^8 - 16c^6h + 4c^4h^2 - 12c^4 + 8c^2h - h^2 + 1}}{2c^2 - h},\\ & \frac{-1 + \sqrt{16c^8 - 16c^6h + 4c^4h^2 - 12c^4 + 8c^2h - h^2 + 1}}{2c^2 - h}.\end{aligned}$$

Since $\tilde{p} > 1-2c^2$, we discard the first three solutions, and this completes the proof. □

4.2.4 Comparison with the infinitely long RC circuit

In this section, we will relate the reduced RC circuit with four nodes shown in Figure 4.7 to the infinitely long RC circuit as shown in Figure 2.2. We will then verify if we can derive the same expressions of $\alpha^*_{T,0}$ and $\alpha^*_{R,0}$ for the infinitely long RC circuit using the expression of optimized $\alpha^{[4]*}$ for RC circuit with four nodes given by (4.51).

We proved in Section 4.1.3 that for the nonoverlapping OWR method, the value of h for the reduced RC circuit with both two and four nodes is given by $h = \lambda_2(\omega_{\min})$. Using this value of h, we find $\alpha^{[4]*}$ for the infinitely long RC circuit. Our analysis for four nodes RC circuit is only valid when $h = \lambda_2(\omega_{\min}) \in \mathbb{R}$, and hence we consider only one type of asymptotic analysis, the one with respect to $\epsilon \to 0$. In this analysis, $h = \lambda_2(0) \in \mathbb{R}$.

4.2.4.1 Asymptotics with respect to $\epsilon \to 0$

We saw in Section 4.1.3.2 that for asymptotic analysis with respect to $\epsilon \to 0$, where $b = -(2+\epsilon)a$, the constants are $c^2 = 1 + \frac{\epsilon}{2}$ and $h = 1 - \sqrt{\epsilon} + \mathcal{O}(\epsilon)$. For this analysis, using the expression of p^* given by (4.52), we arrive at

$$\begin{aligned} p^* &= \frac{-1 + \sqrt{16c^8 - 16c^6h + 4c^4h^2 - 12c^4 + 8c^2h - h^2 + 1}}{2c^2 - h}\\ &= \frac{-1 + \sqrt{2\sqrt{\epsilon} + \mathcal{O}(\epsilon)}}{1 + \sqrt{\epsilon} + \mathcal{O}(\epsilon)} = \frac{-1 + \sqrt{2}\epsilon^{1/4} + \mathcal{O}(\epsilon^{1/2})}{1 + \sqrt{\epsilon} + \mathcal{O}(\epsilon)}\\ &= -1 + \sqrt{2}\epsilon^{1/4} + \mathcal{O}(\epsilon^{1/2}).\end{aligned}$$

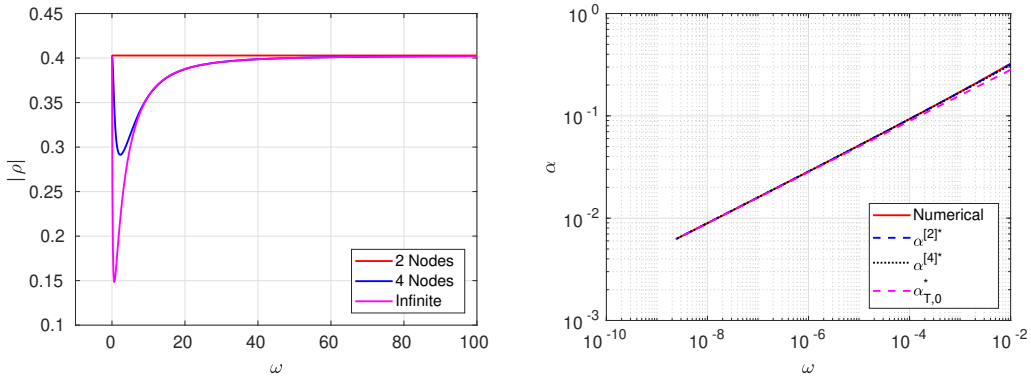

Figure 4.13: Solution given by equioscillation for different lengths of the RC circuits (left) and comparison of the optimized α for $\epsilon = 0$ (right).

Finally, using (4.51), we arrive at

$$\alpha^{[4]*} = 2c^2 - 1 + p^* = \sqrt{2}\epsilon^{1/4} + \mathcal{O}(\epsilon^{1/2}).$$

This is the same expression for $\alpha^*_{R,0}$ derived in Theorem 2.4.3.

4.3 Numerical Experiments

We perform three major numerical experiments to verify whether the method of reduction of the infinitely long RC circuit to a smaller RC circuit produces fairly good results. In other words, we would like to see that the optimized α^* given by Theorems 4.1.3 and 4.2.3 can be used in the transmission conditions of the nonoverlapping OWR method when applied to infinitely long RC circuit.

First of all, we observe numerically that the solution of the min-max problems (4.15) and (4.38) of the reduced RC circuits with two and four nodes respectively are found by equioscillation. For this example, we consider $R = 0.5k\Omega$, $C = 0.63pF$, $\epsilon = 0.01$ and $\omega_{\max} = 100$. The left plot of Figure 4.13 shows that for all RC circuits whether they are infinitely long or reduced circuits with two or four nodes, the solution of the min-max problems is given by equioscillation. Note that $\alpha^{[2]*}$ and $\alpha^{[4]*}$ are calculated using equations (4.20) and (4.51) respectively, while $\alpha^*_{T,0}$ by Theorem 2.4.1. It is interesting to observe that for the RC circuit with two nodes, equioscillation occurs for all $\omega \in [\omega_{\min}, \omega_{\max}]$, while for the other cases, equioscillation occurs between $\omega = \omega_{\min}$ and $\omega = \omega_{\max}$. Further, the right plot of Figure 4.13 shows that the optimized α^* found by all methods is very close to numerically optimized α^*.

Next, we observe the effect of the optimized α^* derived by the different ways on the convergence of the nonoverlapping OWR methods. We consider the case of the RC circuit which could not be considered in Chapter 2. that is, an infinitely long RC

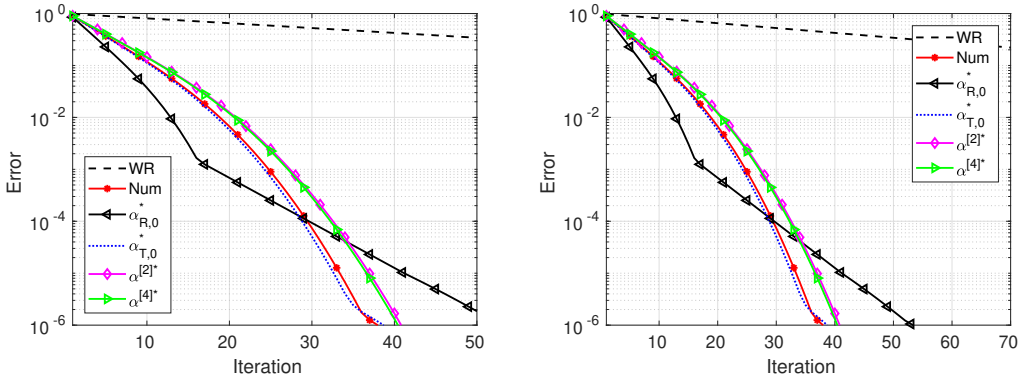

Figure 4.14: Convergence plots of OWR using α^* found by different methods for $N = 150$ and $T = 1000$ (left) and for $N = 200$ and $T = 2000$ (right).

circuit with $\epsilon = 10^{-4}$, with finite time $t \in (0, T]$ and time discretization $\Delta t = 0.1$. We perform two similar experiments: one with a length of the RC circuit of $N = 150$ and $T = 1000$ and the other with $N = 200$ and $T = 2000$. For the OWR method, we use the optimized α^* derived by four different analysis, that is, asymptotic analyses with respect to $T \to \infty$, asymptotic analysis with respect to $\epsilon \to 0$, using the reduced RC circuit of two nodes and the reduced RC circuit of four nodes. We observe that the convergence rate of the nonoverlapping OWR method is far greater than that of the classical nonoverlapping WR method. In both plots of Figure 4.14, we observe that our method of reducing circuits and then solving the min-max problem produces convergence plots which are very close to the numerically optimized convergence.

4.4 Conclusion

We developed a new methodology for analyzing convergence of nonoverlapping OWR when applied to infinitely long RC circuits, which can be also extended to other electric circuits. We showed how long circuits can be reduced to smaller circuits by a method of back-substitution which is similar to the calculation of a Schur complement. One of the most important hurdles is to find a best approximation of h, which contains the information of the remaining circuit. We proved that for the application of the nonoverlapping OWR to the RC circuit, h can be chosen as $h = \lambda_2(\omega_{\min})$.

In Chapter 2, we could not prove that the solution of the min-max problem given by equioscillation is unique. Also, we had to use asymptotic analysis to find expressions for the optimized α^*. Moreover, we considered two separate asymptotic analyses: one with respect to $T \to \infty$ with $\epsilon = 0$ and the other with respect to $\epsilon \to 0$ with $T = \infty$. However, the reduction of this infinitely long RC circuit to a smaller circuit overcomes all these issues. We proved that the solution of the min-max problem is uniquely given by equioscillation (without using asymptotic analysis). With these

reduced circuits, we can treat a combined situation, that is, $\epsilon > 0$ and $T < \infty$.

Further, for fixed $h \in (0, 1)$, we solved the min-max problems for the reduced RC circuit of two nodes and four nodes, and found an explicit expression for the optimized $\alpha^{[2]*}$ and $\alpha^{[4]*}$ respectively. We then compared our newly derived $\alpha^{[2]*}$ and $\alpha^{[4]*}$ with those of $\alpha^*_{T,0}$ and $\alpha^*_{R,0}$ derived in Chapter 2. Finally, we performed some numerical experiments to support our theoretical results, and compare reduced circuits with the infinitely long RC circuit.

However, for the overlapping OWR, we have not yet found a way to approximate h. We know that $h = \lambda_2(\omega)$ for some $\omega \in [\omega_{\min}, \omega_{\max}]$. The solution of the min-max problem for the overlapping OWR is also given by equioscillation, but its behavior is different from the nonoverlapping case. The equioscillation takes place between $\omega = \omega_{\min}$ and $\omega = \bar{\omega}$, where $\bar{\omega} \in (\omega_{\min}, \omega_{\max})$ and $\bar{\omega}$ close to $\omega_{\min}$. This makes the analysis to approximate $h = \lambda_2(\omega)$ difficult. This is work in progress and expected to finish soon.

Chapter 5

Conclusion and Future work

This thesis was devoted to the study of the application of nonoverlapping and overlapping WR methods to electric circuits. We studied two types of circuits: the infinitely long RC circuit and the infinitely long RLCG transmission line. These circuits are an integral part of most of the integrated circuits and hence their quick simulation is important. Moreover the systems of ODEs representing these circuits are the same as the discretized heat and Maxwell's equations respectively.

In Chapter 2, we first developed the mathematical model of an infinitely long RC circuit using the well known MNA formulation. We then applied the WR algorithm to this circuit and studied its convergence in Laplace space. The classical WR method converges superlinearly for small time windows, but has a slow linear rate of convergence when large time windows are employed. To tackle this problem, we introduced optimized transmission conditions, which now exchange at the interface a combination of voltages and currents instead of only voltages in case of the classical WR method. However the introduction of these new transmission conditions leads to an optimization problem. Solving this min-max problem yields the best combination of voltage and current, which are transferred at the interfaces. This min-max problem cannot be solved using the available complex analysis tools and hence we use asymptotic analysis with respect to two different parameters: one with respect to the final time going to infinity and the other with respect to a reaction term going to zero. Both of these asymptotic analyses have been performed for both nonoverlapping and overlapping cases, and it has been found that the optimized parameters for the nonoverlapping OWR behave differently to that of the overlapping OWR. We showed that the convergence of both WR and OWR methods increases by overlapping more nodes. Further, we proved that the improvement in the convergence in WR methods due to optimized transmission conditions is far more than that because of overlapping nodes. Finally, though all these analyses are done only for the two subdomain case, we numerically checked that these optimized parameters can be used for the multiple subdomain case and for the discretized heat equation.

We presented similar analyses for the infinitely long RLC transmission lines in Chapter 3. We considered both nonoverlapping and overlapping WR methods. We developed optimized transmission conditions for both of these cases. One interesting and novel study was based on the way of partitioning the system of ODEs corresponding to transmission lines. In this case, both the voltages at the nodes and currents in between are unknowns, and are arranged in a systematic manner one after the other. Thus the splitting of this system of ODEs becomes interesting. We observed that the type of splitting does not affect the convergence of the classical WR method, but the convergence for OWR is faster when partitioning is at a current node. We then derived asymptotic expressions for the optimization parameters in the optimized transmission conditions for all possible cases, that is, nonoverlapping OWR, overlapping OWR with splitting at a voltage node and overlapping OWR with splitting at a current node.

Due the complicated expression of the convergence factor for both circuits, the process of finding the optimized parameters in the transmission conditions was complicated. In Chapter 4, we therefore develop a new strategy for this analysis, where we first reduce the infinitely long circuit into a smaller circuit with minimal nodes required for the analysis of OWR method. This reduction procedure is performed via back substitution which is similar to the calculation of a Schur compliment. This analysis was done for the application of nonoverlapping OWR to the infinitely long RC circuit.

There are many questions which are open. One needs to study the reduction strategy to the infinitely long RLCG transmission lines. Further, this reductions strategy needs to be extended to the overlapping OWR methods. We would also like to apply these methods to other electric circuits like the low pass filter, PEEC circuit and so on. The considered RC circuit and RLCG transmission lines are in 1D, that is, in one direction. One could also consider 2D circuits. Along with parallelism in the space domain, we can also combine WR methods with other time parallel methods to gain extra parallelism, that is, in the time domain.

Bibliography

[1] M. D. Al-Khaleel, M. J. Gander, and A. E. Ruehli. Optimized waveform relaxation solution of RLCG transmission line type circuits. In *9th International Conference on Innovations in Information Technology (IIT)*, pages 136–140, March 2013.

[2] M. D. Al-Khaleel, M. J. Gander, and A. E. Ruehli. A mathematical analysis of optimized waveform relaxation for a small RC circuit. *Applied Numerical Mathematics*, 75:61 – 76, 2014. 10th IMACS International Symposium on Iterative Methods in Scientific Computing.

[3] M. D. Al-Khaleel, M. J. Gander, and A. E. Ruehli. Optimization of transmission conditions in waveform relaxation techniques for RC circuits. *SIAM Journal on Numerical Analysis*, 52(2):1076–1101, 2014.

[4] L. Bortot, B. Auchmann, I. C. Garcia, A. M. F. Navarro, M. Maciejewski, M. Mentink, M. Prioli, E. Ravaioli, S. Schöps, and A. P. Verweij. STEAM: A hierarchical cosimulation framework for superconducting accelerator magnet circuits. *IEEE Transactions on Applied Superconductivity*, 28(3):1–6, April 2018.

[5] M. Bouajaji, V. Dolean, M. J. Gander, and S. Lanteri. Optimized Schwarz methods for the time-harmonic Maxwell's equations with damping. *SIAM Journal on Scientific Computing*, 34(4):A2048–A2071, 2012.

[6] J. Bourgat, R. Glowinski, P. Le Tallec, and M. Vidrascu. Variational formulation and algorithm for trace operation in domain decomposition calculations. Research Report RR-0804, INRIA, 1988.

[7] S. Brenner and R. Scott. *The Mathematical Theory of Finite Element Methods*. Texts in Applied Mathematics. Springer New York, 2007.

[8] F. Chaouqui. *Optimal Coarse Space Correction for Domain Decomposition Methods*. PhD thesis, 09/18 2018. ID: unige:121801.

[9] F. Chaouqui, G. Ciaramella, M. J. Gander, and T. Vanzan. On the scalability of classical one-level domain-decomposition methods. *Vietnam Journal of Mathematics*, 46(4):1053–1088, Dec 2018.

[10] F. Chaouqui, M. J. Gander, and K. Santugini-Repiquet. On nilpotent subdomain iterations. In *Domain Decomposition Methods in Science and Engineering XXIII*, pages 125–133, Cham, 2017. Springer International Publishing.

[11] F. Chaouqui, M. J. Gander, and K. Santugini-Repiquet. A coarse space to remove the logarithmic dependency in Neumann–Neumann methods. In *Domain Decomposition Methods in Science and Engineering XXIV*, pages 159–167, Cham, 2018. Springer International Publishing.

[12] F. Chaouqui, M. J. Gander, and K. Santugini-Repiquet. A local coarse space correction leading to a well-posed continuous Neumann-Neumann method in the presence of cross points. In *accepted for Domain Decomposition Methods in Science and Engineering XXV, LNCSE, Springer-Verlag*. Springer, 2019.

[13] F. Chaouqui, M. J. Gander, and K. Santugini-Repiquet. Optimal coarse spaces for FETI and their approximation. In *Numerical Mathematics and Advanced Applications ENUMATH 2017*, pages 931–939, Cham, 2019. Springer International Publishing.

[14] G. Ciaramella and T. Vanzan. Substructured Two-level and Multilevel Domain Decomposition Methods. *arXiv e-prints*, page arXiv:1908.05537, Aug 2019.

[15] J. de Dieu Nshimiyimana, F. Plumier, P. Dular, C. Geuzaine, and J. Gyselinck. Co-simulation of finite element and circuit solvers using optimized waveform relaxation. In *IEEE International Energy Conference (ENERGYCON)*, pages 1–6, April 2016.

[16] V. Dolean, M. J. Gander, and L. Gerardo-Giorda. Optimized Schwarz methods for Maxwell's equations. *SIAM Journal on Scientific Computing*, 31(3):2193–2213, 2009.

[17] V. Dolean, M. J. Gander, and E. Veneros. Asymptotic analysis of optimized Schwarz methods for Maxwell's equations with discontinuous coefficients. *ESAIM: M2AN*, 52(6):2457–2477, 2018.

[18] V. Dolean, P. Jolivet, and F. Nataf. *An Introduction to Domain Decomposition Methods*. Society for Industrial and Applied Mathematics, Philadelphia, PA, 2015.

[19] C. Farhat, J. Mandel, and F. X. Roux. Optimal convergence properties of the FETI domain decomposition method. *Computer Methods in Applied Mechanics and Engineering*, 115(3):365 – 385, 1994.

[20] C. Farhat and F. X. Roux. A method of finite element tearing and interconnecting and its parallel solution algorithm. *International Journal for Numerical Methods in Engineering*, 32(6):1205–1227, 1991.

[21] M. J. Gander. *Overlapping Schwarz for Linear and Nonlinear Parabolic Problems*, pages 97–104. 9th International Conference on Domain Decomposition Methods. 1996.

[22] M. J. Gander. Optimized Schwarz methods. *SIAM J. Numer. Anal.*, 44(2):699–731, February 2006.

[23] M. J. Gander. 50 Years of Time Parallel Time Integration. In *Multiple Shooting and Time Domain Decomposition Methods*, pages 69–113, Cham, 2015. Springer International Publishing.

[24] M. J. Gander. Time parallel time integration. *Unpublished, University of Geneva*, November 2018.

[25] M. J. Gander, M. D. Al-Khaleel, and A. E. Ruchli. Optimized waveform relaxation methods for longitudinal partitioning of transmission lines. *IEEE Transactions on Circuits and Systems I: Regular Papers*, 56(8):1732–1743, Aug 2009.

[26] M. J. Gander, M. D. Al-Khaleel, and A. E. Ruehli. Waveform relaxation technique for longitudinal partitioning of transmission lines. In *IEEE Electrical Performane of Electronic Packaging*, pages 207–210, Oct 2006.

[27] M. J. Gander and L. Halpern. Méthodes de relaxation d'ondes (SWR) pour l'équation de la chaleur en dimension 1. *Comptes Rendus Mathematique*, 336(6):519 – 524, 2003.

[28] M. J. Gander, L. Halpern, and M. Kern. A Schwarz waveform relaxation method for advection-diffusion-reaction problems with discontinuous coefficients and non-matching grids. In *Domain Decomposition Methods in Science and Engineering XVI*, pages 283–290, Berlin, Heidelberg, 2007. Springer Berlin Heidelberg.

[29] M. J. Gander, L. Halpern, and F. Nataf. Optimal convergence for overlapping and non-overlapping Schwarz waveform relaxation. In *11th International Conference on Domain Decomposition Methods*, pages 27–36, 1999.

[30] M. J. Gander, L. Halpern, and F. Nataf. Optimal Schwarz waveform relaxation for the one dimensional wave equation. *SIAM Journal on Numerical Analysis*, 41(5):1643–1681, 2003.

[31] M. J. Gander, Y. L. Jiang, and R. J. Li. Parareal Schwarz waveform relaxation methods. In *Domain Decomposition Methods in Science and Engineering XX*, pages 451–458, Berlin, Heidelberg, 2013. Springer Berlin Heidelberg.

[32] M. J. Gander, P. M. Kumbhar, and A. E. Ruehli. Analysis of overlap in waveform relaxation methods for RC circuits. In *Domain Decomposition Methods in Science and Engineering XXIV*, pages 281–289, Cham, 2018. Springer International Publishing.

[33] M. J. Gander, P. M. Kumbhar, and A. E. Ruehli. Asymptotic analysis for different partitionings of RLC transmission lines. In *accepted for Domain Decomposition Methods in Science and Engineering XXV, LNCSE, Springer-Verlag*, 2019.

[34] M. J. Gander, P. M. Kumbhar, and A. E. Ruehli. Asymptotic Analysis for Overlap in Waveform Relaxation Methods for RC Type Circuits. *arXiv e-prints*, page arXiv:2001.04949, Jan 2020.

[35] M. J. Gander, F. Kwok, and B. C. Mandal. Dirichlet-Neumann and Neumann-Neumann waveform relaxation for the wave equation. In *Domain Decomposition Methods in Science and Engineering XXII*, pages 501–509, Cham, 2016. Springer International Publishing.

[36] M. J. Gander and A. E. Ruehli. Solution of large transmission line type circuits using a new optimized waveform relaxation partitioning. In *IEEE Symposium on Electromagnetic Compatibility. Symposium Record (Cat. No.03CH37446)*, volume 2, pages 636–641 vol.2, Aug 2003.

[37] M. J. Gander and A. E. Ruehli. Optimized waveform relaxation methods for RC type circuits. *IEEE Transactions on Circuits and Systems I: Regular Papers*, 51(4):755–768, April 2004.

[38] M. J. Gander and A. M. Stuart. Space-time continuous analysis of waveform relaxation for the heat equation. *SIAM Journal on Scientific Computing*, 19(6):2014–2031, 1998.

[39] M. J. Gander and S. Vandewalle. On the superlinear and linear convergence of the parareal algorithm. In *Domain Decomposition Methods in Science and Engineering XVI*, pages 291–298, Berlin, Heidelberg, 2007. Springer Berlin Heidelberg.

[40] M. J. Gander and T. Vanzan. Heterogeneous optimized Schwarz methods for coupling Helmholtz and Laplace equations. In *Domain Decomposition Methods in Science and Engineering XXIV*, pages 311–320, Cham, 2018. Springer International Publishing.

[41] M. J. Gander and T. Vanzan. Heterogeneous optimized Schwarz methods for second order elliptic PDEs. *SIAM Journal on Scientific Computing*, 41(4):A2329–A2354, 2019.

[42] M. J. Gander and T. Vanzan. On the derivation of optimized transmission conditions for the Stokes-Darcy coupling. In *accepted for Domain Decomposition Methods in Science and Engineering XXV, LNCSE, Springer-Verlag*, 2019.

[43] M. J. Gander and T. Vanzan. Optimized Schwarz methods for advection diffusion equations in bounded domains. In *Numerical Mathematics and Advanced Applications ENUMATH 2017*, pages 921–929, Cham, 2019. Springer International Publishing.

[44] M. J. Gander and H. Zhang. Optimized Schwarz methods with overlap for the Helmholtz equation. In *Domain Decomposition Methods in Science and Engineering XXI*, pages 207–215, Cham, 2014. Springer International Publishing.

[45] M. J. Gander and H. Zhao. Overlapping Schwarz waveform relaxation for the heat equation in N dimensions. *BIT Numerical Mathematics*, 42(4):779–795, Dec 2002.

[46] I. C. Garcia, S. Schöps, M. Maciejewski, L. Bortot, M. Prioli, B. Auchmann, and A. Verweij. Optimized field/circuit coupling for the simulation of quenches in superconducting magnets. *IEEE Journal on Multiscale and Multiphysics Computational Techniques*, 2:97–104, 2017.

[47] P. Gervasio and A. Quarteroni. The INTERNODES method for non-conforming discretizations of PDEs. *Communications on Applied Mathematics and Computation*, 1(3):361–401, Sep 2019.

[48] L. Halpern and J. Szeftel. Nonlinear nonoverlapping Schwarz waveform relaxation for semilinear wave propagation. *Mathematics of Computation*, 78(266):865–889, 2009.

[49] C. W. Ho, A. E. Ruehli, and P. Brennan. The modified nodal approach to network analysis. *IEEE Transactions on Circuits and Systems*, 22(6):504–509, June 1975.

[50] A. Klawonn, P. Radtke, and O. Rheinbach. FETI-DP methods with an adaptive coarse space. *SIAM Journal on Numerical Analysis*, 53(1):297–320, 2015.

[51] F. Kwok. Neumann–Neumann waveform relaxation for the time-dependent heat equation. In *Domain Decomposition Methods in Science and Engineering XXI*, pages 189–198, Cham, 2014. Springer International Publishing.

[52] F. Kwok and B. W. Ong. Schwarz waveform relaxation with adaptive pipelining. *SIAM Journal on Scientific Computing*, 41(1):A339–A364, 2019.

[53] E. Lelarasmee, A. E. Ruehli, and A. L. Sangiovanni-Vincentelli. The waveform relaxation method for time-domain analysis of large scale integrated circuits. *IEEE Transactions on Computer-Aided Design of Integrated Circuits and Systems*, 1(3):131–145, July 1982.

[54] J. Liu and Y. L. Jiang. A parareal algorithm based on waveform relaxation. *Mathematics and Computers in Simulation*, 82(11):2167 – 2181, 2012.

[55] Y. Maday and G. Turinici. A parareal in time procedure for the control of partial differential equations. *Comptes Rendus Mathematique*, 335(4):387 – 392, 2002.

[56] P. Mamooler. *The domain decomposition method of Bank and Jimack as an optimized Schwarz method*. PhD thesis, 06/27 2019. ID: unige:121394.

[57] B. C. Mandal. A time-dependent Dirichlet-Neumann method for the heat equation. In *Domain Decomposition Methods in Science and Engineering XXI*, pages 467–475, Cham, 2014. Springer International Publishing.

[58] J. Mandel. Balancing domain decomposition. *Communications in Numerical Methods in Engineering*, 9(3):233–241, 1993.

[59] J. Mandel and C. R. Dohrmann. Convergence of a balancing domain decomposition by constraints and energy minimization. *Numerical Linear Algebra with Applications*, 10(7):639–659, 2003.

[60] V. Martin. An optimized Schwarz waveform relaxation method for the unsteady convection diffusion equation in two dimensions. *Applied Numerical Mathematics*, 52(4):401 – 428, 2005.

[61] J. C. Maxwell. A Dynamical Theory of the Electromagnetic Field. *Philosophical Transactions of the Royal Society of London*, 155:459–513, 1865.

[62] A. Monge and P. Birken. A multirate Neumann-Neumann waveform relaxation method for heterogeneous coupled heat equations. *SIAM Journal on Scientific Computing*, 41(5):S86–S105, 2019.

[63] F. N. Najm. *Circuit Simulation*. Wiley-IEEE Press, 2010.

[64] B. W. Ong, S. High, and F. Kwok. Pipeline Schwarz waveform relaxation. In *Domain Decomposition Methods in Science and Engineering XXII*, pages 363–370, Cham, 2016. Springer International Publishing.

[65] B. W. Ong and B. C. Mandal. Pipeline implementations of Neumann-Neumann and Dirichlet-Neumann waveform relaxation methods. *Numerical Algorithms*, 78(1):1–20, May 2018.

[66] A. Quarteroni and A. Valli. *Domain Decomposition Methods for Partial Differential Equations*. Oxford University Press, Oxford, UK, 1999.

[67] B. Song and Y-L Jiang. A new parareal waveform relaxation algorithm for time-periodic problems. *International Journal of Computer Mathematics*, 92(2):377–393, 2015.

[68] E. C. Titchmarsh. *The Theory of Functions*. Oxford University Press, 1939.

[69] A. Toselli and O. B. Widlund. *Domain Decomposition Methods- Algorithms and Theory*, volume 34. Springer, Berlin, Heidelberg, 2005.

[70] S. L. Wu and M. D. Al-Khaleel. Optimized waveform relaxation methods for RC circuits: discrete case. *ESAIM: M2AN*, 51(1):209–223, 2017.